Vascular Targeted Agents for the Treatment of Angiosarcoma

Robin Joseph Young

Thesis submitted for the degree of

Doctor of Philosophy

University of Sheffield

Department of Oncology

January 2013

Contents

I Acknowledgements

First and foremost I am indebted to my two supervisors Penella Woll and Nicola Brown; they have supported and inspired me throughout my research, and continue to do so. I also wish to thank Malcolm Reed and Carolyn Staton for all their advice and support.

I wish to thank Yorkshire Cancer Research who funded my clinical research fellowship. I would like to acknowledge Sue Murphy from the Animal Health Trust who generously provided the canine tumour blocks, and Professors Krump-Konvalinkova and Masuzawa who kindly provided the ASM and ISO-HAS cell lines respectively. Pfizer provided axitinib and sunitinib for the drug studies, and Novartis provided DMXAA.

Many other people helped me during my research. By inclusion I risk omission, but I would like to specifically thank Carmel Nichols, Sue Higham, Jenny Globe and Claire Greaves for providing technical support and advice. Thanks also to Sue Newton for helping me with the flow cytometry experiments. I woud like to express my thanks to Lynda Wyld for her help in collecting the sarcoma tumour samples, and to the patients who donated their tissue. I would also like to thank David Hughes and Marlee Fernando for their help, with particular thanks to Malee for giving up so much of her time to guide me through the tumour immunohistochemistry analysis.

I would also like to thank those with whom I was fortunate enough to share lab time and office space, with special mention to Sapna, Matt, Debayan and Sheila.

Finally, I wish to thank my family, especially my wonderful wife Shareen - for sharing the journey and for encouraging me to follow my dreams - and our children, Kamran, Leila and Benjamin.

II Abstract

Background:

Angiogenesis is the process of new blood vessel formation, and is regulated by angiogenic growth factors including vascular endothelial growth factor (VEGF). Angiosarcomas are rare, aggressive vascular tumours. *S*tudies were performed to investigate the expression of angiogenic growth factors in angiosarcoma, and to assess vascular targeted agents for the treatment of angiosarcoma.

Methods:

In vitro studies compared two human cutaneous angiosarcoma cell lines (ASM and ISO-HAS) with human dermal microvascular endothelial cells (HuDMECs). The cell lines were compared in functional assays, including cell viability, cell differentiaiton and cell migration assays, and protein expression profiled using antibody arrays.

Cell responses to vascular targeted agents were compared, including response to bevacizumab an anti-VEGF antibody, axitinib a VEGF receptor (VEGFR) tyrosine kinase inhibitor, selumetinib a MEK inhibitor, and DMXAA a vascular disrupting agent.

Immunohistochemistry studies measured the expression of angiogenic growth factors in angiosarcoma tumour specimens using benign vascular lesions for comparison, and assessed canine angiosarcoma as a model of human angiosarcoma.

Results:

ASM and ISO-HAS demonstrated accelerated growth kinetics, chaotic tubule formation, and increased cell migration compared to HuDMECs.

ASM and ISO-HAS expressed significantly increased VEGF compared to HuDMECs. Only minor responses were observed to VEGF targeted agents in functional assays

despite western blot studies that showed target inhibition of VEGFR2 phosphorylation,. Striking responses were seen however to selumetinib and DMXAA.

Immunohistochemistry studies demonstrated benign and malignant vascular tumours expressed a range of pro-angiogenic growth factors, however analysis did not distinguish malignant from benign vascular tumours.

The morphology of canine angiosarcoma was similar to human angiosarcoma. VEGF and VEGFR2 expression was significantly increased in canine angiosarcoma compared to benign vascular lesions.

Conclusion:

These studies predict limited *in vivo* angiosarcoma tumour response to VEGF targeted agents. Selumetinib and DMXAA are suggested for further study. Canine angiosarcomas represent a potential model of human angiosarcoma to be explored in future studies.

III Abbreviations

4EBP	eIF4E binding protein
ADCC	Antibody-dependent cell-meditated cytotoxicity
aFGF	Acidic fibroblast growth factor
AMPK	AMP-activate protein kinase
Ang	Angiopoietin
ASV	Avian sarcoma virus
ATCC	American type culture collection
ATF	Activating transcription factor
ATM	Ataxia telangiectasia mutant
ATP	Adenosine tri-phosphate
bFGF	Basic fibroblast growth factor
BME	Basement membrane extract
CD	Cluster of differentiation
Chk II	Checkpoint II
C_{max}	Maximal concentration
CSF-1R	Colony stimulating factor-1R
CXCL	Chemokine ligand
DAB	3,3'-diaminobenzidine
DCE	Dynamic contrast-enhanced
Dil-Ac-LDL	Dioctadecyl acetylated low density lipoprotein
DLL	Delta-like ligand
DNA	Deoxyribonucleic acid
DMSO	Dimethyl sulfoxide
DPPIV	Dipeptidyl peptidase IV
DPX	Distyrene plasticiser xylene
EBM	Endothelial basal medium

ECGM	Endothelial cell growth media
ECL	Electrochemiluminescence
EDTA	Ethylenediaminetetraacetic acid
EGF	Epidermal growth factor
eIF4E	Eukaryotic initiation factor 4E
ELISA	Enzyme-linked immunosorbent assay
eNOS	Endothelial nitric oxide synthase
ERK	Extracellular signal-regulated kinase
ESMO	European Society for Medical Oncology
FACS	Fluorescence activated cell sorting
FAK	Focal adhesion kinase
FCS	Fetal calf serum
FFPE	Formalin fixed paraffin embedded
FGF	Fibroblast growth factor
FLT	FMS-related tyrosine kinase
FSC	Forward scatter
GDNF	Glial cell-derived neurotrophic factor
GIST	Gastro-intestinal stromal tumur
GM-CSF	Granulocyte macrophage colony stimulating factor
GSK-3	Glycogen synthase kinase-3
HB-EGF	Heparin binding EGF-like growth factor
HDF	Human dermal fibroblast
HGF	Hepatocyte growth factor
HHV8	Human herpes virus 8
HIF	Hypoxia-inducible factor
HRP	Horseradish peroxidise
HSP 27	Heat shock protein 27
HuDMEC	Human dermal micro-vascular endothelial cell
HUVEC	Human umbilical vein endothelial cell

IC	Inhibitory concentration
IFN	Interferon
IGFBP1	Insulin-like growth factor binding protein-1
IGF-1R	Insulin-like growth factor-1 receptor
IL	Interleukin
iTRAQ	Isobaric tags for relative and absolute quantification
Jag	Jagged
NCCN	National Comprehensive Cancer Network
MAPK	Mitogen-activated protein kinase
MCP-1	Monocyte chemotactic protein-1
MDM2	Murine double minute2
MEK	Mitogen-activated protein kinase kinase
MMP	Matrix metalloproteinase
MRI	Magnetic resonance imaging
MST	Serine/threonine protein kinase 3
mTOR	Mammalian target of rapamycin
MTS	Dimethylthiazol tetrazolium salt
MVD	Micro-vessel density
NF-κB	Nuclear factor kappa B
NICD	Notch intracellular domain
NRP	Neuropilin
PBS	Phosphate buffered saline
PDGF	Platelet derived growth factor
PECAM	Platelet endothelial cell adhesion molecule
PI	Propidium Iodide
PI-3-K	Phosphatidylinositol-3-kinase
PKC	Protein kinase C
PLCγ	Phospholipase-Cγ
PlGF	Placental growth factor

pRTK	Phosphorylated receptor tyrosine kinase
PTEN	Phosphatase and tensin homolog
pTK	Phosphorylated tyrosine kinase
RB	Retinoblastoma
REC	Research ethics committee
RET	Rearranged during transfection
RNA	Ribonucleic acid
ROR1	Receptor tyrosine kinase-like orphan receptor-1
SEM	Standard error of the mean
SMA	Smooth muscle actin
SSC	Side scatter
STAT	Signal transducer and activator of transduction
STH	Sheffield Teaching Hospitals
sVEGFR	Soluble vascular endothelial growth factor receptor
TEMED	Tetramethylethylenediamine
TGF-β	Transforming growth factor-β
Tie	Tyrosine kinase with immunoglobulin-like and EGF-like domains
TIMP	Tissue inhibitor of matrix metalloproteinase
TKI	Tyrosine kinase inhibitor
TNFα	Tissue necrosis factor α
TSP-1	Thrombospondin-1
UEA-1	Ulex europaeus agglutinin-1
uPA	Urokinase plasminogen activator
VEGF	Vascular endothelial growth factor
VEGFR	Vascular endothelial growth factor receptor
vGPCR	Viral G protein coupled receptor
vIL6	Viral interleukin 6
vWF	Von Willebrand factor
WT-1	Wilms tumour-1

IV List of tables

Results

Discussion

V List of Figures

1 Introduction

1.1 Angiogenesis

Angiogenesis is the process of new blood vessel formation from existing vasculature[1]. It maintains vascular homeostasis, and is stimulated during menstruation, in wound healing, and in skeletal muscles in response to exercise. Physiological angiogenesis is tightly regulated by exquisite control across a spectrum of pro and anti-angiogenic growth factors.

Angiogenesis is also important in a variety of pathological processes. Angiogenesis is a critical step in cancer progression and is one of the Hallmarks of Cancer[2]. Tumours are unable to grow beyond 2-3mm^3 without a vascular supply, and the tumour vasculature also provides passage for tumour dissemination. Genetic abnormalities, including mutations in p53, Ras and von Hippel-Lindau (VHL), or changes within the tumour micro-environment, particularly tissue hypoxia, stimulate a shift to a pro-angiogenic state. A switch to uncontrolled release of pro-angiogenic growth factors results in dysregulated angiogenesis and the formation of chaotic, immature, leaky vessels. Tumour angiogenesis is initiated early in cancer progression, and is up-regulated even in pre-malignant conditions[3]. Numerous studies have correlated increasing tumour angiogenesis with a poorer prognosis[4].

The main signalling components regulating angiogenesis are:

- Vascular Endothelial Growth Factors (VEGF)
- Angiopoietins
- Platelet Derived Growth Factors (PDGF)
- Fibroblast Growth Factors (FGF)
- Notch

1.1.1 Vascular Endothelial Growth Factors

Vascular endothelial growth factors are a family of five glycoproteins, VEGF A, B, C, D and placental growth factor (PlGF), with VEGFA the most important member (hereafter referred to as VEGF)[5]. The VEGF gene, located at chromosome 6p12, consists of eight exons. mRNA splice variants involving exons 6 and 7 result in different VEGF isoforms, including $VEGF_{121}$, $VEGF_{165}$, $VEGF_{189.}$ These isoforms have distinct matrix binding properties that modify their solubility and biological activity, of which $VEGF_{165}$ is the most abundant and biologically active[6]. Exon 8 splice variants with anti-angiogenic properties have also been described (e.g. $VEGF_{165b}$)[7].

VEGF expression may be induced in all cell types however basal expression is usually low. In contrast, VEGF is over-expressed in tumours. Tumour cells secrete VEGF in response to hypoxia, other growth factors including epidermal growth factor (EGF), fibroblast growth factor (FGF), platelet derived growth factor (PDGF), transforming growth factor (TGF)-β, interleukin (IL)-6 and oestrogen, and mutations of Ras, Src, p53 and phosphatase and tensin homolog (PTEN)[6].

VEGF stimulates angiogenesis through the tyrosine kinase receptors VEGFR1-3 (figure 1.1). VEGFR1 is the most abundant VEGF receptor, and also binds VEGFB and PlGF. VEGFR1 is expressed by endothelial cells as both a transmembrane receptor and in a soluble truncated form (sVEGFR1). VEGFR1 is also expressed by monocytes, and stimulates macrophage infiltration of tumours. VEGF binding to VEGFR1 induces a weak intracellular signal, and the receptor's primary function appears to be to trap circulating VEGF to limit binding to VEGFR2[8]. However, tumour secretion of VEGFB and PlGF displaces VEGF from VEGFR1 and so increases VEGFR2 signalling[9].

VEGFR2 is principally expressed on endothelial cells, and is the main receptor mediating VEGF signalling[8]. VEGFR2 also forms complexes with neuropilin (NRP) co-receptors, enhancing the response to VEGF[10]. VEGFR2 activation induces endothelial cell survival, proliferation, migration and invasion[11]. Cell surface

expression of VEGFR2 is not static, but cycles within endocytic compartments[12], and VEGF binding to VEGFR2 also stimulates receptor ubiquitination and degradation[12]. VEGFR2 processing is therefore an important mechanism regulating endothelial cell sensitivity to VEGF.

VEGFR3 is chiefly expressed by lymphatic endothelial cells, and is the main receptor for VEGFC and D. VEGFR3 is not expressed on mature vascular endothelial cells, but is expressed by tip endothelial cells of angiogenic sprouts[13].

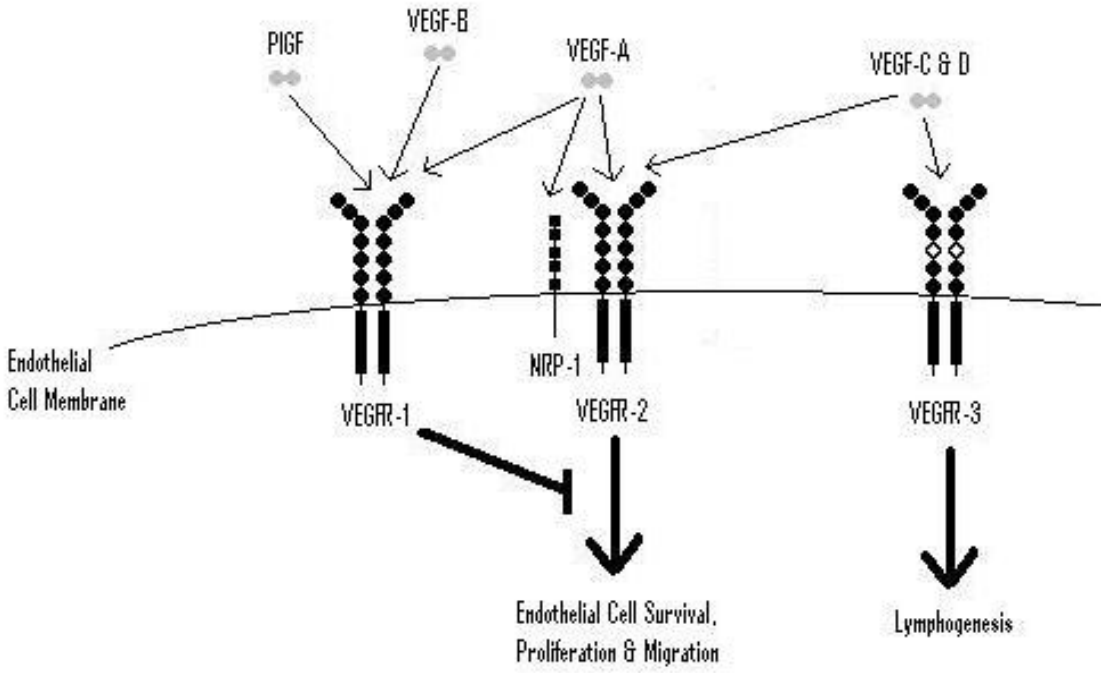

Figure 1.1: VEGF receptors and their ligands.

1.1.2 Angiopoietins

Four angiopoietin ligands have been identified (Ang1-4). Ang-1 and Ang-2 are the most important isoforms[14]. The angiopoietins signal through the Tie tyrosine kinase receptors, with Tie2 the primary receptor[14]. Tie2 receptors are principally found on endothelial cells, although they are also expressed on haemopoetic cells and are required for normal haematopoeisis[15].

Ang-1 is constitutively produced by pericytes[15]. Ang-1 stabilises the vasculature by promoting endothelial cell survival, and maintaining tight intercellular junctions between endothelial and perivascular cells[14, 16]. Ang-2 is produced by endothelial cells. It binds to, but does not activate Tie2, and antagonises Ang-1 signalling[14]. The effect of Ang-2 is to increase endothelial cell plasticity[14]. In the presence of VEGF this results in endothelial cell proliferation, but in the absence of VEGF leads to vascular regression[16]. Ang-2 is therefore intimately involved in vascular re-modelling[14].

A meta-analysis of pathology studies comparing tumour expression of Ang-1 and Ang-2 concluded that angiopoietin expression was increased in tumours compared to benign controls, and that tumour expression of Ang-2 was higher than Ang-1. Ang-1 was principally expressed by tumour cells, whilst Ang-2 was expressed by both tumour and tumour endothelial cells[17].

1.1.3 Platelet Derived Growth Factors

PDGFs consist of four homodimeric ligands, AA, BB, CC and DD, which signal through two tyrosine kinase receptors, PDGFRα and β[18]. The PDGFRs are closely related to the VEGFR family, and have a wide range of cellular functions. PDGF-BB and PDGFRβ are involved in the regulation of angiogenesis; PDGF-B is secreted by vascular endothelial cells, whilst PDGFRβ is expressed by pericytes[19]. PDGF-B stimulates pericyte migration and proliferation, and recruits pericytes to blood vessels during the process of vessel maturation[19].

Pericyte coverage of the tumour vasculature may protect tumour endothelial cells from VEGF targeted agents. Co-inhibition of VEGF signalling with agents to target PDGFRβ may therefore enhance the anti-angiogenic response[20]. PDGFRβ expression is not limited to pericytes however, and it is also expressed by stromal cells throughout the tumour, suggesting PDGFRβ inhibition may have broader anti-tumour effects[18]. Specific pathogenic abnormalities of PDGF signalling have been identified in a number of different tumours: a translocation between chromosomes 17 and 22,

t(17:22)(q22:q13.1), results in synthesis of a collagen type 1 alpha 1 (COL1A1)-PDGF-BB fusion protein which causes dermatofibrosarcoma protuberan (DFSP) tumour formation[21], and activating mutations in PDGFRα have been demonstrated in a third of c-kit wild-type gastrointestinal stromal tumours (GISTs)[22].

1.1.4 Fibroblast Growth Factors

FGF stimulated angiogenesis mediates tumour resistance to VEGF targeted agents[23]. FGFs are a family of 22 growth factors which signal through four tyrosine kinase receptors (FGFR1-4). They are secreted by a variety of cell types, including tumour cells, and have a wide range of effects beyond promoting angiogenesis[24]. Endothelial cells express FGFR1 and FGFR2 through which the pro-angiogenic FGFs, acidic FGF (aFGF, also known as FGF-1) and basic FGF (bFGF, also known as FGF-2), promote degradation of the extracellular matrix, and endothelial cell proliferation and migration[24]. As well as directly stimulating endothelial cells, FGFs also promote angiogenesis through the up-regulation of other pro-angiogenic pathways, including increased expression of VEGF and Ang-2[24]. As growth factors that stimulate a broad range of cellular processes, including proliferation, survival, migration and invasion, it is unsurprising that aberrant FGF signalling has been identified in a wide range of tumours[25]. Drugs to target FGF signalling are in development, including tyrosine kinase inhibitors (TKIs) such as Brivanib and BIBF1120, however these agents also inhibit VEGF and PDGF receptors[26]; newer agents under investigation including AZD4547 are more potent and selective inhibitors of FGFRs [27].

1.1.5 Notch

The Notch signalling system is an evolutionary conserved system that controls branching morphogenesis[28]. Notch consists of five distinct ligands, Delta-like ligand (DLL) 1, 3 and 4, Jagged 1 and 2, and four Notch receptors. The endothelial specific signalling components of Notch are DLL-1, DLL-4, Jag-1, Jag-2 and Notch 1 and 4[29]. Unlike other angiogenic growth factors which are secreted, both the Notch ligand and its receptor are bound to the cell membrane. This restricts the effects of Notch

signalling to cells immediately adjacent to each other. In response to endothelial cell stimulation with VEGF, DLL-4, expressed on the surface of the leading tip endothelial cell, binds to the Notch receptor in neighbouring stalk endothelial cells. This releases the Notch intracellular domain (NICD), which translocates to the cell nucleus to stimulate transcription of Notch target genes such as Hey and Hes[29]. Notch stimulation decreases stalk endothelial cell expression of VEGFR2, 3 and NRP1, and increases their expression of VEGFR1. Different receptor expression results in different functional responses to VEGF stimulation, with endothelial tip cells guiding angiogenic sprout formation and stalk endothelial cells proliferating behind[30].

Notch signalling is important in the development of the vasculature including tumour angiogenesis, but is also considered to play an important role in cancer by maintaining cancer stem cells. Together with Wnt and Heghehog, Notch signalling pathways form an inter-linked signalling network which controls stem cell differentiation and is dysregulated in a wide range of cancers[31]. Therapeutic agents to target Notch are currently in development, particularly inhibitors of γ-secretase which cleaves the Notch receptor to release the NCID[32].

1.1.6 VEGF targeted therapy

The importance of VEGF in tumour angiogenesis has led to a focus on the development of drugs that target VEGF. Key therapeutic agents include the humanised monoclonal antibody to VEGF bevacizumab (Avastin), and TKIs such as sunitinib (Sutent) and axitinib (Inlyta).

1.1.6.1 Bevacizumab

The feasibility of VEGF targeted therapy was confirmed in studies using the anti-VEGF antibody A4.6.1 (a bevacizumab prototype), which demonstrated no direct effect on tumour growth *in vitro*, but reduced tumour micro-vessel density (MVD) and tumour growth *in vivo*[33]. The precise mechanism through which bevacizumab exerts its anti-angiogenic effects has yet to be fully elucidated. Suggested mechanisms include

inhibition of new blood vessel formation, pruning of existing immature tumour vessels, and functional normalisation of the tumour vasculature[34, 35].' An imaging study of tumour xenografts, using *ex vivo* micro-computed tomography and *in vivo* dynamic contrast-enhanced (DCE) ultrasound, showed anti-VEGF antibody reduced tumour perfusion and tumour blood volume within 24 and 48 hours of administration respectively[36]. In patients with colorectal liver metastasis, DCE magnetic resonance imaging (MRI) showed a similarly rapid reduction in tumour blood volume within just 4 hours of bevacizumab infusion. In phase III clinical trials, in combination with standard chemotherapy, bevacizumab improved progression free survival in metastatic breast cancer and improved overall survival in metastatic colorectal cancer, advanced non small cell lung cancer, and advanced ovarian cancer (table 1.1).

1.1.6.2 Tyrosine kinase inhibitors

Protein kinases are enzymes that transfer a phosphate group from adenosine tri-phosphate (ATP) on to tyrosine, serine or threonine residues of substrate molecules, which are themselves often other protein kinases[37]. Tyrosine kinases are essential for translating extracellular signals into an intracellular response including signals that promote angiogenesis. Ligand binding to the extracellular domain of tyrosine kinase receptors causes receptor dimerisation and phosphorylation of tyrosine residues on the intracellular domain. This leads to the sequential recruitment and activation of a cascade of intracellular signalling proteins, finishing with an end biological effect. For example, VEGF binding to VEGFR2 triggers receptor dimerisation and subsequent auto-phosphorylation of tyrosine residues including tyrosine^{1175}. Phosphorylated tyrosine^{1175} activates phospholipase-Cγ (PLCγ) and, through protein kinase C (PKC), stimulates the mitogen-activated protein kinase (MAPK) pathway, Raf-MEK-ERK, inducing endothelial cell proliferation[38].

TKIs are small molecules that readily diffuse through the cell surface membrane to inhibit protein kinase activity and thus inhibit signal transduction. Most TKIs are competitive inhibitors of ATP binding. There are a number of different TKIs in clinical

development, each with a different profile of kinases they inhibit[39]. Sunitinib is a broad spectrum TKI, inhibiting VEGFR1-3, PDGFRs, KIT, FLT3, CSF-1R and RET[40]. Sunitinib extends overall survival in patients with renal cell carcinoma and GISTs (table 1.2). Axitinib is more selective and principally inhibits VEGFR1-3, PDGFRs and KIT[41]. Axitinib has shown benefit in renal cell carcinoma, and is currently under study in a national phase II clinical trial for advanced soft tissue sarcoma.

TKIs have a potential therapeutic advantage over bevacizumab, as their broad spectrum of activity inhibits angiogenic pathways beyond VEGF which are implicated in anti-angiogenic drug resistance mechanisms. Furthermore TKIs that inhibit angiogenesis may also inhibit tumour progression by directly targeting aberrant signalling pathways within the tumour cell. A broad spectrum of activity however also increases the potential for side effects.

There is debate about how anti-angiogenic therapy should be integrated with standard treatment regimens. Vessel normalisation as a consequence of anti-angiogenic therapy may improve tumour oxygenation and reduce interstitial pressure, improving the delivery and efficacy of combined cytotoxic therapy[42]. In addition, radiation or chemotherapy-induced tumour cell death releases pro-survival signals, including pro-angiogenic cytokines, which would be inhibited by concurrent anti-angiogenic therapy. It has also been hypothesised however that anti-angiogenic therapy could reduce the efficacy of concurrent cytotoxic therapy as vasoconstriction and destruction of the tumour vasculature, as a consequence of anti-angiogenic therapy, would decrease tumour perfusion with cytotoxic chemotherapy, and increase tumour hypoxia inducing radiation resistance[42].

Reference	Trial	Trial Design	Comparison	Patient Numbers	Median PFS, Bz vs Control	*p*	Median OS, Bz vs Control	*p*
Metastatic Colorectal Cancer								
[43]	Study 2107	Randomised placebo-controlled phase III	IFL +/- Bz	813	10.6 vs 6.2 mths`	<0.001	20.3 vs 15.6 mths	<0.001
[44]	NO16966	Randomised placebo-controlled phase III	XELOX or FOLFOX +/-Bz	1401	9.4 vs 8.0 mths	0.002	21.3 vs 19.9 mths	0.077
Advanced Non Small Cell Lung Cancer								
[45]	E4599	Randomised open-label phase III	PC +/- Bz	878	6.2 vs 4.5 mths	<0.001	12.3 vs 10.3 mths	0.003
[46, 47]	AVAiL	Randomised placebo-controlled phase III	CG +/- Bz (15 or 7.5mg/kg)	1043	6.5 or 6.7 vs 6.1 mths	0.03 or 0.003	13.4 or 13.6 vs 13.1 mths	0.761 or 0.420
Ovarian Cancer								
[48]	ICON7	Randomised open-label phase III	Carbotaxol +/- Bz	1528	19.0 vs 17.3 mths	0.004	NA	NA
		High risk (FIGO III/IV) cohort		465	16.0 vs 10.5	0.002	36.6 vs 28.8 mths	0.002
Metastatic Breast Cancer								
[49]	E2100	Randomised open-label phase III	P +/- Bz	722	11.8 vs 5.9 mths	<0.001	26.7 vs 25.2 mths	0.16
[50]	AVADO	Randomised placebo-controlled phase III	D +/- Bz (15 or 7.5mg/kg)	736	10.1 or 9.0 vs 8.2 mths	0.006 or 0.12	NA	NA
[51]	RIBBON-1	Randomised placebo-controlled phase III	Cape +/- Bz or	1237	8.6 vs 5.7 mths	<0.001	1 yr OS: 81% vs 74%	0.27
			Tax/Anthra +/- Bz		9.2 vs 8.0 mths	<0.001	81% vs 83%	0.83
Metastatic Renal Cancer								
[52, 53]	CALGB 90206	Randomised open-label phase III	IFNα +/- Bz	732	8.5 vs 5.2 mths	<0.001	18.3 vs 17.4 mths	0.097
[54]	AVOREN	Randomised placebo-controlled phase III	IFNα +/- Bz	649	5.4 vs 10.2 mths	<0.001	23.3 vs 21.3 mths	0.336
Recurrent Glioblastoma Multiforme								
[55]		Open-label phase II	Bz	85	NA	NA	9.3 mths	NA
Advanced Pancreatic Cancer								
[56]	CALGB 80303	Randomised placebo-Controlled phase III	Gem +/- Bz	602	3.8 vs 2.9 mths	0.07	5.8 vs 5.9 mths	0.95

Table 1.1: Clinical trials of bevacizumab

PFS – progression free survival; OS – overall survival; Bz – Bevacizumab; p – p value presented from hazard ratio analysis; IFL – irinotecan + fluorouracil + leucovorin; XELOX – oxaliplatin + capecitabine; FOLFOX – oxaliplatin + fluorouracil/folinic acid; PC – paclitaxel + carboplatin; P – paclitaxel; D – docetaxol; Cape – Capecitabine; Tax/Anthra – Taxane/Anthracycline; IFNα – interferon alpha; Gem – Gemcitabine; NA – not available.

Tumour	Trial Design	Comparison	Patient Numbers	Median PFS, Drug vs Control	*p*	Median OS, Drug vs Control	*p*
Sunitinib							
Metastatic Renal Cancer[57, 58]	Randomised open-label phase III	Sunitinib vs IFNα	750	11 vs 5 mths	<0.001	26.4 vs 21.8 mths	0.051
GIST[59]	Randomised placebo-controlled phase III	Second-line Sunitinib vs Placebo	312	24.1 vs 6.0 weeks	<0.0001	NA	0.007
Metastatic Breast Cancer[60]	Randomised open-label phase III	P + Sunitinib vs P + Bz	485	7.4 vs 9.2 mths	0.999	NA	NA
Sorafenib							
Metastatic Renal Cancer[61]	Randomised placebo-controlled phase III	Second-line Sorafenib vs Placebo	903	5.5 vs 2.8 mths	<0.001	NA vs 14.7 mths	0.02
Hepatocellular Cancer[62]	Randomised placebo-controlled phase III	Sorafneib vs placebo	602	5.5 vs 2.8 mths	<0.001	10.7 vs 7.9 mths	<0.001
Advanced NSCLC[63]	Randomised placebo-controlled phase III	PC +/- Sorafenib	926	4.6 vs 5.4 mths	0.433	10.7 vs 10.6 mths	0.915
Axitinib							
Advanced Pancreatic Cancer[64]	Randomised placebo-controlled phase III	Gem +/- Axitinib	632	4.4 vs 4.4 mths	0.520	8.5 vs 8.3 mths	0.544
Pazopanib							
Metastatic Renal Cancer[65]	Randomised placebo-controlled phase III	Pazopanib vs Placebo	435	9.2 vs 4.2 mths	<0.0001	NA	NA
Soft Tissue Sarcoma[66]	Randomised placebo-controlled phase III	Pazopanib vs Placebo	369	4.6 vs 1.6 mths	<0.0001	12.5 vs 10.7 mths	0.25
Vandetanib							
Advanced NSCLC[67]	Randomised placebo-controlled phase III	Second-line D +/- Vandetanib	1391	4 vs 3.2 mths	<0.0001	10.3 vs 9.9 mths	0.371

Table 1.2: Clinical trials of tyrosine kinase inhibitors

PFS – progression free survival; OS – overall survival; p – p value presented from hazard ratio analysis; GIST – gastro-intestinal stromal tumour; NSCLC – non small cell lung cancer; IFNα – interferon alpha; P – paclitaxel; Bz – Bevacizumab; PC – paclitaxel + carboplatin; Gem – Gemcitabine; D – docetaxol

1.2 Angiosarcoma

Angiosarcomas are a subtype of soft tissue sarcoma, which are rare aggressive tumours derived from malignant endothelial cells of vascular or lymphatic origin[68]. Angiosarcomas are included within the spectrum of vascular tumours which ranges from benign capillary haemangioma and pyogenic granuloma, through intermediate grade haemangioendotheliomas, to the malignant Kaposi's sarcoma and angiosarcoma[69].

1.2.1 Epidemiology

Angiosarcomas represent 2% of all soft tissue sarcomas[70] and 5.4% of cutaneous soft tissue sarcomas[71]. They can arise in any soft tissue structure or viscera but cutaneous disease predominates (table 1.3). Clinically, angiosarcomas can be sub-divided into primary cutaneous, breast or soft tissue disease, and secondary lymphoedema-associated or radiation-induced tumours[69]. Genetic analysis has shown that primary and secondary angiosarcoma have distinct molecular profiles[72], and there is clinical evidence to suggest behaviour may differ dependent on site of origin[73, 74]. Typically however study numbers are too small to allow extensive subgroup analysis, and it is not clear to what extent differences between angiosarcoma subgroups are due to primary biological differences, or to differences in their clinical presentation and subsequent treatment.

Angiosarcomas can develop in any age group, but are more frequent in older patients. Classically, angiosarcomas present as cutaneous disease of the head and neck in white elderly men. Breast angiosarcomas however are the second most common tumour group, and therefore overall the distribution of disease is similar between sexes.

Site	Number	Percentage
Head and neck	144	27.0
Breast	105	19.7
Extremities	82	15.3
Trunk	51	9.5
Liver	32	6.0
Heart	25	4.7
Bone	19	3.6
Spleen	14	2.6
Other or unknown	62	11.6
Total	**534**	**100**

Table 1.3: Distribution of angiosarcoma; pooled data from 534 cases was used to compile this table (Fury *et al*[73], Mark *et al*[75], Abraham *et al*[76], Naka *et al*[77] and Fayette *et al*[78]).

1.2.2 Aetiology

Most angiosarcomas arise *de novo,* though there are a few reports of malignant transformation within a pre-existing benign vascular lesion[79]. Chronic lymphoedema of any origin is associated with the development of angiosarcoma, a phenomenon known as Stewart-Treves Syndrome[80]. Lymphoedema after treatment for breast cancer is one aetiological factor in the development of breast angiosarcoma. Radiotherapy is an independent aetiological factor with a peak incidence 10 years after treatment[81]. There are also case reports suggesting mutations in the DNA repair proteins, BRCA 1 and BRCA 2, predispose to the development of angiosarcoma following breast cancer therapy[82].

Hepatic angiosarcomas are associated with occupational exposure to vinyl chloride[83] and thorium dioxide (Thorotrast), used in the 1930-40's as a radiology contrast medium[84]. Other chemical carcinogens include arsenic, radium and anabolic steroids[85].

There are reports of angiosarcoma in association with foreign bodies, including accidentally retained surgical gauzes[86, 87], vascular[88, 89], and orthopaedic prostheses[90, 91] and even in association with a gouty tophus[92].

1.2.3 Clinical presentation

Cutaneous angiosarcoma may initially resemble a bruise, or a purplish-red raised papule (figure 1.2). With increasing size these lesions are associated with marked tissue infiltration, surrounding oedema, tumour fungation and areas of ulceration and haemorrhage [69]. Deeper soft tissue lesions present as an expanding mass associated with pain or discomfort (figure 1.3). Tissue infiltration and multi-focal disease are particular features, and positive microscopic margins despite radical surgery are common[76, 78, 93, 94].

Angiosarcomas principally disseminate haematogenously and in keeping with this the lung is the most common site for metastases to develop. This may manifest as pleural disease, haemorrhagic pleural effusion or pneumothorax. Other common metastatic sites include liver, bone, soft tissue structures and lymph nodes[73, 75-77, 93, 95, 96].

Figure 1.2: Cutaneous angiosarcoma arising in a mastectomy scar 5 years after surgery and radiotherapy for a primary breast cancer.

Figure 1.3: Hepatic angiosarcoma. CT scan showing multifocal tumour in the right lobe of liver (arrowed).

1.2.4 Pathology

Abnormal pleomorphic malignant endothelial cells are the hallmark of angiosarcoma (figure 1.4). They are infiltrative tumours and do not have a capsule or clear demarcating border separating them from normal tissue. In well differentiated areas the abnormal endothelial cells form functioning vascular channels, but in poorly differentiated areas they form continuous sheets with areas of haemorrhage and necrosis, and may be difficult to differentiate from anaplastic carcinoma or melanoma[69, 97, 98].

Angiosarcomas typically express endothelial markers including von Willebrand factor (vWF), cluster of differentiation 31 (CD31), CD34, ulex europaeus agglutinin-1 (UEA-1) and VEGF. vWF, UEA-1 and CD31 are most useful in poorly differentiated cases, although progressive tumour de-differentiation can lead to loss of these markers[99].

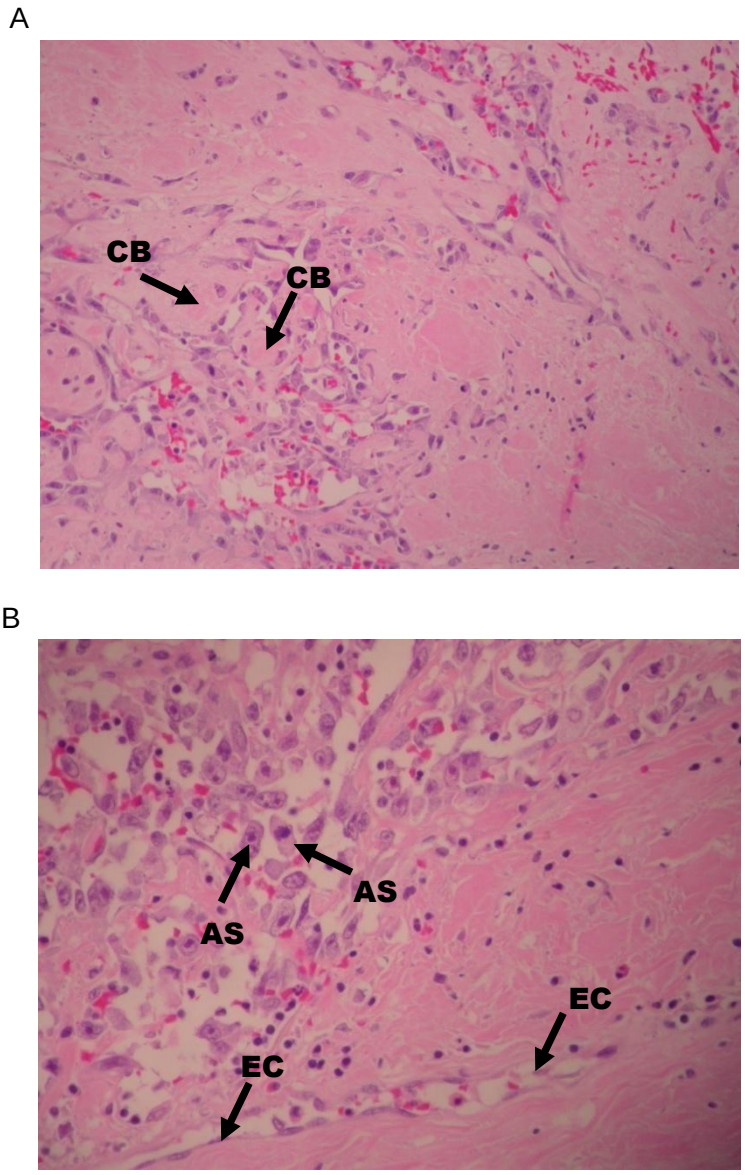

Figure 1.4: Haematoxylin and eosin stained sections of angiosarcoma. (A) shows the neoplastic vascular structures dissected by collagen bundles (CB) (magnification x20); (B) contrasts the varied shapes of the large malignant endothelial cells (AS) with the endothelial cells a normal capillary vessel below (EC) (magnification x40).

1.2.5 Treatment

Most of the published reports of angiosarcoma treatment describe retrospective case series. There are no randomised trials, and few prospective studies. To date, their treatment has been encompassed by management guidelines for other soft tissue sarcomas such as those published by ESMO[100] and NCCN[101].

As rare tumours angiosarcomas present specific challanges to their study. Currently there are no established *in vitro* or *in vivo* models of angiosarcoma, and archived tumour material for molecular analysis is limited. Typically two or three patients per year present to the Sheffield Sarcoma Network with angiosarcoma and their rarity limits the feasibility of performing adequately powered randomised clinical trials. National and international collaborations are therefore necessary to progress clinical studies of angiosarcoma. Angiosarcomas have been included in larger studies of soft tissue sarcomas, such as the PALETTE study (Pazopanib for metastatic soft tissue sarcoma)[66], however patient numbers restrict sub-group analysis of trial results by histology. Furthermore, tumour response to therapeutic agents is usually assessed using Response Evaluation Criteria in Solid Tumours (RECIST)[102]. RECIST employs radiological measurements (CT or MRI) to assess disease response. Angiosarcomas however often present as superficial, cutaneous lesions and radiological assessment may not be helpful to assess disease. Criteria other than RECIST may be more appropriate including use of clinical photographs.

1.2.5.1 Local disease

Radical surgery with complete (R0) resection is the primary treatment of choice. Involved margins (R1 or R2 resection) are common due to the invasive and often multi-focal nature of angiosarcomas[73, 76, 78, 93]. Because of the high risk of local recurrence, adjuvant radiotherapy is recommended using large doses (>50Gy) and wide treatment fields[75, 93].

1.2.5.2 Advanced disease

Cytotoxic chemotherapy using anthracyclines or taxanes is the primary treatment option for metastatic disease, although supporting evidence is limited (table 1.4). Taxanes have anti-angiogenic activity and have been of particular interest in the management of angiosarcoma. A retrospective study of 32 patients with angiosarcoma reported an overall response rate of 20/32 (63%), with progression free survival of 7.6 months[74]. The only prospective phase II study of taxane for advanced disease

demonstrated responses in 5/30 (17%), though two were deemed a pathological complete response[103]. A retrospective analysis comparing the response of metastatic angiosarcoma to doxorubicin with the response to weekly paclitaxel suggested similar efficacy[104].

1.2.5.3 Biological agents

Vascular-targeted biological therapies have led to a renewed interest in angiosarcomas. The results from phase II clinical trials are summarised in table 1.5.

Preliminary results from a phase II study of single agent bevacizumab in 29 patients with angiosarcoma showed 3 partial responses and 13 with stable disease[105].

Tyrosine kinase inhibitors for the treatment of soft tissue sarcomas have been assessed in several phase II studies. The largest study, using sorafenib, included a cohort of 37 angiosarcomas within a larger study of 122 advanced soft tissue sarcomas[106]. 4 partial responses and 1 complete response were seen within the angiosarcoma group, giving an overall response rate of 14%. In contrast, only one partial response was seen in the other sarcoma patients. Another phase II study of sorafenib in 41 patients with angiosarcoma reported responses in 4 (10%)[107]. Final results from a phase II study of sunitinib in 48 patients with metastatic soft tissue sarcomas included 2 patients with angiosarcoma; one partial response and 10 stable disease were reported, but none in angiosarcoma[108].

There are also scattered case reports of angiosarcoma responses to thalidomide, which has documented anti-angiogenic properties[109].

Reference	Study design	Patient Numbers	Chemotherapy	ORR	Median PFS	Median OS	Comments
[110]	Review of RCTs	33	Doxorubicin regimens	33%	NR	NR	Pooled data from AS patients in four prospective RCTs in advanced STS
[104]	Case series	117	Doxorubicin vs Weekly paclitaxel	29% vs 53%	3.0 vs 5.8 mths (p>0.05)	5.5 vs 10.3 mths (p=0.002)	On multivariate analysis performance status was the only factor associated with survival
[73]	Case series	71	Doxorubicin regimens vs Paclitaxel	NR	3.7-5.4 mths 4.0 months	NR	Taxane response for disease above and below the neck (6.8 vs 2.8 mths)
[111]	Case series	9	Paclitaxel	89%	5 mths	NR	
[112]	Case series	9	Docetaxel	67%	9.5 mths	NR	
[74]	Case series	32	Paclitaxel	63%	7.6 mths	NR	ORR 75% (PFS 9.5 mths) for face & scalp, ORR 58% (PFS 7 mths) for other sites
[103]	Single arm phase II	30	Weekly Paclitaxel	17%	4 mths	7.6 mths	

Table 1.4: Studies of palliative chemotherapy for locally advanced or metastatic angiosarcoma

ORR - overall response rate; PFS - progression free survival; OS - overall survival; AS - angiosarcoma; NR - not reported; RCT - randomised controlled trial; STS - soft tissue sarcoma

Author	Evaluable Patient Numbers	Treatment	ORR	Median PFS	Median OS
Ryan CW *et al*. [113]	38 STS	Sorafenib	2 PR/ 14 SD (ORR 5%) overall	3 months overall	13 months overall
	Including 9 AS		1 PR/ 6 SD (ORR 11%) in AS	4.7 months in AS	13.5 months in AS
Maki RG *et al*.[106]	122 STS	Sorafenib	1 CR/ 5 PR/ 62 SD (ORR 5%) overall	3.2 months overall	14.9 months overall
	Including 37 AS		1 CR/ 4 PR/ 21 SD (ORR 14%) in AS	3.8 months in AS	14.2 months in AS
Ray-Coquard *et al*.[107]	26 cutaneous AS	Sorafenib	1 CR/ 1 PR/ 4 SD (ORR 8%)	1.8 months	12.0 months
	15 visceral AS		0 CR/ 2 PR/ 4 SD (ORR 13%)	3.8 months	9.0 months
George *et al*. 2009.[108]	48 STS	Sunitinib	1 PR/ 10 SD (ORR 2%) overall	NR	NR
	Including 2 AS		No responses in AS		
Agulnik *et al*. 2009.[105]	26 AS	Bevacizumab	3 PR/ 13 SD	NR	NR
			(ORR 12%)		

Table 1.5: Phase II trials of biological therapies in soft tissue sarcoma, including angiosarcoma

ORR - overall response rate; PFS - progression free survival; OS - overall survival; STS - soft tissue sarcoma; AS - angiosarcoma; CR - complete response; PR - partial response; SD - stable disease; NR - not reported

1.3 The Molecular Pathology of Angiosarcoma

Published reports of the molecular changes in angiosarcoma typically explore the expression of one or two markers in a small series of tumours, with limited correlation to clinical or pathological features, and are usually insufficient to compare subgroups such as cutaneous, visceral or radiation-induced disease. Recently however, several studies have highlighted differences between angiosarcoma subgroups. An RNA array analysis of 22 angiosarcomas demonstrated, in keeping with their endothelial nature, up-regulated genes for VEGFR1, VEGFR2, TIE-1, and TIE-2, as well as other endothelial markers such as CD31 and vWF[72]. Cluster analysis suggested two groups of angiosarcoma – primary disease with over expression of VEGFR1 and the protein kinase AKT3, and radiation-induced or lymphoedema-associated secondary disease with increased expression of the protein kinases LYN and PKCθ. Other studies have confirmed differences between the genetic abnormalities of primary and secondary angiosarcoma, with amplifications of MYC in secondary but not primary disease[114].

Cancer cells are characterised by a set of molecular abnormalities, the “Hallmarks of Cancer”[2]. These abnormalities include insensitivity to programmed cell death (apoptosis), aberrant growth, a propensity towards invasion and metastasis, and the stimulation of angiogenesis. Angiosarcomas demonstrate a variety of molecular abnormalities in keeping with their malignant phenotype. None of these abnormalities however are unique to angiosarcoma, and they have also been described in other cancers, including other soft tissue sarcomas[115].

1.3.1 Chromosomal abnormalities

Cytogenetic analysis of angiosarcomas has been published for nine cases[116]. Most of these samples were derived from metastases, poorly differentiated angiosarcomas or radiation induced tumours. In keeping with this, a wide range of disparate

chromosomal abnormalities have been identified, none of which are specific to angiosarcoma. Common themes include trisomy 5, deletions on the short arm of chromosome 7, varied abnormalities on chromosomes 8, 20 and 22, and loss of chromosome Y.

1.3.2 Immortality

p53 has a central role in controlling cell growth and programmed cell death. Abnormalities in p53 are frequently described in tumours, including angiosarcomas. Naka *et al* showed half of human angiosarcomas (17/33) had at least one mutation involving the p53 gene[117]. An immunohistochemistry study by Zietz *et al* demonstrated high levels of sequestered defective p53 tetramers in 10/19 (53%) of angiosarcomas, and p53 inactivation by increased levels of MDM2 in 13/19 (68%)[118]. In this study p53 and MDM2 expression did not correlate with tumour site or grade, although benign vascular controls demonstrated lower levels of p53 accumulation. In contrast, a recent study by Italiano *et al* found p53 mutations in only 2/52 (4%) of angiosarcomas. Despite this, p53 accumulation was observed in 23/46 (50%) of tumours, and was associated with a significantly worse prognosis[119].

In a genetic study of vascular abnormalities, 5/6 head and neck angiosarcomas demonstrated loss of heterozygosity at p53 (17p13), 4/6 at the RB allele (13q14) and 3/5 at WT-1 (11p13)[120]. Similar abnormalities, although less frequent, were also identified in benign hemangiomas (3/5, 3/5, 1/5 respectively).

1.3.3 Abnormal growth signals

Myc is a key transcription factor, stimulating cell growth and proliferation, and is important in tumourigenesis. MYC amplifications have been reported in secondary but not primary angiosarcomas. Combined results from four studies using fluorescence *in situ* hybridisation (FISH) have shown MYC amplification in 0/54 primary angiosarcomas and 74/90 (82%) secondary angiosarcomas (range 55 – 100%)[114, 121-123]. Secondary angiosarcomas with MYC amplification were not histologically

distinguishable from other tumours, but were associated with co-amplification of VEGFR3 in 8/55 (15%)[114, 121].

Abnormalities in Ras, an intracellular growth signal, have been found in many different cancers. K-ras-2 mutations have been found in 5/19 (26%) sporadic and 2/5 (40%) Thorotrast induced liver angiosarcomas[124]. Liver angiosarcomas induced by vinyl chloride have shown similar K-ras-2 mutations (8/15)[125]. A small study of primary cardiac angiosarcomas demonstrated K-ras mutations in 3/5 (60%)[126].

In vitro human umbilical vein endothelial cells (HUVECs) with inducible H-RAS demonstrated up-regulation of ERK and Akt signalling pathways. Functionally this was associated with increased HUVEC cell survival, proliferation and reduced tube formation in co-culture assays with fibroblasts. Up-regulated ERK controlled increased proliferation whilst Akt controlled vascular morphogenesis. Both ERK and Akt contributed to increased endothelial cell survival[127].

SVR cells, an immortalised murine endothelial cell line over expressing H-ras, form angiosarcoma tumours *in vivo*[128]. *In vitro* studies with SVR cells showed that down-regulation of MEK (MAPKK), by using clones with dominant negative MEK or by inhibition of MEK with the drug PD98059, resulted in a significant reduction in colony formation[129]. Despite this, inhibition of MEK had no effect on *in vivo* tumour development. Wortmannin inhibition of the phosphatidylinositol-3-kinase (PI-3-kinase) pathway in SVR cells did result in significantly smaller angiosarcoma tumours *in vivo*[128], although independent over expression of Akt1 in murine endothelial cells resulted in benign vascular malformations distinct from angiosarcomas[130]. The viral oncogene v-p3k, of the avian sarcoma virus ASV16, codes for a gene homologous to the catalytic subunit of PI-3-kinase. This oncogene is implicated in the pathogenesis of haemangiosarcomas in chickens[131]. However, whilst mutations in the PI-3-KCA gene have been described in 13/33 (39%) human angiosarcomas, the PI-3KCA mutations

identified were not manifest in the transcriptome, and thus were unlikely to be biologically relevant[119].

Activating transcription factor 2 (ATF2) and signal transducer and activator of transduction 3 (STAT3) are important downstream transcription factors involved in cell growth and proliferation. A study by Chen *et al* demonstrated over expression of phosphorylated ATF2 and STAT3 in cutaneous angiosarcoma (13/14 and 14/14 respectively) compared to normal blood vessels[132]. However this study also demonstrated over expression in benign vascular proliferations, suggesting these factors were simply a measure of increased cellular proliferation rather than of malignancy.

Yamamoto *et al* showed an increased number of mast cells in cutaneous angiosarcoma lesions[133]. Angiosarcoma tumour cells were shown to express stem cell factor and thus to recruit mast cells. Mast cells produce various cytokines including VEGF and FGF-2 which may in turn stimulate endothelial cells. Because of the success of KIT inhibitors in treating other sarcomas, particularly GISTs, investigators have studied KIT expression in angiosarcoma. Results pooled from three separate series showed KIT positivity in 38/76 (50%), with diffuse KIT expression in 18/38 (47%)[134-136]. KIT mutation analysis has been performed for a handful of angiosarcomas, none of which identified activating mutations in the key juxtamembrane and tyrosine kinase domains, exon 11 and 17 respectively[134].

Finally a study of epidermal growth factor receptor (EGFR) expression in soft tissue sarcomas included a small subset of angiosarcomas, with 3/4 (75%) demonstrating increased EGFR expression[137].

1.3.4 Invasion and metastasis

Disruption of the extracellular matrix releases sequestered growth factors, promoting malignant growth and facilitating tumour invasion and migration. The matrix is digested by a variety of different proteases, including matrix metalloproteinases (MMPs), and the

urokinase plasminogen activator system (uPAS). A comparative immunohistochemistry study of different cutaneous vascular lesions by Thewes *et al*, showed no evidence of inhibitors or activators of uPAS in 15 normal skin controls. In contrast, activators of uPAS were found in both benign and malignant vascular lesions. 4/4 (100%) cutaneous angiosarcomas showed diffuse expression of uPA, and its corresponding receptor uPA-R. uPAS inhibitors (PAI-1 and PAI-2) however were found only in benign vascular proliferations[138].

Synthesis of the Ets-1 transcription factor is stimulated through VEGF and bFGF activation of ERK. Ets-1transcription factor promotes the expression of matrix metalloproteinases, including MMP1, MMP3, and uPA[139]. A study by Naito *et al* showed Ets-1 and MMP1 expression were increased in 7 cutaneous angiosarcomas, compared to hemangioma and pyogenic granuloma controls[140].

Decreased levels of the major basement membrane components (laminin, collagen type IV, fibronectin and heparin sulfate proteoglycan) were also shown in angiosarcomas compared to benign vascular proliferations such as capillary hemangioma[141].

Finally the actin bundling motility protein fascin was uniformly over expressed in a study of 20 angiosarcomas compared to a small control group of benign hemangiomas[142].

1.3.5 Angiogenesis

Immunohistochemistry studies have investigated the expression of VEGF and its receptors in angiosarcoma, but there is little data on the expression of other angiogenic cytokines such as angiopoietins.

Several studies have shown VEGFA is expressed at higher levels in angiosarcomas compared to benign vascular or normal tissue controls. A study by Tokuyama *et al* showed VEGFA was expressed in 13/17 (76%) cutaneous angiosarcomas compared to

2/34 (6%) of benign vascular tumours[143], and a study by Zietz *et al* showed expression in 18/19 (95%) of angiosarcomas compared to 1/10 (10%) of benign vascular lesions[144].

The study by Tokuyama *et al* also reported that tumour endothelial expression of VEGFR2 and R3 correlated significantly with Ki-67 expression, with VEGFR2 and R3 expression significantly increased in angiosarcomas compared to the benign vascular tumour controls[143]. A study of 34 cutaneous and soft tissue angiosarcomas by Itakura *et al* however demonstrated increased expression of VEGFR2 was associated with an improved survival, whilst VEGFR1 and R3 expression were not related to outcome[145]. A study by Yonemori *et al* in a separate panel of 34 angiosarcomas confirmed VEGFR2 expression correlated with survival, whilst PDGFRβ expression was inversely related to survival; VEGFR1, R2, R3, and PDGFRα and PDGFRβ expression were not associated with tumour site or size[146]. These studies suggest tumour cell expression of VEGFR2 in angiosarcoma is a marker of endothelial differentiation, rather than a pathogenic feature.

Murine endothelial cells (MS1) transfected with VEGF 121 over-expressed VEGFR1 and VEGFR2 in comparison to the parent cell line[147]. Inoculation of the MS1-VEGF cell line into nude mice produced slow growing well-differentiated angiosarcomas similar to, although less rapidly growing than those formed by the Ras modified MS1 (SVR) cell line.

No evidence of increased copy numbers of VEGFR2 were observed by FISH in 9 angiosarcoma patients studied by Antonescu *et al*[72]. Point mutations were identified in 4/39 (10%) angiosarcoma patients; 2 primary breast angiosarcoma had point mutations in the transmembrane domain of VEGFR2 (exon 16 T771R) and 2 radiation-induced breast angiosarcoma had mutations, one in the extracellular domain (exon 15 D717V) and one in the kinase domain (exon 24 A1065T). Transfection of COS-7 cells with D717V or A1065T mutated VEGFR2 demonstrated constitutive phosphorylation in

the absence of VEGF stimulation. VEGFR2 autophosphorylation was sensitive to tyrosine kinase inhibition with either sorafenib or sunitinib.

The expression of angiopoietins in angiosarcoma is less well studied. The Tie2 kinase inhibitor 4-(6-methoxy-2-naphthyl)-2-(4-methylsulfinylphenyl)-5-(4-pyridyl)-1 H-imidazole inhibited SVR and MS1-VEGF cell viability *in vitro*, and inhibited angiosarcoma tumour growth *in vivo*[148]. In this study, sunitinib also inhibited SVR and MS-1 tumour growth *in vivo*, and combination therapy with the Tie2 kinase inhibitor was more effective than either agent alone[148].

Wang *et al* investigated the effects of introducing a point mutation into the Tie2 kinase domain (a glycine to aspartic acid substitution at residue 833 found in 22% (8/37) of human intramuscular haemangiomas) of the murine endothelial cell line MSS31[149]. Compared to wild type MSS31, endothelial cells with the Tie2 mutation showed no significant difference in Tie2 protein expression, but demonstrated an increase in Tie2 phosphorylation and increase in VEGF expression. Interestingly, *in vivo* the Tie2 mutant cell line produced angiosarcomas rather than haemangiomas.

There is minimal evidence for the role of other pro-angiogenic factors in the development of angiosarcomas. An immunohistochemistry study of 7 cutaneous angiosarcomas by Yamamoto *et al* identified increased expression of FGF-2 and its receptor compared to normal skin controls, with serum FGF-2 also elevated in 4/7 (57%)[150]. DNA abnormalities in the Notch signalling pathway have been identified in a small series of angiosarcoma patients[151]. Interestingly, pan inhibition of Notch signalling resulted in liver sinusoidal endothelial cell proliferation, intussusceptive angiogenesis, and the formation of hepatic vascular abnormalities, including angiosarcomas, *in vivo*[152, 153].

In summary, angiosarcomas are rare aggressive tumours of endothelial cells. A variety of molecular abnormalities have been described, none of which are specific to angiosarcoma.

1.4 Hypothesis

It was hypothesised that angiogenic growth factors drive the biology of angiosarcomas, and represent targets for the treatment of angiosarcoma.

1.5 Aims

A series of laboratory studies were planned to investigate this hypothesis:

- To characterise established angiosarcoma cell lines, and tumour cell isolates derived from fresh angiosarcoma tumour samples, and to compare them with primary cell cultures of dermal microvascular endothelial cells.
- To profile endothelial cell expression of angiogenic cytokines, and to compare their behaviour in functional assays including cell differentiation and cell migration assays.
- To assess the *in vitro* response to vascular targeted therapies in functional assays including cell viability, cell differentiation and cell migration assays.
- To compare the expression of angiogenic growth factors and their receptors in a panel of angiosarcoma tumour samples using a series of benign vascular tumours as a control.

2 Methods

2.1 Cells

The online catalogues of the American Type Culture Collection (ATCC), the Health Science Research Resources Bank (Japanese Collection of Research Bioresources – JCRB) the German Collection of Microorganisms and Cell Cultures (Deutsche Sammlung von Mikroorganismen und Zellkulturen – DSMZ), and the published literature were searched to identify malignant endothelial cell lines as potential *in vitro* models of angiosarcoma.

The cell lines subsequently obtained were:

i) **ASM** – provided courtesy of Professor V Krump-Konvalinkova, Institute of Pathology, Johannes Gutenburg University Mainz, Germany. The cell line was developed from an 80 year old male with primary cutaneous angiosarcoma of the scalp[154]. ASM cells were cultured in Endothelial Cell Growth Media (ECGM; PromoCell) with ECGM Supplement Pack (PromoCell) plus 10% fetal calf serum (FCS; Gibco), 0.5% v/v penicillin, 0.5% v/v streptomycin and 0.5% v/v amphotericin.

ii) **ISOS-1** – provided courtesy of Professor M Masuzawa, Cell Resource Centre for the Biomedical Research Institute of Development, Aging and Cancer, Tohoku University, Japan. This cell line was developed from an 84 year old male with locally metastatic cutaneous angiosarcoma of the scalp by subcutaneous implantation of tumour fragments into severe combined immunodeficient (SCID) mice[155]. The cell line derived from the resultant growth, designated ISOS-1, expressed murine major histocompatibility complex (MHC) class I antigens and murine telocentric chromosomes. ISOS-1 cells were cultured in Dulbecco's modified Eagle's media (DMEM;

Lonza) plus 10% FCS, 0.5% v/v penicillin, 0.5% v/v streptomycin and 0.5% v/v amphotericin.

iii) **ISO-HAS** – provided courtesy of Professor M Masuzawa. The cell line was developed concurrently with ISOS-1 from the patient described above[156]. As per its developmental protocol ISO-HAS was initially grown in ISOS-1 conditioned media: ISOS-1 cells were grown to confluency in DMEM media, and this media was collected at 72 hours and passed through a 0.2μm filter. Complete ISO-HAS media consisted of 50% ISOS-1 conditioned media in combination with 50% fresh DMEM supplemented with 10% FCS, 0.5% penicillin, 0.5% streptomycin and 0.5% amphotericin to total volume. After initial passages, flasks of ISO-HAS cells were conditioned for four weeks in 100% DMEM with 10% FCS, 0.5% penicillin, 0.5% streptomycin and 0.5% amphotericin, or ECGM as described for ASM. ISO-HAS growth was poor in 100% DMEM, and cell morphology altered to a spindle shape. ISO-HAS grown in ECGM remained healthy with similar growth kinetics. Therefore, following initial studies, ISO-HAS was grown in ECGM media, supplemented as described for ASM. ISO-HAS cells were well-maintained under these conditions and this allowed for direct cell comparisons in subsequent studies.

iv) **SVR** – purchased from ATCC. The SVR cell line was developed from a primary murine endothelial cell line (MS-1) transfected with retrovirus encoding SV40 large T antigen and H-Ras[128]. *In vivo* SVR produces haemorrhagic tumours consistent with well differentiated angiosarcomas. SVR was grown in DMEM media supplemented with 10% FCS, 0.5% v/v penicillin, 0.5% v/v streptomycin and 0.5% v/v amphotericin.

v) **EAhy926** – provided courtesy of Dr Edgell, University of North Carolina, USA. EAhy926 was formed by fusion of the lung cancer cell line A549 with human umbilical vein endothelial cells (HUVECs)[157]. *In vitro* these transformed cells express vWF, CD31, VEGFR1, VEGFR2, and form cord-

like structures on the extracellular matrix Matrigel, consistent with an endothelial phenotype[158]. EAhy926 cells were cultured in DMEM media with 10% FCS, 0.5% v/v penicillin, 0.5% v/v streptomycin and 0.5% v/v amphotericin.

Adult human dermal micro-vascular endothelial cells (HuDMECs) were sourced as experimental controls. HuDMECs were purchased from Promocell and grown in ECGM media and ECGM Supplement Pack. Human dermal fibroblasts (HDFs) and human umbilical vein endothelial cells (HuVECs) were used in several studies. HDFs were kindly donated by Dr Canton, Kroto Research Institute, University of Sheffield, who purchased them from ATCC (PCS-201-010). HDFs were grown in DMEM media with 10% FCS, 0.5% v/v penicillin, 0.5% v/v streptomycin and 0.5% v/v amphotericin. HuVECs were kindly provided by Dr Holmes, Microcirculation Research Group, University of Sheffield who sourced them from Promega. HuVECs were grown in endothelial basal media (EBM-2; Lonza) with 10% FCS.

Unless otherwise stated, all cells were cultured in T75 flasks (Nunc) within a humidified incubator (SANYO), in 21% O_2, 5% CO_2, at 37^{o}C. Flasks were regularly monitored to assess cellular health. Media was changed every 2 or 3 days; the old media was discarded, cells washed with phosphate buffered saline (PBS; Lonza), and 10mls of fresh growth medium applied. Cells were passaged as they approached confluency. Old media was removed and the cells washed with PBS. 2mls of trypsin 0.05% (Lonza) were added and the flask returned to the incubator for 1 – 2 minutes. Flasks were viewed under a microscope and cell detachment assisted if necessary with a gentle tap. Trypsin was neutralised with an equal volume of growth media and the cells divided, typically 1:3, between new flasks with 10mls of fresh growth media added.

For primary endothelial cell cultures (HuDMECs and early cell passages from angiosarcoma tumour samples), cells were passaged using Promocell trypsin solution and trypsin neutralising solution. Cell suspensions were transferred to a 15ml tube and

centrifuged at 1000 x g for 3 minutes. The supernatant was tipped off, and cells re-suspended in fresh media, and split (1:3) into new flasks.

2.2 Characterisation Studies

2.2.1 Immunocytochemistry characterisation

Immunocytochemistry studies were performed to demonstrate the expression of endothelial cell markers including CD31, CD34 and vWF. CD31, also known as platelet endothelial cell adhesion molecule (PECAM-1), is a transmembrane glycoprotein cell adhesion molecule expressed by endothelial cells, platelets and inflammatory cells[159]. CD34 is a transmembrane glycoprotein and a haematopoietic stem cell and endothelial progenitor cell marker[159]. vWF is stored in Weibel-Palade bodies of endothelial cells and also expressed by platelets. It stabilises factor VIII and is important for thrombus formation[159].

2.2.1.1 Slides

Slides of each cell line were created for immunocytochemistry profiling. Semi-confluent flasks of cells were trypsinised, centrifuged and then re-suspended in 10mls of full media. Clean glass slides were placed in large petri dishes and 1ml of cell suspension pipetted on to each slide. Slides were incubated overnight, washed briefly in PBS and fixed in ice-cold methanol at –20^{o}C for 10 minutes. Slides were air dried and stored in cardboard racks covered in aluminium foil at –20^{o}C until used.

2.2.1.2 Immunocytochemistry protocol

Slides prepared as above were washed for 3 minutes in PBS. 10% blocking serum in PBS was applied to each slide and incubated at room temperature for 1 hour. Primary antibodies in 2% serum were applied and incubated at 4^{o}C overnight (Table 2.1). Following this, slides were washed twice for 5 minutes in PBS, 0.1% Tween (PBST). Secondary antibodies in 2% serum were applied and slides incubated at room temperature for 1 hour (Table 2.1). Slides were again washed twice for 5 minutes in PBST before ABC Elite solution (Vector Laboratories) was applied for 40 minutes.

Slides were washed twice for 5 minutes in PBST and then DAB solution (Vector Laboratories) was applied for 3 minutes. Slides were washed in tap water for 5 minutes, stained with Gills Haematoxylin for 1 minute, and then washed in running tap water for 3 minutes. Finally slides were dehydrated in successive ethanol baths using 70%, 90%, 95% and 100% ethanol, 2 minutes each, followed by a xylene bath for 5 minutes. Coverslips were affixed using DPX. Pilot studies were performed to optimise the procedure and determine the final antibody concentration for each antigen until a working protocol was finalised.

Slides of ASM and ISO-HAS cells were stained and scored for the expression of endothelial cell markers. Slides of HuDMEC cells were used as a positive control and slides of HDF cells as a comparison. Slides of HuDMEC cells incubated with PBS rather than the primary antibody were used as a negative control. Each slide was studied to calculate a staining score: a score for the proportion of stained cells (0 = <1%, 1 = 1-10%; 2 = 11-50%; 3 = >50%) was summed with a score for the staining intensity (1 = weak, 2 = moderate, 3 = strong) to provide a total score (range 0-6). Immunocytochemistry studies were performed three times using slides of cells from different passages, and a mean staining score for each marker was calculated.

Antibody	Primary	Secondary
CD31 (sc-0.N.100)	1:50	1:250
CD34 (sc-19587)	1:50	1:250
vWF (sc-53466)	1:50	1:250
αSMA (ab5694)	1:300	1:500
VEGF (sc-152)	1:100	1:200
VEGFR1 (ab2350)	1:50	1:200
VEGFR2 (ab39256)	1:100	1:200

Table 2.1: Concentration of antibodies used in immunocytochemistry characterisation studies

2.2.1.3 Permanox slides

ASM and ISO-HAS exhibited a mixed morphology in tissue culture, and immunocytochemistry studies suggested a mixed pattern of staining. Cell morphology however was not maintained on glass slides. In order to correlate cell morphology with immuno-staining, cells were grown on plastic 4-chambered Permanox slides (Lab-Tek). These slides permitted cells to be grown directly on the slides, and the four chamber system allowed concurrent staining with four different antibodies on one slide. 30,000 cells in 0.75mls full growth media were seeded into each chamber and incubated at 37^{o}C. Permanox slides of ASM, ISO-HAS, and HuDMECs were established. Growth was observed over several days and the media replenished at 48 hours. Cell growth was very slow however, and the majority of cells were non-adherent. Permanox slides were fixed in ice-cold methanol for 10 minutes after 72 hours. Fixed cells were stained for CD31, CD34, vWF and αSMA as per the protocol in 2.2.1.2. Staining quality was also poor and this methodology was not pursued further.

2.2.2 Flow cytometry

Flow cytometry studies were performed to investigate the expression of CD31, VEGF, VEGFR1 and VEGFR2 in ASM and ISO-HAS in order to demonstrate the presence of cell sub-populations indicated in the immunocytochemistry studies.

Flow cytometry measures the scatter of light directed through a stream of cells to quantify their attributes. Light detectors collect data on forward scatter (FSC), a measure of cell size, and side scatter (SSC), a measure of cell granularity. Flurochromes excited by light present distinct emission spectra, and so antibodies labelled with different fluorochromes are used to simultaneously assess the expression of different cellular antigens[160]. Data collected can be presented as a dot plot (also known as a cytogram) (Figure 2.1), or as a histogram (Figure 2.2).

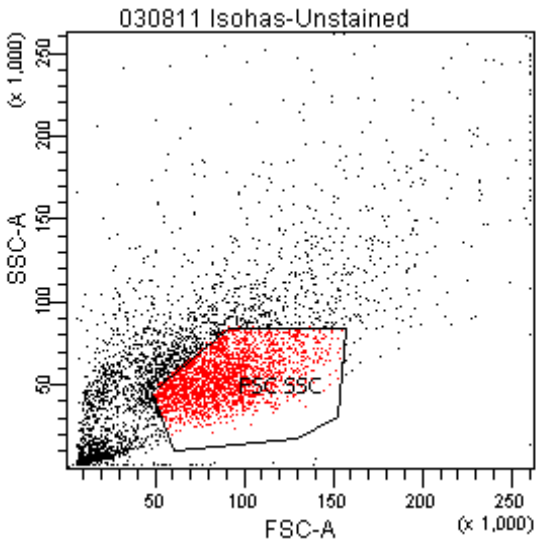

Figure 2.1: Cytogram of unstained ISO-HAS cells plotting forward scatter (FSC) against side scatter (SSC). Subsequent results were gated to a main study population (shown in red) to reduce signal noise, particularly from non-viable cells.

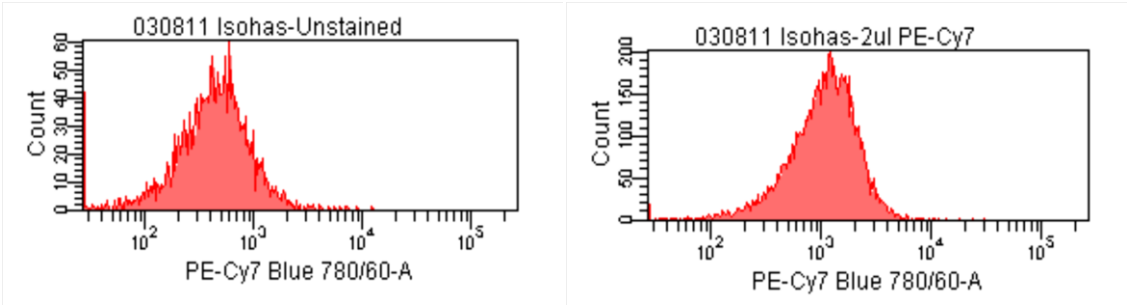

Figure 2.2: Histogram showing a population shift in fluorescence intensity from a median of 432 to 1,104 demonstrating the presence of bound PE-Cy7 labelled antibody (in this case CD31).

Prior to their use in flow analysis, primary antibodies were prepared by conjugating them to a fluorochrome (table 2.2) using the Lightning Link Conjugation Kit (Innova Biosciences). As per manufacturer instructions, 1µl of Lightning Link Modifier reagent was added per 10µl of antibody and mixed gently. 10µgs of Lightning Link Mix were added to the antibody and incubated for 3 hours in the dark at room temperature. 1µl of Lightning Link Quencher was added per 10µl of antibody and the vials of conjugated antibodies were wrapped in aluminium foil and stored at 4^{o}C until used.

Semi-confluent T175 flasks of cells were washed in PBS twice, trypsinised, centrifuged, and re-suspended in flow cytometry buffer solution (PBS with 1% FCS). 500,000 viable cells were aliquoted into tubes, centrifuged and re-suspended in 200µls of buffer solution. Separate tubes were established to analyse cells without the addition of antibody, with each individual antibody, and with a combination of the four conjugated primary antibodies (table 2.2). Tubes were incubated on ice for 30 minutes following the addition of antibody. Then, cells were washed twice, re-suspended in 300µls of buffer solution, and transferred to flow cytometry tubes for analysis. Flow cytometry was performed using a BD LSR II analyser and BD FACS Diva Software (version 6.0). Preliminary studies were performed using a series of increasing antibody concentrations to optimise the protocol, including antibody concentrations beyond that which induced a maximum cell population shift, indicating antigen-antibody specific binding.

Antibody	Fluorochrome	Emission Spectra	Volume of antibody per 500,000 cells (µl)
CD31 (sc-0.N.100)	PE-Cy7	Blue 780/60-A	2.5
VEGF (sc-152)	PerCP-Cy5.5	Blue 695/40-A	2.5
VEGFR1 (ab2350)	RPE (R-Phycoerythrin)	Blue 575/26-A	5
VEGFR2 (ab2349)	APC (Allophycocyanin)	Red 660/20-A	5

Table 2.2: Fluorochromes and volume of antibody used.

2.2.3 Dil-Ac-LDL

Dil-Ac-LDL is an acetylated-low density lipoprotein labelled with the fluorescence 1,1'-dioctadecyl-3,3,3',3'-tetramethyl-indocarbocyanine perchlorate, and is selectively taken up by macrophages and endothelial cells via the receptor-mediated scavenger cell pathway. Dil-Ac-LDL is metabolised in lysosomes, and the fluorescent probe accumulates in the lysosome intracellular membrane[161]. ASM and ISO-HAS uptake of Dil-Ac-LDL was compared with HuDMEC and HDF cells to confirm their endothelial nature.

Semi-confluent flasks of cells were washed in PBS twice. 2mls of growth media with Dil-Ac-LDL (Biomedical Technologies Inc) 10µg/ml were added and cells were incubated at 37^{o}C for 4 hours. The Dil-Ac-LDL media was removed and flasks were washed twice in PBS. 2mls of normal growth media (Dil-Ac-LDL free) were added and fluorescent cells were observed through a Leica DM IL microscope.

2.3 Functional Assays

In vitro studies were performed to compare ASM and ISO-HAS cells with HuDMECs in functional assays:

2.3.1 Growth kinetics

Preliminary studies were performed with HuDMECs, ASM, and ISO-HAS to compare their growth curves: 30,000 viable cells in 1ml were seeded in 12-well plates in full growth media. Viable cell counts were calculated at 24, 48, 72 and 96 hours. Supernatant from the wells were collected in individual 15ml tubes. Wells were washed with PBS, trypsin applied, and the wells monitored until the cells had detached. Cells were collected, the wells rinsed twice and these washes collected. The tubes were centrifuged at 1000 x g for 3 minutes, the media was tipped off and the cells re-suspended in 1ml of fresh media. Cells were counted using the Beckman Coulter Vi-CELL, and the %viability, viable and total cell count recorded. 3 wells were assessed at each time point and a mean cell count calculated. At 48 hours uncounted wells were washed and replenished with equal volumes of fresh media.

2.3.2 Differentiation

Endothelial differentiation assays were used to model the angiogenic process *in vitro*, including endothelial cell attachment, migration, alignment and tubule formation[162]. For these studies, semi-confluent T75 flasks of cells were starved overnight in EBM-2 media with 1% FCS. Meanwhile, a 96-well plate and cassette of 200µl pipette tips were chilled at -20^{o}C, and aliquots of growth factor reduced basement membrane matrix (Matrigel; BD Biosciences) defrosted overnight on ice at 4^{o}C. Then, 40µls of matrigel

were added to wells of the 96-well plate and incubated at 37^{o}C for half an hour. 10,000 viable cells in 100µls media +/- 50ng/ml carrier free recombinant $VEGFA_{165}$ (R&D Systems) were added to wells, a minimum of 3 wells per condition. Tubule formation was assessed at 6 hours. The well centres were imaged, and the number of tubules formed and the tubule length counted manually.

Pilot studies were performed to establish the optimum conditions for endothelial tubule formation. Studies were performed with cells in full growth media using cell seeding densities of 15,000, 20,000 and 25,000 cells per well with serial images taken at 4, 6, 8, 12 and 24 hours. These preliminary studies showed analysis of HuDMEC differentiation at seeding densities greater than 15,000 cells per well was limited by large islands of proliferating cells. In contrast, optimum ASM and ISO-HAS tubule formation in these preliminary studies required 25,000 cells per well. The number of tubules formed peaked after 6 – 8 hours, and rapidly regressed thereafter (figure 2.3).

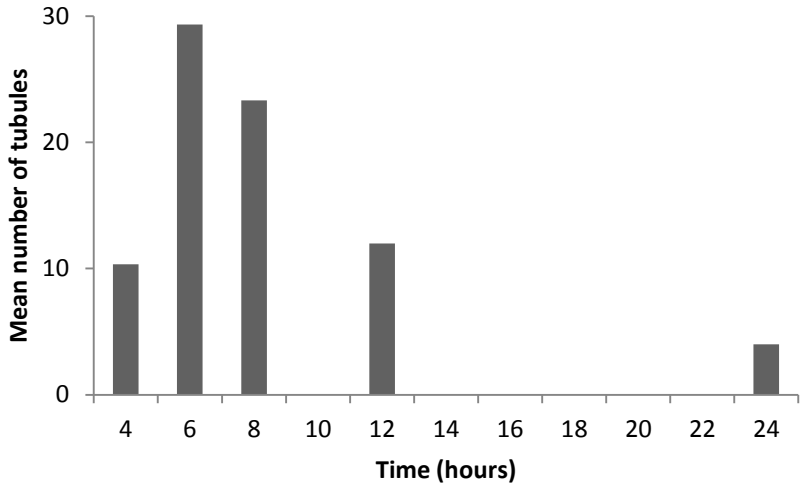

Figure 2.3: Number of tubules formed in the differentiation assay using ASM cells at 25,000 cells per well in full media. Data shown represents mean of 3 wells (n=1).

Preliminary studies to compare tubule formation between cell lines and investigate response to the TKI axitinib were performed using 15,000 HuDMECs per well and 25,000 cells per well of ASM and ISO-HAS, +/- 20ng/ml VEGF, with cell differentiation assessed at 8 hours. These preliminary studies showed no evidence of increased

tubule formation in response to VEGF stimulation and no significant effects of axitinib 50ng/ml (figure 2.4). Repeat assays were performed to validate these findings, and to extend the doses of axitinib up to 250ng/ml with VEGF increased to 50ng/ml. These studies were performed using ASM and ISO-HAS cells recovered from a different vial of cryo-preserved cells frozen down at an earlier passage. These, and subsequent cells, formed extensive islands of proliferating cells at 25,000 cells per well, and the protocol was modified to 10,000 cells per well of HuDMECs, ASM and ISO-HAS, with tubule formation assessed at 6 hours and these conditions were maintained in all subsequent differentiation assays.

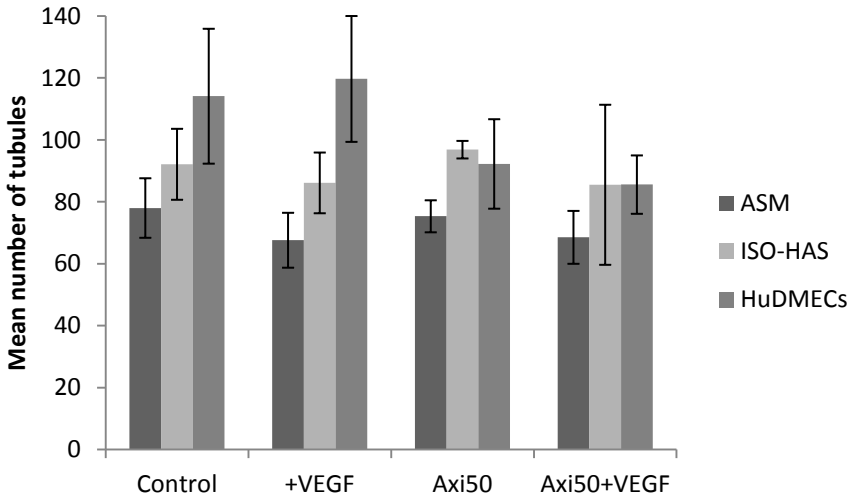

Figure 2.4: Number of tubules formed in preliminary endothelial differentiation studies with HuDMECs 15,000 cells/well, ASM and ISO-HAS 25,000 cells/well, axitinib 50ng/ml and VEGF 20ng/ml. Data shown represents mean +/- SEM; n=3.

2.3.3 Migration

Cell migration may be assessed *in vitro* by several different methods[163]. The scratch assay requires a monolayer of cells to which a 'wound' (scratch) is applied. Serial images to measure gap closure are used to assess migration. Addition of an anti-proliferative drug such as Mitomycin-C is used to exclude gap closure due to cell proliferation. Problems with this assay include difficulties in consistently producing a uniform scratch, the absence of a chemokine gradient, and toxicity from adding the

anti-proliferative agent. Alternatively, both cell migration and cell invasion (which also requires digestion of an extracellular matrix) can be assessed using a chamber system such as the Boyden chamber. This assay measures the movement of cells from an upper to a lower chamber, across a matrix coated porous membrane. Chemoattractants may be added to the lower chamber to mimic migration *in vivo* along a chemokine gradient. The assay is fiddly to set up however, and laborious to quantify.

The Boyden chamber was used in these studies: Cells were starved overnight in EBM-2, 1% FCS. The Boyden chamber was washed, thoroughly dried and placed in an incubator at 37^{o}C. Polycarbonate porous membranes (25 x 80mm, 8µm pores; NeuroProbe) had the bottom right hand corner clipped for orientation. 20µls of 1mg/ml collagen IV (Sigma Aldrich) were mixed in 2mls PBS. The membrane was immersed in this collagen IV solution for 10 minutes each side and allowed to air dry. The membrane was then immersed in EBM-2, 1% FCS media, for 10 minutes each side, and again allowed to dry. Meanwhile, cells were trypsinised and re-suspended to form a suspension of 300,000 viable cells/ml in EBM-2, 1% FCS media. 30µls of EBM-2, 1% FCS media +/- 20ng/ml recombinant VEGF were then added to lower wells. The dry porous membrane was carefully placed across the lower wells, and the top plate secured in place. 50µls (15,000 cells) of cell suspension were added to the upper wells with a minimum of 6 wells established for each condition. The chamber was incubated for 4 hours, then the Boyden chamber plates were separated and the membrane carefully removed. The upper surface of the membrane was scraped and washed in PBS to remove adherent cells that had not migrated through. The membrane was fixed in methanol for 5 minutes, stained with Gills Haematoxylin for 5 minutes and washed in PBS for a further 5 minutes. The membrane was placed on glass slides and a coverslip affixed using DPX. Once dry, migration was assessed. The lower surface of the membrane was viewed at x4 magnification to locate the well centres and then imaged at x20 magnification. Cells were counted manually. Those with a complete nucleus

visible at the photograph margins were included in the count. An average migration count from 3 wells was calculated for each condition.

Initial assays were performed with 10,000, 15,000, 20,000 and 25,000 ASM and ISO-HAS cells/well to optimise the assay conditions.

2.3.4 *In vivo* tumour formation

Preliminary studies were performed to assess ASM and ISO-HAS tumour formation *in vivo*. These studies were performed by Sapna Lunj under the Home Office Project Licence PPL40/3531. Female CD1 nude mice were purchased from Charles River Laboratories. 5 x 10^6 viable ASM or ISO-HAS cells in 0.5mls PBS, were injected subcutaneously into the mammary fat pads of the nude mice, six animals for each cell line. The animals were then followed over 8 weeks. Their general health and weight were monitored, and the inoculation sites checked for cutaneous tumour formation. Macroscopic tumours did not develop, and the animals remained healthy and active throughout. They were culled after 8 weeks with no evidence of gross pathology.

2.4 Protein Expression Profiling

2.4.1 Protein arrays

R&D Systems protein arrays (ARY 001, 003, 007) were used to investigate the expression of 55 angiogenesis related proteins, 42 phosphorylated receptor tyrosine kinases (pRTK) and 46 phosphorylated tyrosine/serine/threonine kinases (pTK) in cell lysates. The expression of angiogenic proteins was also investigated in cell supernatants. The arrays were similar in principle to the sandwich enzyme-linked immunosorbent assay (ELISA). Briefly, they consisted of nitrocellulose membranes with duplicate spots of antibody for each individual protein. Study samples were added, followed by a second antibody with a horseradish peroxidise (HRP) tail. Chemiluminescence was applied and the membranes then imaged. Spot densities subsequently developed in proportion to the quantity of bound protein.

These studies were performed according to supplied manufacturer instructions; the method for the angiogenesis array is described below, but pTK and pRTK array methods were similar. First, the membranes were washed in array buffer (supplied) for 1 hour at room temperature during which time equivalent quantities of study sample proteins were incubated at room temperature with array buffer and biotinylated detection antibody mix (supplied). The membranes were then incubated overnight at $4^{o}C$ with the study sample/antibodies, and subsequently washed for 10 minutes three times in wash buffer (supplied). Streptavidin-HRP (supplied) was diluted in array buffer and added to the membrane and then incubated for 30 minutes at room temperature. The membranes were again washed in wash buffer for 10 minutes three times, and then incubated with Immobilon Western Chemiluminescent HRP substrate (Millipore) for 3 minutes in a dark room. The arrays were arranged in a Hypercassette and exposed to Amersham Hyperfilm ECL (GE Healthcare) for up to 10 minutes and the film developed. The film was scanned and peak density measured for each antibody spot on the protein array using a GS-710 Callibrated Imaging Densitometer (Bio-Rad) and Quality One (version 4.6.8) 1-D image analysis software. An average peak density for each protein was calculated from the paired duplicate spots, a background reading was subtracted, and the density then presented as a ratio of the averaged peak densities from the positive control spots. An example image of a protein array study is shown in figure 2.5.

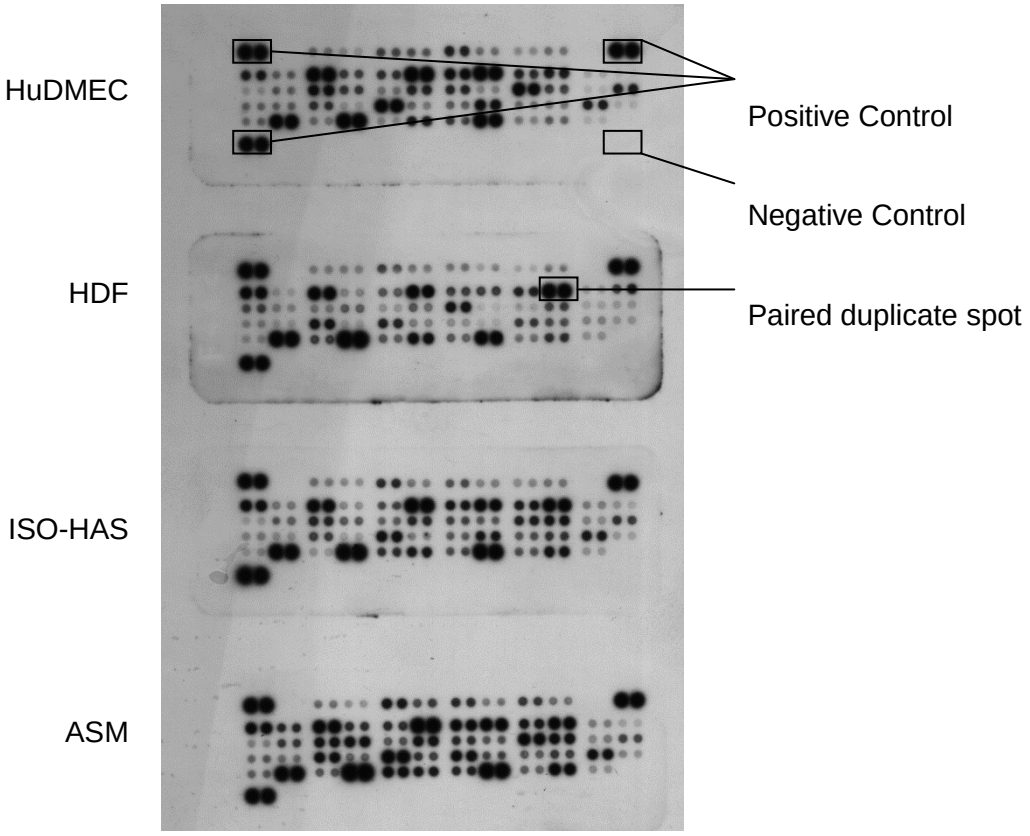

Figure 2.5: Example image of an array to assess the expression of angiogenesis related proteins in HuDMEC, HDF, ISO-HAS and ASM cell lysates.

To generate the cell lysate samples for analysis, T75 flasks of semi-confluent cells were starved overnight in EBM-2 media with 1% FCS. Lysis buffer was created according to 1% NP-40, 20mM Tris-HCL (pH 8.0), 137 mM NaCl, 10% glycerol, 2mM EDTA, Complete Mini EDTA-free protease inhibitor cocktail tablets (Roche) +/- PhosSTOP phosphatase inhibitor cocktail tablets (Roche) for the pRTK arrays. The lysis buffer was mixed, aliquoted and stored at -20^{o}C until use. Lysis buffer supplied with ARY 003 was used for the pTK array.

Flasks were washed in PBS, 500µls of lysis buffer were added, and the flasks gently rocked on ice for 20 minutes. Flasks were scraped and the lysate collected and transferred to 1.5ml eppendorf tubes. The lysate was agitated through a 22 gauge needle and then centrifuged at 4^{o}C for 5 minutes at 14,000 rpm. Lysates were stored at

-80^{o}C until use. Prior to use, quantification of protein content in the cell lysates was performed using protein standards of 0.0, 0.05, 0.25, 0.5, 0.75 and 1.0mg/ml from Bovine Serum Albumin (BSA) 2mg/ml (Sigma-Aldrich) diluted with lysis buffer. 20µl's of standard or sample were aliquoted in triplicate in a 96 well plate and absorbance measured at 570nm using a FLUOstar Galaxy plate reader after 30 minutes incubation at 37^{o}C following the addition of 200µl of bicinchoninic acid and copper II sulphate solution (8mls BCA to 200µl $CuSO_4$; Sigma-Aldrich). Absorbance readings from the BSA standards were used to plot a standard absorbance curve from which the protein concentration in the study samples was calculated.

The expression of angiogenic proteins in hypoxic conditions was also investigated in cells starved overnight in EBM-2, 1% FCS in a hypoxic chamber (1% O_2). Cell lysates were generated as described above. For investigating angiogenic protein expression in cell supernatant, T175 flasks of semi-confluent cells were washed in PBS and incubated overnight at 37^{0}C following the addition of 20mls of EBM-2 with 1% FCS. The supernatant was removed, filtered using a 0.2µm filter (Sarstedt), and concentrated [x20] using Amicon Ultra-15 10K Centrifugal Filter Units (Millipore) centrifuged at 4^{o}C for 20 minutes at 4000 x g.

2.4.2 VEGF ELISA

T75 flasks of semi-confluent cells were washed in PBS and starved overnight in 10mls EBM-2 media with 1% FCS. The cell supernatant was collected, filtered (0.2µm) and stored at -80^{o}C until use. Cell lysates were prepared on ice following the addition of triple lysis buffer (section 2.4.3) and protein quantification performed as previously described. Samples were also prepared from flasks of cells starved overnight in 1% FCS EBM-2 media in a hypoxic chamber (1% O_2). VEGF ELISA (R&D Systems) was performed according to manufacturer instructions. VEGF protein standards were re-constituted in calibrator diluent (supplied) and serially diluted. 50µls of assay diluent were added to each well of a 96-well plate pre-coated with a monoclonal antibody specific for all VEGF isoforms, followed by 200µls of sample. Duplicate wells were used

for the measurement of VEGF in cell supernatant. The plate was covered and incubated at room temperature for 2 hours. The wells were then washed three times with wash buffer (supplied) using a squirter bottle. 200µls of VEGF conjugate (supplied) were added, the plate covered, and again incubated at room temperature for a further 2 hours. The plate was washed three times with wash buffer and then 200µls of substrate solution added (supplied). The plate was covered with aluminium foil and incubated for 20 minutes before 50µls of stop solution were added (supplied). Colour developed relative to the proportion of bound VEGF. Colour intensity was measured using a FLUOstar Galaxy plate reader at 450nm and corrected using absorbance readings at 520nm. A standard curve was calculated from the VEGF protein standards and used to estimate VEGF concentrations in the study samples. VEGF secretion in to the cell supernatant was expressed relative to the total protein concentration in cell lysates.

2.4.3 Western blot

Protein expression of VEGF, VEGFR1, VEGFR2, phosphorylated VEGFR2 (pVEGFR2) and phosphorylated extracellular signal-regulated kinase (pERK) was investigated by western blot.

To investigate VEGF expression, semi-confluent T175 flasks of cells were starved overnight in 10mls of EBM-2, 1% FCS. The supernatant was collected, filtered (0.2µm) and concentrated [x10] (Centrifugal Filter Units, Millipore). Cell lysate samples were derived concurrently. To create these lysates, 500µl of triple lysis buffer per T75 flask was added on ice. This lysis buffer comprised of 50mM Tris-HCl (pH 8.0), 150mM NaCl, 0.02% sodium azide, 0.1% SDS, 1% NP-40, 0.5% sodium deoxycholate and Complete Mini EDTA-free protease inhibitor cocktail tablets +/- PhosSTOP phosphatase inhibitor cocktail tablets. The lysis buffer was mixed, aliquoted and stored at -20^{o}C until use. Following addition of the lysis buffer, flasks were gently agitated for 10 minutes and scraped. The lysate was transferred to an eppendorf and aspirated through a 22 gauge needle ten times. The lysate was incubated on ice for 20 minutes and then centrifuged for 10 minutes at 15,000rpm at 4^{o}C.The lysate was transferred to

a fresh eppendorf, leaving behind any residual cell debris that had settled during centrifugation, and stored at -80^{o}C until use. Prior to use protein quantification was performed as previously described.

To investigate baseline expression of VEGFR1, VEGFR2, pVEGFR2 and to quantify the effects of axitinib (0ng/ml, 50ng/ml and 250ng/ml) and bevacizumab (0mg/ml, 0.25mg/ml) on pVEGFR2, semi-confluent T75 flasks of cells were starved overnight in EBM-2, 1% FCS. Flasks were washed in PBS and then incubated for 1 hour at 37^{o}C with 2mls of EBM-2 media plus VEGF targeted agent, with DMSO or bevacizumab control vehicle (see section 2.5) added as necessary to ensure equal quantities throughout. 50ng/ml recombinant VEGF was added and flasks were incubated for a further 3 minutes at 37^{o}C before cells were lysed. pVEGFR2 expression was also investigated in hypoxia following incubation of semi-confluent T75 flasks of cells overnight in EBM-2, 1% FCS in a hypoxic chamber (37^{o}C, 1% O_2). Lysates were generated as described above.

The effect of axitinib (0ng/ml, 50ng/ml and 250ng/ml) and bevacizumab (0mg/ml, 0.25mg/ml) on pERK expression was investigated. Semi-confluent T75 flasks of cells were starved overnight in EBM-2, 1% FCS. Flasks were washed in PBS and then incubated for 1 hour at 37^{o}C with 2mls of media and VEGF targeted agent, with DMSO/control vehicle quantities added as necessary. 50ng/ml recombinant VEGF was added and separate flasks of cells lysed at 0, 5, 10 and 20 minutes. Lysates were generated as described above.

For the western blot procedure, the gel apparatus was constructed using a 1.5mm plate. Separating gels were prepared for each plate according to the quantities shown in table 2.3. 12% gels were used for the VEGF studies, the 10% gels for VEGF and pERK studies and 7.5% gels for the VEGFR studies. Butanol was layered on top of the separating gel and then washed off once this had set (40 minutes). Stacking gel was prepared from 6.1ml distilled water, 2.5ml 0.5M Tris-HCl (Geneflow), 100µl 10%

sodium dodecyl sulphate (SDS; Geneflow), 1.3ml 30% Acrylamide (Geneflow), 100µl 10% ammonium persulphate (APS; Sigma-Aldrich) and 10µl Tetramethylethylenediamine (TEMED; Sigma-Aldrich), added and a 9 well comb inserted.

% Acrylamide	12%	10%	7.5%
Distilled Water	3.35ml	2.5ml	2.5ml
1.5M Tris-HCl	2.5ml	2.5ml	2.5ml
10% SDS	100µl	100µl	100µl
30% Acrylamide	4ml	3.3ml	2.5ml
10% APS	50µl	50µl	50µl
TEMED	5µl	5µl	5µl

Table 2:3: Separating gel preparation.

Whilst the stacking gel was setting (20 minutes) the samples for running were prepared from 4µl NuPAGE sample reducing buffer [10x] (Invitrogen), 10µl NuPAGE sample buffer [4x] (Invitrogen), sample and distilled water 26µl; sample volumes were varied to ensure equivalent protein loads were used. Samples were heated at 70^{o}C for 10 minutes using a Techne DRI-Block DB-2A. The gel cassette was placed in the running apparatus and the tank filled with running buffer (100ml UltraPure [10x] Tris/Glycine/SDS (Geneflow), 900ml distilled water). The combs were removed and each well flushed with running buffer using a 25 gauge needle. 10µl of Precision Plus Protein Standards Kaleidoscope (Bio-Rad) molecular weight marker was loaded into the first well and subsequent wells loaded with sample. The gel was then run at 100V using a Bio-Rad PowerPac Basic. Once the samples had passed through the stacking gel the voltage was increased to 150V. Running time was approximately 2 hours. Once the samples had run off the gel, the apparatus was disassembled, the plates prised open and the bottom right hand corner of the gel sliced off for orientation. The gel was then washed in transfer buffer (100ml UltraPure [10x] Tris/Glycine, 200ml methanol, 700ml distilled water) on a shaking platform (Luckham Shaker R100) for 10 minutes twice. Polyvinylidene fluoride (PVDF) membrane was cut to size and activated in

methanol for 5 minutes before being washed in transfer buffer during which time Bio-Rad Extra Thick filter paper was soaked in transfer paper. The transfer plates (Trans-Blot SD Semi-Dry Tansfer Cell, Bio-Rad) were cleaned with methylated spirit and the blotter stacked with filter paper, membrane, gel, filter paper. Air bubbles were rolled out following the addition of each layer to ensure an even transfer of proteins. The BioRad PowerPac HD was set at 15V and the Transfer Cell run for 20 minutes for 1 gel, 33 minutes for 2 gels. After transfer the bottom right hand corner of the membrane was cut for orientation and placed in blocking solution.

The protocol describing blocking conditions, washes and concentration of antibodies were adjusted independently for each antibody to optimise the blots produced. The final protocols are described here.

For VEGF, VEGFR1, VEGFR2 and pERK studies, membranes were blocked in PBS, 0.1% Tween (PBST) with 5% powdered milk (Marvel) for 1 hour at room temperature and then overnight at 4^{o}C with the primary antibody in blocking solution (table 2.4). Membranes were then washed for 10 minutes, 3 times with PBST and the secondary antibody applied (ECL anti-mouse/anti-rabbit IgG horseradish peroxidise linked whole antibody; GE Healthcare) also in blocking solution, for 1 hour at room temperature. The membrane was again washed in PBST for 10 minutes, 3 times and then covered with 1ml of Immobilon Western Chemiluminescent HRP substrate (Millipore) for 3 minutes in a dark room. The membranes were arranged in a Hypercassette and exposed to Amersham Hyperfilm ECL (GE Healthcare) for up to 10 minutes and the film developed.

For pVEGFR2 studies, membranes were blocked in TBST (TBS [x10] – TrisHCl 24.23g, 80.06g NaCl, 800ml distilled water, pH to 7.6 with HCl and top with distilled water to 1L. For [1x] – 100ml TBS[x10], 900ml distilled water, 0.1% Tween), 5% bovine serum albumin (Sigma-Aldrich) overnight at 4^{o}C. Primary antibody was applied in blocking solution for 2 hours at room temperature and the membranes then washed in

TBST for 15 minutes, 4 times and secondary antibody then applied for 1 hour at room temperature. Membranes were again washed in TBST for 15 minutes, 4 times and then covered with 1ml of Pierce ECL Western Blotting Substrate (Thermo Scientific) for 3 minutes. The membranes were arranged in a Hypercassette and exposed to Amersham Hyperfilm ECL (GE Healthcare) for up to 20 minutes and the film developed.

	Primary Antibody	Secondary Antibody
VEGF (sc-152)	1:500	1:1000
VEGFR1 (Cell Signalling #2893)	1:500	1:1000
VEGFR2 (Cell Signalling #2479S)	1:1000	1:2000
pVEGFR2 (Cell Signalling #2478)	1:1000	1:2000
pERK (Sigma M8159)	1:10,000	1:15,000
β-actin (Sigma A5441)	1:10,000	1:15,000

Table 2.4: Antibody concentrations used in western blotting

To demonstrate equivalent protein loading of wells membranes for pVEGFR2 probing were run concurrently with VEGFR2 studies. Following probing for VEGF and pERK, membrane was immersed in Restore Western Blot Stripping Buffer (Thermo Scientific) for 20 minutes at room temperature and washed for 10 minutes, 3 times in PBST. Primary antibody to β–actin was added and incubated for 20 minutes, the membranes were washed again 3 times in PBST for 10 minutes, secondary antibody was applied for 30 minutes, washed again for 10 minutes, 3 times in PBST. Finally the membranes were covered with 1ml of Immobilon Western Chemiluminescent HRP substrate (Millipore) for 3 minutes in a dark room. The membranes were arranged in a Hypercassette and exposed to Amersham Hyperfilm ECL (GE Healthcare) for up to 5 minutes and the film developed.

2.5 Drug Studies

A series of studies were performed to investigate the effects of vascular targeted agents on ASM and ISO-HAS, with HuDMECs as a comparison.

Doxorubicin (D1515, Sigma Aldrich) and paclitaxel (T7402, Sigma Aldrich) were purchased. Axitinib (AG-13736) and sunitinib (SU-11248) were provided by Pfizer. Akt inhibitor (MK2206, Selleck), Chk2 inhibitor (C3742, Sigma Aldrich) and mTOR inhibitor everolimus (RAD001, Selleck) were purchased. 1mg of each drug was dissolved in 1ml DMSO prior to use and stored in 10µl aliquots at -20^{o}C. Prior to use, a fresh aliquot was re-constituted in 10mls of media to provide a working solution of 1µg of drug/ml of media. 10µls of DMSO were dissolved in another 10mls of media to provide a control solution. Quantities of each were used to provide different drug concentrations with equal quantities of DMSO as illustrated in table 2.5.

The MEK inhibitor selumetinib (S1008, Selleck) was purchased, 1mg of drug was dissolved in 50µls of DMSO, and 10µl aliquots stored at -20^{o}C. DMXAA (ASA404) was initially provided by Novartis with additional supplies purchased from Santa Cruz (sc-207592). 25mgs DMXAA were dissolved in 1.25mls DMSO and stored at 4^{o}C until use. DMSO was added as required in studies of selumetinib and DMXAA to control for DMSO concentration.

Bevacizumab (Roche, Avastin) was purchased and supplied in a control vehicle at 25mg/ml. Additional control vehicle was prepared according to 51 mM sodium phosphate and 60 mg/ml trehalose dihydrate (pH 6.2) and 0.04% Tween[164], and added as necessary to ensure equal volumes throughout. Both bevacizumab and control vehicle were stored at 4^{o}C until use.

2.5.1 Chemosensitivity assays

A series of studies were performed to investigate the effects of vascular targeted agents on endothelial cell proliferation and cell viability. The principal assays available to measure this were[165]:

Clonogenic assay – these assays are considered the gold standard approach for determining chemosensitivity. Cells are first exposed to the drug of interest, plated, and then colonies that subsequently develop are counted. This assay measures cell proliferation and can be used to distinguish cytostatic from cytotoxic drug effects. Colonies must grow sufficiently large to be visualised for counting, and thus this assay may overestimate drug response. These assays are also tedious, labour intensive and are impractical for screening a large number of samples.

DNA synthesis – these assays measure the uptake of a DNA precursor (e.g. ^{3}H-thymidine) to assess cell proliferation. These assays do not distinguish between viable, non-replicating cells and cells that have died, and do not distinguish DNA replication from repair.

Cell membrane integrity assays – or dye exclusion assays, use the differential uptake of a dye to distinguish viable from dead cells. Trypan blue is excluded by viable cells but not by those that have died. This is used to estimate a viable cell count. Trypan blue may underestimate drug toxicity as dying cells may still exclude the dye, and fully lysed cells will not appear. A Beckman Coulter Vi-CELL haemocytometer was available within the laboratory and provided consistent, reproducible results. The Vi-CELL uses trypan blue staining, a microscope and image analysis to calculate % viability, viable and total cell count.

Metabolic assays – including the MTS assay, measures the mitochondrial reduction by metabolically active cells of the yellow tetrazolium salt (3-(4,5-dimethylthiazol-2-yl)-5-(3-carboxymethoxyphenyl)-2-(4-sulfophenyl)-2H-tetrazolium), in the presence of phenazine ethosulphate (PES), to a formazan compound. Plate reader measurement of colour change (absorbance) is used as a surrogate measure for the number of viable cells. Comparing absorbance measurements from plates analysed at different time points (e.g. 24 and 48 hrs) provides an estimate of drug effects on cell proliferation, assuming mitochondrial activity (and MTS metabolism) remains constant over time.

The MTS assay is easy to replicate but only measures viable cells, and the results may be affected by chemical composition of the media including its pH.

Studies of drug effects on ASM and ISO-HAS were performed with a cell membrane integrity assay, using the Vi-CELL to produce semi-automated cell counts. It was not practical to perform these assays using HuDMECs, as the assay demanded a large number of cells and HuDMECs required stringent conditions to maintain growth. The MTS assay was therefore used to assess drug effects on HuDMEC viability and cell proliferation. Supplementary MTS studies were performed with ASM and ISO-HAS to ensure comparisons of drug effects were fair.

Initial drug viability studies were performed with ASM cells. 100,000 viable cells in 1 ml of full growth media were seeded in 12-well plates and incubated at 37^{o}C. After 60 hours for cultures to establish, wells were washed in PBS and chemotherapy drugs added in fresh growth media. A different drug concentration was used for each 12-well plate. Viable cell counts were performed using the Beckman Coulter Vi-CELL 0, 48, 72 and 96 hours after drug addition. 3 wells were assessed at each time point and results averaged. The protocol described in 2.5.1.1 was subsequently used to assess drug effects on cell viability.

2.5.1.1 Cell membrane integrity assay

100,000 viable cells in 1ml were seeded in 12-well plates in full growth media. At 48 hours the wells were washed with PBS and any residual PBS aspirated. Solutions of drug and fresh growth media were added to each well, 3 wells for each condition (tables 2.5). Following a further 120 hours, cells were counted as previously described.

Drug Concentration (ng/ml)	Drug (µls) (@1µl(1µg)/ml media)	DMSO (µls) (@1µl/ml media)	Growth Media (µls)
0	0	250	750
25	25	225	750
50	50	200	750
100	100	150	750
150	150	100	750
200	200	50	750
250	250	0	750

Table 2.5: Example doses used in vascular targeted drug studies.

2.5.1.2 MTS assay

Semi-confluent flasks of cells were starved for 4 hours in EBM-2 with 1% FCS. Cells were trypsinised, centrifuged, and re-suspended in EBM-2 with 1% FCS, and a viable cell count calculated using the Vi-Cell. Tubes of different drug concentrations were established containing 50,000 viable cells/ml in EBM-2, 1% FCS. 100µls (5,000 cells) were pipetted into wells of a 96-well plate, 6 wells per condition. 6 wells held media only (no cells) to provide a background reading. 3 hours prior to the assessment of cell viability, 20µls of MTS (Promega) were added per well. The plate was then covered in aluminium foil and incubated at 37^{o}C. Colour intensity developed proportional to mitochondrial activity (a surrogate marker for cell viability), and absorbance measured using a FLUOstar Galaxy plate reader at 420nm. A background reading from the blank wells was subtracted from the absorbance measurements, and an average reading calculated for each condition. A preliminary study with serial plates read at 24, 48 and 72 hours showed minimal change in absorbance measurements between 48 and 72 hours, and thus the subsequent studies assessed proliferation at 24 and 48 hours only.

A study of drug concentrations in the absence of cells was performed to control for any direct chemical effects of the study drugs on the tetrazolium salt. Figure 2.6 shows the drugs did not have a direct chemical effect.

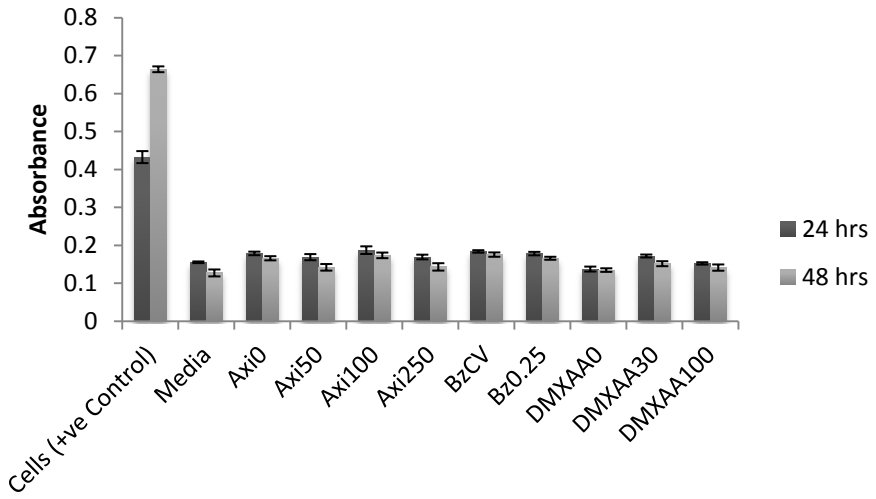

Figure 2.6: Absorbance measurements from an MTS study performed in the absence of cells. Axi - axitinib (0-250ng/ml), BzCV - bevacizumab control vehicle, Bz - bevacizumab (0.25mg/ml), DMXAA (0-100µg/ml). Data is represented as mean of 5 wells ±SEM; n=1.

2.5.2 Functional studies

Studies were performed to investigate the effects of vascular targeted agents on endothelial cell function in differentiation, migration and invasions assays.

2.5.2.1 Differentiation

The effects of axitinib, bevacizumab, selumetinib and DMXAA on endothelial cell tubule formation were studied. The differentiation assay protocol described in 2.3.2 was followed. After plating the Matrigel, tubes of 100,000 viable cells per ml were prepared, in different drug concentrations, +/- 50ng/ml recombinant VEGF. Volumes of DMSO or bevacizumab control vehicle were added to ensure equal quantities were used throughout.

2.5.2.2 Migration

The effects of axitinib and bevacizumab on endothelial cell migration were studied. The Boyden chamber assay protocol described in 2.3.3 was followed. Tubes of different drug concentrations with 300,000 viable cells/ml were prepared for the upper chambers and tubes of drug concentrations +/- 20ng/ml recombinant VEGF were prepared for the

lower chambers. Volumes of DMSO or bevacizumab control vehicle were added to tubes to ensure equal volumes throughout.

2.5.2.3 Invasion

Endothelial cell invasion was investigated using the CULTREX 96-well Basement Membrane Extract (BME) Cell Invasion Assay (Trevigen), a modified trans-well assay. The assay was prepared as per manufacturer instructions: The supplied reagents were first prepared. 500µls of [10x] Coating Buffer were diluted in 4.5mls of distilled water. 50µls of growth factor reduced basement membrane extract (BME) purchased separately (Trevigen) were reconstituted in 450µls of [x1] Coating Buffer to produce a working BME solution of [x0.1]. 3mls of [x10] Cell Dissociation Solution were diluted in 27ml of distilled water, and 30µls of dimethyl sulfoxide (DMSO) were used to form a Calcein-AM solution. 50µls of [x0.1] BME were then pipetted into the top chambers of the supplied 96-well plate. The plate was covered and incubated overnight at 37^{o}C to allow the matrix to set and a semi-confluent flask of cells were starved overnight in EBM-2, 1% FCS. Tubes were prepared of 1 x 10^{6} viable cells/ml of EBM-2, 1% FCS +/- axitinib, and 50µls (50,000 cells) pipetted into upper chambers, 3 wells per condition, 3 wells containing media only. Tubes of EBM-2, 1% FCS +/- axitinib +/- recombinant VEGF 20ng/ml were prepared, and 150µls aliquoted into lower chambers. The plate was covered and incubated for 24 hours at 37^{o}C. Following incubation the lower plate was exchanged for a black 96-well base-plate (supplied). 100µls of [x1] Cell Disassociation + Calcein-AM (1.2µls/ml) were pipetted into chambers of the black base-plate. The reconstructed plates were then covered and incubated at 37^{o}C for a further hour. The base-plate was gently tapped at 30 and 60 minutes to release adherent cells. Calcein fluorescence of cells released into the lower chambers was measured at 1 hour using the FLUOstar Galaxy plate reader at 485nm excitation, 520nm emission. A background measurement from the 3 wells of media only was subtracted from readings, and an average measurement calculated for each drug condition from the wells prepared in triplicate.

A preliminary study was performed using BME [x1] supplied (not growth factor reduced). Fluorescence measurements were not increased above baseline readings from the blank wells of media only, suggesting the absence of cell invasion. As per kit instructions, a subsequent study was performed using serial BME concentrations (x0.1 – x1.0) diluted with coating buffer, 3 wells per condition (figure 2.7). These studies showed no increase in fluorescence measurements above a BME concentration of 0.25. A 10% concentration [x0.1] BME was therefore used in all the subsequent studies as described above.

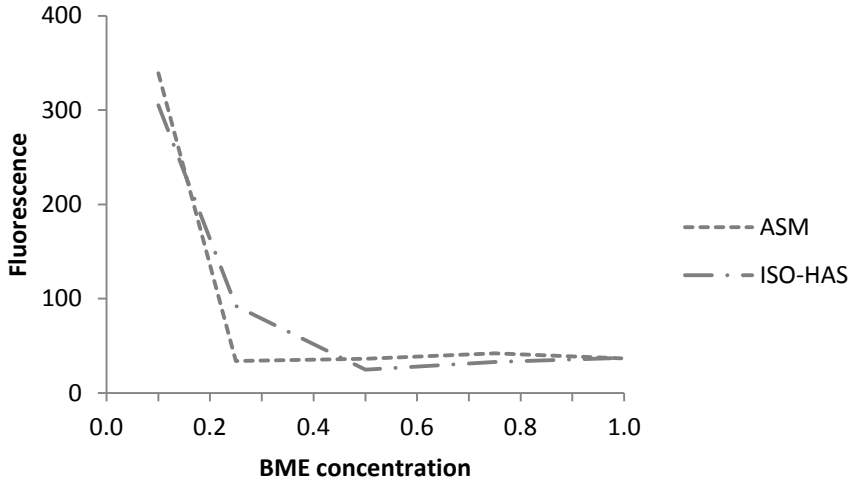

Figure 2.7: Mean fluorescence from invasion assay using serial dilutions of basement menbrane extract (BME); n=1.

Initial studies were then performed using BME extract [x0.1] supplied, to compare ASM and ISO-HAS invasion in control media +/- axitinib, +/- VEGF 20ng/ml (figure 2.8). These studies showed no significant change in fluorescence readings, indicating no increase in cell invasion following the addition of the chemotractant VEGF, and no difference in cell invasion in the presence of axitinib 50ng/ml. The BME supplied with the invasion assay kit however was not growth factor reduced. As growth factors contained within the BME may have influenced these results subsequent studies were performed, as described in the protocol above, using growth factor reduced BME purchased separately, comparing endothelial cell invasion with axitinb concentrations of 0, 50 and 250ng/ml.

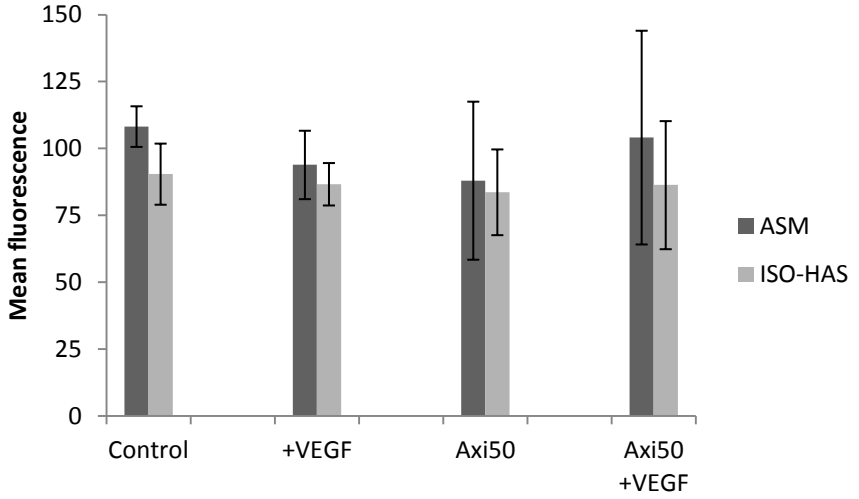

Figure 2.8: Mean fluorescence measurements from invasion assays using basement membrane extract [x0.1] supplied, in 1% EBM (control), plus 20ng/ml VEGF, axitinib 50ng/ml, and axitinib 50ng/ml plus VEGF. Data shown represents mean ± SEM; n=3.

Calcein-AM is absorbed and cleaved by viable cells to produce AM and fluorescent free Calcein. Fluorescence measured in this invasion assay was therefore proportional to the number of viable cells in the lower chamber. These viable cells had invaded from the upper chambers through the BME, remained adherent to the underside of the upper chamber, to then be released into the lower chamber by the Cell Disassociation solution. Baseline studies were performed to convert the fluorescence readings into estimated cell numbers (figure 2.9): Semi-confluent T75 flasks of cells were starved overnight in EBM-2, 1% FCS. Cells were trypsinised, centrifuged at 1000 x g for 3 minutes, and re-suspended to form a suspension of 1 x 10^6 viable cells/ml in [1x] Cell Disassociation Solution. 0-50µls of cell suspension were pipetted into wells to produce wells of 0, 1,000, 2,500, 5,000, 10,000, 25,000 and 50,000 cells per well, 3 wells per condition. Volumes of [1x] Cell Disassociation Solution were added to produce equal volumes of 50µls per well. A solution of [1x] Cell Disassociation Solution + Calcein-AM (2.4µl/ml) was prepared and 50µls pipetted into each well. The plate was covered and incubated at 37^{o}C for 1 hour. The plate was read with a FLUOstar Galaxy plate reader at 485nm excitation, 520nm emission. Background readings were subtracted and the

average readings plotted to produce a standard curve used to transform fluorescent reading from the invasion assay into an estimate of cell numbers.

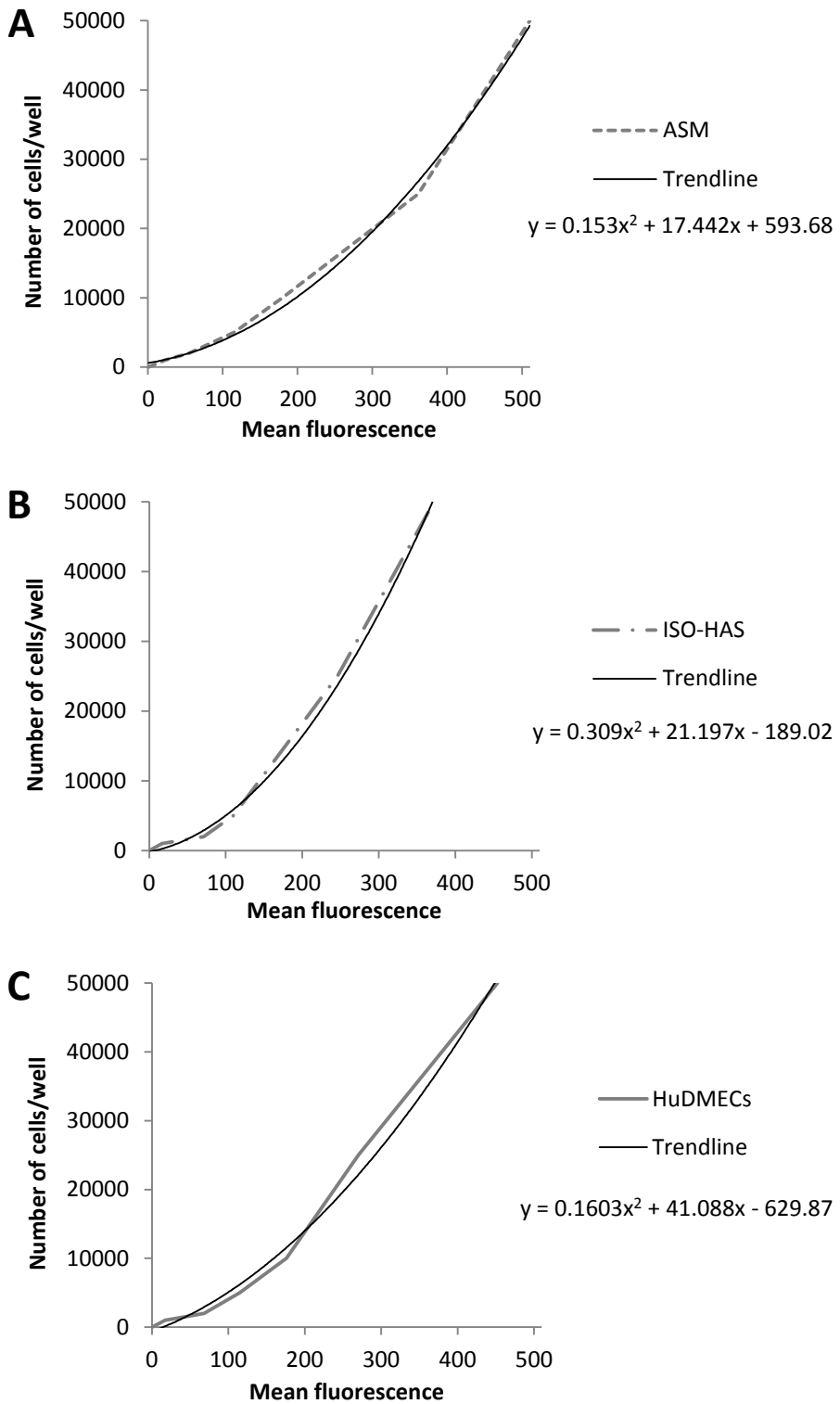

Figure 2.9: Mean fluorescence for (A) ASM, (B) ISO-HAS and (C) HuDMECs for known cell concentrations. Trendline equations shown were used to estimate the number of invaded cells from fluorescence readings in subsequent assays.

2.6 Tumour Samples

2.6.1 Cell line development

I obtained approvals from the Research Ethics Committee (REC), and the Sheffield Teaching Hospital's (STH) Research department for obtaining intra-operative tumour tissue samples from patients undergoing a planned surgical procedure for soft tissue sarcoma including angiosarcoma (REC number: 09/H1313/52; STH project number: 15394; Appendix I). Potential research participants were identified from clinical review at the local sarcoma multi-disciplinary team meeting. Patients were approached by their treating physician during an outpatient assessment and provided with a patient information sheet. A signed consent form was obtained from the patient by a study investigator at a follow-up visit. At resection the surgical specimen was transferred on ice to histopathology for tumour sampling. Samples were obtained by blind biopsy of the tumour specimen by the collaborating histopathologists. Fresh samples were taken for cell line development and other samples stored in RNAlater (Ambion) at -80^{o}C, or fixed in formaldehyde and embedded in paraffin wax for later molecular analysis. Samples were pseudo-anonymised with a soft tissue sarcoma (STS) study number.

Multiple methods were simultaneously trialled to isolate malignant endothelial cells from fresh tumour biopsies. Protocols 3 and 4 detailed below were based on methods described by Krump-Konvalinkova *et al*[154] and Masuzawa *et al*[156], yielding ASM and ISO-HAS respectively.

Protocol 1:

A 2mm^3 sample of tumour was finely minced with a scalpel in a small petri dish, and transferred to T25 Nunc flasks containing full growth media (ECGM, ECGM Supplement Pack, plus 10% FCS, 0.5% v/v penicillin, 0.5% v/v streptomycin and 0.5% v/v amphotericin).

Protocol 2:

A 2mm^3 sample of tumour was minced with a scalpel and incubated in trypsin 0.04% (PromoCell) for 30 minutes at 37^{o}C. After 10 minutes the supernatant was removed and centrifuged at 1000 x g for 5 minutes, and plated in a T25 flask in full growth media. Additional trypsin 0.04% was added to the residual minced tumour tissue and the process repeated 3 times.

Protocol 3:

A 2mm^3 sample of tumour was minced with a scalpel and then digested with the collagenase dispase (Sigma Aldrich), 2mg, at 4^{o}C for 4 hours. Cells were centrifuged at 1000 x g for 5 minutes and re-suspended in trypsin 0.04% and incubated at 37^{o}C degrees for 2 hours. Cells were again centrifuged at 1000 x g for 5 minutes, re-suspended in full growth media and plated in T25 flasks.

Protocol 4:

A 2mm^3 sample of tumour was minced with a scalpel and incubated in 0.04% trypsin at 37^{o}C for 15 minutes. The cell solution was centrifuged at 1000 x g for 5 minutes and plated in T25 flasks in full growth media.

To encourage endothelial cell adhesion some T25 flasks were first coated with gelatin 0.2%: 1ml of 2% gelatin (Sigma Aldrich) was warmed at 37^{o}C until the solution became clear (approximately 1 hour) and then diluted in 9mls PBS. 1ml of 0.2% gelatin was aliquoted into T25 flasks, and incubated at 37^{o}C for 1 hour. Excess gelatin in the flask was then pipetted off prior to use.

Flasks were regularly monitored to observe for cell adherence and subsequent growth. Small aliquots of fresh growth media were added every 72 hours. 2 to 3 weeks were typically required before any growth was seen. Cells were then trypsinised, centrifuged, and re-plated as a monolayer in a T75 flask. Once semi-confluent, T75 flasks of cells were split gently (ratio of 1:2 – 1:3) and early cell passages used for *in vitro* studies. Protocol 3 proved the most effective method at yielding cells for further study.

Tumour samples from four patients were obtained (STS0510, 2110, 2210 and 1011). Tumour details are presented in the relevant section of the results chapter (see section 3.5).

STS0510

MACS microbeads (Miltenyi Biotec) were used to isolate CD31 positive cells. As previously described CD31 is a transmembrane glycoprotein cell adhesion molecule expressed on the surface of endothelial cells, platelets and monocytes[166], as well as by tumour cells of angiosarcoma[99]. The protocol used to isolate CD31 positive cells was followed as per manufacturer instructions: A semi-confluent flask of cells were washed in PBS, trypsinised and centrifuged for 3 minutes at 1000 x g. Cells were re-suspended in 60µls of full growth media. 20µls of Fc receptor Blocking Reagent (supplied) were added, the sample was briefly vortexed, 20µls of CD31 microbeads added, and the sample incubated on ice for 15 minutes. 1ml of media was added, centrifuged again for 3 minutes at 1000 x g and re-suspended in 1 ml of media. Meanwhile, an LS Column (Miltenyi Biotec) was placed in the Midi-MACS Separator – a magnetic retainer, and rinsed with 3 mls of media. The cell suspension was added and the column again rinsed with 3 mls of media 3 times. Cells that bound to the magnetic CD31+ microbeads were held within the LS Column and were flushed out using 5mls of full growth media into a T25 flask once the Column was removed from the magnetic Midi-MACS Separator.

Glass slides of cells were prepared for immunocytochemistry staining (as per 2.2.1). Early cell passages were stored in liquid nitrogen for subsequent recovery and study in functional assays: Flasks were trypsinised, centrifuged at 1000 x g for 3 minutes, re-suspended in 1ml full growth media with 10% DMSO and transferred to a cryo-vial, placed in -80^{o}C freezer for 24 hours, and then to liquid nitrogen. For cell recovery the vials were extracted, warmed in a water bath at 37^{o}C for 1 minute and rapidly transferred to a flask with full growth media. Unfortunately none of the vials cryo-

preserved were successfully recovered, despite also using flasks coated in 0.2% gelatin or 50ng/ml fibronectin (Sigma Aldrich).

STS2110, STS2210

Insufficient cells grew from these tumour samples for immunocytochemistry and functional studies.

STS1011

CD31 extraction was not performed with cells grown from STS1011 in order to study the whole tumour cell population in functional assays. Slides of an early cell passage were prepared for immunocytochemistry staining (as per section 2.2.1). Functional assays were performed on early cell passages (P2 – P7) to investigate the effects of axitininb and bevacizumab on proliferation and differentiation as per the protocols described in section 2.5.

2.6.2 Angiogenesis related protein array of human tumours

Human angiosarcoma specimens were obtained from two sources:

i) Peri-operative tumour sampling described in section 2.6.1.

ii) Baseline biopsies of angiosarcoma lesions from patients who participated in the national cancer research network (NCRN) multi-centre study of axitininb for advanced soft tissue sarcoma (Axi-STS; International Standard Randomised Controlled Trials Number (ISRCTN): 60791336).

All biopsies were placed in RNAlater immediately after sampling. Samples from the Axi-STS study were sent to the University of Sheffield at room temperature. Samples were stored in RNAlater at -80^{o}C until analysis. Samples were analysed using the angiogenesis related protein array (R&D Systems). Tumour samples from two de-differentiated liposarcomas collected peri-operatively (STS1711, STS1810) were also analysed using the angiogenesis related protein array

2.6.2.1 Protein extraction

Tumour samples were minced in 15 second bursts, in 500µls of Cell Disruption Buffer (Ambion), using an Ultra-Turrax T8 (IKA Labortechnik). Samples were then incubated for 2 hours on ice, and then centrifuged at 15,000rpm for 12 minutes at 4^{o}C. Cell supernatant was transferred to a fresh eppendorf, leaving behind residual cell debris settled during centrifugation, and stored at -20^{o}C overnight until analysis.

2.6.2.2 Protein array

Methods described in section 2.4.1 were followed for performing the array studies. Prior to analysis, total protein quantification of study samples was performed as previously described. Identical quantities of protein (120µg/ml) were used for each array.

2.6.3 Immunohistochemistry study of human vascular tumours

I obtained REC and STH Research department approvals for retrieving archived formalin-fixed paraffin embedded (FFPE) pathology specimens for analysis (REC number: 09/H1313/30; STH project number: 15355; Appendix I). The STH pathology archive was searched for angiosarcoma and benign vascular tumours processed between1999 – 2009. Archived haematoxylin and eosin (H&E) slides of identified vascular tumours were reviewed for quality control, to confirm the underlying histology, and to ensure adequate material for further study. Angiosarcoma tumour samples collected prospectively (see section 2.6.1) were also included in these studies. Basic clinical parameters from angiosarcoma specimens were recorded including the patient's age, sex, and disease site.

Slides were cut from FFPE tumour blocks by University of Sheffield technical staff. Tumour blocks were first chilled on ice, and 6µm sections cut onto glass slides with a Biocut 2035 (Leica). The slides were dried at 37^{o}C for 24 hours before use.

2.6.3.1 Immunohistochemistry protocol

Slides were stained simultaneously for each antibody to enable direct comparison across the tumour groups. Preliminary studies were performed to optimise the study protocol for each antibody. Slides were racked and rehydrated for 5 minutes in xylene twice, then 3 minute baths of 100%, 100%, 95%, 90% and 70% ethanol, then washed in distilled water. Antigen retrieval was performed using citric acid (0.01M citric acid, pH6.0 with 0.1% Tween). Slides were immersed in citric acid, covered and heated on high in a 700W microwave (Panasonic NN6308) for 3 minutes and then 7 minutes on medium. During heating the bath was regularly topped up with additional citric acid to ensure the slides remained submerged. Slides were then allowed to cool on ice in the citric acid bath for 20 minutes. Slides were washed briefly in distilled water and endogenous peroxidase was blocked with 0.3% hydrogen peroxidase (270mls methanol and 30mls of 3% hydrogen peroxidase (Sigma Aldrich)) at 37^{o}C for 30 minutes. Slides were again washed with distilled water and the tumour sections edged with an ImmEdge wax pen. Blocking solution was applied (9mls PBS, 1ml serum, 1ml [10x] casein) at room temperature for 1 hour. Primary antibody as per table 2.6 was applied in 2% serum and incubated overnight at 4^{o}C. Slides were then washed in PBST (0.1% Tween) for 5 minutes, twice. Secondary antibody was applied for 1 hour at room temperature, during which time ABC solution (Elite) was prepared (5mls PBS, 2 drops tube A, 2 drops tube B). Slides were again washed in PBST for 5 minutes, twice. ABC solution was applied for 40 minutes. Slides were washed again, and then stained with DAB (Elite; 5mls distilled water, 2 drops buffer, 4 drops DAB, 2 drops hydrogen peroxide) for up to 3 minutes. Slides were washed in tap water and stained in Gills Haematoxylin for 1.5 minutes and allowed to ‘blue’ in running tap water for 3 minutes. Slides were then dehydrated in sequential baths of 70%, 90%, 95%, 100% and 100% ethanol for 3 minutes each and then immersed in xylene for 5 minutes twice. Finally coverslips were affixed using DPX and allowed to dry before immuno-scoring.

As in the immunocytochemistry staining studies, slides were scored for the number of cells stained (0 = <1%, 1 = 1-10%; 2 = 11-50%; 3 = >50%) combined with a score for staining intensity (1 = weak, 2 = moderate, 3 = strong). Slides of placental tissue were used as a positive control. Tumour slides processed with the primary antibody substituted with PBS were used as a negative control. Staining of normal tissue adjacent to the vascular tumour was used to assess endothelial specific staining.

Antibody	Primary	Secondary
VEGF (sc-152)	1:100	1:200
VEGFR1 (ab2350)	1:50	1:200
VEGFR2 (ab39256)	1:100	1:200
NRP1 (ab81321)	1:250	1:500
bFGF (ab106245)	1:250	1:500
FGFR1 (ab71928)	1:250	1:500
Ang-1 (ab8451)	1:250	1:500
Ang-2 (ab65835)	1:75	1:250
Tie2 (AF-313)	1:50	1:250
HGF (AF-294-NA)	1:250	1:500
MET (ab51067)	1:250	1:500

Table 2.6: Concentration of primary and secondary antibodies used in the immunohistochemistry studies

2.6.4 Immunohistochemistry study of canine vascular tumours

In contrast to human disease, angiosarcomas represent 10% of all canine tumours[167]. FFPE tumour samples of benign canine vascular tumours and cutaneous and visceral angiosarcomas were obtained through collaboration with the Animal Health Trust (Cambridge, UK). The Animal Health Trust pathology archive was searched for vascular tumours and retrieved tumour blocks sent to the University of Sheffield for analysis. Canine specific antibodies are not available commercially and therefore the immunohistochemistry protocols used to study the human tumour samples were folowed, as described in section 2.6.3.1.

2.7 Statistical Methods

The biological characteristics of ASM, ISO-HAS and HuDMEC cells, as assessed by cell differentiation and cell migration functional assays, were compared using the independent t test. Proteins of interest were selected from the protein array expression profiles, by comparing the size of the protein peak densities between cell lines (a more than two fold difference in protein peak density was considered of interest), and by identifying statistically significant differences between peak densities using the one-way ANOVA test. ASM, ISO-HAS and HuDMEC expression of VEGF, as quantified by ELISA, were compared using the independent t test. Responses to vascular targeted agents were analysed using the paired t test, by comparing cell response to increasing drug exposure in cell viability, cell differentiation or cell migration assays, with or without the presence of VEGF stimulation. The immuno-staining of the vascular tumour samples were compared between tumour groups using the Kruskall-Wallis or Mann-Whitney test.

All statistical analysis was performed using PASW Statistics 18; *p* values less than 0.05 were considered significant.

3 Results

3.1 Characterisation of Angiosarcoma Cell Lines

ASM and ISO-HAS have been identified as malignant endothelial cell lines[154, 156, 158]. Characterisation studies were performed to confirm that ASM and ISO-HAS cells were endothelial. As ASM and ISO-HAS cells were derived from cutaneous vascular tumours, dermal microvascular endothelial cells (HuDMECs) were selected as a positive control. As angiosarcomas are classified with mesenchymal tumours, dermal fibroblasts (HDFs), cells of mesenchymal origins that do not usually express endothelial cell markers, were selected as a negative control. The morphology of ASM and ISO-HAS cells were compared to HuDMECs and HDFs, immunocytochemistry studies quantified the expression of endothelial cell markers, and uptake of the fluorescent endothelial cell specific marker Dil-Ac-LDL was assessed.

3.1.1 Cell morphology

Images of cultured cells are presented in figure 3.1. Images were taken using phase contrast microscopy (x4 magnification). HuDMECs had a cobblestone morphology typical of endothelial cells in culture. HuDMEC morphology was maintained up to passage 6, beyond which an increasing proportion of cells demonstrated a spindle morphology. HuDMECs were therefore utilised up to passage 6 for these experiments. HDFs demonstrated a spindle morphology typical of fibroblasts, which was maintained by cells up to passage 8 used for these experiments. ASM and ISO-HAS cells exhibited a mixed morphology. A proportion of cells appeared polygonal, whilst others were spindle shaped. ASM and ISO-HAS cells were studied in experiments up to passage 20. ASM cells passaged beyond this adopted a homogenous spindle morphology, and were negative for endothelial cell markers including CD31.

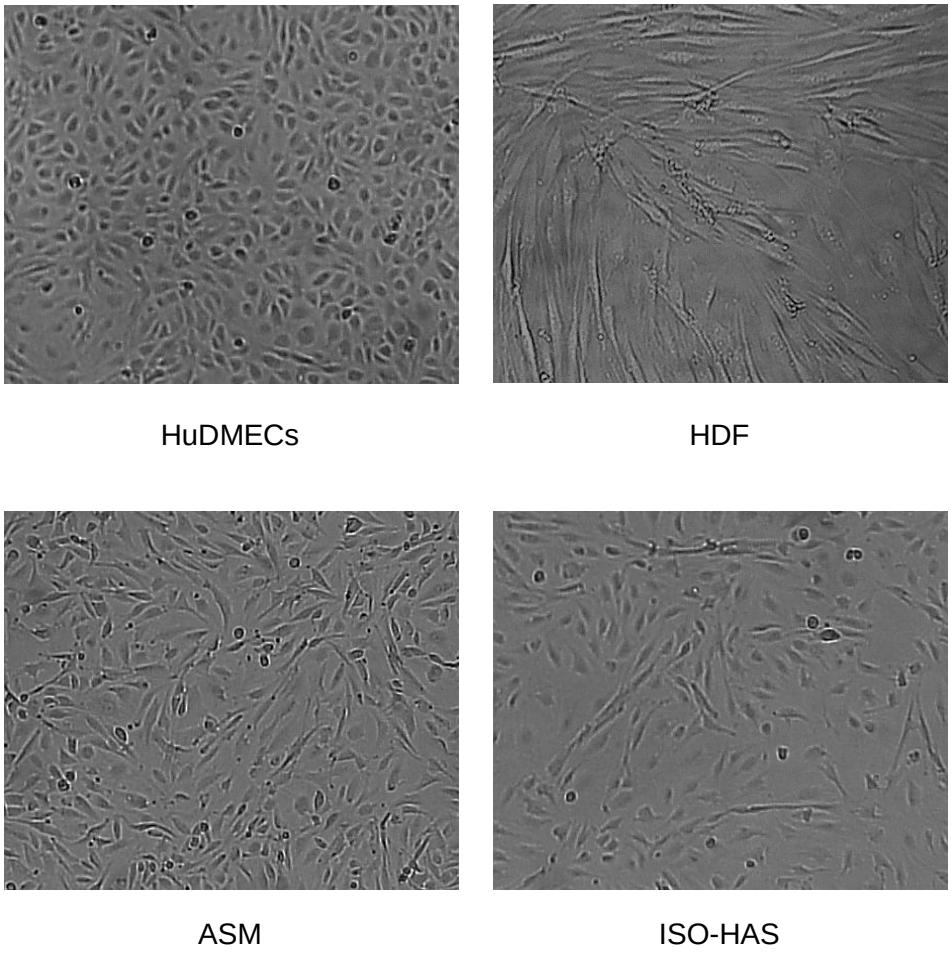

Figure 3.1: Cell morphology in full growth media (x4 magnification).

3.1.2 Immunocytochemistry studies

Immunocytochemistry studies were performed to compare the expression of endothelial cell markers by ASM and ISO-HAS cells with HuDMEC and HDF cells. The results are summarised in table 3.1. HuDMECs stained strongly for the endothelial cell markers CD31, CD34 and vWF, and also for VEGF, VEGFR1 and VEGFR2. Unexpectedly HuDMECs also showed staining for αSMA. Pericytes and vascular smooth muscle cells would be expected to stain for αSMA but not endothelial cells. HuDMEC expression of aSMA may have been induced, perhaps as a consequence of *in vitro* culture on glass slides, or show contamination of the HuDMEC cell line with pericytes; alternatively this staining may represent a false positive finding. In contrast HDFs did not stain for the endothelial cell markers CD31, CD34 or vWF, but stained strongly for αSMA. HDFs also showed staining for VEGF, VEGFR1 and VEGFR2.

Whilst VEGF and VEGFR1 are not endothelial specific markers, VEGFR2 is principally expressed on endothelial cells. HDF expression of VEGFR2 was not predicted and suggests a false positive result.

ASM and ISO-HAS cells showed staining for the endothelial cell markers. However, in contrast to HuDMECs which showed a uniform staining pattern, ASM and ISO-HAS cells demonstrated a range of staining intensities to CD31 and vWF (figure 3.2). ASM and ISO-HAS cells also stained for VEGF, VEGFR1, VEGFR2 and αSMA.

Pilot studies of other putative endothelial cell lines found EAhy926 stained for CD31 but not vWF, whilst SVR and ISOS-1 stained for neither CD31 nor vWF. EAhy926, SVR and ISOS-1 stained for both VEGF and VEGFR2.

	HuDMEC	ASM	ISO-HAS	HDF
CD31	6.0	4.0	4.7	0.0
CD34	4.3	2.7	2.7	0.0
vWF	6.0	4.3	4.3	0.0
αSMA	4.3	4.0	4.7	6.0
VEGF	4.7	5.3	5.0	5.0
VEGFR1	5.7	5.7	5.3	5.3
VEGFR2	5.0	4.7	5.7	4.0

Table 3.1: Immunocytochemistry studies of HuDMEC, ASM, ISO-HAS and HDF cells. Immunocytochemistry staining was semi-quantified using a composite score for the number of stained cells and the staining intensity (see section 2.2.1.2). Data shown represents mean score; n=3.

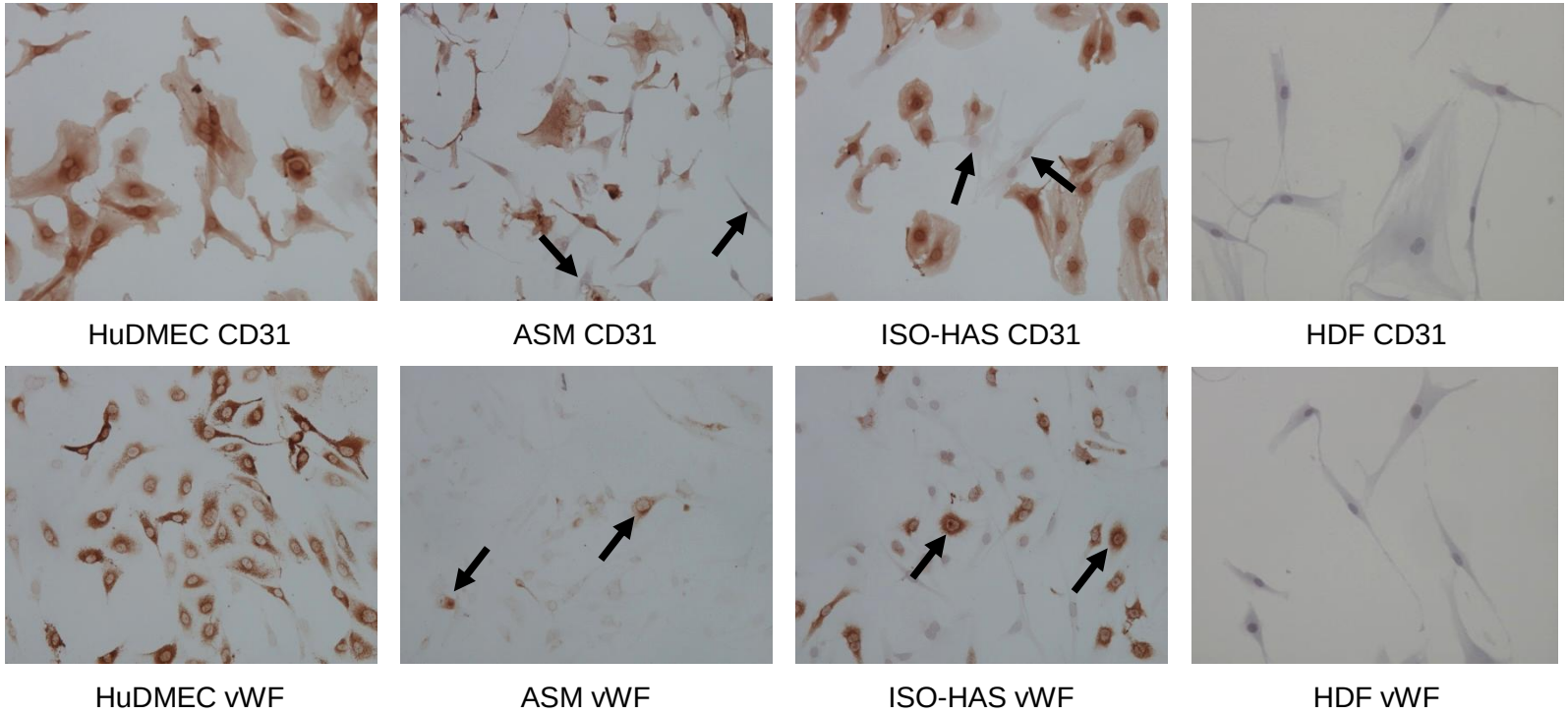

Figure 3.2A: Images from immunocytochemistry studies (x20 magnification). HuDMECs stained strongly for the endothelial cell markers CD31 and vWF. ASM and ISO-HAS cells in contrast showed a mix of staining intensity (arrows indicate ASM and ISO-HAS cells that stained weakly for CD31, and cells that stained strongly for vWF). HDFs did not stain for either CD31 or vWF.

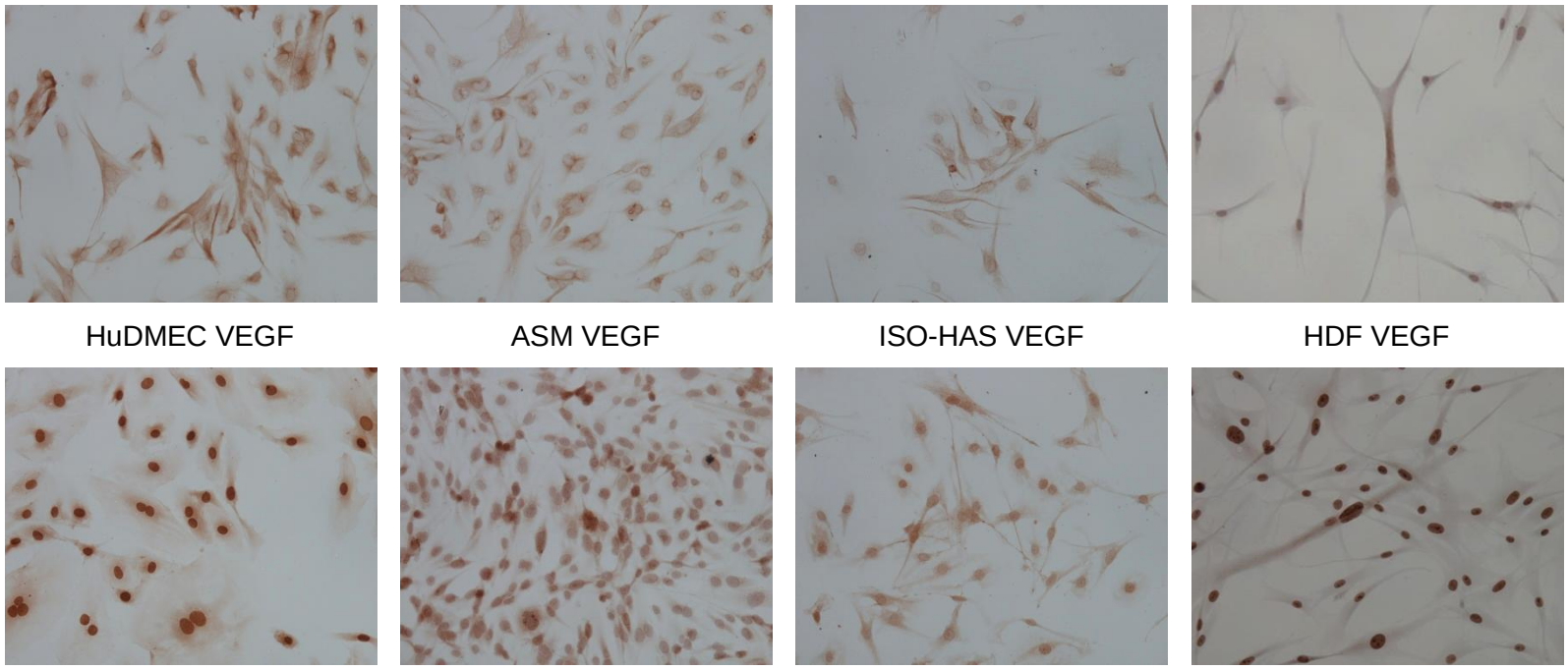

Figure 3.2B: Images from immunocytochemistry studies (x20 magnification). HuDMEC, ASM, ISO-HAS and HDF cells stained for VEGF and VEGFR2.

3.1.3 Dil-Ac-LDL

Consistent with other endothelial cells, ASM and ISO-HAS cells demonstrated uptake of the endothelial cell specific marker Dil-Ac-LDL (figure 3.3). Control studies showed Dil-Ac-LDL uptake by HuDMECs but not HDFs.

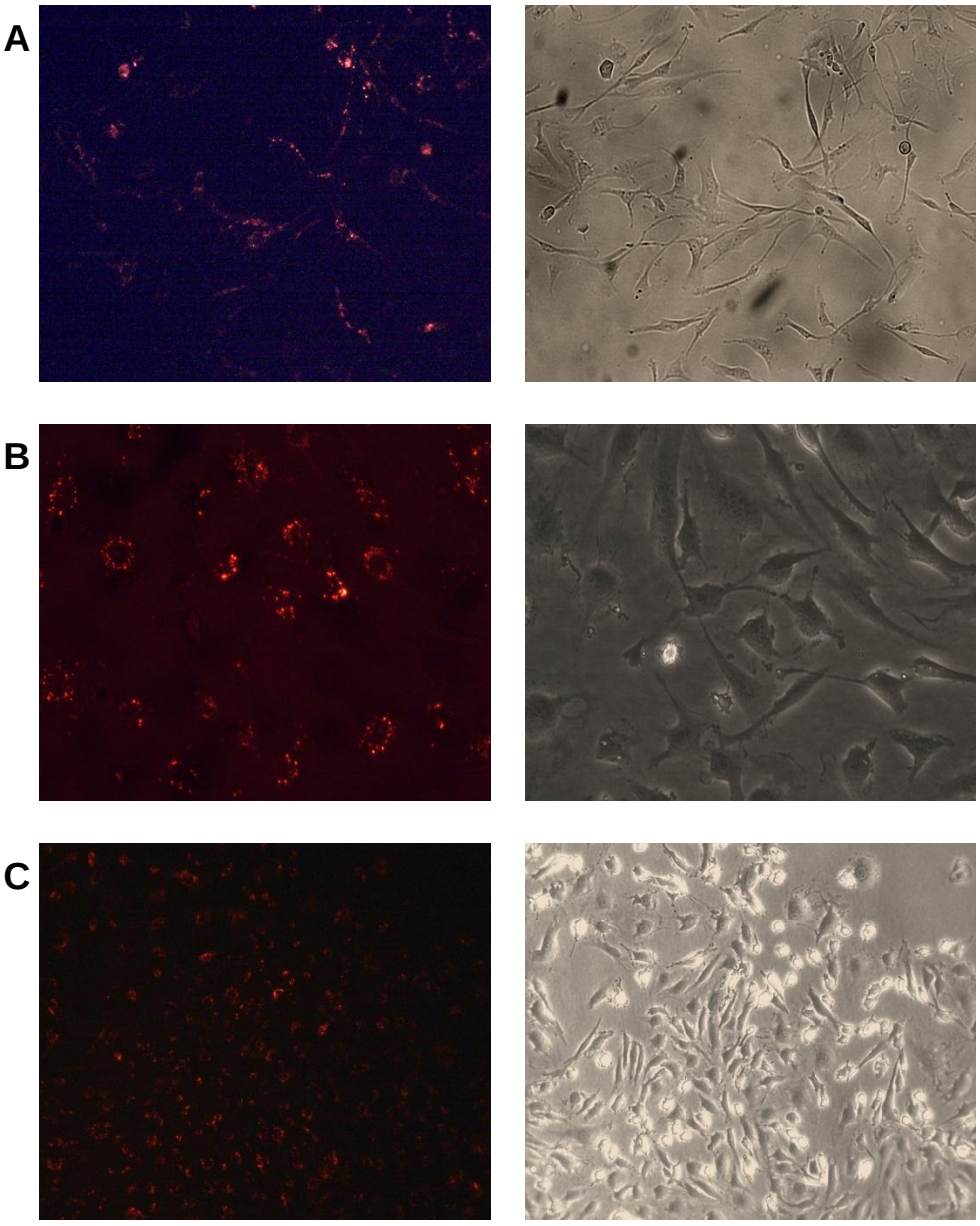

Figure 3.3: Replica images of (A) ASM cells (x10 magnification), (B) ISO-HAS cells (x20 magnification) and (C) HuDMECs (x10 magnification), taken with white light and with fluorescence following incubation with the fluorescent endothelial cell marker Dil-Ac-LDL.

3.1.4 Flow cytometry

ASM and ISO-HAS cultures showed cells with a mixed morphology, and immunocytochemistry studies of ASM and ISO-HAS showed cells with a range of staining intensity for endothelial cell markers. Cell morphology was poorly preserved on the glass slides used in the immunocytochemistry studies. ASM and ISO-HAS cells were therefore grown on Permanox multi-chamber slides to correlate cell morphology with endothelial cell marker expression. However, ASM and ISO-HAS cell growth were limited on the Permanox multi-chamber slides. Flow cytometry studies were therefore performed using fluorescent labelled CD31, VEGF, VEGFR1 and VEGFR2 antibodies to investigate for sub-populations of cells within ASM and ISO-HAS cultures.

To analyse endothelial cell marker expression, the total cell population was gated to select a study population by excluding non-viable cells, cell debris and cell doublets. Cytometric analysis of ASM and ISO-HAS study populations demonstrated a shift in fluorescence intensity consistent with endothelial cell marker expression, with no evidence of distinct sub-populations of cells that over or under expressed endothelial cell markers (figure 3.4 and 3.5).

3.1.5 Characterisation of angiosarcoma cell lines summary

The characterisation studies confirmed ASM and ISO-HAS cells expressed CD31, vWF, VEGFR2, and uptook Dil-Ac-LDL, consistent with cells of endothelial origin. The morphology and immunocytochemistry studies suggested ASM and ISO-HAS consisted of a mixed population of cells, however the flow cytometry studies were consistent with cells of a single population that expressed endothelial cell markers with differing intensities.

A

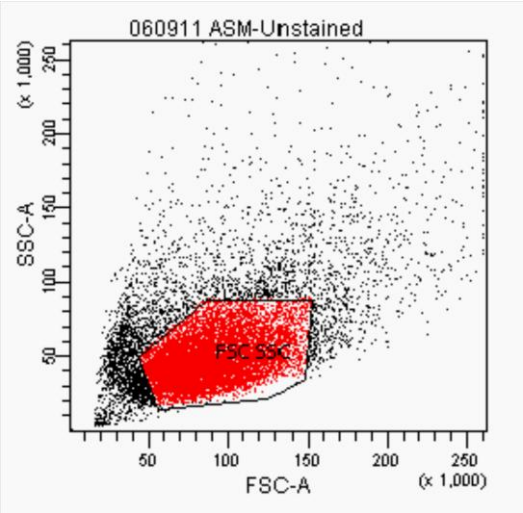

B

	Median Fluorescence Intensity	
	Unstained	Stained
CD31 (PECy7)	381	924
VEGF (PerCp Cy5.5)	293	551
VEGFR1 (R-PE)	158	275
VEGFR2 (APC)	280	353

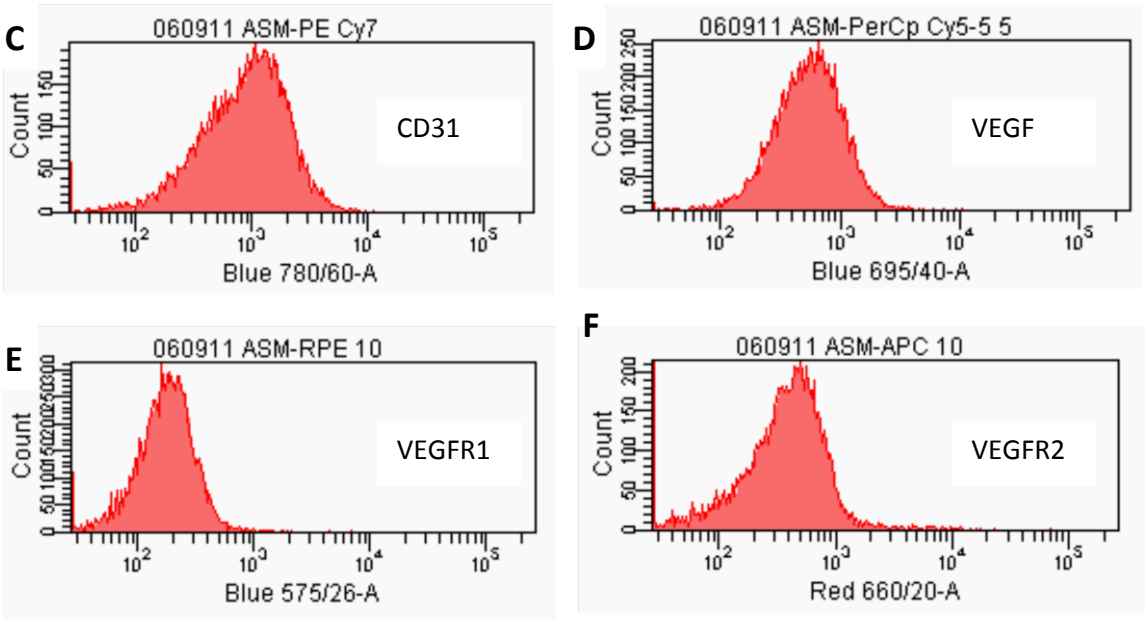

Figure 3.4: Flow cytometry results for ASM: (A) Plot by forward and side scatter of total and gated study population. (B) Median shift in fluorescence intensity for each antibody compared to measurements in the unstained population. (C)-(F) Plot of fluorescence intensity for each antibody in the gated population.

A

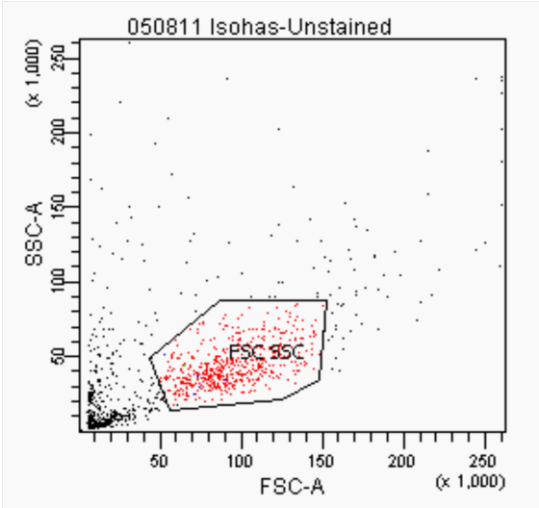

B

	Median Fluorescence Intensity	
	Unstained	Stained
CD31 (PECy7)	548	1329
VEGF (PerCp Cy5.5)	409	748
VEGFR1 (R-PE)	214	261
VEGFR2 (APC)	373	615

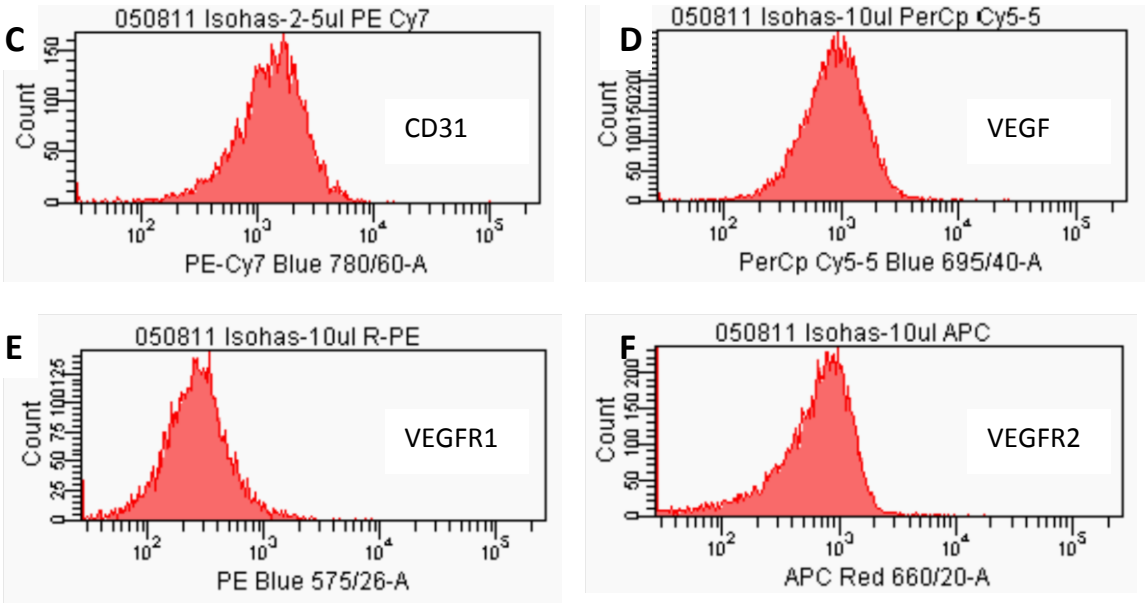

Figure 3.5: Flow cytometry results for ISO-HAS: (A) Plot by forward and side scatter of total and gated study population. (B) Median shift in fluorescence intensity for each antibody compared to measurements in the unstained population. (C)-(F) Plot of fluorescence intensity for each antibody in the gated population.

3.2 Protein Expression

ASM and ISO-HAS cells were studied using R&D Systems Proteome Profiler Antibody Arrays, to establish a profile of the proteins they expressed, and to identify putative drug targets for the treatment of angiosarcoma. The protein expression profiles of HuDMEC and HDF cells were used for comparison.

3.2.1 Protein arrays

Protein array studies determined the expression of 55 angiogenesis related proteins, 46 phosphorylated intracellular kinases, and 42 phosphorylated receptor tyrosine kinases in ASM, ISO-HAS, HuDMEC and HDF cell lysates in normoxic conditions. Array studies were also performed to compare angiogenesis related proteins secreted by ASM and ISO-HAS cells into the supernatant. As hypoxia stimulates angiogenesis and tumours *in vivo* are typically hypoxic, additional array studies were performed to compare the expression of angiogenesis related proteins in ASM, ISO-HAS and HuDMEC cell lysates in hypoxic conditions. Duplicate studies were performed using different cell passages; however protein array costs limited the number of replicates.

3.2.1.1 Angiogenesis related proteins

In normoxic conditions the expression profile of angiogenesis related proteins derived from HuDMEC cells were distinct from HDFs (figure 3.6). The expression of a number of proteins were increased more than two-fold in HuDMEC cells compared to HDFs; significantly increased proteins included Ang-2 (p=0.022), endostatin (p=0.002), endothelin-1 (p=0.021), heparin-binding EGF-like growth factor (HB-EGF) (p=0.019), insulin growth factor binding protein-2 (IGFBP-2) (p=0.018), interleukin-8 (IL-8) (p=0.013), PDGF-AA (p=0.031) and PDGF-BB (p=0.027). HuDMEC expression of coagulation factor III, FGF-7, glial cell-derived neurotrophic factor (GDNF) and VEGF were less than half that of HDFs, but differences were not statistically signifcant. The distinct profiles of HuDMEC and HDF cells suggested the angiogenesis related protein

array was a useful tool for studying the expression of these proteins in ASM and ISO-HAS cells.

In normoxic conditions the angiogenesis related protein expression profiles of ASM and ISO-HAS were broadly similar to HuDMECs (figure 3.6). ASM and ISO-HAS protein expressions were calculated as a ratio of HuDMEC values to identify proteins with a greater than two-fold difference in expression (figure 3.7). ASM and ISO-HAS expression of coagulation factor III, TIMP-4 (tissue inhibitor of metalloproteinase-4) and VEGF were increased compared to HuDMECs, whilst Ang-2, MCP-1 (monocyte chemotactic protein-1) and prolactin were decreased relative to HuDMECs. A one-way ANOVA analysis was performed to compare the expression profiles. Only VEGF expression was significantly increased ($p=0.029$). A post-hoc Tukey's analysis of VEGF expression showed mean ± SEM difference in peak density between ASM and HuDMECs 0.63 ± 0.12 ($p=0.027$), and mean ± SEM difference between ISO-HAS and HuDMECs 0.43 ± 0.12 ($p=0.07$).

Secreted angiogenesis related proteins may promote tumour growth by stimulating neighbouring tumour and stromal cells within the tumour micro-environment. However, proteins expressed in cell lysates may not reflect proteins secreted into the cell supernatant, and a comparison may suggest different drug targets. The expression of angiogenesis related proteins in ASM and ISO-HAS cell supernatant was therefore studied, and contrasted with cell lysate data (figure 3.8). Cell supernatant was collected from semi-confluent cells incubated overnight in normoxia and concentrated [x20] prior to study. These arrays showed differences in the expression of a number of proteins: Activin A, angiogenin, GDNF, GM-CSF (granulocyte macrophage colony-stimulating factor), HGF, IGFBP-1 and -3, MCP-1 and PDGF-AA were increased in cell supernatant compared to the lysates, whilst coagulation factor III, aFGF, bFGF and TSP-1 (thrombospondin-1) were decreased.

As hypoxia stimulates angiogenesis, the expression of angiogenesis related proteins was studied in lysates from ASM, ISO-HAS and HuDMEC cells incubated overnight in hypoxic conditions (1% O_2) (figure 3.9). The profile of angiogenesis related proteins obtained from HuDMECs cultured in normoxic conditions was broadly similar to the expression profile of HuDMECs in hypoxic conditions. However, the relative peak density of some of the proteins expressed by HuDMECs in hypoxia, including Ang-1, EGF, HGF, MMP-9, PDGF-AA and VEGF, were less than half that of HuDMECs in normoxia.

A comparison of the expression profiles from ASM and ISO-HAS cells in hypoxia with HuDMECs identified a number of proteins with a greater than two-fold difference in expression (figure 3.10). Angiogenin, Ang-1, aFGF, HGF and VEGF showed increased expression in ASM and ISO-HAS cells compared to HuDMECs. ASM and ISO-HAS expression of Ang-2, CXCL16 (chemokine ligand 16), GDNF, IL-1β, MCP-1 and prolactin were decreased relative to HuDMECs. The difference in VEGF expression in hypoxia was especially pronounced; VEGF expression was twenty-five times greater in ASM and ISO-HAS lysates than in HuDMECs. This finding supported further study of VEGF expression, and the subsequent study of ASM and ISO-HAS cell response to agents targeting VEGF.

If resources had permitted, additional protein array studies to assess the expression of angiogenesis related proteins in supernatant collected from cells incubated under hypoxic conditions would have been of interest, and also supernatant from HuDMECs in normoxic conditions.

3.2.1.2 Phosphorylated protein kinases

Phosphorylated tyrosine, serine and threonine residues on intracellular protein kinases regulate cell function, and are drug targets of small molecule kinase inhibitors. Basal phosphorylation of 46 protein kinases were assessed in lysates from semi-confluent ASM, ISO-HAS, HuDMEC and HDF cells starved overnight (figure 3.11). There were

few objective differences between the phosphorylated protein kinase profiles of HuDMEC and HDF cells, and the phosphorylated protein kinase profiles were broadly similar across all four studied cell lines. HuDMEC levels of phosphorylated endothelial nitric oxide synthase (eNOS) was more than double HDF levels (p=0.009), and HuDMEC levels of phosphorylated ERK were less than half that of HDFs (p=0.07), but other differences between HuDMEC and HDF cells were not significant.

Only phosphorylated checkpoint II (ChkII) differed more than two-fold between both ASM, ISO-HAS and HuDMEC cells (p=0.15) (figure 3.12). A one-way ANOVA analysis identified a statistically significant difference in p53 phosphorylation at serine 15 (p=0.010). The difference measured was small (mean ± SEM difference in relative peak density of phosphorylated $p53^{S15}$ between ASM and HuDMECs 0.14 ± 0.02 (p=0.009), and between ISO-HAS and HuDMECs 0.09 ± 0.02 (p=0.034)), however as both ChkII and $p53^{S15}$ are activated by ATM (ataxia telangiectasia mutant) in response to DNA double strand breaks this finding may be biologically relevant.

3.2.1.3 Phosphorylated receptor tyrosine kinases

Ligand binding to receptor tyrosine kinases induces receptor dimerisation and phosphorylation of tyrosine residues on the receptor's intracellular domain, which in turn activate downstream intracellular signalling networks leading to a cellular response. Phosphorylated receptor tyrosine kinases were profiled to identify key cell signalling pathways stimulated in basal conditions, and to identify potential drug targets. Basal phosphorylation of 42 receptor tyrosine kinases (RTKs) in lysates from semi-confluent ASM, ISO-HAS, HuDMEC and HDF cells starved overnight was also assessed (figure 3.13). Compared to ASM and ISO-HAS, both HuDMEC and HDFs had a broader profile of phosphorylated RTKs. Basal phosphorylation of VEGFR1, VEGFR2, VEGFR3, Tie2 and EphrinB1 and B2 were identified in HuDMECs. Basal phosphorylation of EGFR, PDGFRs, IGF-1R (insulin-like growth factor-1 receptor), Ret, Axl and ROR1 and 2 (receptor tyrosine kinase-like orphan receptor) were identified in HDFs. Only basal phosphorylation of EGFR (epidermal growth factor receptor) and

VEGFR2 were observed in ASM, and VEGFR1, VEGFR2, Tie2, EphrinA7, IGF-1R and ROR2 in ISO-HAS.

3.2.1.4 Protein array summary

A table summarising key findings from the array studies is shown below (table 3.2).

Array	HuDMEC protein expression compared to HDFs	ASM and ISO-HAS protein expression compared to HuDMECs
Angiogenesis related proteins (*normoxia*)	↑Ang-2 ↑Endostatin ↑Endothelin-1 ↑HB-EGF ↑IGFBP-2 ↑IL-8 ↑PDGF-AA ↑PDGF-BB	↑Coagulation Factor III ↑TIMP-4 ↑VEGF
	↓Coagulation Factor III ↓FGF-7 ↓GDNF ↓VEGF	↓Ang-2 ↓MCP1 ↓Prolactin
Angiogenesis related proteins (*hypoxia*)		↑Angiogenin ↑Ang-1 ↑aFGF ↑HGF ↑VEGF
		↓Ang-2 ↓CXCL16 ↓GDNF ↓IL-1β ↓MCP-1 ↓Prolactin
Phosphorylated kinases	↑eNOS	↑p70 S6 kinase ↑p53 ↑ChkII
	↓ERK1/2	
Phosphorylated RTKs	↑VEGFR1-3 ↑Tie2	
		↔VEGFR2
	↓EGFR ↓IGF-1R ↓PDGFRs	↓Tie2 ↓VEGFR3

Table 3.2: Key findings from protein array studies.

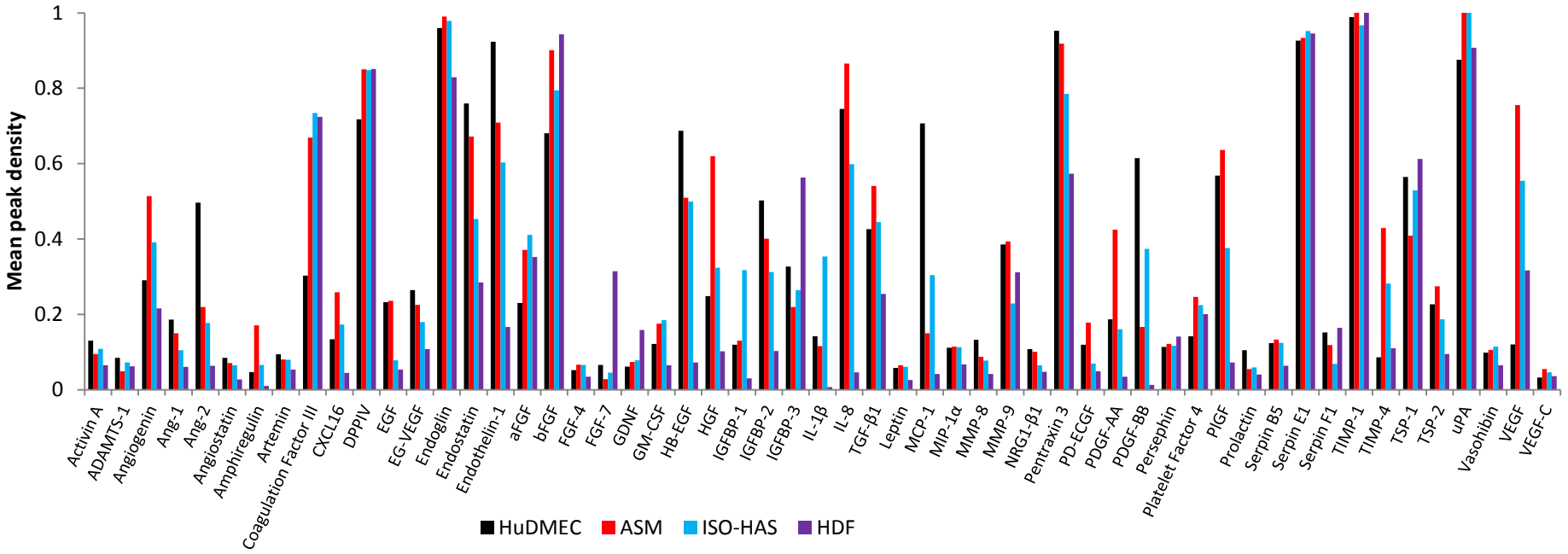

Figure 3.6: Expression profiles of angiogenesis related proteins from HuDMEC, ASM, ISO-HAS and HDF cell lysates. Data shown represents mean peak densities standardised relative to internal positive controls; n=2.

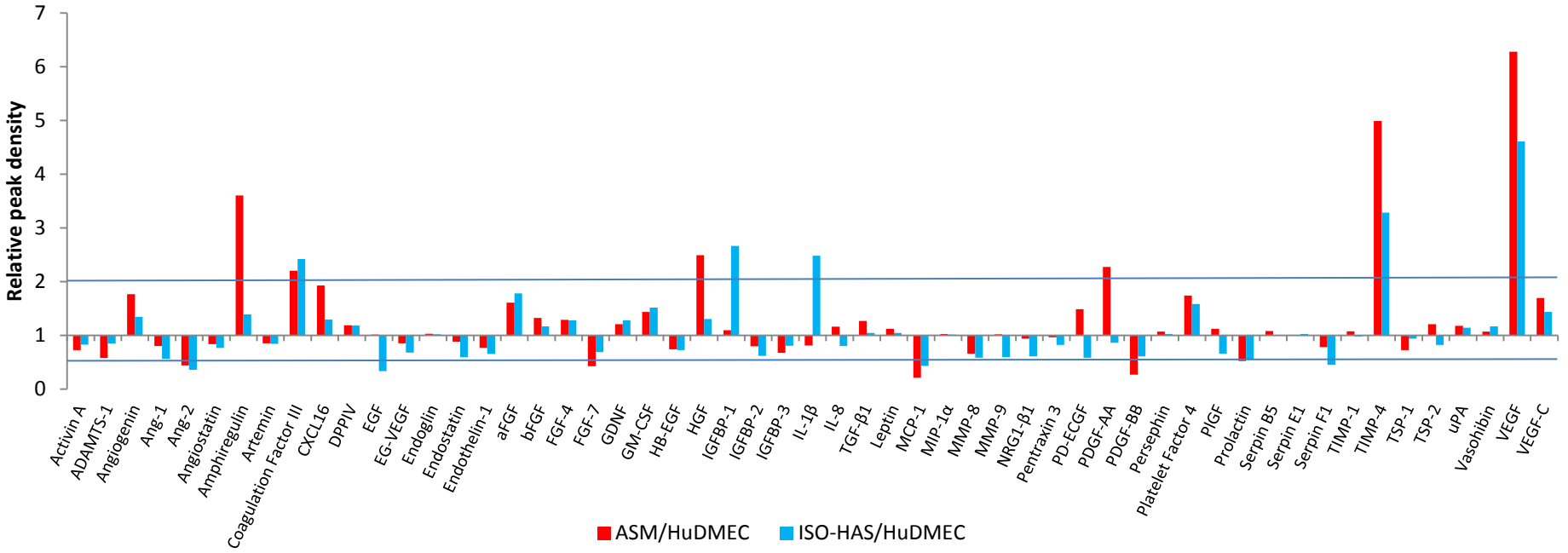

Figure 3.7: Expression profiles of angiogenesis related proteins from ASM and ISO-HAS cell lysates. Data shown represents relative peak densities expressed as a ratio of HuDMEC values. Gridlines identify proteins with a greater than two-fold difference in expression.

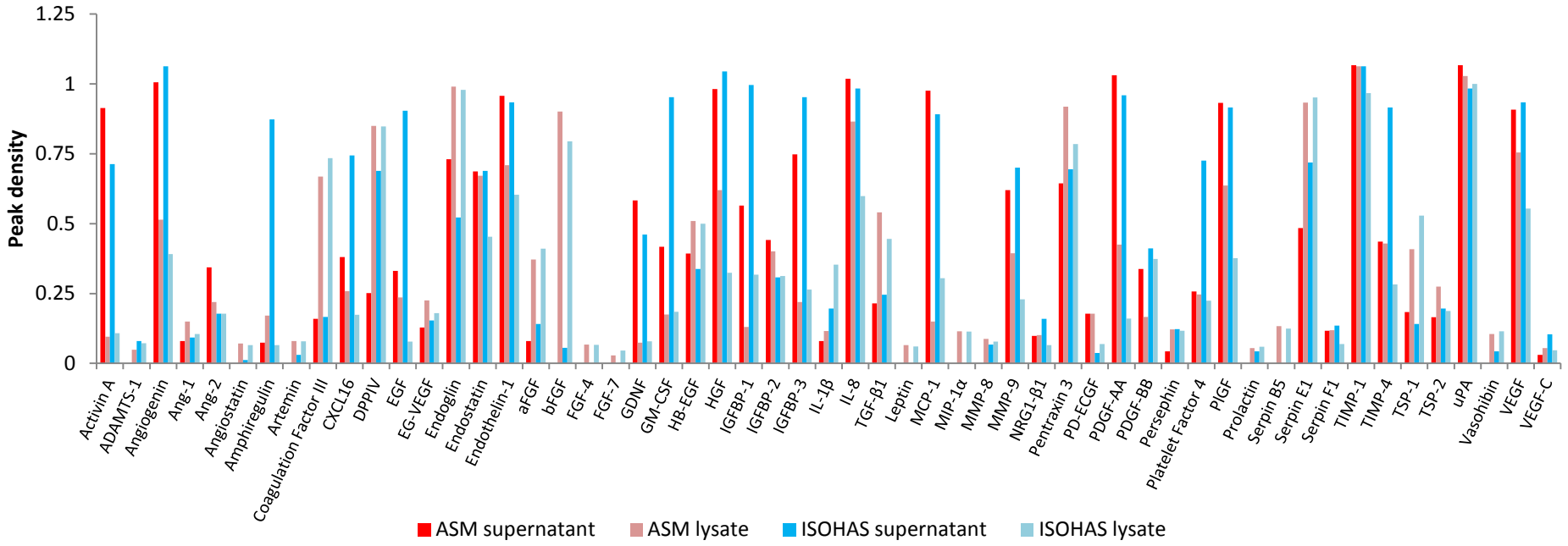

Figure 3.8: Expression profiles of angiogenesis related proteins in ASM and ISO-HAS supernatants (concentrated x20), and comparison with expression profiles from cell lysates. Data shown represents peak densities standardised relative to internal positive controls; n=1.

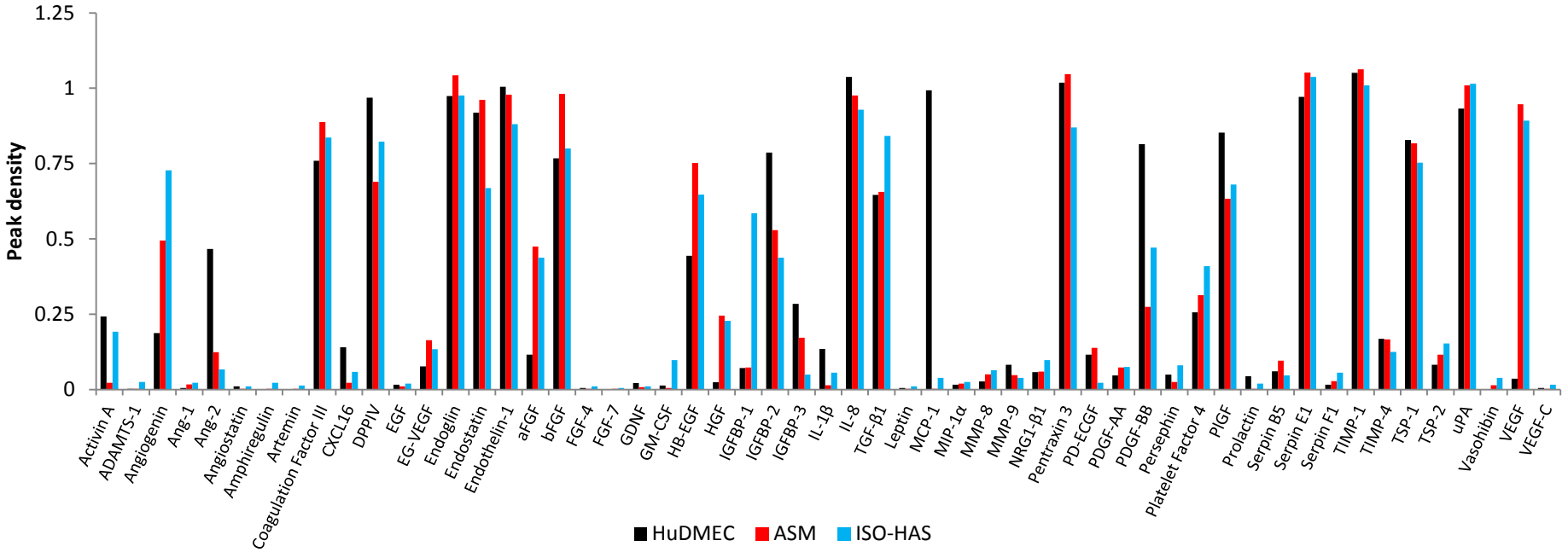

Figure 3.9: Expression profiles of angiogenesis related proteins from HuDMEC, ASM and ISO-HAS cells incubated overnight in hypoxic conditions (1% O_2). Data shown represents peak density values standardised relative to internal positive controls; n=1.

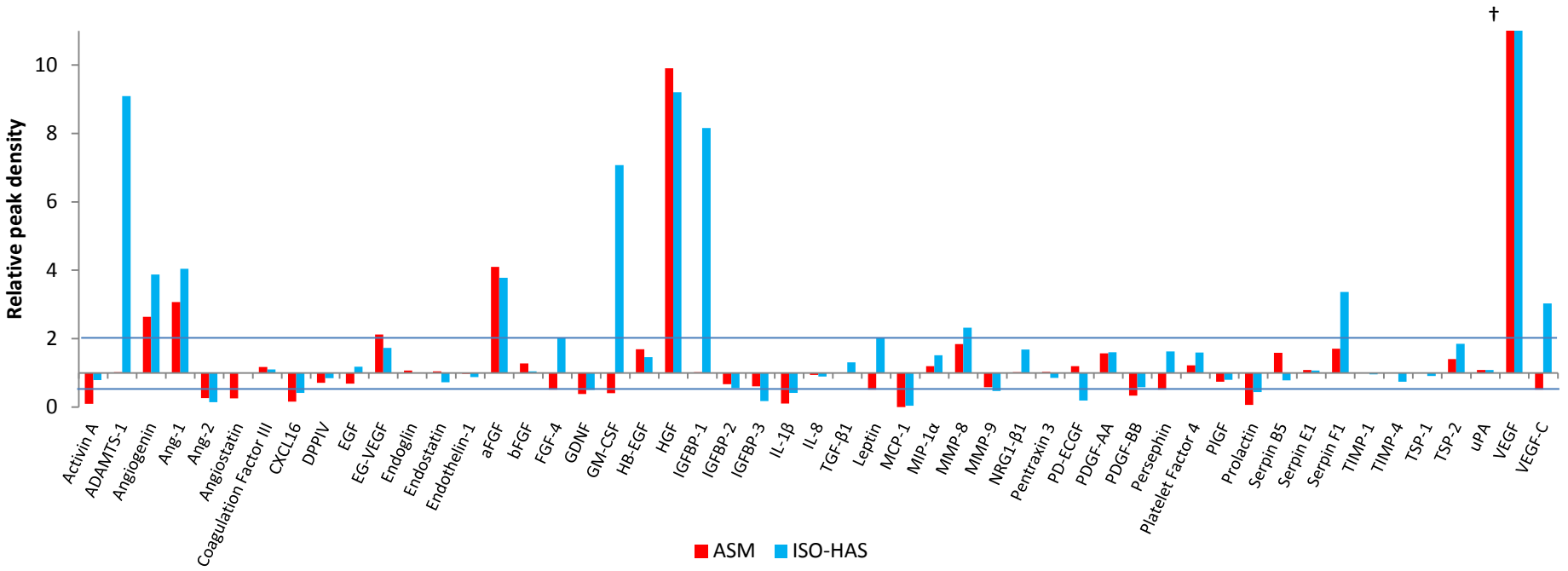

Figure 3.10: Expression profiles of angiogenesis related proteins from cells incubated overnight in hypoxic conditions (1% O_2). Data shown represents ASM and ISO-HAS peak density values expressed as a ratio of HuDMEC values. Gridlines identify proteins with a greater than two-fold difference in expression. Comparison of amphiregulin, artemin and vasohibin has not been included in this graph as expression in HuDMECs was undetected, prohibiting a direct comparison as a ratio. † VEGF data censored – ASM value 26.4; ISO-HAS value 24.9.

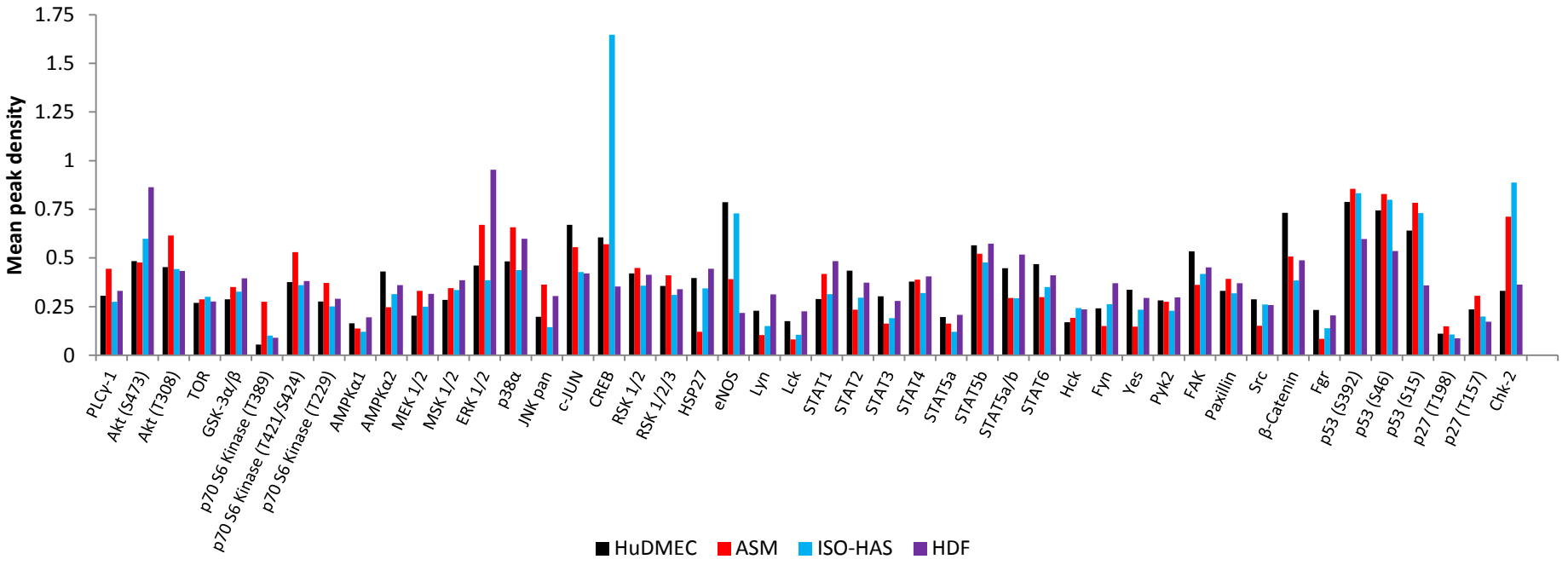

Figure 3.11: Expression profile of phosphorylated intracellular kinases in HuDMEC, ASM, ISO-HAS and HDF cell lysates. Data shown represents mean peak densities standardised relative to internal positive controls; n=2.

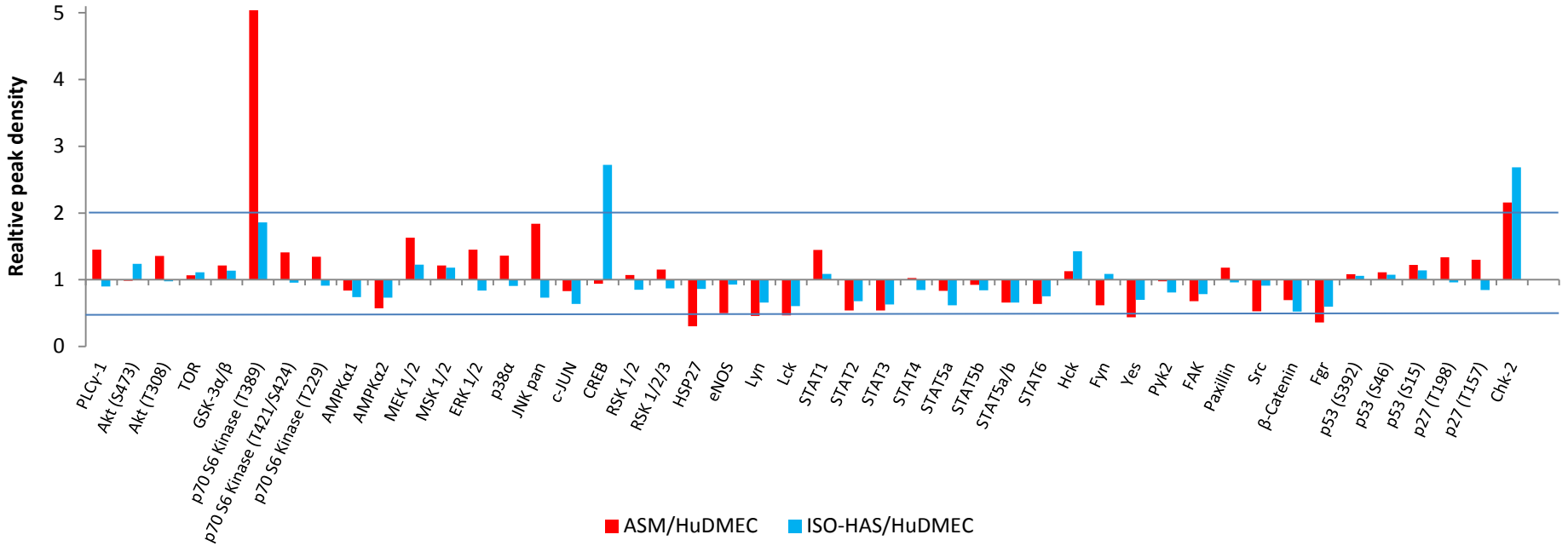

Figure 3.12: Expression profiles of phosphorylated intracellular kinases from ASM and ISO-HAS cell lysates. Data shown represents ASM and ISO-HAS peak density values expressed as a ratio of HuDMEC values. Gridlines identify proteins with a greater than two-fold difference in expression.

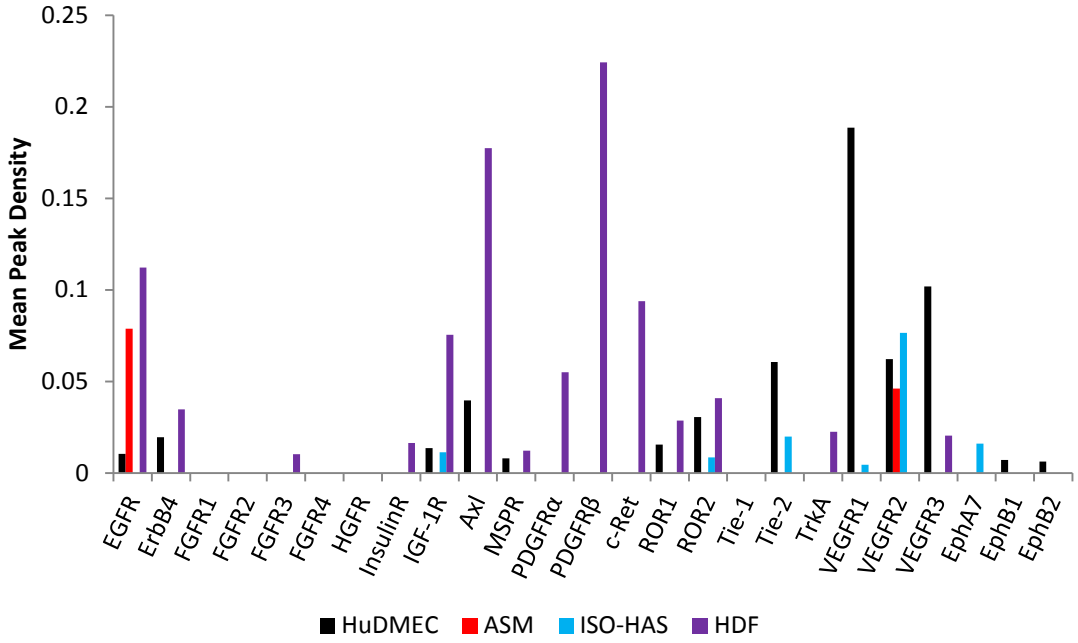

Figure 3.13: Expression profiles of basal receptor tyrosine kinase (RTK) phosphorylation in HuDMEC, ASM, ISO-HAS and HDF cell lysates. Data shown represents mean peak density standardised relative to internal positive controls; n=2. Levels of 42 RTKs were studied in total, with a summary of the positive and important negative findings shown here.

3.2.2 VEGF ELISA

The angiogenesis related protein array studies demonstrated increased VEGF in ASM and ISO-HAS cell lysates compared to HuDMECs in both normoxia and hypoxia. The secretion of VEGF into supernatant from cells incubated overnight in normoxic and hypoxic conditions (21% versus 1% O_2) was therefore quantified by ELISA (figure 3.14). These studies showed VEGF released into cell supernatant increased in hypoxic compared to normoxic conditions, but was statistically significant for ISO-HAS only (mean ± SEM VEGF secretion in pg/ml of ISO-HAS cells in normoxia vs hypoxia 149.9 ± 57.5 vs 829.4 ± 176.0 (p=0.025)). VEGF secretion in supernatant collected from ASM and ISO-HAS cells in normoxic conditions was higher than HuDMECs (mean ± SEM VEGF pg/ml HuDMEC vs ISO-HAS vs ASM cells, 23.8 ± 9.0 vs 149.9 ± 57.5 vs 179.5 ± 58.1 (p=0.07 and 0.038 respectively)). VEGF expression was significantly higher in supernatant from ASM and ISO-HAS cells incubated overnight in hypoxic conditions compared to HuDMECs (mean ± SEM VEGF pg/ml HuDMEC vs ISO-HAS vs ASM cells, 64.9 ± 31.9 vs 829.4 ± 176.0 vs 855.5 ± 309.0 (p=0.005 and 0.044 respectively)). All data was adjusted to show VEGF concentration secreted per mg of total protein in the corresponding cell lysates, as determined by the BSA assay (see section 2.4.1).

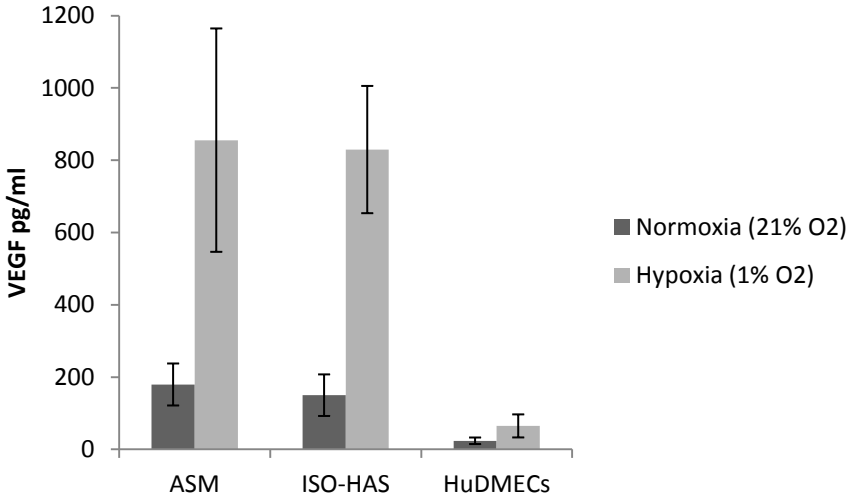

Figure 3.14: VEGF expression in ASM, ISO-HAS and HuDMEC supernatant, collected from cells incubated overnight in normoxic and hypoxic conditions. Data shown represents mean VEGF expression (pg/ml) adjusted per mg of total protein content measured in the cell lysates ± SEM; n=4.

3.2.3 Western blot studies

ASM and ISO-HAS expression of VEGF and VEGFRs was assessed by western blot.

3.2.3.1 VEGF

Cleavage of VEGFA mRNA results in different VEGFA isoforms with distinct biological characteristics: $VEGFA_{121}$, $VEGFA_{165}$ and $VEGFA_{189}$. $VEGFA_{165}$, the most biologically active isoform, is expressed as a glycosylated homodimer with a molecular weight of 42kDa; however monomers and heterodimers with other VEGFA isoforms may also occur. The expression of VEGFA in ASM and ISO-HAS cell lysates and cell supernatant was investigated by western blotting (figure 3.15). Multiple protein bands of different molecular weights were detected around 25 and 42kDa which may represent the expression of multiple VEGFA isoforms.

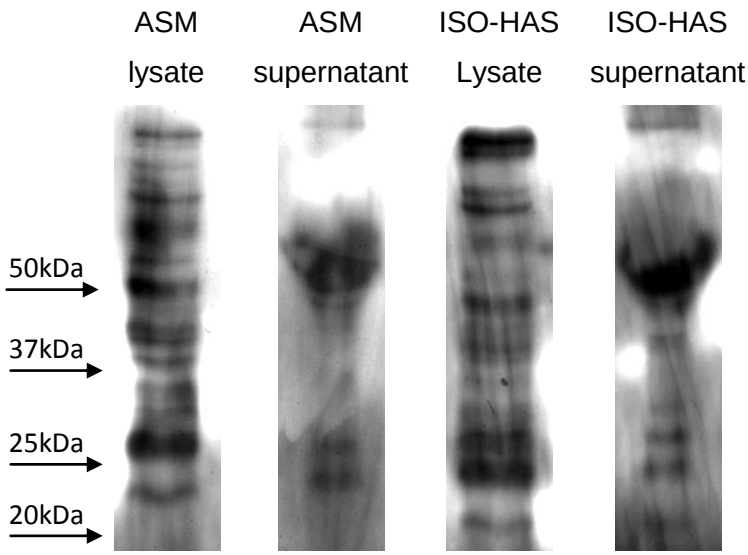

Figure 3.15: Images of western blots probing for VEGFA in ASM and ISO-HAS cell lysates and cell supernatant (concentrated x10). Blots were performed 3 times, and representative images are shown.

3.2.3.2 VEGFR2

VEGFR2 is the main receptor mediating the pro-angiogenic effects of VEGFA. Phosphorylation of VEGFR2 in ASM and ISO-HAS lysates from semi-confluent cells starved overnight in normoxia and hypoxia were investigated by western blotting (figure 3.16). These studies showed low or absent VEGFR2 phosphorylation in cells in

normoxic conditions without the addition of exogenous VEGF stimulation. VEGFR2 phosphorylation was seen in normoxic conditions following the addition of exogenous VEGF (50ng/ml). In contrast in hypoxic conditions, VEGFR2 phosphorylation was observed in ASM and ISO-HAS cells even in the absence of exogenous VEGF stimulation.

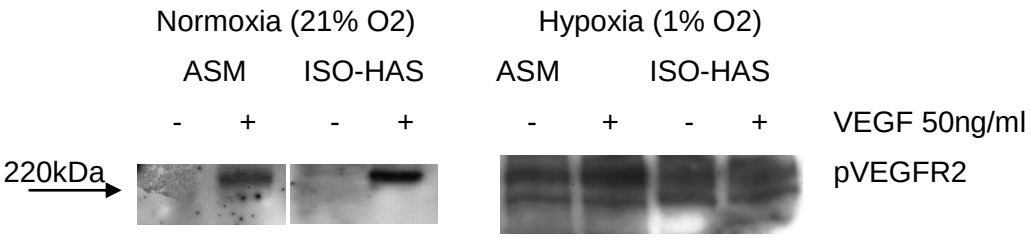

Figure 3.16: Images of western blots probing for phosphorylated VEGFR2 in ASM and ISO-HAS cells incubated overnight in normoxic or hypoxic conditions +/- stimulation with exogenous VEGF 50ng/ml 3 minutes before lysate preparation.

Despite adjustments to the working protocol described in section 2.4.3, western blot studies did not demonstrate expression of VEGFR1 in ASM, ISO-HAS or HuDMEC lysates.

3.2.4 Protein expression summary

Compared to HuDMECs, VEGF was significantly over-expressed by ASM and ISO-HAS cells, in both normoxic and hypoxic conditions. There was no evidence of autophosphorylation of VEGFR2 in ASM or ISO-HAS cells in normoxic conditions, but VEGFR2 was autophosphorylated in hypoxic conditions.

3.3 Functional Assays

Functional assays were performed to contrast the biological characteristics of ASM, ISO-HAS and HuDMEC cells. Assays were performed to compare endothelial cell proliferation using the semi-automated Vi-CELL to measure viable cell counts over time, endothelial cell differentiation by studying tubule formation on the extracellular matrix Matrigel, and cell migration using the Boyden chamber (see section 2.3).

3.3.1 Growth kinetics

The growth curves of ASM, ISO-HAS and HuDMEC cells plated in full growth media were compared at an initial seeding density of 5 x 10^4 viable cells per ml. There was a lag phase of 48 hours after seeding before mean viable cell counts increased from baseline (figure 3.17). At 72 hours after seeding, ASM and ISO-HAS growth curves separated from HuDMECs and showed an exponential growth phase, whilst HuDMEC proliferation became variable.

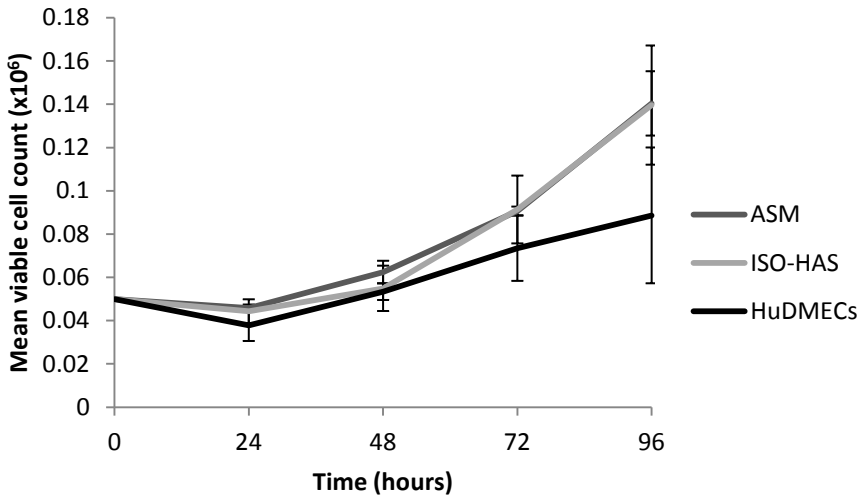

Figure 3.17: Growth curves from cells plated in full media, with an initial seeding density of 5 x 10^4 cells per ml. Viable cell counts were measured every 24 hours from seeding. Data shown represents mean viable cell count ± SEM; n=3.

3.3.2 Differentiation (tubule formation) assay

The differentiation assay, used to model angiogenesis *in vitro*, assessed endothelial tubule formation on an extracellular matrix (see section 2.3.2). Baseline studies

compared the number of tubules formed at 6 hours by HuDMEC, ASM and ISO-HAS cells on growth factor reduced basement membrane extract (Matrigel) in the presence or absence of exogenous VEGF (50ng/ml). The morphology of tubule structure was very different between cell lines. HuDMECs formed an elegant network of tubules, ISO-HAS formed numerous short tubules and ASM formed fewer, short tubules (figure 3.18 and 3.19). ASM and ISO-HAS formed significantly shorter tubules than HuDMECs (mean ± SEM difference in tubule length (arbitrary units) between HuDMECs and ASM 2.0 ± 0.3 ($p<0.001$), and between HuDMECs and ISO-HAS 1.8 ± 0.3 ($p<0.001$)). ISO-HAS and HuDMEC formed significantly more tubules than ASM cells (mean ± SEM number of tubules ASM vs ISO-HAS vs HuDMECs, 31 ± 9.5 vs 108 ± 17.2 vs 106 ± 11.7 ($p=0.006$ and 0.008 respectively)). In these studies no increase was seen in the number of tubules formed following stimulation with exogenous VEGF. The total length of the tubule network formed by ASM, ISO-HAS and HuDMECs strongly correlated with the number of tubules formed, and therefore in subsequent drug studies only the number of tubules formed was measured.

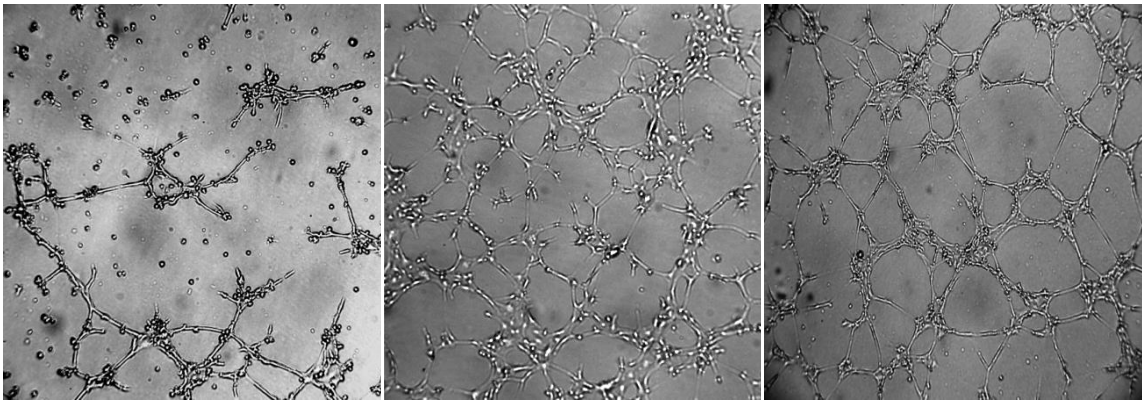

ASM ISO-HAS HuDMECs

Figure 3.18: Images of tubule formation by ASM, ISO-HAS and HuDMEC cells on Matrigel (x4 magnification).

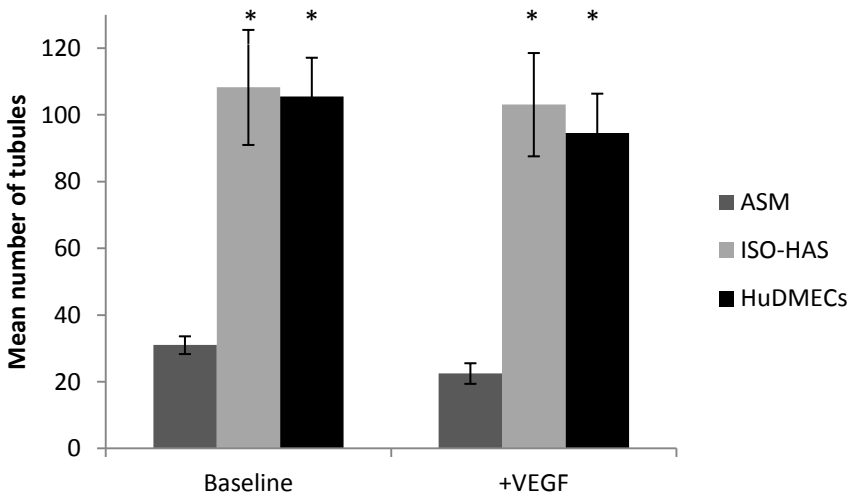

Figure 3.19: Number of tubules formed by ASM, ISO-HAS and HuDMEC cells on growth factor reduced basement membrane extract ± exogenous VEGF (50ng/ml); * increased compared to ASM ($p<0.01$), p value calculated using the independent t test. Data shown represents mean number of tubules ± SEM; n=4.

3.3.3 Migration

The Boyden chamber was used to compare the migration of endothelial cells across a porous membrane (see section 2.3.3). Studies compared the number of migrated ASM, ISO-HAS and HuDMEC cells at 4 hours, in the presence or absence of VEGF 20ng/ml added to lower chambers (figure 3.20). In the absence of VEGF, an increased number of ASM and ISO-HAS cells migrated compared to HuDMECs (mean ± SEM number per x20hpf of migrated HuDMEC vs ASM vs ISO-HAS cells, 19.6 ± 3.2 vs 91.0 ± 9.8 vs 60.7 ± 13.4 ($p=0.001$ and 0.025 respectively)). Cell migration did not increase in response to the addition of VEGF chemotractant to lower chambers in studies of ASM and ISO-HAS cell lines. In contrast, a tendency towards increased migration was observed in studies with HuDMECs (mean ± SEM number per x20hpf of migrated HuDMECs with and without VEGF 20ng/ml, 22.3 ± 2.1 and 19.6 ± 3.2 ($p=0.056$)). Comparisons between cell lines in the presence of VEGF 20ng/ml showed significantly increased ASM cells migrated, and a tendency towards increased ISO-HAS cells migrated, compared to HuDMECs (mean ± SEM number per x20hpf of migrated cells

in the presence of VEGF 20ng/ml HuDMECs vs ASM vs ISO-HAS, 22.3 ± 2.1 vs 86.2 ± 3.0 vs 57.1 ± 10.3 ($p<0.001$ and 0.075 respectively)).

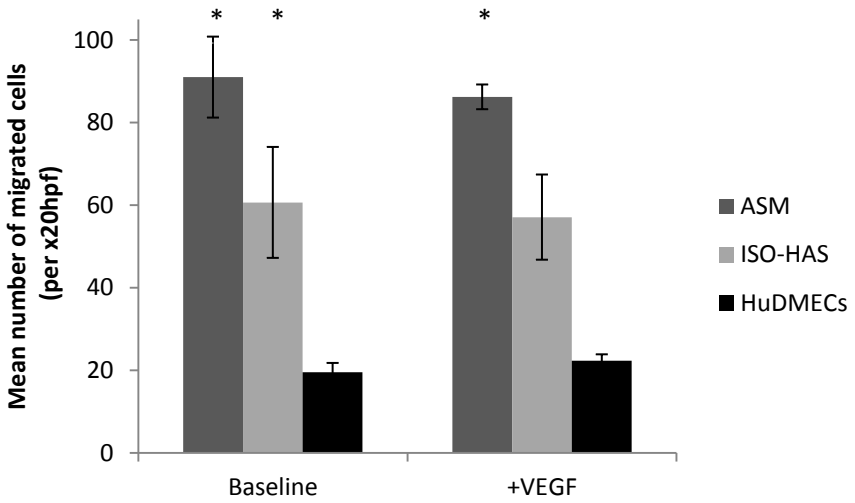

Figure 3.20: ASM, ISO-HAS and HuDMEC cell migration in Boyden chamber studies, in the presence or absence of VEGF 20ng/ml; * increased cell migration compared to HuDMECs ($p<0.05$), calculated using the independent t test. Data shown represents mean number of migrated cells per high power field (hpf) x20 magnification ± SEM; n≥3.

3.3.4 Functional assays summary

These studies demonstrated ASM and ISO-HAS cells had biological characteristics distinct from HuDMEC cells and were consistent with a malignant phenotype, including increased growth kinetics, chaotic tubule formation, and increased cell migration. These characteristics were measureable in a series of *in vitro* functional assays, which were subsequently used to quantify and compare ASM, ISO-HAS and HuDMEC cell response to vascular targeted agents.

3.4 Drug Studies

Drug studies were performed to compare the response of ASM, ISO-HAS and HuDMECs to vascular targeted agents. Baseline cell viability assays were performed to demonstrate chemosensitivity of ASM and ISO-HAS cells to doxorubicin and paclitaxel chemotherapy, which are used as first and second line agents for the treatment of advanced angiosarcoma. The effects of VEGF targeted agents were selected for study as protein array and ELISA studies identified that ASM and ISO-HAS cells expressed significantly more VEGF compared to HuDMECs. Bevacizumab, the humanised monoclonal antibody to VEGF, and the tyrosine kinase inhibitors (TKIs) axitinib and sunitinib were studied as examples of drugs targeting the VEGF signalling pathway. The MEK inhibitor selumetinib was studied after western blot studies showed persistent phosphorylation of downstream ERK in ASM and ISO-HAS cells despite the inhibition of VEGFR2 phosphorylation by VEGF targeted agents. Response to the Akt inhibitor MK2206 and mTOR inhibitor everolimus in ASM and ISO-HAS cells was investigated following results from an immunohistochemistry study by Lahat *et al* showing increased expression of pAkt, p4EBP1 and eIF4E in angiosarcoma tumour samples[168], although the phosphorylated kinase protein array studies presented here suggested only a modest increase in pAkt expression by ASM or ISO-HAS cells compared to HuDMECs, and increased p70 S6 kinase in ASM cells only. In contrast, the phosphorylated kinase array demonstrated increased phosphorylation of ChkII in ASM and ISO-HAS cells and therefore response to the ChkII inhibitor C3742 was studied. Finally, as an example of a direct vascular targeting agent, the vascular disrupting agent DMXAA was studied, with mechanisms of action distinct from the other agents selected for study.

3.4.1 Chemotherapeutic agents

Preliminary viability studies were performed to assess response of ASM cells to doxorubicin or paclitaxel chemotherapy (0 - 50ng/ml) (figure 3.21). 1 x 10^5 viable cells were seeded in full growth media and allowed 60 hours to establish before

chemotherapy agents were added. Viable cell counts were then measured using the Vi-CELL at 0, 48, 72 and 96 hours following the addition of chemotherapy. Viable cell counts 96 hours after treatment were expressed as a percentage of cell counts at 96 hours in the absence of drug (0ng/ml; Figure 3.22). From the trendlines, the half maximal inhibitory concentrations (IC_{50}) were estimated at 12.5ng/ml and 31.5ng/ml for paclitaxel and doxorubicin respectively.

All drug studies performed subsequently used the protocol described in section 2.5.1.1. 1x 10^5 viable cells were plated in full growth media and allowed 48 hours to establish. Therapeutic agents were then added and cell counts performed 120 hours later using the Vi-CELL. Further viability studies with doxorubicin and paclitaxel using this protocol confirmed a chemotherapy dose response at 120 hours of decreasing ASM and ISO-HAS % viability and viable cell counts with increasing chemotherapy dose. Estimated IC_{50} from these studies were similar to the preliminary estimates, with an IC_{50} for paclitaxel of 7.5ng/ml for both ASM and ISO-HAS and IC_{50} for doxorubicin of 22.5ng/ml and 20ng/ml for ASM and ISO-HAS respectively (figure 3.23).

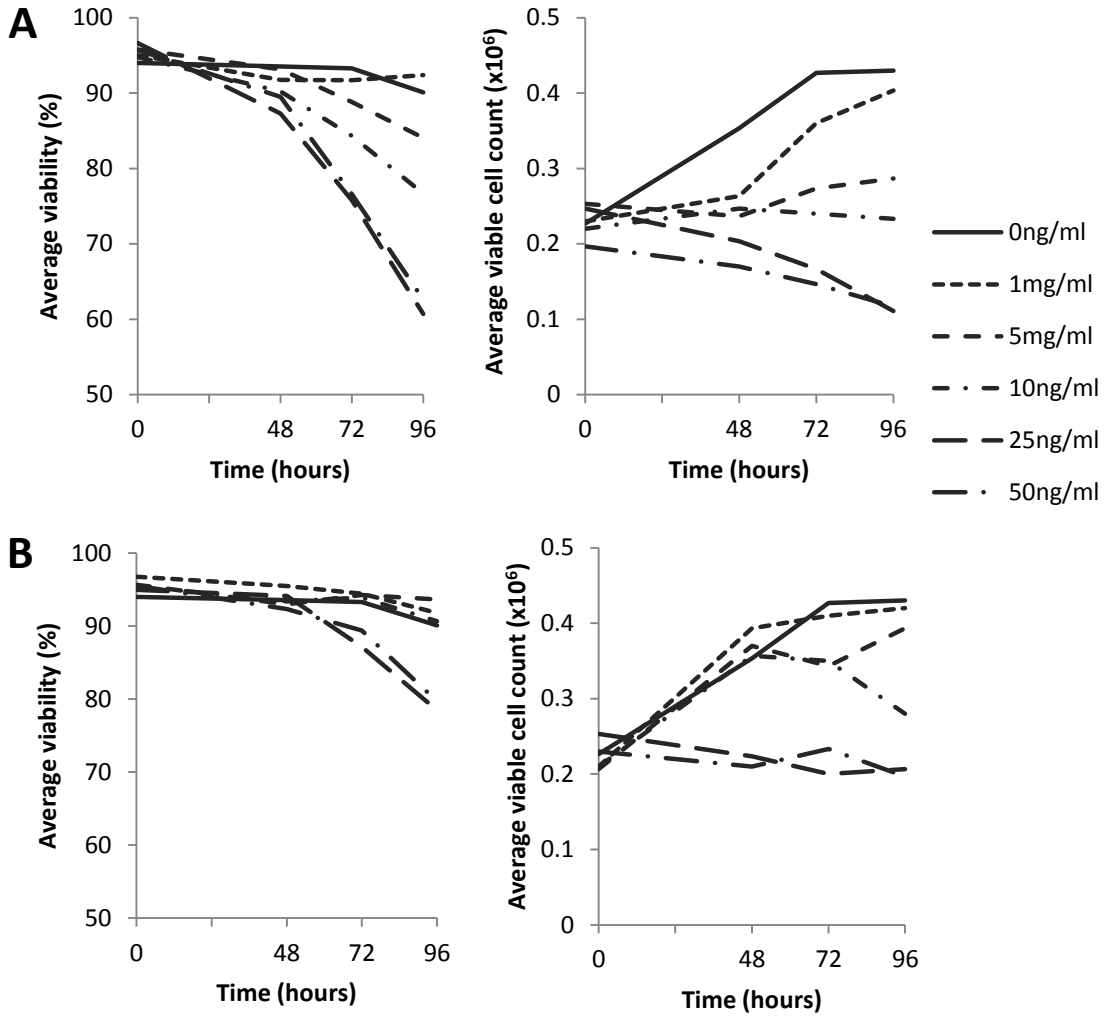

Figure 3.21: ASM viability and viable cell count at 0, 48, 72 and 96 hours after the addition of (A) paclitaxel and (B) doxorubicin. Data shown is the mean of 3 wells; n=1.

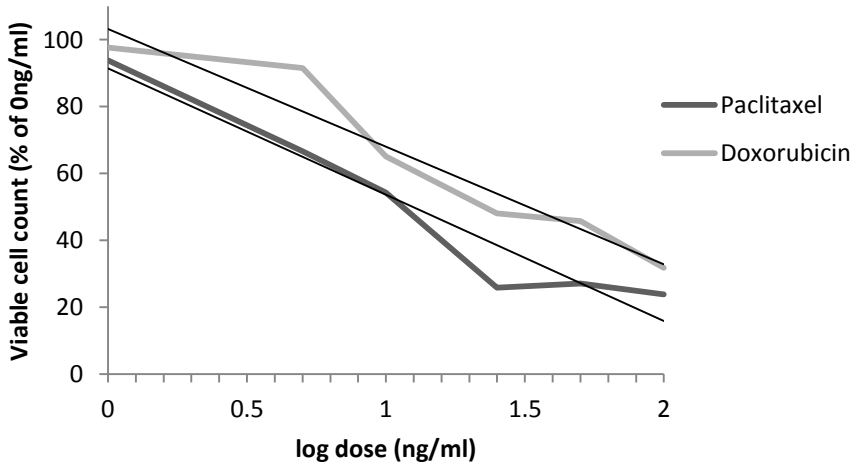

Figure 3.22: ASM viable cell count at 96 hours. Log dose response to paclitaxel and doxorubicin chemotherapy shown with trendlines fitted; n=1.

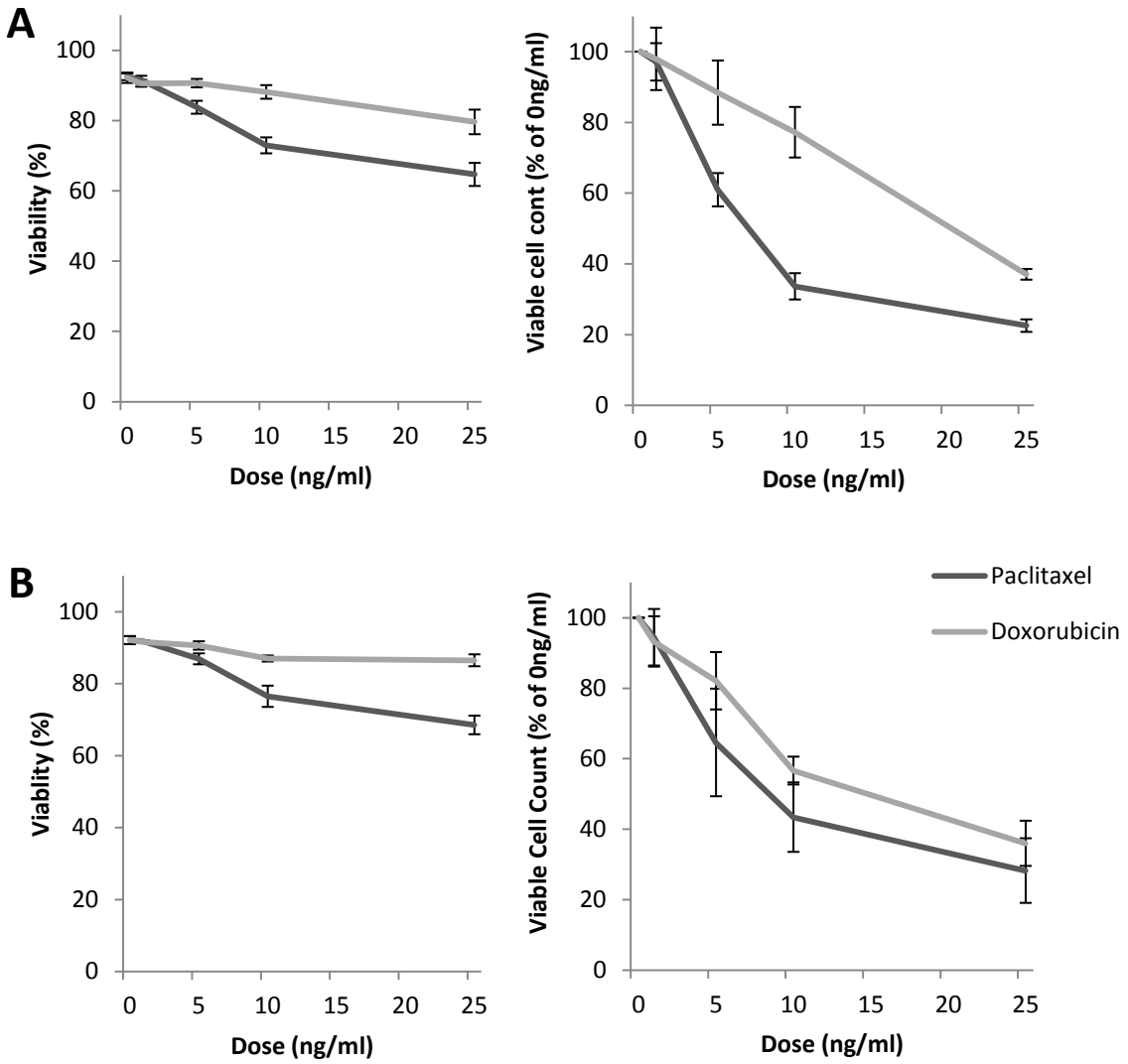

Figure 3.23: (A) ASM and (B) ISO-HAS viability and viable cell counts in response to paclitaxel and doxorubicin chemotherapy. Data shown represents mean ± SEM; n≥3.

3.4.2 VEGF targeted agents

The angiogenesis protein array and VEGF ELISA studies provided a clear rationale for studying the effects of VEGF targeted therapy.

3.4.2.1 Tyrosine kinase inhibitors

3.4.2.1.1 Cell viability studies in the presence of TKI

Response to the broad spectrum TKI sunitinib (0 - 250ng/ml) and the more selective VEGFR TKI axitinib (0 - 250ng/ml) was studied. Drug response was studied across a range of doses based on published data from phase I trials reporting a C_{max} of 72ng/ml and 63ng/ml for sunitinib and axitinib with recommended treatment doses (50mg daily and 5mg twice daily respectively)[169, 170]. Minimal responses were seen at 120 hours in ASM or ISO-HAS % viability or viable cell counts with either agent (figure 3.24A and B). Comparison studies investigated HuDMEC response to axitinib at 24 and 48 hours using the MTS assay (see section 2.5.1.2). These studies showed modest effects on HuDMEC cell viability (figure 3.25) with a trend towards decreased absorbance with increased axitinib concentrations (Kendall's tau b=-0.35, p=0.14), whilst parallel studies confirmed minimal response in ASM and ISO-HAS cells (figure 3.26). HuDMEC response to sunitinib was not studied.

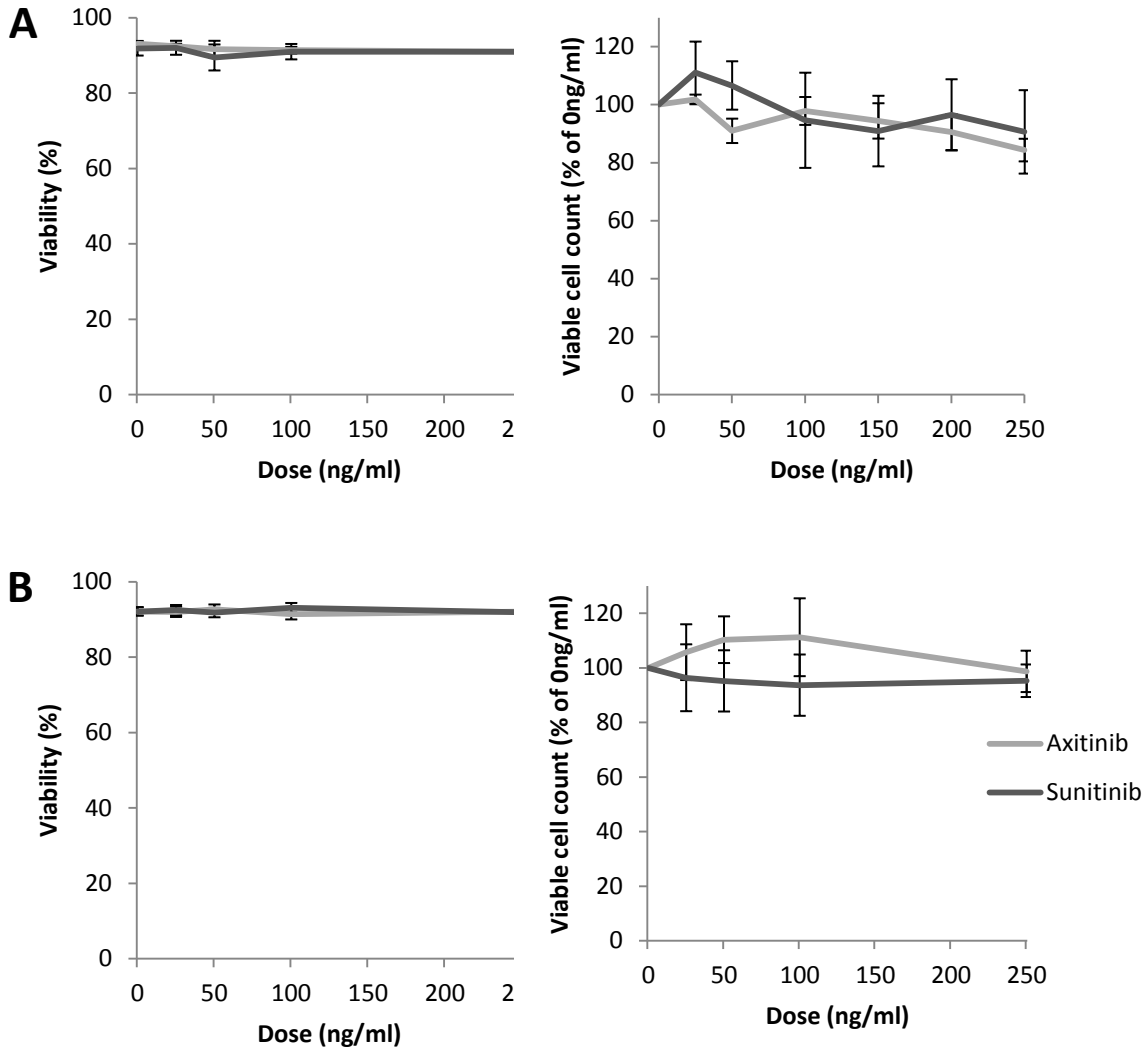

Figure 3.24: (A) ASM and (B) ISO-HAS viability and viable cell counts in response to axitinib (0 - 250ng/ml) and sunitinib (0 - 250ng/ml). Data shown represents mean ± SEM; n≥3.

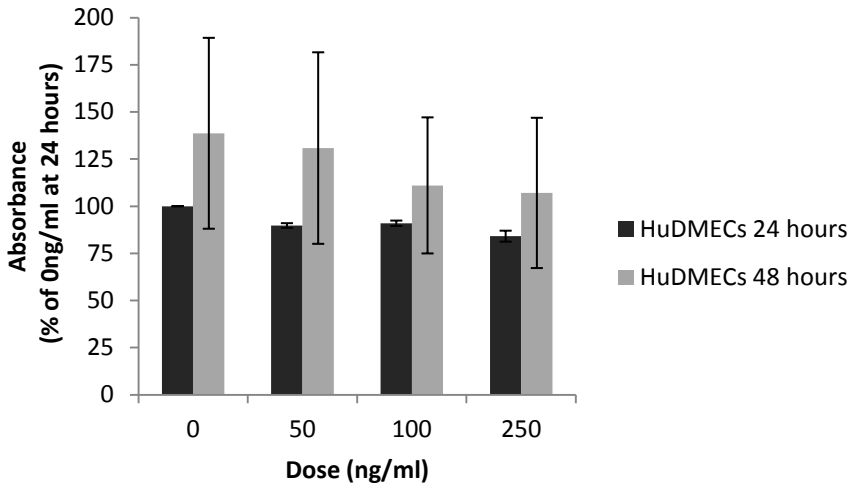

Figure 3.25: MTS assay of HuDMECs with axitinib (0 - 250ng/ml). Absorbance was measured at 24 and 48 hours. Data shown represents mean relative absorbance expressed as a % of baseline (0ng/ml at 24 hours) ± SEM; n=3.

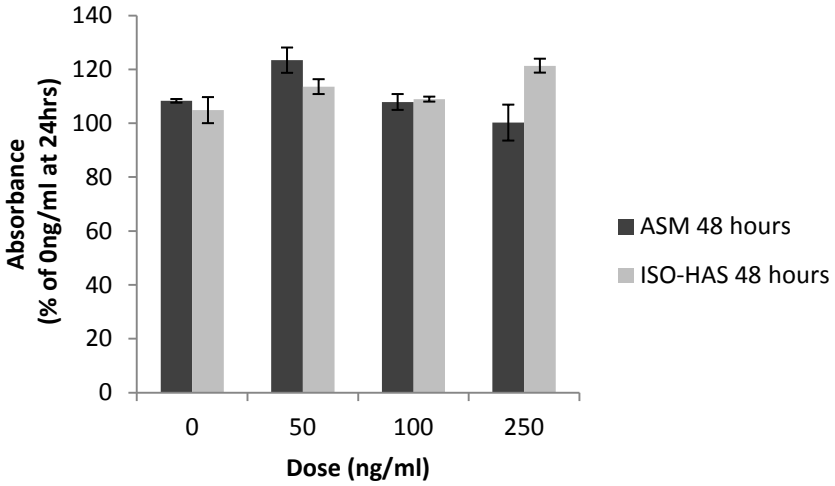

Figure 3.26: MTS assay of ASM and ISO-HAS with axitinib (0 - 250ng/ml). Data shown represents mean relative absorbance at 48 hours expressed as a % of baseline (0ng/ml at 24 hours) ± SEM; n≥2.

As minimal response in viable cell counts were observed in TKI studies (0 - 250ng/ml) with ASM and ISO-HAS, studies were performed using extended drug doses (up to 10,000ng/ml). Significantly reduced viable cell counts were observed at doses over 500ng/ml suggesting off target effects (figure 3.27).

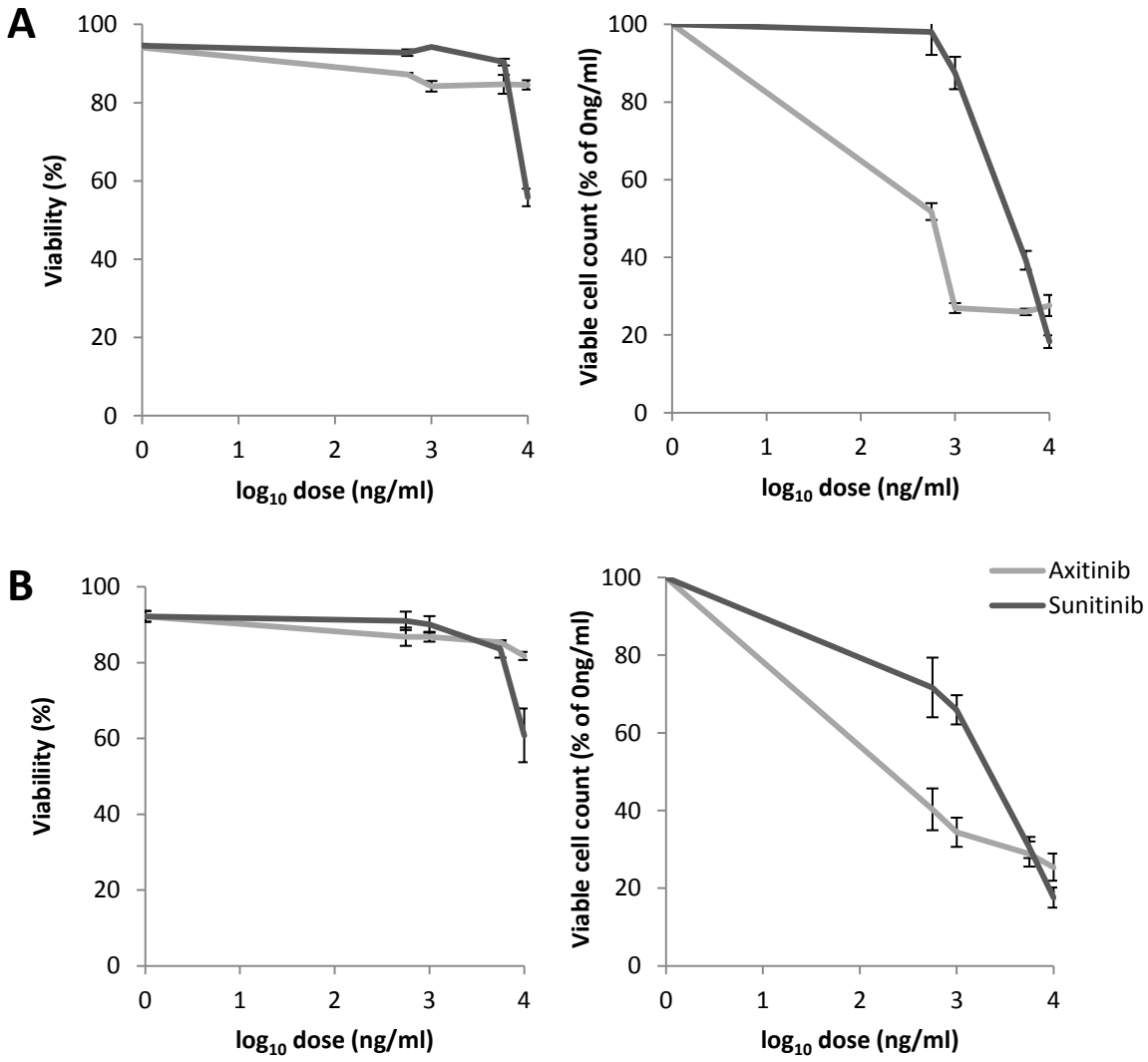

Figure 3.27: (A) ASM and (B) ISO-HAS viability and viable cell counts in extended dose studies (0 - 10,000ng/ml) with axitinib and sunitinib. Data shown represents mean ± SEM; n=3. TKI dose is shown on a logarithmic scale.

Studies were then performed to investigate any changes in ASM and ISO-HAS viable cell counts with TKI and chemotherapy drug combinations. In order to explore these effects, the dose of paclitaxel used (5ng/ml) was below the estimated IC_{50} and this was combined with axitinib (0 - 50ng/ml) and sunitinib (0 - 50ng/ml). Although responses to single agent TKI were demonstrated using higher doses, it was decided more clinically relevant doses should be used when testing in combination with chemotherapy. These studies suggested the effect of combining TKI with cytotoxic chemotherapy was additive rather than synergistic (figure 3.28).

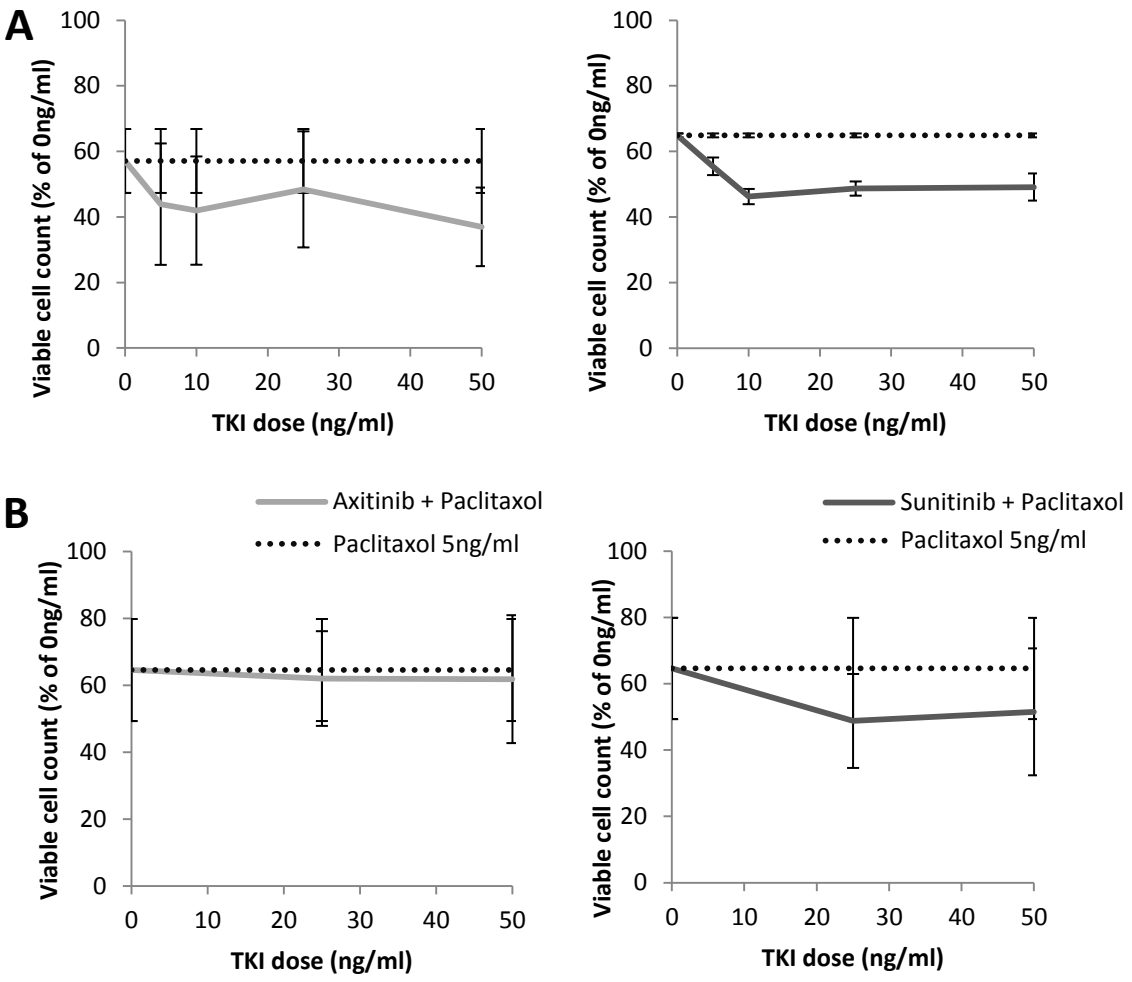

Figure 3.28: (A) ASM and (B) ISO-HAS viability and viable cell counts in response to combination therapy with TKI (0 - 50ng/m) and paclitaxel chemotherapy (5ng/ml). Data shown represents mean ± SEM; n=3.

3.4.2.1.2 Cell differentiation studies in the presence of TKI

Studies were then performed to compare the biological effects of TKIs on endothelial cell function in differentiation (tubule formation), migration and invasion assays. Axitinib, as a selective and more potent inhibitor of VEGFR phosphorylation than sunitinib, was chosen for further study using these assays. Response to axitinib 0ng/ml, 50ng/ml and 250ng/ml were compared; 0ng/ml as a control, 50ng/ml as a clinically relevant dose, and 250ng/ml as a dose that demonstrated modest evidence of efficacy in cell viability assays with ASM and HUDMEC cells.

The number of tubules formed by ASM, ISO-HAS and HuDMEC cells on growth factor reduced Matrigel, in response to axitinib (0 – 250ng/ml) with or without the addition of exogenous VEGF (50ng/ml), were compared to assess drug response *in vitro* (see section 2.3.2). Consistent with the baseline differentiation studies previously described (see section 3.3.2), the endothelial cell lines developed distinct patterns of tubule formation, and exogenous VEGF did not affect these.

Axitinib, in the presence and absence of exogenous VEGF 50ng/ml, did not significantly reduce the number of tubules formed by ASM cells at the doses studied (figure 3.29).

Axitinib 50ng/ml significantly reduced the number of tubules formed by ISO-HAS cells (mean ± SEM difference between the number of tubules formed by ISO-HAS cells with axitinib 0ng/ml and 50ng/ml, 44.2 ± 12.4 (p=0.038)). This inhibition was not reversed by adding VEGF, with a trend towards fewer tubules with increasing axitinib concentrations in the presence of exogenous VEGF 50ng/ml (Kendall's tau b=-0.64, p=0.008). Other paired comparisons of the number of ISO-HAS tubules formed however were not statistically significant.

Compared to axitinib 0ng/ml, fewer tubules were formed by HuDMECs with axitinib 50ng/ml (p=0.058) and 250ng/ml (p=0.071) (Kendall's tau b=-0.45, p=0.07). A trend towards fewer HuDMEC tubules with increasing axitinib concentration was also seen in

the presence of exogenous VEGF 50ng/ml (Kendall's tau b=-0.36, p=0.14), with significantly fewer HuDMEC tubules formed with axitinib 250ng/ml compared with axitinib 0ng/ml (mean ± SEM difference in the number of HuDMEC tubules formed with axitinib 0ng/ml and axitinib 250ng/ml in the presence of exogenous VEGF 50ng/ml, 23.4 ± 5.1 (p=0.019)).

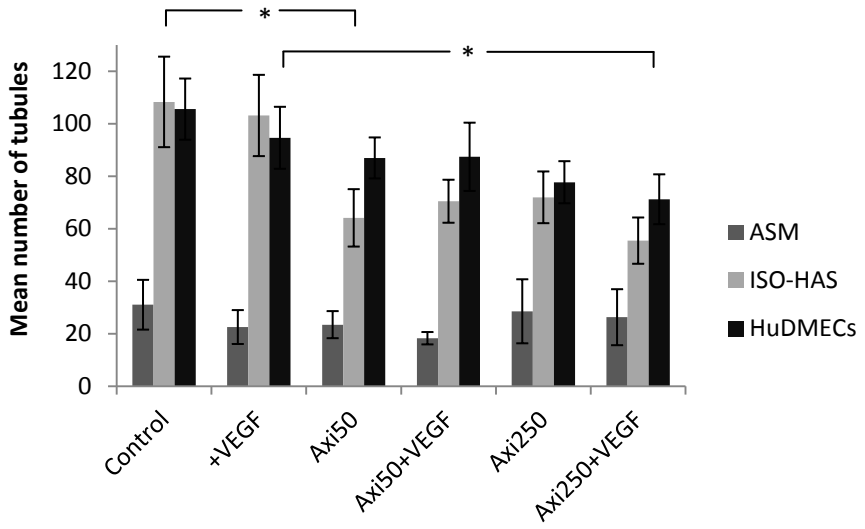

Figure 3.29: Number of tubules formed in the differentiation assay with axitinib (0 - 250ng/ml) ± VEGF (50ng/ml); * decreased tubule formation ($p<0.05$), calculated using the paired t test; comparisons between ISO-HAS cells with axitinib 0ng/ml and 50ng/ml, and between HuDMEC cells with axitinib 0ng/ml and 250ng/ml in the presence of exogenous VEGF are shown. Data shown represents mean ± SEM; n=4.

3.4.2.1.3 Cell migration studies in the presence of TKI

Endothelial cell migration was assessed using the Boyden chamber assay (see section 2.5.2.2). Consistent with the baseline migration studies previously described (see section 3.3.3), ASM, ISO-HAS and HuDMECs demonstrated distinct patterns of migration (figure 3.30). Cell migration was not significantly altered in the presence of exogenous VEGF 20ng/ml; HuDMEC cell migration was increased but not significantly (p=0.11)

A dose dependent inhibition of HuDMEC migration was seen with increasing axitinib dose, but results were not significant (Kendall's tau b=-0.55, p=0.059). In the presence of exogenous VEGF, a significant dose dependent inhibition of HuDMEC migration was observed (Kendall's tau b=-0.72, p=0.014) (mean ± SEM number per hpf of migrated HuDMECs in the presence of exogenous VEGF 20ng/ml with axitinib 0ng/ml vs axitinib 50ng/ml vs axitinib 250ng/ml, 22.8 ± 2.1 vs 16.0 ± 3.7 vs 8.3 ± 1.2 (p=0.085 and 0.013 respectively)). In contrast, axitinib at 50ng/ml or 250ng/ml did not significantly inhibit ASM or ISO-HAS cell migration, either in the presence or absence of exogenous VEGF.

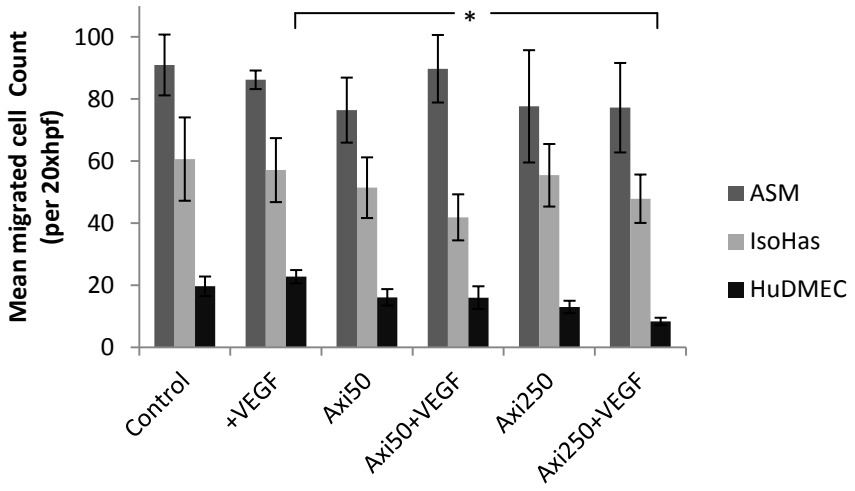

Figure 3.30: Number of migrated ASM, ISO-HAS and HuDMEC cells seen per x20 hpf with the addition of axitinib 0ng, 50ng and 250ng/ml ± the chemoattractant VEGF 20ng/ml; * decreased HuDMEC migration ($p<0.05$), calculated using the paired t test. Data shown represents mean ± SEM; n=3.

3.4.2.1.4 Cell invasion studies in the presence of TKI

Invasion was assessed using a modified trans-well assay in a 96-well plate format (see section 2.5.2.3). A plate reader was used to quantify the cellular conversion of Calcein-AM to fluorescent Calcein in lower wells, to estimate the number of viable endothelial cells that invaded through from upper chambers across a porous membrane coated in a basement membrane extract.

Control studies with ASM, ISO-HAS and HuDMEC cells in axitinib 0ng/ml contrasted with results from the Boyden chamber migration assays (figure 3.31). Results showed a similar number of ASM and HuDMEC cells invaded across the basement membrane extract, but significantly fewer ISO-HAS cells (mean ± SEM number of invaded ISO-HAS vs ASM vs HuDMEC cells, 598 ± 120 vs 1739 ± 229 vs 1583 ± 311 ($p=0.012$ and 0.042 respectively)). Furthermore no significant increase in cell invasion was seen by either cell line in response to the chemotractant VEGF (20ng/ml).

No significant differences were seen in fluorescent readings in response to axitinib 50ng/ml or 250mg/ml, with or without the addition of exogenous VEGF (20ng/ml), and correspondingly therefore there were also no significant differences in the estimated number of invaded cells (figure 3.). Fluorescent readings with ASM cells decreased with the addition of axitinib 50ng/ml, however these differences were not significant (mean ± SEM difference in fluorescence between ASM cells with axitinib 0ng/ml and axitinib 50ng/ml 22.6 ± 12.1 ($p=0.20$)).

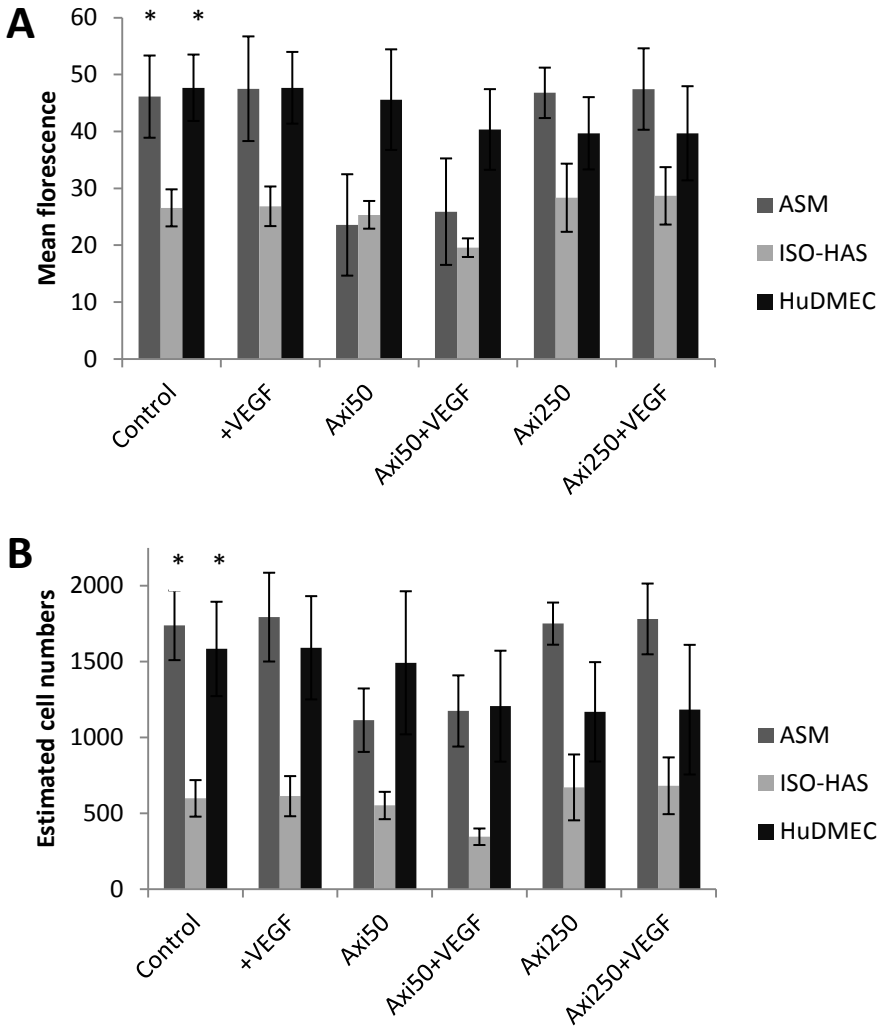

Figure 3.31: Invasion assay results comparing baseline studies with the addition of axitinib 50ng/ml or 250ng/ml, ± VEGF 20ng/ml. (A) mean fluorescence (raw data) and (B) fluorescence readings expressed as estimated cell numbers (using the equations shown in section 2.5.2.3); * increased ASM and HuDMEC cell invasion compared to ISO-HAS ($p<0.05$), calculated using the independent t test. Data shown represents mean ± SEM; n=3.

3.4.2.2 Bevacizumab

Preliminary studies were performed to assess endothelial cell response to the humanised monoclonal antibody to VEGF bevacizumab 5mg/ml, however in control studies, similar endothelial cell responses were also seen with 5mg/ml drug vehicle (51mM sodium phosphate and 60mg/ml trehalose dehydrate (pH 6.2) and 0.04%

Tween[164]; see section 2.5). A Boyden chamber migration study was performed to assess endothelial cell response to serial dilutions of the bevacizumab control vehicle. This study identified 0.25mg/ml of vehicle as the maximum dose with no significant effect on cell migration compared to vehicle free. Response to bevacizumab 0.25mg/ml has previously been studied *in vitro* in assays with retinal microvascular endothelial cells[171], and was therefore selected as an appropriate dose for further study. Only modest responses were seen in these subsequent studies, and therefore the effects of bevacizumab at doses lower than 0.25mg/ml were not assessed.

3.4.2.2.1 Cell viability studies in the presence of bevacizumab

The effects of bevacizumab (0.25mg/ml) on ASM and ISO-HAS cell viability were measured with the trypan blue dye exclusion assays using the Vi-CELL (see section 2.5.1.1) in both single agent and drug combination studies with paclitaxel (5ng/ml). No significant differences were seen in viable cell counts compared to control vehicle in either monotherapy or combination studies with chemotherapy (figure 3.32). In these studies the response to paclitaxel chemotherapy by ISO-HAS was less than that observed in the initial chemotherapy studies previously described (figure 3.23). This was repeated using cells recovered from a different vial of ISO-HAS cells stored in liquid nitrogen, but similar results were found.

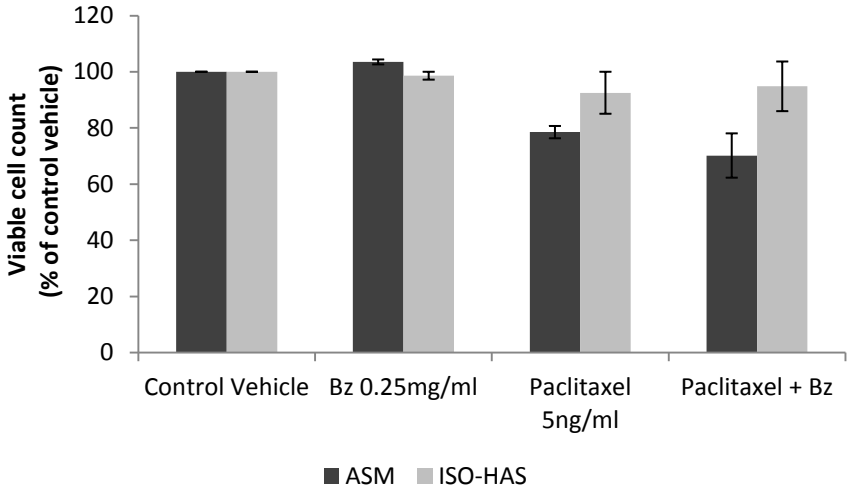

Figure 3.32: Viable cell counts for ASM and ISO-HAS in response to bevacizumab (Bz) 0.25mg/ml ± paclitaxel 5ng/ml. No significant differences were seen in response to bevacizumab. Data shown represents mean ± SEM; n=3.

Comparison studies were performed to investigate the effects of bevacizumab on HuDMEC viability using the MTS assay (see section 2.5.1.2). These studies demonstrated no significant changes in viability or proliferation at 24 and 48 hours (figure 3.33). Parallel studies confirmed minimal response to bevacizumab in ASM and ISO-HAS cells (figure 3.34).

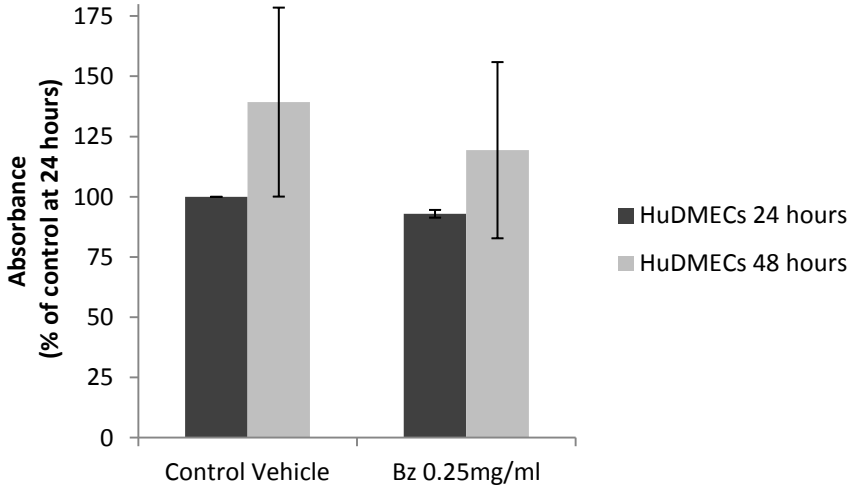

Figure 3.33: MTS assay of HuDMECs with bevacizumab (Bz) 0.25mg/ml. Absorbance was measured at 24 and 48 hours. Data shown represents mean relative absorbance expressed as a % of baseline (control vehicle at 24 hours) ± SEM; n=4.

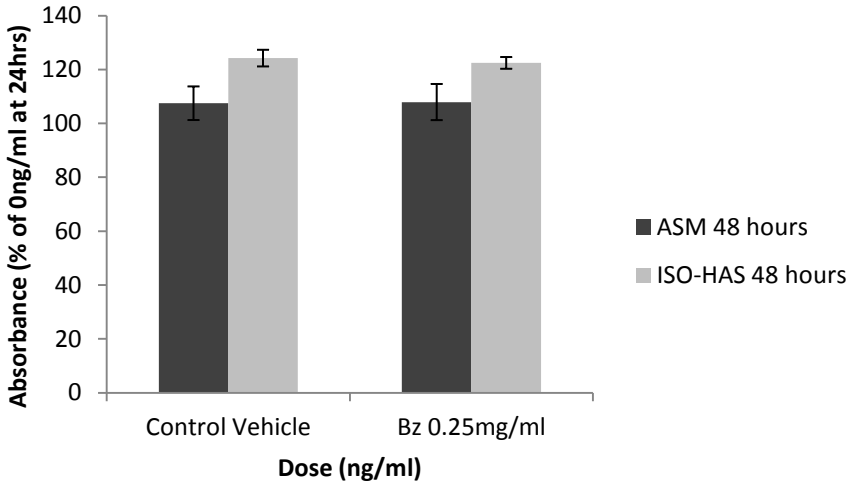

Figure 3.34: MTS assay of ASM and ISO-HAS with bevacizumab (Bz) 0.25mg/ml. Data shown represents mean relative absorbance at 48 hours expressed as a % of baseline (control vehicle at 24 hours) ± SEM; n≥2.

3.4.2.2.2 Cell differentiation studies in the presence of bevacizumab

ASM, ISO-HAS and HuDMEC cell response to bevacizumab 0.25mg/ml was studied in differentiation assays at 6 hours (see section 2.5.2.1). Endothelial cell tubule formation was similar to baseline studies. In the bevacizumab studies the number of tubules formed by ASM and ISO-HAS cells did not differ significantly with the addition of VEGF (50ng/ml), however the number of tubules formed by HuDMEC cells significantly increased in response to VEGF (mean ± SEM number of HuDMEC tubules formed in control vehicle vs control vehicle plus VEGF 50ng/ml, 57 ± 5.1 vs 75 ± 7.4 (p=0.019)) (figure 3.35).

No significant change was observed in the number of ASM or ISO-HAS tubules formed in response to bevacizumab 0.25mg/ml, either in the presence or absence of exogenous VEGF (figure 3.35). In contrast, bevacizumab 0.25mg/ml inhibited HuDMEC tubule formation stimulated by VEGF 50ng/ml (mean ± SEM number of HuDMEC tubules formed in control vehicle vs bevacizumab 0.25mg/ml + VEGF 50ng/ml, 57 ± 5.1 vs 51 ± 8.1 (p=0.67)).

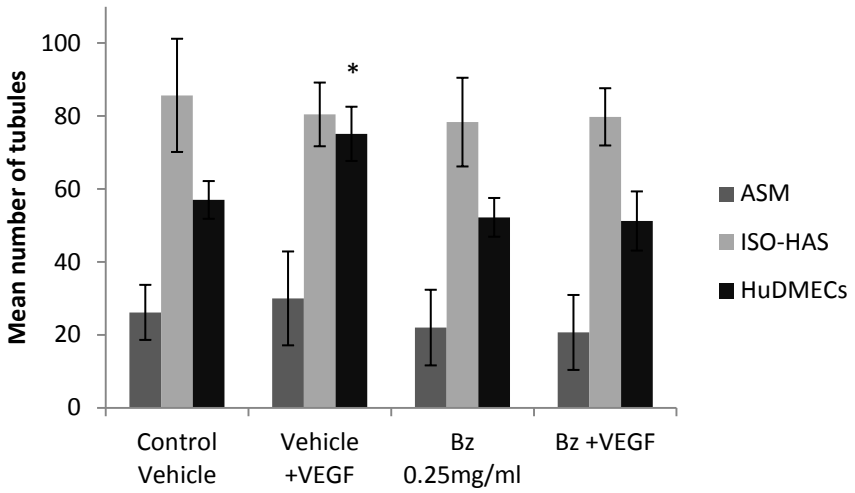

Figure 3.35: Number of tubules formed in the differentiation assay with bevacizumab (Bz) 0.25mg/ml ± VEGF 50ng/ml; * increased number of tubules formed by HuDMEC cells in response to VEGF stimulation ($p<0.05$), calculated using the paired t test. Data shown represents mean ± SEM; $n \geq 3$.

3.4.2.2.3 Cell migration studies in the presence of bevacizumab

Cell migration was assessed using the Boyden chamber (see section 2.3.3). Cell migration was similar to baseline studies. The number of migrated ASM or ISO-HAS cells did not significantly increase with the addition of VEGF (20ng/ml) however, the number of migrated HuDMEC cells significantly increased in response to stimulation with VEGF (mean ± SEM number per 20x hpf of migrated HuDMEC cells with bevacizumab 0ng/ml vs bevacizumab 0ng/ml plus VEGF 20ng/ml, 14 ± 2.2 vs 23 ± 2.6 ($p=0.022$)) (figure 3.36).

No significant change was observed in the number of migrated ASM or ISO-HAS cells in response to bevacizumab 0.25mg/ml (figure 3.36). In contrast Bevacizumab 0.25mg/ml significantly inhibited VEGF stimulated HuDMEC cell migration, and reduced HuDMEC migration to levels below the established baseline (mean number of migrated HuDMEC cells per 20x hpf with control vehicle vs bevacizumab 0.25mg/ml plus VEGF 20ng/ml 14 +/- 2.2 vs 10 +/- 1.6 ($p=0.028$)).

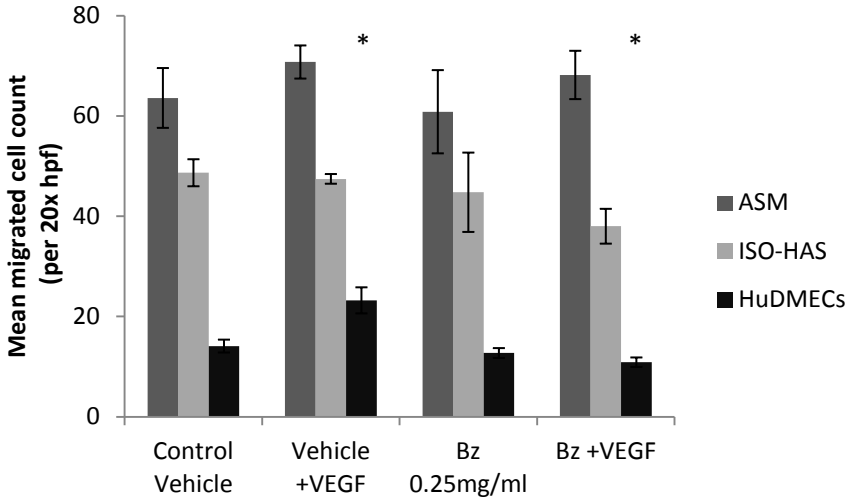

Figure 3.36: Number of migrated ASM, ISO-HAS and HuDMEC cells per x20 hpf with bevacizumab (Bz) 0.25 mg/ml ± the chemotractant VEGF 20ng/ml; * significant difference in HuDMEC cell migration compared to control ($p<0.05$), calculated using the paired t test. Data shown represents mean ± SEM; n≥3.

3.4.2.3 VEGF targeted agents in hypoxia

Tumours are typically hypoxic. Hypoxia stimulates the expression of VEGF and thus tumour angiogenesis. The VEGF ELISA studies showed a dramatic increase in ASM and ISO-HAS expression of VEGF in hypoxia (1% O_2) compared to HuDMECs (figure 3.14). Drug studies were therefore performed to assess the response of ASM and ISO-HAS to VEGF targeted therapy in hypoxic conditions. HuDMECs did not tolerate hypoxic conditions of 1% O_2 well, and their response to VEGF targeted therapy was therefore not assessed.

3.4.2.3.1 Cell viability in hypoxia

Cell viability was assessed using the trypan blue dye exclusion assay with viable cell counts measured 120 hours after the addition of drugs (see section 2.5.1.1). ASM and ISO-HAS % viability and viable cell counts were lower in hypoxia (1% O_2) than normoxia (21% O_2) (table 3.3).

		Normoxia (21% O_2)	Hypoxia (1% O_2)	*p*
ASM	Viability (%)	91.8 ± 1.6	78.7 ± 6.0	0.054
	Viable cell count (x10^6)	0.36 ± 0.04	0.15 ± 0.01	0.004
ISO-HAS	% viability	92.1 ± 1.1	66.8 ± 8.3	0.09
	Viable cell count (x10^6)	0.24 ± 0.05	0.15 ± 0.07	0.31

Table 3.3: ASM and ISO-HAS % viability and viable cell counts in normoxia (21% O_2) and hypoxia (1% O_2); *p* values calculated using the independent t test. Data shown represents mean ± SEM; n=3.

As shown in figure 3.37 axitinib 50ng and 250ng/ml, and bevacizumab 0.25mg/ml did not significantly alter ASM or ISO-HAS viable cell counts in hypoxia (1% O_2).

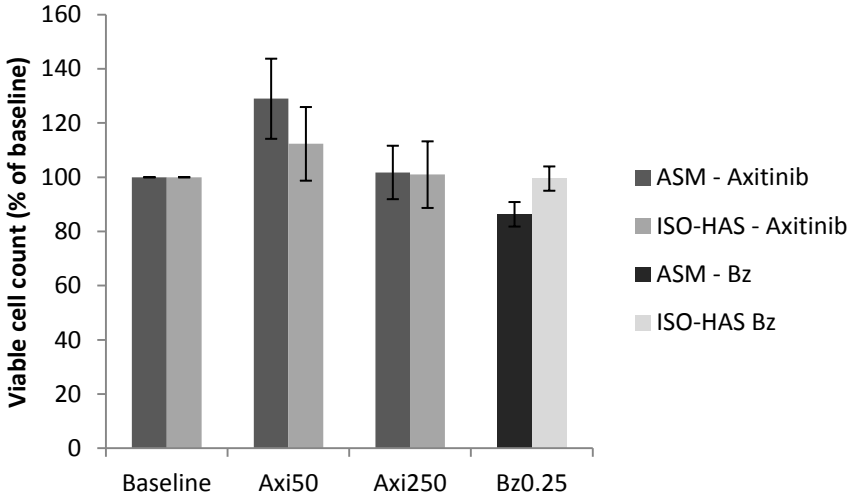

Figure 3.37: ASM and ISO-HAS viable cell counts in hypoxia (1% O_2) without VEGF targeted agents, and with the addition of axitinib 50ng/ml, 250ng/ml, and bevacizumab 0.25mg/ml. Data represents mean ± SEM; n=3.

3.4.2.3.2 Cell differentiation in hypoxia

Studies were performed to quantify changes in the number of tubules formed by ASM and ISO-HAS cells in hypoxia (1% O_2). Both ASM and ISO-HAS cells formed fewer tubules in hypoxia than normoxia but these differences were not significant, and as in normoxia, ASM cells formed fewer tubules than ISO-HAS. No significant differences were observed between the numbers of tubules formed by ASM or ISO-HAS cells in hypoxia in baseline studies, with exogenous VEGF (50ng/ml), or with the addition of axitinib 50ng or 250ng/ml, or bevacizumab 0.25mg/ml (figure 3.38A and B).

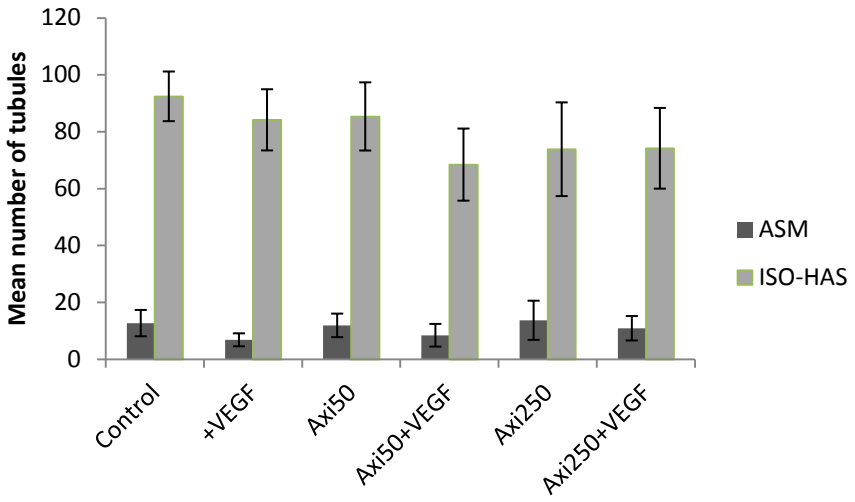

Figure 3.38A: Number of tubules formed by ASM and ISO-HAS cells in hypoxia (1% O_2) with axitinib 50ng/ml and 250ng/ml ± VEGF 50ng/ml. Data shown represents mean ± SEM; n=3.

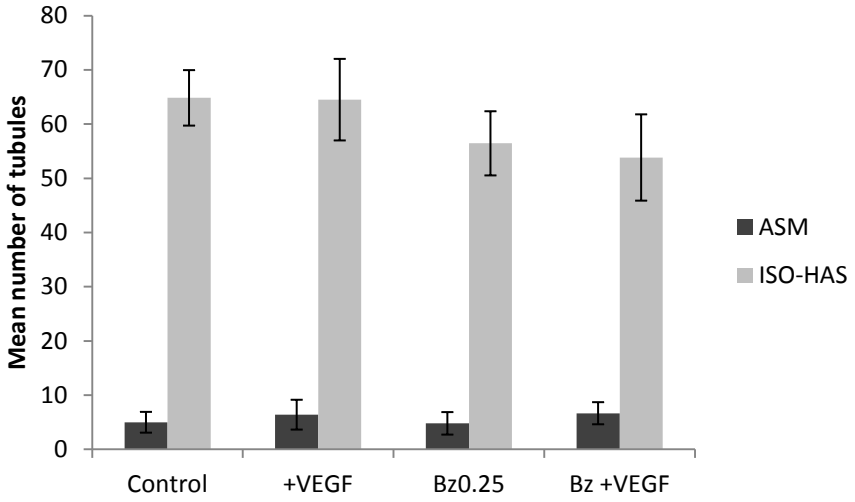

Figure 3.38B: Number of tubules formed by ASM and ISO-HAS cells in hypoxia (1% O_2) with bevacizumab 0.25mg/ml ± VEGF 50ng/ml. Data shown represents mean ± SEM; n=3.

3.4.2.4 Endothelial cell differentiation with ASM and ISO-HAS conditioned media

The protein expression studies demonstrated ASM and ISO-HAS cells secreted a broad panel of pro-angiogenic growth factors (figure 3.8), and increased VEGF secretion under hypoxic conditions (figure 3.14). Malignant endothelial cell secretion of pro-angiogenic growth factors may promote tumour growth through autocrine or paracrine stimulation of malignant endothelial cells. However, these growth factors may also stimulate other cells within the tumour microenvironment including non-neoplastic endothelial cells. An exploratory study was performed to investigate whether growth factors secreted by ASM and ISO-HAS would stimulate a response in non-malignant endothelial cells. The cell differentiation assay was used to assess the response of HuVECs to ASM or ISO-HAS cell conditioned media at 6 hours, and to assess whether VEGF targeted therapy (axitinib or bevacizumab) would inhibit any response. HuVECs rather than HuDMECs were used for this study, as HuDMECs were not available within the laboratory at that time.

A small reduction was observed in the number of HuVEC tubules formed in response to exogenous VEGF (20ng/ml). In contrast, an increase in the number of HuVEC

tubules was seen with both ASM and ISO-HAS cell conditioned media. This increase was reduced by the addition of axitinib 50ng/ml or 250ng/ml, and to a lesser extent by bevacizumab 0.25mg/ml.

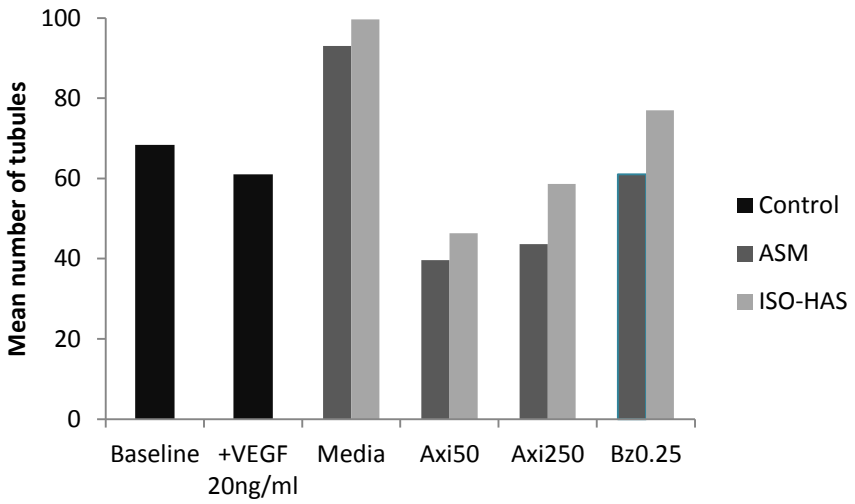

Figure 3.39: Number of tubules formed by HuVECs in control studies (baseline and in response to exogenous VEGF 20ng/ml), and following the addition of ASM or ISO-HAS conditioned media, and with conditioned media plus axitinib 50ng/ml, 250ng/ml and bevacizumab 0.25mg/ml. Data shown represents mean number of tubules from 3 wells; n=1.

3.4.2.5 VEGFR2 phosphorylation status

As the observed responses to axitinib and bevacizumab in functional assays with ASM and ISO-HAS cells were minimal, a series of western blots were performed to assess change in VEGFR2 phosphorylation status (pVEGFR2) following stimulation with VEGF in cells pre-incubated in axitinib and bevacizumab (figure 3.40). These studies demonstrated pVEGFR2 was undetectable in the absence of exogenous VEGF stimulation. VEGFR2 phosphorylation was observed following stimulation with VEGF 50ng/ml, which was reduced following treatment with axitinib 50ng/ml, 250ng/ml, and with bevacizumab 0.25mg/ml, indicating a biological effect of VEGF targeted agents on these cells.

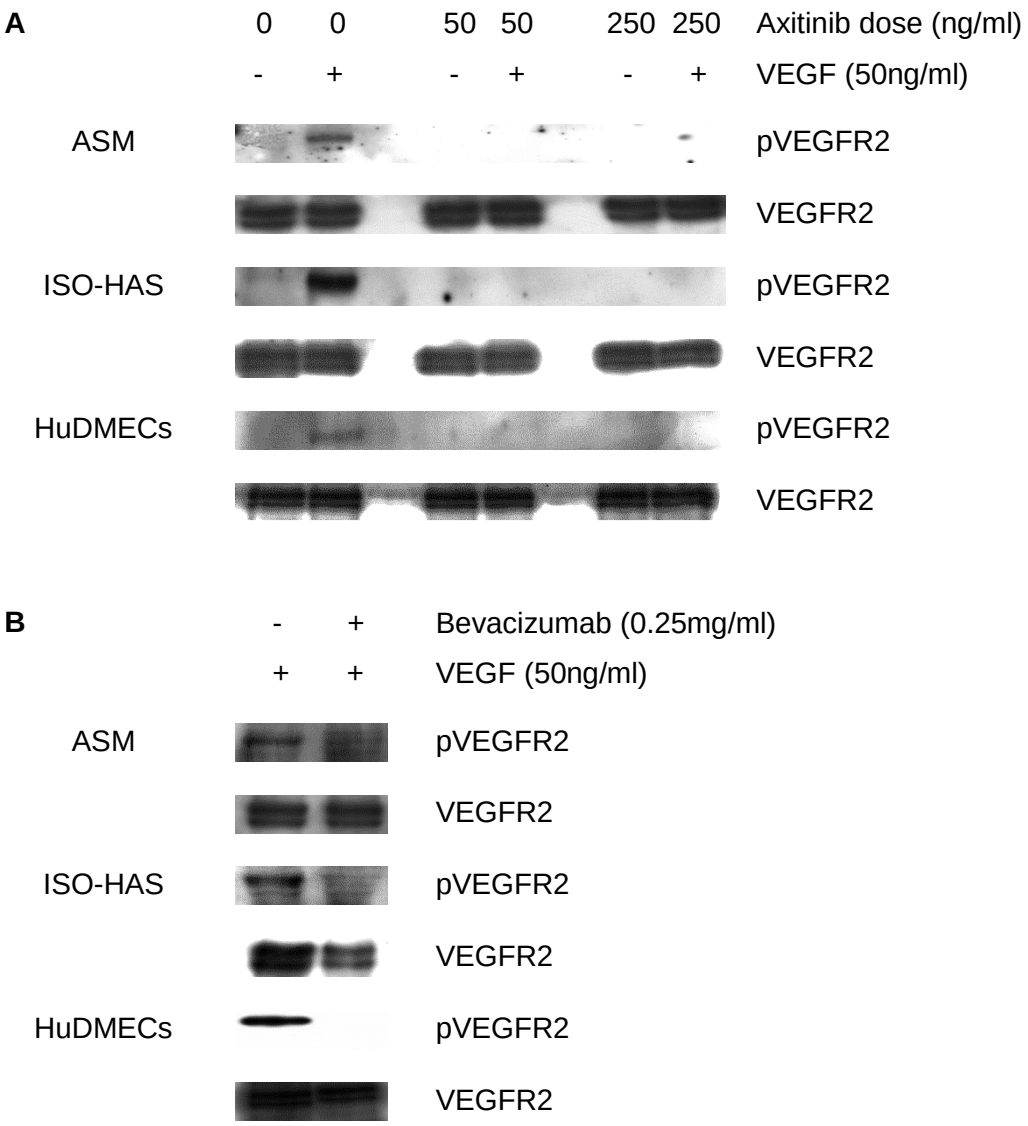

Figure 3.40: Representative western blot studies comparing ASM, ISO-HAS and HuDMEC levels of total and pVEGFR2 (220 kDa) in response to exogenous VEGF stimulation, following pre-incubation with (A) axitinib and (B) bevacizumab. Blots were repeated on at least three occasions.

3.4.2.6 Downstream signalling - phosphoERK

Studies were performed to assess levels of the phosphorylated downstream signalling intermediary protein ERK (pERK) (figure 3.41a and b). Baseline levels of pERK were established in control studies, and a transient increase in pERK observed five minutes after stimulation with exogenous VEGF (50ng/ml). Baseline and peak pERK levels

were reduced, but not absent, in the presence of axitinib 50ng/ml, 250ng/ml and bevacizumab 0.25mg/ml (figure 3.42a and b).

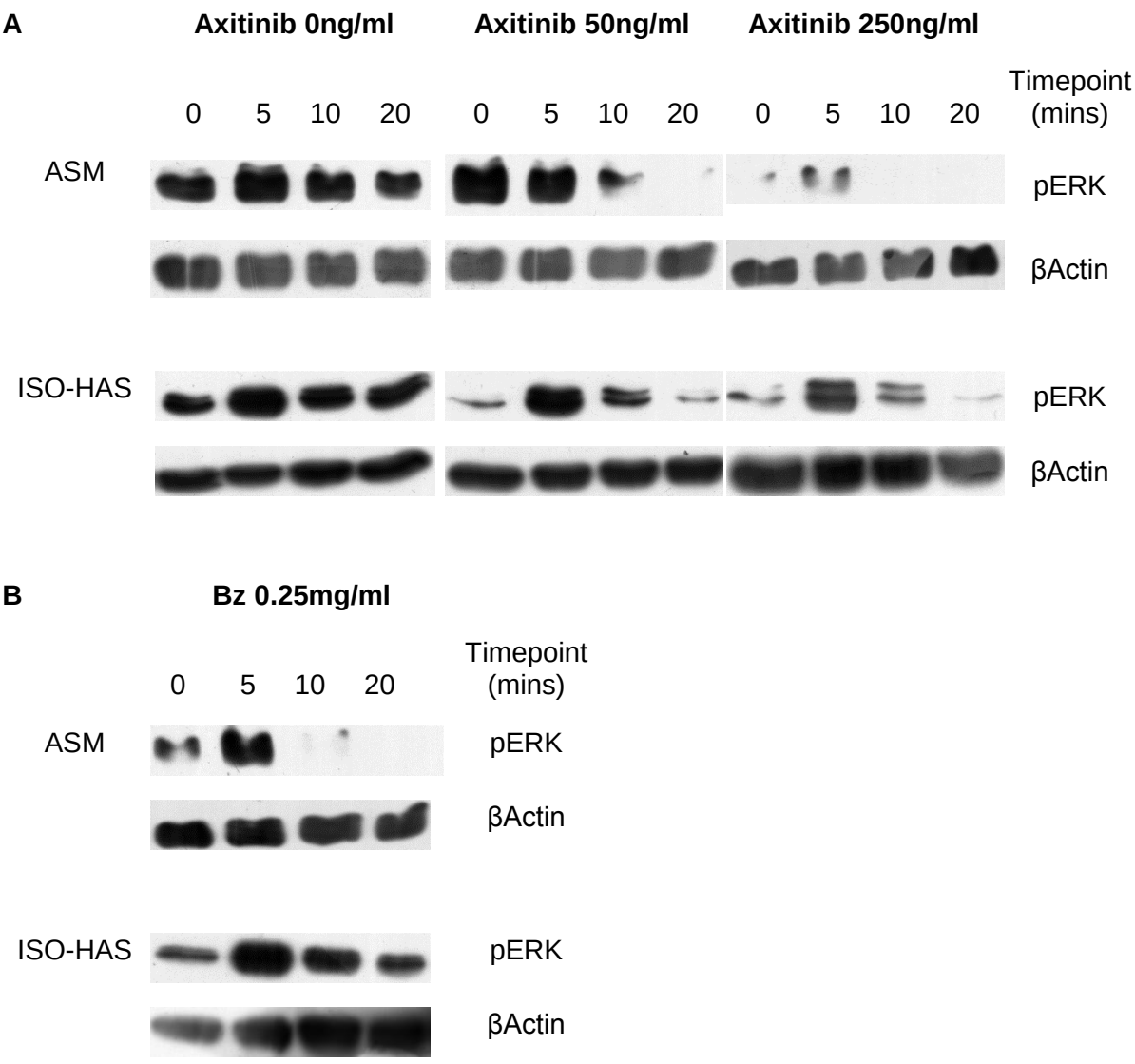

Figure 3.41: Representative western blot studies of pERK in ASM and ISO-HAS cells pre-incubated in (A) axitinib or (B) bevacizumab for 1 hour prior to stimulation with VEGF 50ng/ml. pERK probed in lysates collected at 0, 5, 10 and 20 minutes after stimulation. Blots were repeated on two occasions.

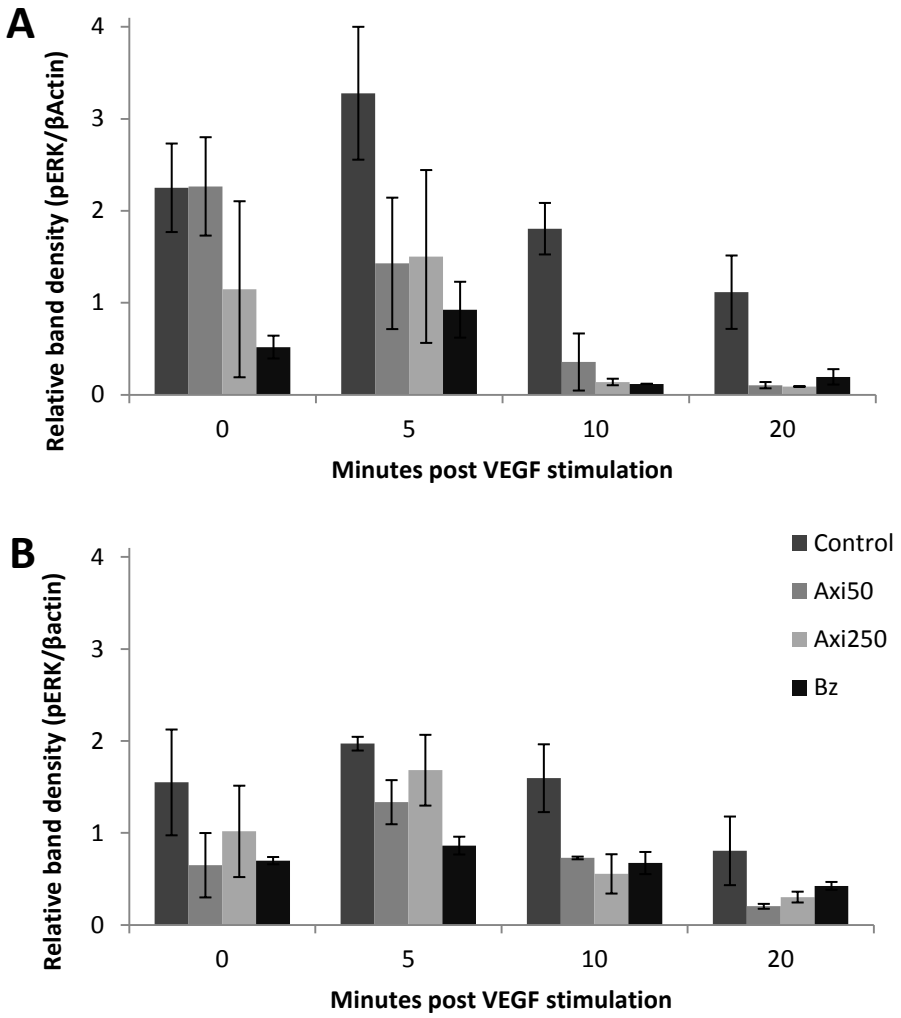

Figure 3.42: Summary data from western blot studies of pERK expression in (A) ASM and (B) ISO-HAS cells pre-incubated in axitinib or bevacizumab before and after stimulation with VEGF 50ng/ml. Data shown represents mean relative density ± SEM; n=2.

3.4.3 MEK inhibition

Western blot studies of pERK expression (see section 3.4.2.6) identified basal pERK levels in ASM and ISO-HAS cells, and demonstrated persistent ERK phosphorylation despite treatment with axitinib or bevacizumab. Consistent with results from the phosphorylated kinase protein array, pERK expression by western blot was higher in ASM than ISO-HAS cells (figures 3.12 and 3.42). The array also showed increased levels of phosphorylated MEK in ASM and ISO-HAS cells relative to HuDMECs (figure

3.12). Together, these results provided a strong rationale for studying the effects of a MEK inhibitor. Response to selumetinib, a selective inhibitor of MEK1/2, was studied across a dose range of 0 - 2000ng/ml as results from a phase I trial reported mean plasma C_{max} of 1436 ng/ml at the recommended selumetinib treatment dose of 75mg bd[172].

3.4.3.1 Cell viability studies MEK inhibition

The effect of selumetinib on ASM and ISO-HAS cell viability were studied using the trypan blue dye exclusion assay (see section 2.5.1.1). Selumetinib significantly reduced ASM viable cell counts with an estimated IC_{50} of 1750ng/ml, but had minimal effects on ISO-HAS cell viability (figure 3.43).

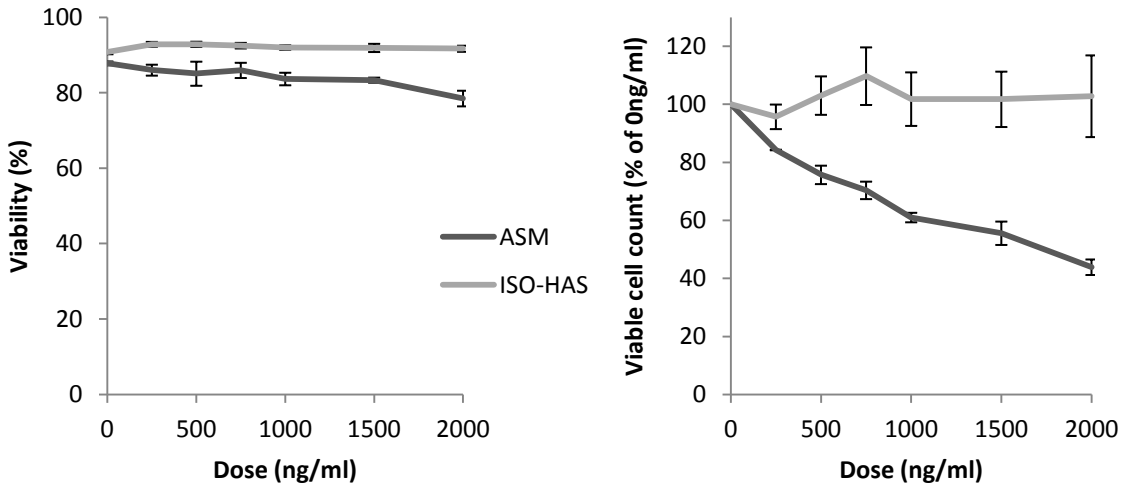

Figure 3.43: ASM and ISO-HAS viability and viable cell counts in response to the MEK inhibitor selumetinib. Data shown represents mean ± SEM; n≥3.

3.4.3.2 Cell differentiation studies with MEK inhibition

ASM and ISO-HAS response to selumetinib were studied using the cell differentiation assay (see section 2.5.2.1). Endothelial cell differentiation was similar to baseline studies. In these studies exogenous VEGF (50ng/ml) increased ISO-HAS tubule formation, though not significantly (p=0.08) (figure 3.43).

Selumetinib reduced ISO-HAS tubule formation in studies with the addition of exogenous VEGF 50ng/ml, but not in studies without it (mean ± SEM number of ISO-

HAS tubules with exogenous VEGF 50ng/ml, selumetinib 0ng/ml vs 750ng/ml vs 1500ng/ml, 108.6 ± 11.0 vs 84.6 ± 7.0 vs 82.6 ± 8.1 (p=0.021 and p=0.006 respectively)) (figure 3.43). Selumetinib significantly reduced the number of tubules formed by ASM cells, both in the presence and absence of exogenous VEGF 50ng/ml (mean ± SEM number of ASM tubules with VEGF 50ng/ml and selumetinib 0ng/ml vs 1500ng/ml, 10.7 ± 1.2 vs 3.2 ± 0.5 (p=0.015), and mean ± SEM number of ASM tubules without additional VEGF and selumetinib 0ng/ml vs 1500ng/ml, 12.1 ± 1.3 vs 5.7 ± 1.3 (p=0.050)).

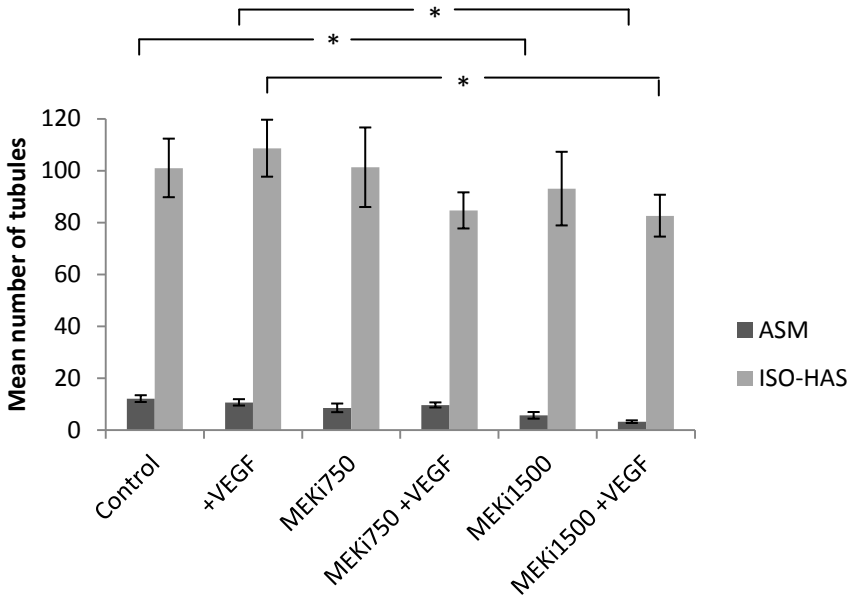

Figure 3.44: Number of tubules formed in the differentiation assay in response to the MEK inhibitor (MEKi) selumetinib at 0ng/ml, 750ng/ml and 1500ng/ml ± VEGF 50ng/ml; * decreased tubule formation ($p<0.05$), calculated using the paired t test, comparisons between ISO-HAS cells with exogenous VEGF and selumetinib 0ng/ml and 1500ng/ml, and ASM cells with selumetinib 0ng/ml and 1500ng/ml in the presence and absence of exogenous VEGF are shown. Data shown represents mean ± SEM; n≥3.

3.4.4 mTOR inhibition

ASM and ISO-HAS cell responses to the mTOR inhibitor everolimus, and the Akt inhibitor MK2206, were studied in cell viability assays using the trypan blue dye exclusion assay (see section 2.5.1.1). mTOR inhibitors reduce VEGF synthesis through

reduced production of HIF-1α[173]. Akt was also identified as a potential drug target, as a key intra-cellular signalling molecule upstream of mTOR. Results from the phosphorylated kinase protein array provided supporting evidence for studying ASM and ISO-HAS response to these agents, with increased Akt and S6 kinase phosphorylation observed in ASM cells relative to HuDMECs, and increased phosphorylation of AMPKα, an intra-cellular inhibitor of mTOR, in HuDMEC cells relative to ASM and ISO-HAS.

A phase I study reported mean plasma C_{max} of 61ng/ml with an everolimus dosing schedule of 10mg per day, and mean plasma C_{max} of 174ng/ml with a dosing schedule of 70mg per week[174]. The effects of everolimus were therefore studied over a dose range of 0 – 250ng/ml. MK2206 was also studied over a dose range of 0 – 250ng/ml, supported by a phase I study that reported mean MK2206 plasma C_{max} of 36ng/ml with the recommended dosing schedule of 60mg alternate days[175].

3.4.4.1 Cell viability with mTOR inhibition

Neither everolimus nor MK2206 affected % viability (figure 3.45). Minor effects to viable cell counts were observed with the pAkt inhibitor. Modest responses were seen with exposure to everolimus, with maximal inhibition achieved by doses of 50ng/ml. Response to everolimus was subsequently studied in combination with doxorubicin chemotherapy (10ng/ml), as mTOR inhibitors would likely be used clinically in combination with chemotherapeutics. These combination studies suggested an additive rather than synergistic effect (figure 3.46). Effects in functional assays were not studied due to time constraints and indications that these agents were unlikely to have a profound effect.

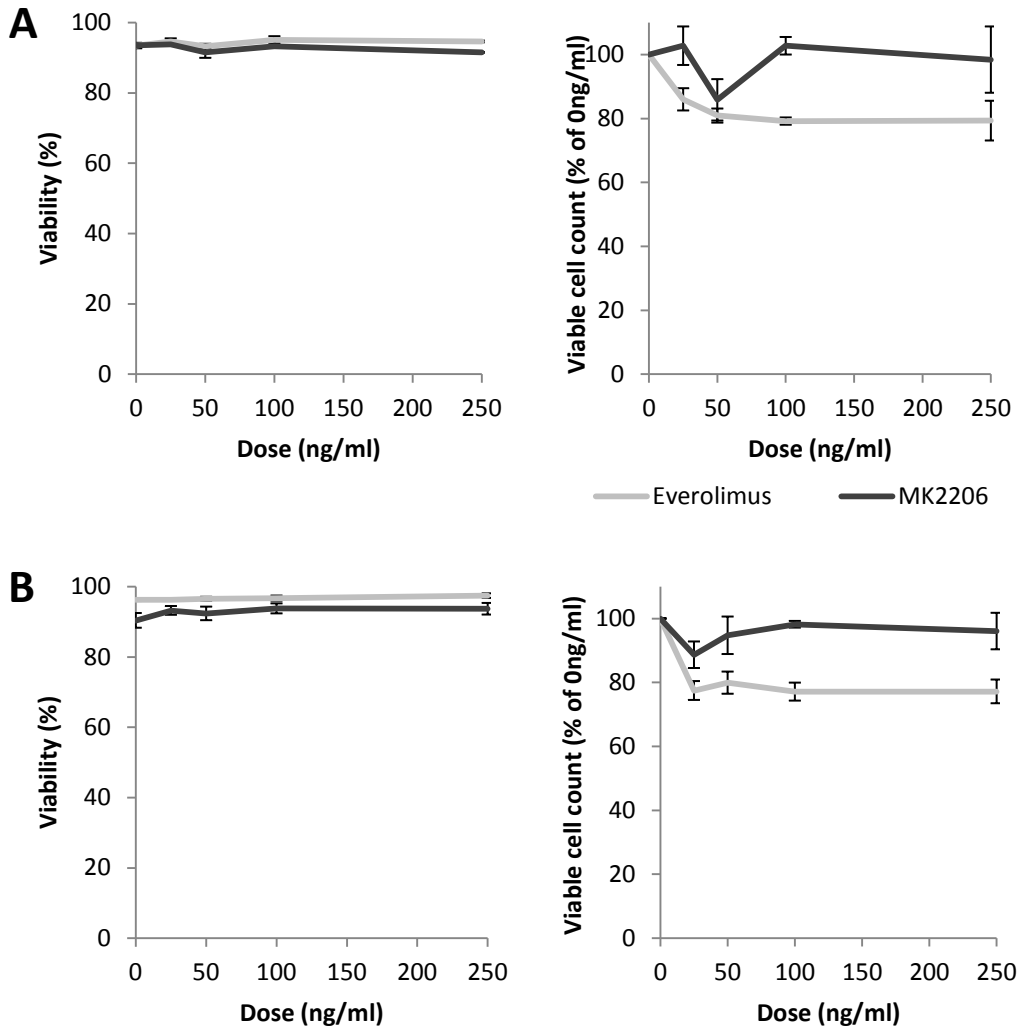

Figure 3.45: (A) ASM and (B) ISO-HAS viability and viable cell counts in response to everolimus (0 – 250ng/ml) and MK2206 (0 – 250ng/ml). Data shown represents mean ± SEM; n=3.

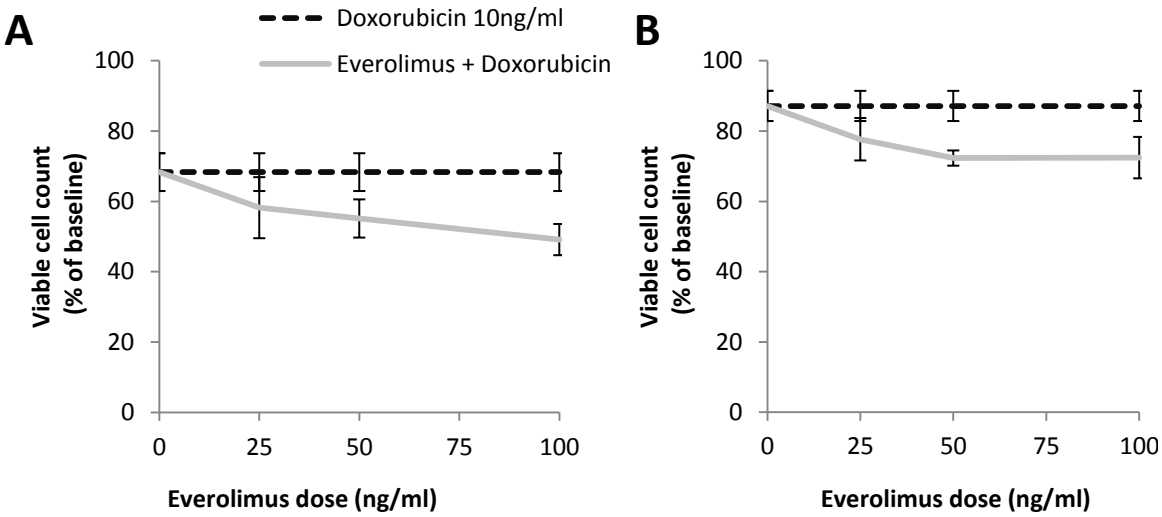

Figure 3.46: (A) ASM and (B) ISO-HAS viable cell counts in response to combination therapy with everolimus (0 – 250ng/ml) and doxorubicin chemotherapy 10ng/ml. Data shown represents mean ± SEM; n=3.

3.4.5 Summary of studies with VEGF targeted agents

Only minor responses to the VEGF targeted agents axitinib and bevacizumab were observed in functional assays of ASM and ISO-HAS cells, despite western blot studies that demonstrated target inhibition of VEGFR2 phosphorylation. Increased cell responses were observed to the mTOR inhibitor everolimus, and to targeting the cell signalling pathway downstream of VEGFR2 with the MEK inhibitor selumetinib.

3.4.6 Checkpoint II inhibition

The phosphorylated kinase protein array identified checkpoint II (ChkII) as a potential drug target. ChkII is phosphorylated in response to double strand DNA breaks, including double strand breaks caused by treatment with radiotherapy or chemotherapeutic agents such as doxorubicin[176]. A variety of checkpoint II inhibitors are currently in pre-clinical development. C3742 (0 – 250ng/ml) was selected for study (IC_{50} 15nM) as a selective ChkII inhibitor[176].

3.4.6.1 Cell viability with checkpoint II inhibition

ASM and ISO-HAS cell response to the ChkII inhibitor C3742 were studied in cell viability assays using the trypan blue dye exclusion assay (2.5.1.1). No response to C3742 was observed in ASM cells (figure 3.47), whilst in ISO-HAS the single agent ChkII inhibitor had a significant protective effect (mean ± SEM ISO-HAS viable cell count ($x10^6$) 0ng/ml vs 100ng/ml, 0.31 ± 0.02 vs 0.37 ± 0.01 (p=0.040). The ChkII inhibitor also protected ISO-HAS cells from response to doxorubicin (mean ± SEM ISO-HAS cell count ($x10^6$) with doxorubicin 10ng/ml and ChkII inhibitor 0ng/ml vs 100ng/ml, 0.24 ± 0.01 vs 0.29 ± 0.002 (p=0.006)) (figure 3.48).

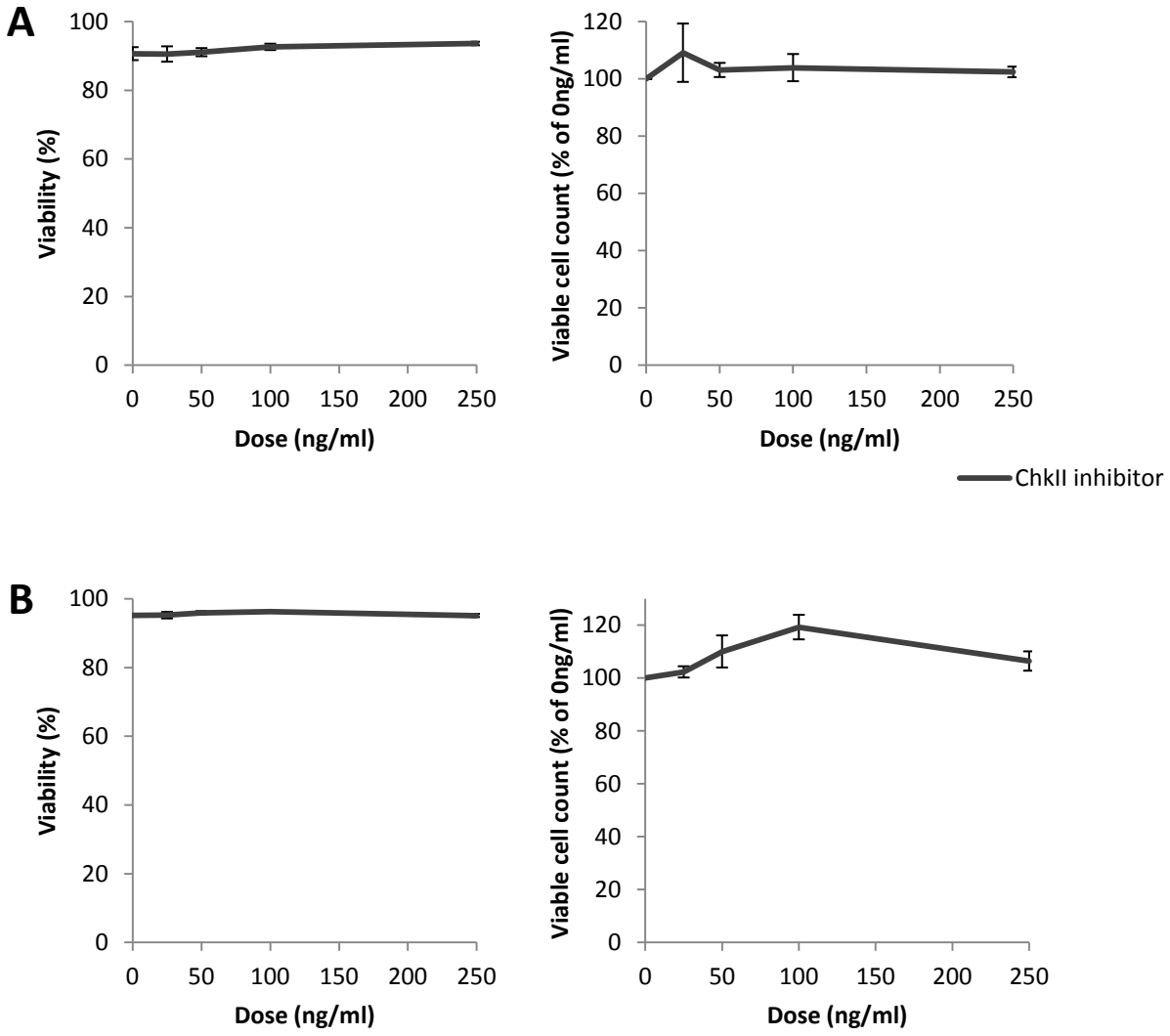

Figure 3.47: (A) ASM and (B) ISO-HAS viability and viable cell counts in response to the ChkII inhibitor C3742 (0 – 250ng/ml). Data shown represents mean ± SEM; n=3.

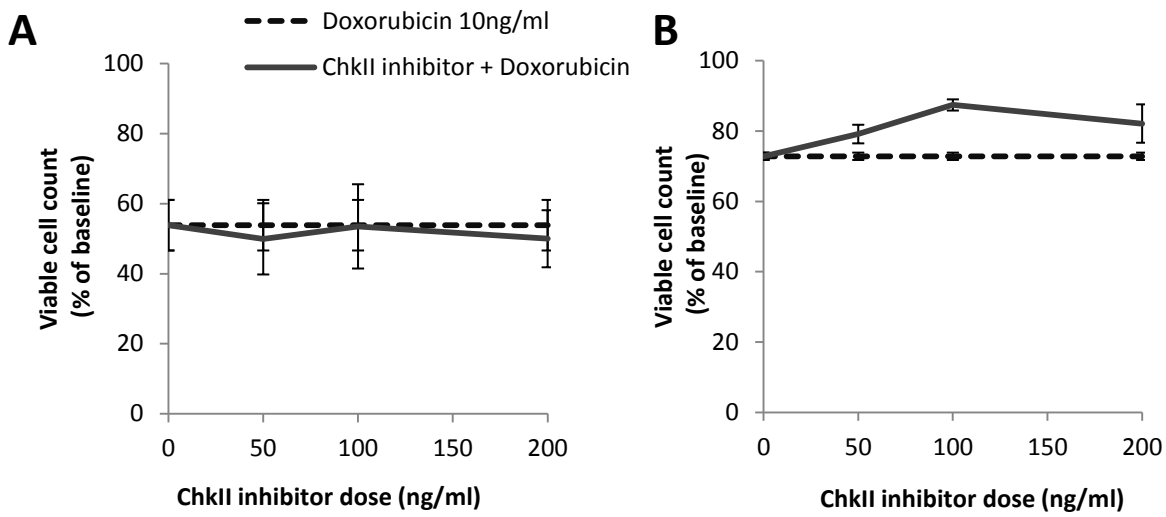

Figure 3.48: (A) ASM and (B) ISO-HAS viable cell counts in response to combination therapy with ChkII inhibitor (0 – 250ng/ml) and doxorubicin chemotherapy 10ng/ml. Data shown represents mean ± SEM; n=3.

3.4.7 Vascular disrupting agent

The anti-angiogenic agents studied thus far target tumour angiogenesis through inhibition of the cell signalling pathways stimulated by pro-angiogenic growth factors such as VEGF. In contrast, DMXAA is a vascular disrupting agent that induces apoptosis in tumour endothelial cells, resulting in collapse of the tumour vasculature and thus tumour hypoxia and necrosis[177]. With DMXAA treatment at 1800mg/m^2, the dose used in phase III clinical trials in combination with chemotherapy[178], a phase I trial of single agent DMXAA reported an estimated plasma C_{max} of 1000µM[179]. A DMXAA dose range of 0 – 300µg/ml was therefore initially studied. However after a preliminary study, the DMXAA re-constituted in distilled water crystallised out of solution following storage at 4^{0}C. Thereafter DMXAA was re-constituted in DMSO, however this limited the maximum dose studied to 100µg/ml, as DMXAA doses beyond this used DMSO volumes above 1% which were toxic to cells.

3.4.7.1 Cell viability with vascular disrupting agent

ASM and ISO-HAS cell response to DMXAA was studied in cell viability assays using the trypan blue dye exclusion assay (2.5.1.1). DMXAA significantly reduced viable cell

counts in both ASM and ISO-HAS with an IC_{50} of 90 and 150 µg/ml respectively (figure 3.49). Modest decreases in % viability were also observed. Comparison studies were performed to investigate the effects of DMXAA on HuDMEC viability using the MTS assay (see section 2.5.1.2). DMXAA significantly reduced HuDMEC viability and proliferation (mean ± SEM HuDMEC relative absorbance at 48 hours with DMXAA 0µg/ml vs 30µg/ml vs 100µg/ml, 151.4 ± 14.7 vs 95.8 ± 14.1 and 76.7 ± 9.0 (p=0.053 and 0.012 respectively)) (figure 3.50). Parallel studies of ASM and ISO-HAS cell viability confirmed response to DMXAA at 48 hours using the MTS assay (figure 3.51).

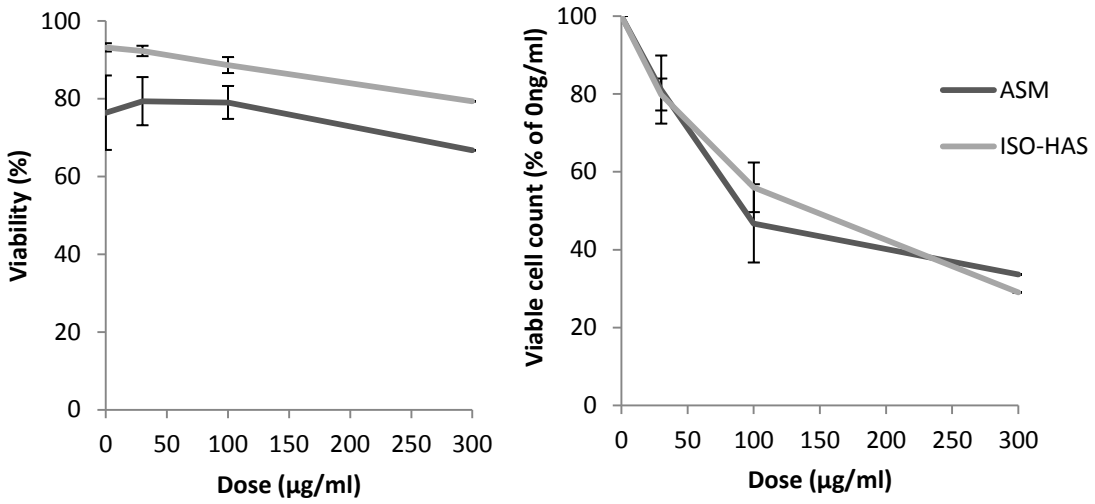

Figure 3.49: ASM and ISO-HAS viability and viable cell counts in response to the vascular disrupting agent DMXAA (0 - 300µg/ml). Data shown represents mean ± SEM; n=3.

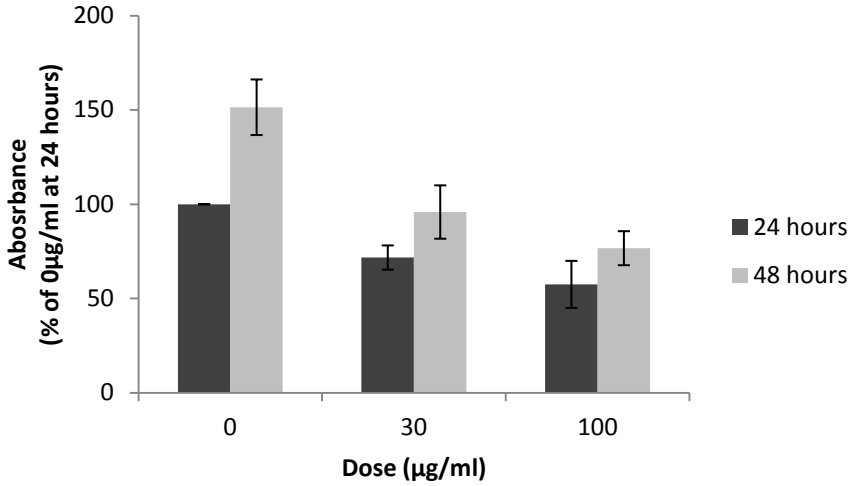

Figure 3.50: Results from the MTS assay of HuDMECs with DMXAA (0 – 100µg/ml). Absorbance was measured at 24 and 48 hours. Data shown represents mean relative absorbance expressed as % of baseline (0µg/ml at 24 hours) ± SEM; n=3.

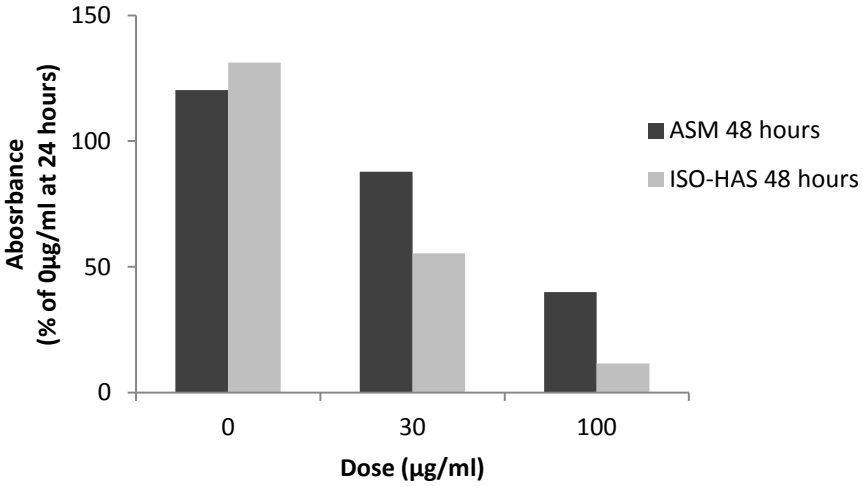

Figure 3.51: Results from the MTS assay of ASM and ISO-HAS cells with DMXAA (0 – 100µg/ml). Data shown represents mean relative absorbance at 48 hours expressed as % of baseline (0µg/ml at 24 hours); n=1.

3.4.7.2 Cell differentiation with vascular disrupting agent

Endothelial cell response to DMXAA (0 - 100µg/ml) was studied using the cell differentiation assay (see section 2.5.2.1). The number of tubules formed by ASM, ISO-HAS and HuDMEC cells in these assays were consistent with previous studies. DMXAA significantly reduced endothelial cell tubule formation in a dose dependent

manner (mean ± SEM number of ASM tubules in DMXAA 0µg/ml vs 100µg/ml, 21.1 ± 7.2 vs 5.8 ± 2.4 (p=0.086), mean ± SEM number of ISO-HAS tubules in DMXAA 0µg/ml vs 100µg/ml, 108.2 ± 8.3 vs 61.0 ± 8.8 (p=0.009), and mean ± SEM number of HuDMEC tubules in DMXAA 0µg/ml vs 100µg/ml, 79.4 ± 19.1 vs 46.8 ± 18.8 (p=0.025)) (figure 3.52).

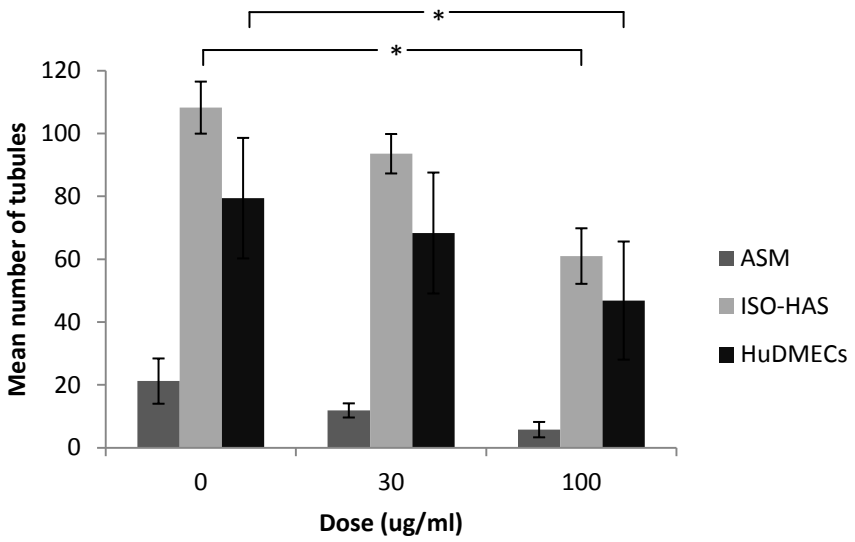

Figure 3.52: Number of tubules formed in the differentiation assay in response to DMXAA at 0, 30 and 100µg/ml; * decreased tubule formation compared to 0µg/ml ($p<0.05$), calculated using the paired t test, comparisons between ISO-HAS cells with DMXAA 0µg and 100µg/ml, and between HuDMEC cells with DMXAA 0µg and 100µg/ml are shown. Data shown represents mean ± SEM; n≥3.

3.4.7.3 DMXAA drug mechanisms

Studies were performed to investigate the mechanisms of drug response seen in the angiosarcoma cell lines. The precise methods by which DMXAA exerts its anti-vascular effect are unknown, however it has been postulated that DMXAA stimulates apoptosis in endothelial cells via nuclear factor kappa B (NF-κB) and induces tumour expression of tumour necrosis factor α (TNFα) within 24 hours of exposure[177].

3.4.7.3.1 TNFα

ASM cells were incubated for 4 and 24 hours with DMXAA 0µg/ml or 100µg/ml, and the levels of TNFα in lysates and cell conditioned media quantified by ELISA. TNFα levels

were similar in lysates and conditioned media, and TNFα expression was similar at 4 and 24 hours of drug exposure (figure 3.53). Compared to control samples, TNFα expression was slightly higher in cells treated with DMXAA 100μg/ml but this was not significant.

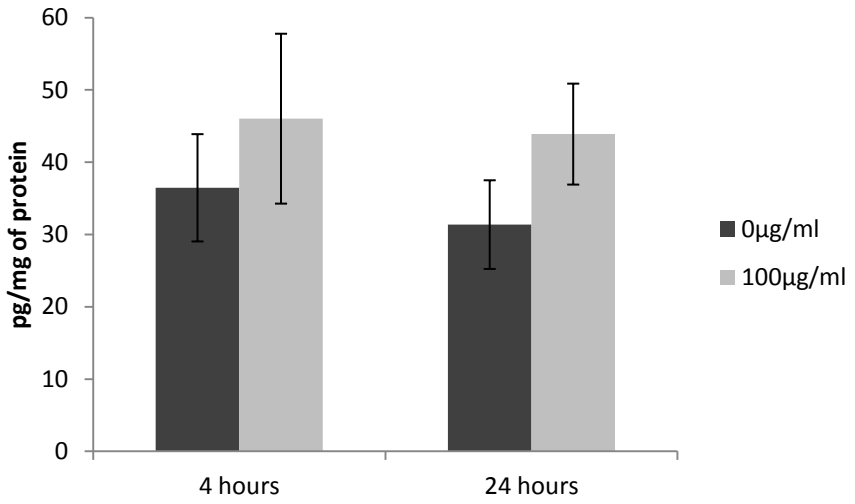

Figure 3.53: Graph comparing the expression of TNFα in ASM cell lysates following 4 and 24 hours incubation with 0 or 100μg/ml DMXAA. Data shown represents mean TNFα values per mg of total protein content in the cell lysates ± SEM; n=4.

3.4.7.3.2 Apoptosis

ASM cells were incubated for 1, 2, 4, 6, 12 and 24 hours with DMXAA 0μg/ml or 100μg/ml. Cell death was assessed by flow cytometry using annexin V antibody and propidium iodide (PI) staining to measure the proportion of apoptotic and necrotic cells respectively. Results showed an increase over time in the proportion of apoptosis and necrosis with both DMXAA 0μg/ml and 100μg/ml (mean ± SEM apoptotic plus necrotic cells (%) with DMXAA 0μg/ml at 1 hour vs 12 hours, 10.3 ± 2.2 vs 19.0 ± 2.5 (p=0.060), and mean ± SEM apoptotic plus necrotic cells (%) with DMXAA 100μg/ml at 1 hour vs 12 hours, 12.2 ± 2.4 vs 19.8 ± 0.8 (p=0.040)) (figure 3.54). However, there was no significant difference in the proportion of apoptosis and necrosis between cells treated with DMXAA 0μg/ml and DMXAA 100μg/ml (table 3.4).

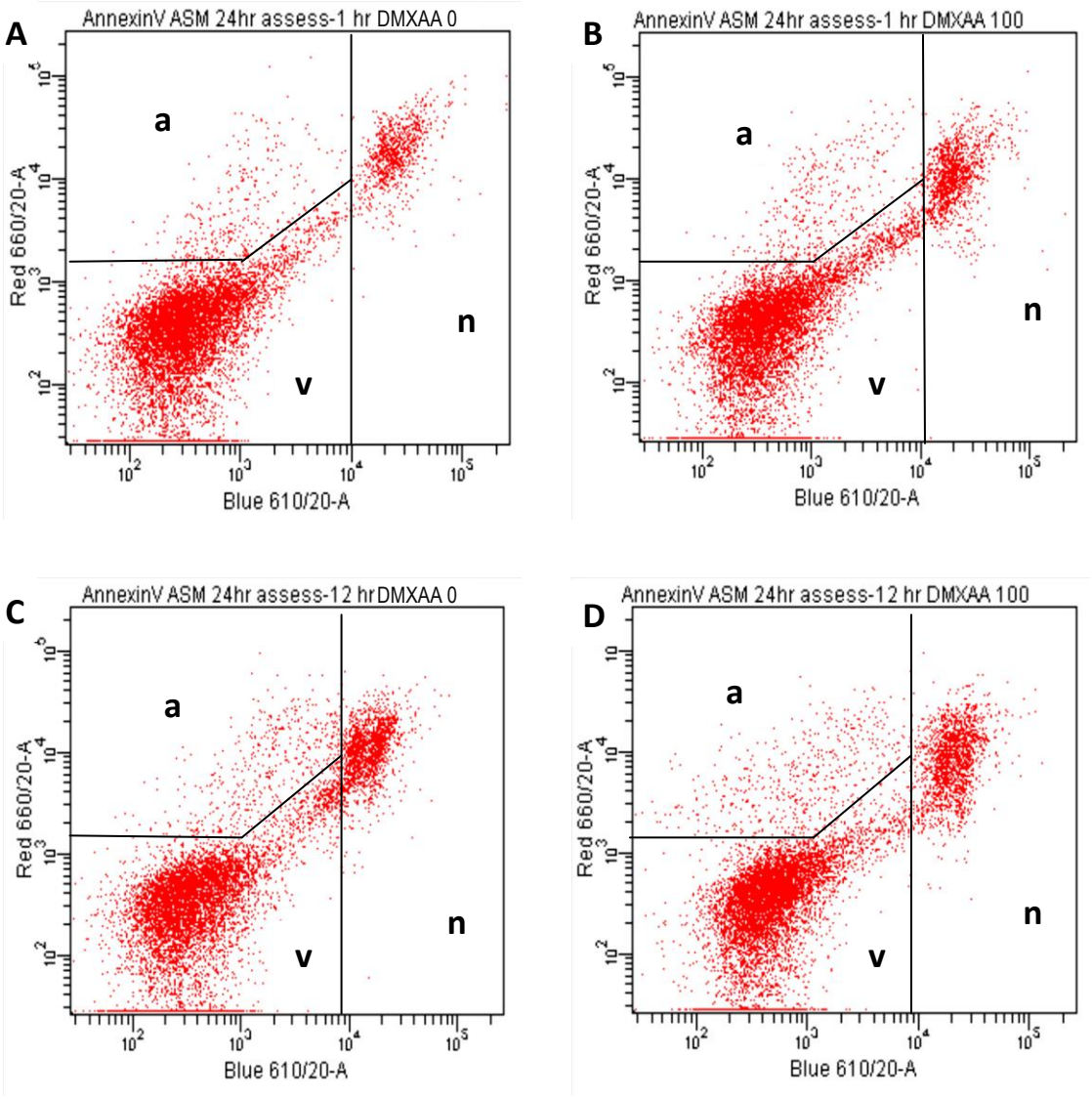

Figure 3.54: Plots from flow cytometry studies to measure the proportion of viable, apoptotc and necrotic cells using annexin V antibody (Red 660/20-A) and propidium iodide staining (Blue 610/20-A). Plots compare ASM cells incubated in DMXAA 0µg/ml and 100µg/ml for 1 hour (A and B) and 12 hours (C and D) respectively. Cells were gated into: a - apoptotic; n - necrotic; v - viable.

Time (hours)	DMXAA (µg/ml)	% Viable	% Apoptotic	% Necrotic	*p*
1	0	89.6	3.3	7.1	0.60
	100	87.8	4.5	7.7	
2	0	85.4	2.2	12.4	0.62
	100	88.0	3.5	8.5	
4	0	85.4	2.8	11.8	0.24
	100	83.6	3.3	13.1	
6	0	83.6	5.3	11.1	0.49
	100	86.7	3.5	9.8	
12	0	81.0	3.6	15.4	0.77
	100	80.2	4.4	15.4	
24	0	81.5	5.6	12.9	0.86
	100	82.9	5.4	11.7	

Table 3.4: The proportion of viable, apoptotic and necrotic ASM cells, as measured by flow cytometry using annexin V and propidium iodide staining. ASM cells were incubated with DMXAA 0µg/ml or 100µg/ml for 1 – 24 hours. *p* values were calculated using the independent t test to compare the proportion of apoptotic plus necrotic cells between DMXAA 0µg/ml and DMXAA 100µg/ml. Data shown represents mean cell count (%); n=3.

3.4.7.4 Vascular disrupting agent summary

Striking responses to the vascular disrupting agent DMXAA were observed in functional assays of ASM, ISO-HAS and HuDMEC cells. The mechanism of this response is uncertain. It has been postulated that DMXAA causes tumour endothelial cell apoptosis, perhaps through induction of TNFα. However, the studies presented here showed DMXAA did not induce TNFα expression, nor increase cell apoptosis, in ASM cells. Further studies in a wider panel of angiosarcoma tumour samples, including *in vivo* studies, are required to support the progression of DMXAA for angiosarcoma to clinical trials, however human angiosarcoma tumour samples are limited.

3.5 Human Angiosarcoma Tumour Samples

Angiosarcoma tumour samples were collected intra-operatively from four patients following informed consent (REC number: 09/H1313/52; STH project number: 15394) (table 3.5). These samples were collected with the aim of isolating viable angiosarcoma tumour cells for *in vitro* study.

Sample number	Patient Age	Patient Sex	Tumour site	Tumour details	Additional notes
STS0510	69	F	Breast - secondary angiosarcoma	70mm well differentiated angiosarcoma	Wide local excision and post operative radiotherapy for primary breast cancer 12 yrs previously
STS2110	69	M	Soft tissue (leg) - secondary angiosarcoma	Large (>50mm) fungating, necrotic tumour	Chronic lymphoedema secondary to an angiogram procedure complicated by aneurysm and chronic infection 12 yrs previously
STS2210	58	F	Breast - secondary angiosarcoma	2mm tumour excised	Mastectomy and post operative radiotherapy for primary breast cancer 8 yrs previously
STS1011	48	F	Breast - primary angiosarcoma	52mm tumour	No known risk factors

Table 3.5: Details of patients donating angiosarcoma tumour tissue.

3.5.1 Tumour cell isolates

Fragments from fresh tumour biopsies were homogenised and plated in T25 flasks in full growth media (see section 2.6.1). Once established, adherent proliferating cell populations were re-plated to form a monolayer in T75 flasks. Immunocytochemistry studies of early cell passages were performed to assess expression of endothelial cell markers including CD31, VEGF and VEGFRs, and the fibroblast marker αSMA.

3.5.1.1 STS0510

Once cultured, STS0510 tumour cell isolates were separated to select CD31+ cells using MACS micro beads coated with antibody for CD31 (see section 2.6.1). The extracted CD31+ cells were then re-plated and re-cultured. These cells had a spindle morphology (figure 3.55), and immunocytochemistry studies showed they were CD31, CD34 and vWF negative, VEGFR2 weakly positive, and αSMA, VEGF and VEGFR1 strongly positive (figure 3.56). This profile was consistent with cells of a fibroblastic rather than endothelial lineage. A similar immunocytochemistry profile was also seen in STS0510 cell isolates which underwent a repeat CD31 separation. Growth of the STS0510 tumour cell isolates arrested at passage 6. Aliquots of cell isolates were stored in liquid nitrogen in 10% DMSO for later study in functional assays, but unfortunately did not survive this process.

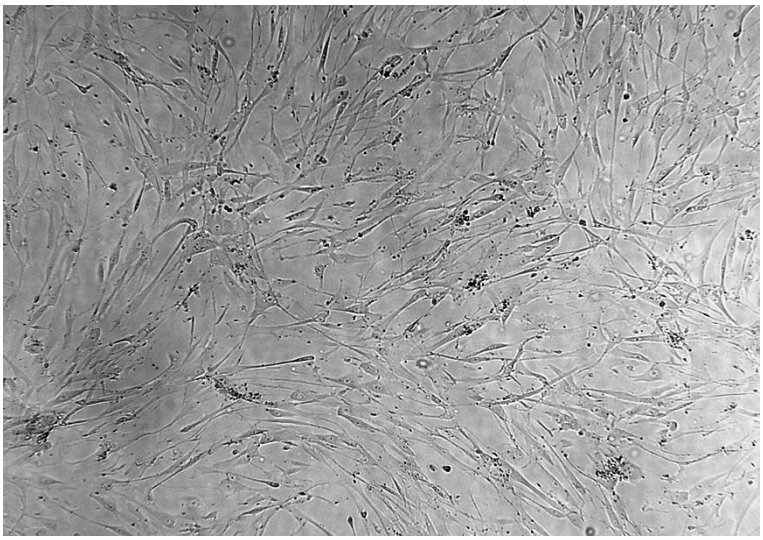

Figure 3.55: Cells isolated by CD31+ MACS micro beads from STS0510, passage 2 (x4 magnification).

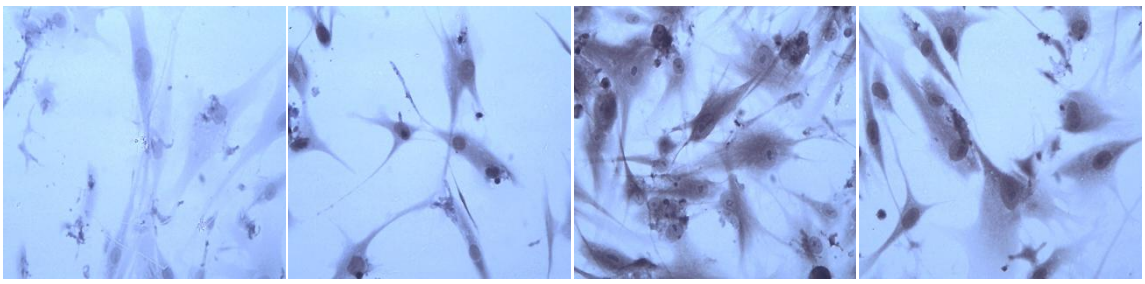

CD31 αSMA VEGF VEGFR1

Figure 3.56: Immunocytochemistry studies of STS0510 passage 2 tumour cell isolates which had previously undergone CD31 separation (x20 magnification). Cells did not stain for CD31 but did stain for αSMA, VEGF and VEGFR1. A similar staining profile was seen with isolates that underwent a secondary CD31 separation.

3.5.1.2 STS2110, STS2210

Insufficient cells settled and grew in culture from these tumour specimens, prohibiting further study.

3.5.1.3 STS1011

Unlike with STS0510, cell separation of STS1011 cell isolates using CD31 antibody coated MACS micro beads was not performed. STS1011 tumour cell isolates had a spindle morphology (figure 3.57), and in immunocytochemistry studies passage 4 cells were CD31 and αSMA negative, but VEGF, VEGFR1 and VEGFR2 positive (figure 3.58). STS1011 cell growth arrested at passage 8.

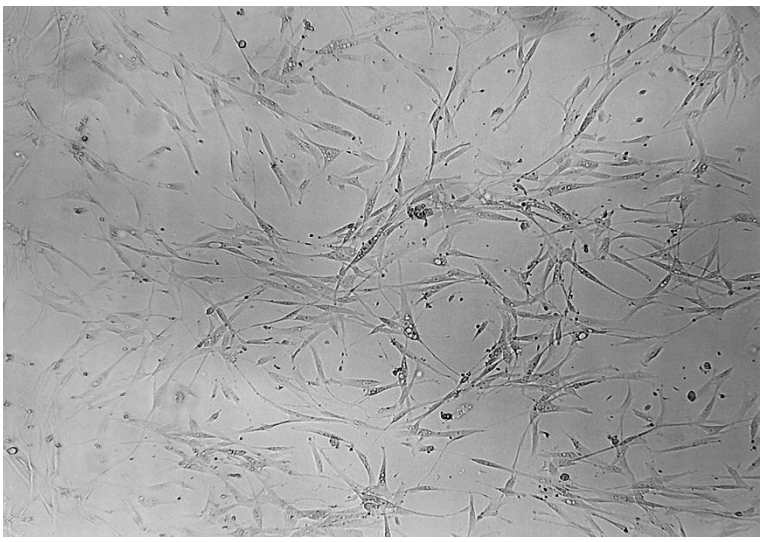

Figure 3.57: Image of cells isolated from STS1011, passage 2 (x4 magnification).

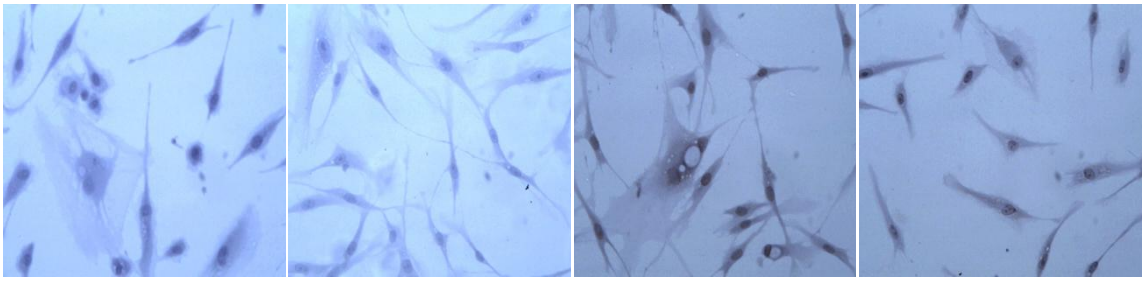

CD31 αSMA VEGF VEGFR1

Figure 3.58: Immunocytochemistry studies of passage 4 cells isolated from STS1011 (x20 magnification). Cells were CD31, αSMA negative, VEGF and VEGFR1 positive.

3.5.1.3.1 Functional *in vitro* studies

The response of STS1011 cell isolates to VEGF targeted agents was studied in functional assays. Response to axitinib (50ng/ml and 250ng/ml) and bevacizumb (0.25mg/m) was assessed. These studies preceded the assays investigating ASM and ISO-HAS response to the MEK inhibitor selumetinib and the vascular disrupting agent DMXAA, and thus STS1011 response to these agents was not studied.

3.5.1.3.1.1 STS1011 cell viability

Cell viability in response to paclitaxel chemotherapy (5ng/ml), and VEGF targeted agents was assessed using the trypan blue dye exclusion assay (see section 2.5.1.1). STS1011 passage 4 cell isolates showed a striking response to single agent paclitaxel

5ng/ml, a modest response to axitinib 250ng/ml, and no response to bevacizumab 0.25mg/ml. In contrast, only minor drug responses were seen with passage 7 cells. No increased response was observed to combinations of paclitaxel with VEGF targeted agents with passage 4 or 7 cells (figure 3.59a and b).

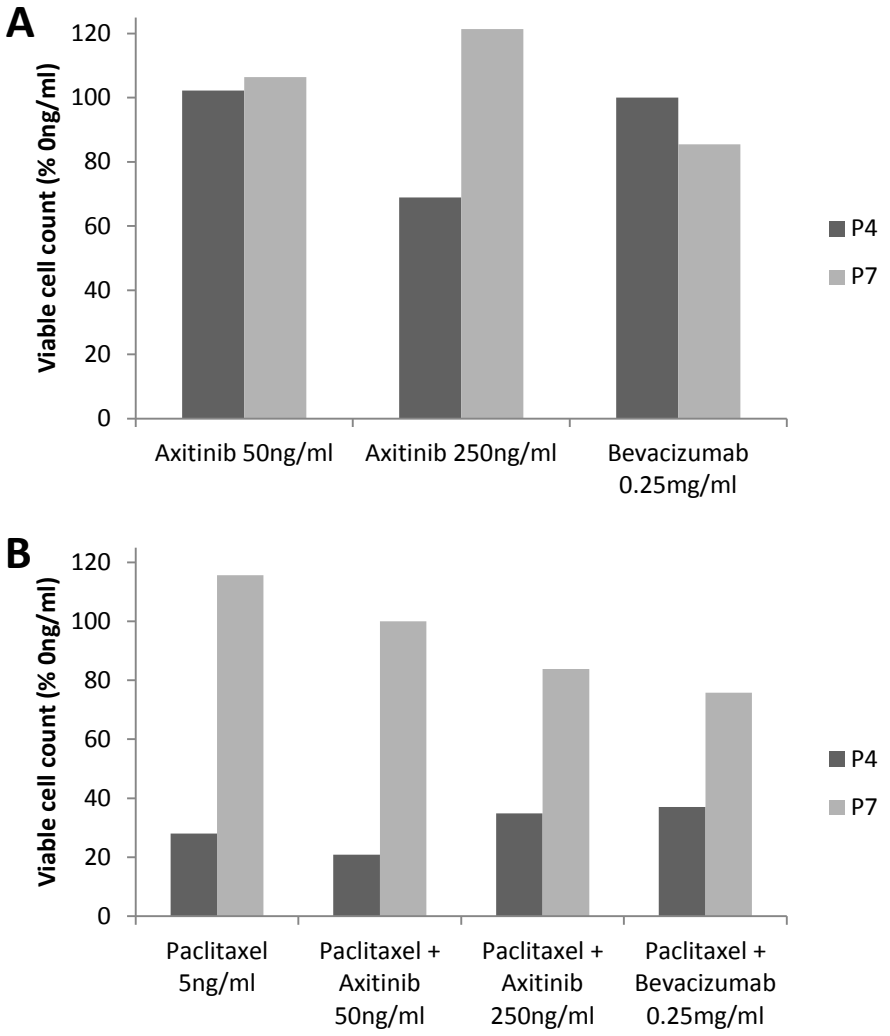

Figure 3.59: Comparison of STS1011 passage 4 and 7 viable cell counts (A) in response to single agent axitinib (50ng/ml, 250ng/ml) or bevacizumab (0.25mg/ml) and (B) in response to single agent paclitaxel (5ng/ml) and in combination with VEGF targeted agents. Data shown represents the mean viable cell count of 2 wells expressed as a percentage of the STS1011 viable cell count without any drug; n=1.

3.5.1.3.1.2 STS1011 cell differentiation

The response of STS1011 tumour cell isolates to VEGF targeted agents was studied in cell differentiation assays (see section 2.5.2.1). Tubule formation by passage 2 STS1011 cells was similar to that observed with ISO-HAS cells. Passage 4 STS1011 cells pre-dominantly formed islands of proliferating cells interconnected by webs of tubules and by passage 7 only a few tubules were seen (figure 3.60).

Overall, no increase was seen in the number of tubules formed by STS1011 passage 2 and 4 cells in response to VEGF 50ng/ml stimulation (mean ± SEM number of tubules formed by passage 2 and 4 cells, with vs without VEGF 50ng/ml, 103.5 ± 5.1 vs 104.9 ± 4.9 (p=0.853)). Axitinib 50ng/ml and 250ng/ml tended to reduce the number of tubules formed, both in the presence and absence of exogenous VEGF 50ng/ml stimulation (in the absence of VEGF mean ± SEM number of tubules with axitinib 0ng/ml vs 50ng/ml vs 250ng/ml, 113.0 ± 2.0 vs 75.4 ± 5.9 vs 79.8 ± 6.8 (p=0.07 and 0.09 respectively); in the presence of VEGF 50ng/ml mean ± SEM number of tubules with axitinib 0ng/ml vs 50ng/ml vs 250ng/ml, 100.3 ± 9.8 vs 77.7 ± 6.0 vs 63.8 ± 26.2 (p=0.39 and 0.27 respectively)) (figure 3.61A). The number of tubules formed did not differ in response to bevacizumab 0.25mg/ml, either in the presence or absence of VEGF 50ng/ml stimulation (figure 3.61B).

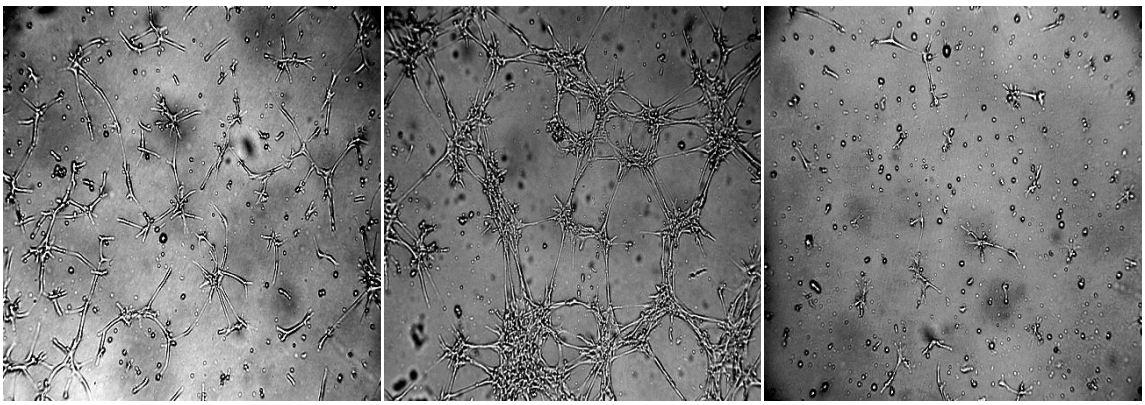

P2 P4 P7

Figure 3.60: Tubule formation on growth factor reduced Matrigel in differentiation assays with cell isolates from STS1011, passage 2, 4 and 7 (x4 magnification).

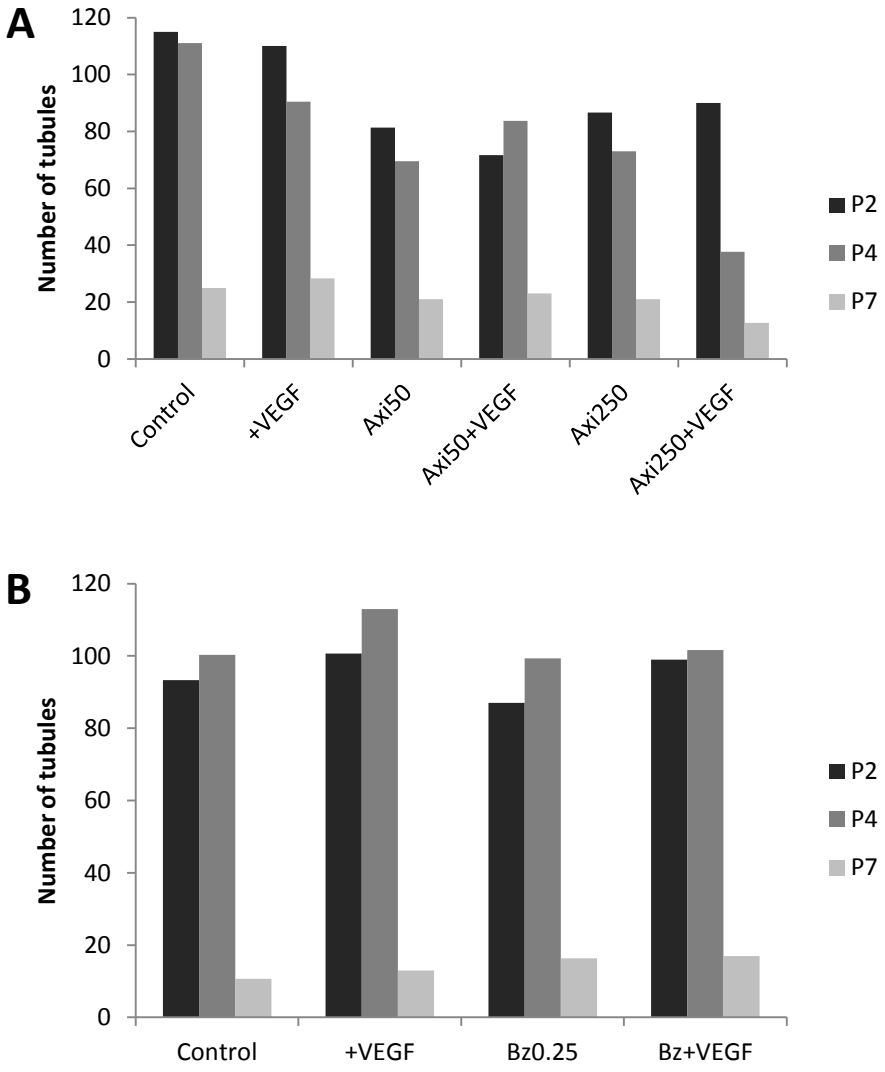

Figure 3.61: Number of tubules formed by STS1011 cell passages (P2, P4 and P7) in cell differentiation assays in response to (A) axitinib (0 – 250ng/ml) and (B) bevacizumab (0.25mg/ml) in the presence or absence of VEGF 50ng/ml stimulation. Data shown represents mean number of tubules from 3 wells; n=1.

3.5.1.4 Tumour cell isolates summary

These studies illustrated some of the difficulties of isolating tumour cells from angiosarcoma samples for *in vitro* study, including the rarity of human angiosarcomas and the rapid adaptation of cells to *in vitro* culture. Protocol 3 (see section 2.6.1) was the most efficient method of isolating cells from tumour samples.

3.5.2 Angiogenesis related protein array of tumour samples

Array studies were performed using the R&D Systems protein array to investigate the expression of angiogenesis related proteins in freshly frozen tumour samples from five human cutaneous angiosarcomas (see section 2.6.2). STS2110 and STS1011 tumour samples were collected intra-operatively from patients with localised disease (REC number: 09/H1313/52; STH project number: 15394). Three other tumour samples were collected pre-treatment from patients with advanced angiosarcoma enrolled on the clinical phase II study of axitinib for soft tissue sarcoma (Axi-STS study; REC number: 09/H1208/42; STH project number: 15195).

The expression profiles of the five tumour samples were generally similar to each other, although factors such as coagulation factor III, bFGF and IL-8 showed a range of expression (figure 3.62). The profiles were also broadly consistent with the expression profiles obtained from ASM and ISO-HAS cells in hypoxia (see figure 3.9). Particular differences of note include increased expression of matrixmetalloproteases (MMP-8 and -9), and decreased expression of HGF, TGF-β, TSP-1 and VEGF in the tumour tissue compared to the cell lines (table 3.6).

Tumour expression increased compared to cell lines		Tumour expression decreased compared to cell lines	
Angiogenin	↑	Coagulation factor III	↓
IGFBP-3	↑	HB-EGF	↓
MMP-8 and -9	↑	HGF	↓
Platelet factor 4	↑	TGF-β	↓
Serpin F1	↑	PDGF-BB	↓
		TSP-1	↓
		uPA	↓
		VEGF	↓

Table 3.6: Summary of angiosarcoma tumour expression of angiogenesis related proteins compared with ASM and ISO-HAS cell lines.

Samples from two de-differentiated liposarcoma tumours collected intra-operatively (STS1711 and STS1810) were also analysed using the angiogenesis related protein array (figure 3.63). The liposarcoma expression profiles were distinct from the angiosarcoma samples. The expression of angiogenin, dipeptidyl peptidase IV (DPPIV), endoglin, serpin F1 and TIMP-1 were similar, but compared to the angiosarcoma specimens the expression of Ang-2, endostatin, IL-8, TGF-β, PlGF, uPA and VEGFC were low or absent in the two liposarcoma samples.

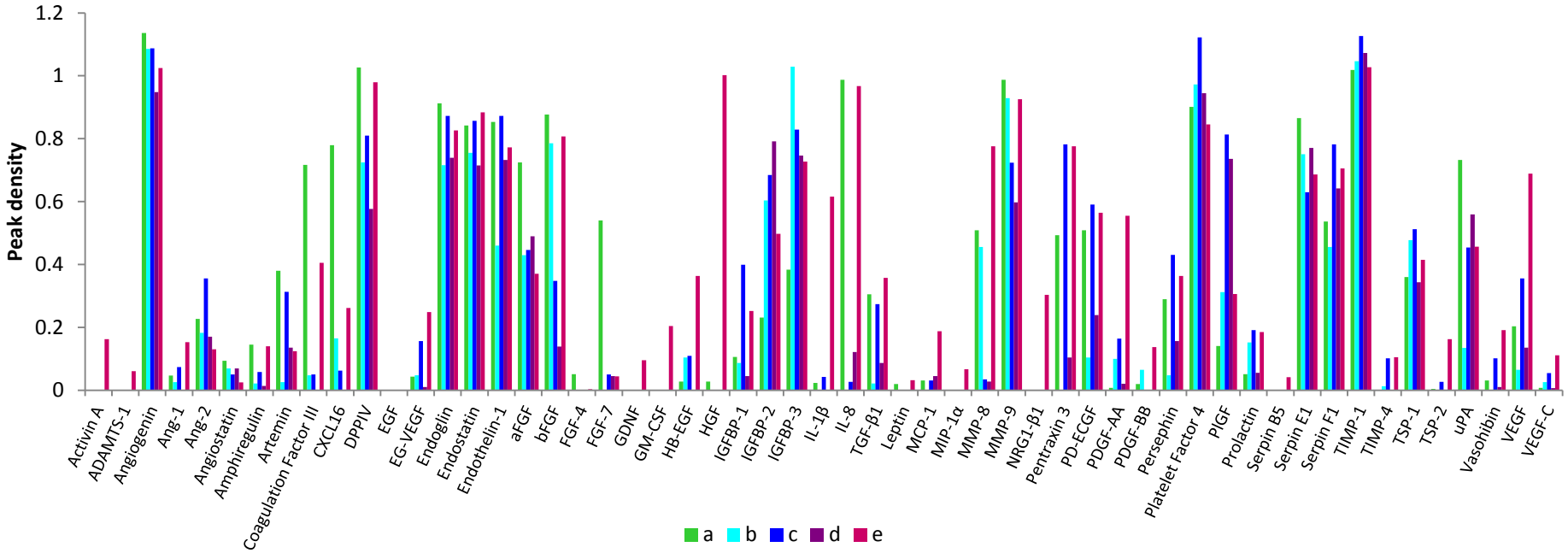

Figure 3.62: Expression profiles of angiogenesis related proteins from freshly frozen angiosarcoma tumour samples (a - STS21010; b - STS1011; c to e - samples collected from Axi-STS study). Data shown represents mean peak density from paired antibody spots (n=1).

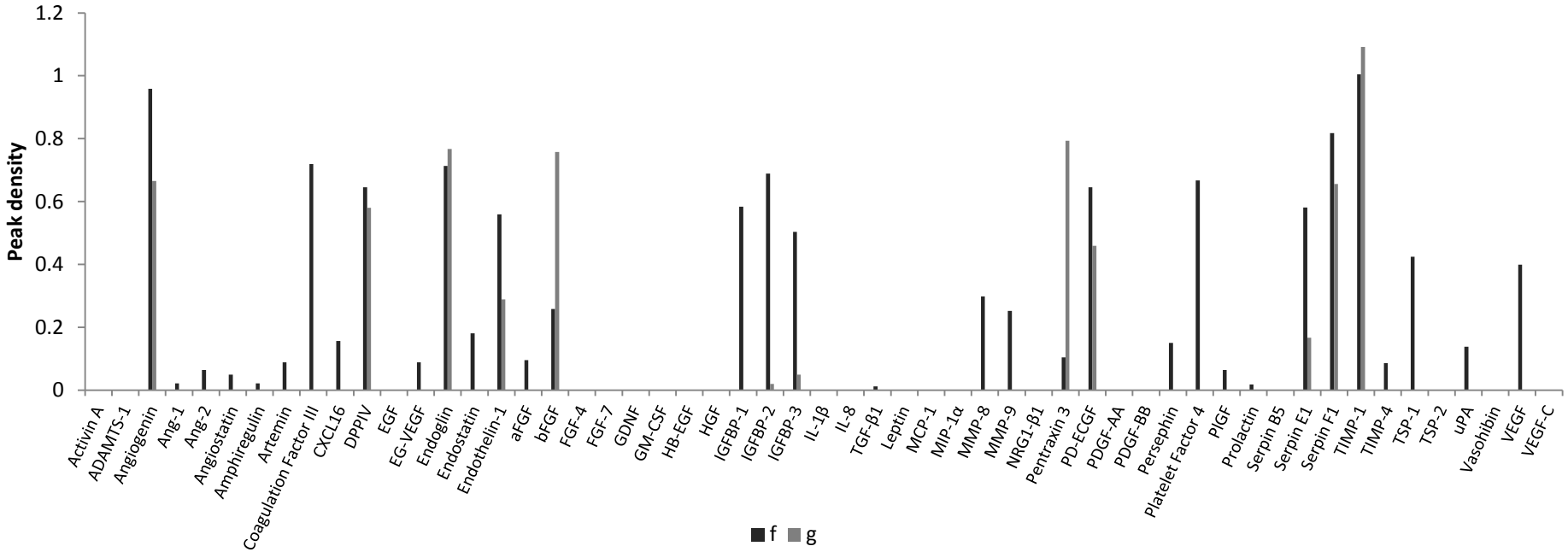

Figure 3.63: Expression profiles of angiogenesis related proteins from two de-differentiated liposarcoma tumour samples (f - STS1711; g - STS1810). Data shown represents mean peak density from paired antibody spots (n=1).

3.5.3 Immunohistochemistry studies of tumour samples

FFPE vascular tumour samples were identified from the pathology archives of Sheffield Teaching Hospitals NHS Trust (REC number: 09/H1313/30; STH project number: 15355). Histology and sample adequacy were confirmed by Dr David Hughes collaborating histopathologist, and 6µm tumour sections cut for immunohistochemistry study (see section 2.6.3). Details of the 39 tissue blocks used for these studies are summarised in table 3.7. Slides of placental tissue were used as a positive control. Tumour slides processed with the primary antibody substituted with PBS were used as a negative control. Staining of normal tissue adjacent to the vascular tumour was examined to identify endothelial specific staining.

Two haemangioendotheliomas were included in the group of malignant vascular tumours. Haemangioendotheliomas are rare vascular tumours of intermediate malignant potential. They typically present as a painful solitary mass in superficial or deep soft tissue and have a low risk for metastasis[180]. Haemangiomas are benign vascular tumours. Capillary haemangiomas are common, typically superficial lesions, whilst cavernous haemangiomas often involve deeper structures[181]. Pyogenic granulomas are rapidly growing exophytic vascular tumours of skin or oral mucosa. They are inflammatory lesions which often bleed and ulcerate. Their aetiology is unknown but may be of traumatic or infective origin. They commonly present in the first trimester of pregnancy (granuloma gravidarum) indicating hormonal influences on tumour growth[181].

Tissue	Histology	Tumour Site	Date	Patient Age	Patient Sex
Malignant Vascular Lesions	16 Angiosarcoma[†] 2 Haemangioendothelioma	8 Breast 6 Cutaneous 4 Soft tissue	2000 - 2011	71 (41 - 83)	5M: 13F
Benign Vascular Lesions	11 Benign Haemangioma	-	2010	-	-
Inflammatory Vascular Lesions	6 Pyogenic Granuloma 3 Granulation Tissue	-	2010	-	-

Table 3.7: Summary of the vascular tumour blocks analysed by immunohistochemistry. [†]17 angiosarcoma specimens were included, 1 breast angiosarcoma was represented twice – as an excision biopsy and a surgical resection specimen.

3.5.3.1 Histological features

Angiosarcomas are infiltrative tumours of malignant endothelial cells that form irregular vascular channels (figure 3.64). Haemangioendotheliomas consist of nests of rounded endothelial cells containing intracytoplasmic vacuoles that sit embedded within a myxoid or hyaline matrix[180]. Capillary haemangiomas consist of a profusion of small blood vessels which in cavernous haemangiomas form large, thin walled vascular spaces lined by flattened endothelial cells. Pyogenic granulomatous lesions in contrast are highly cellular lesions with packed with proliferating endothelial cells arranged in a lobular pattern[181].

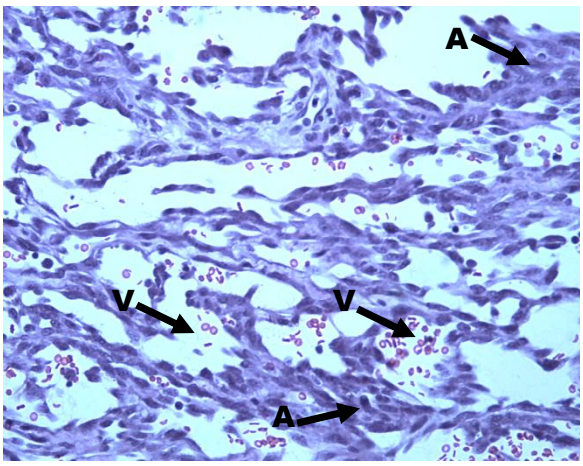

Angiosarcoma: Poorly differentiated vascular channels (V) formed by large malignant endothelial cells (A)

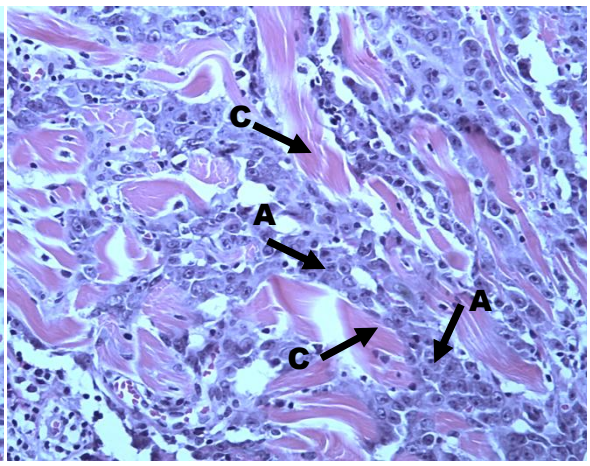

Angiosarcoma: Malignant endothelial cells (A) and dissecting collagen fibres (C)

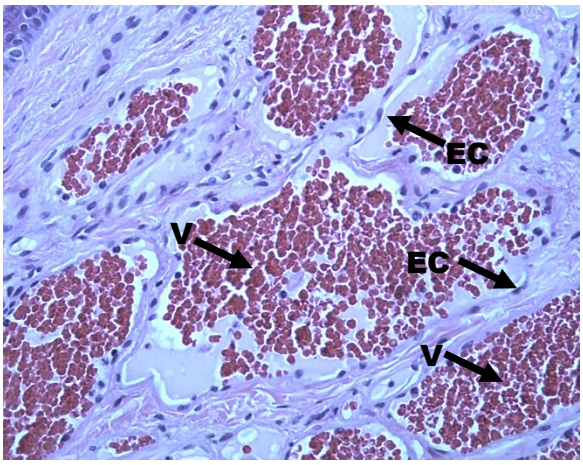

Benign haemangioma: Large vascular spaces (V) lined by endothelial cells with thin cytoplasm (EC)

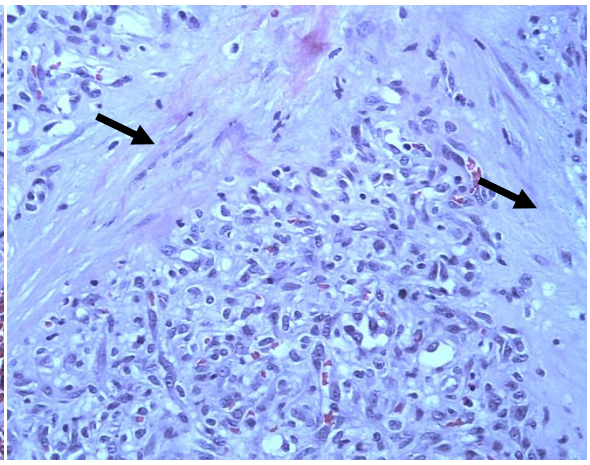

Pyogenic granuloma: Highly cellular tumour of benign endothelial cells bordered by collagen fibres (arrowed)

Figure 3.64: Tumour samples stained with haematoxylin and eosin, comparing the key morphological features of angiosarcomas with benign haemangiomas and pyogenic granulomas (x20 magnification).

3.5.3.2 Tumour expression of angiogenesis related proteins

Tumour expression of VEGF, VEGFR1, VEGFR2, NRP1, bFGF, FGFR1, Ang-1, Ang-2, Tie2, HGF and Met was assessed by immunohistochemistry (see section 2.6.3.1). The immunohistochemistry staining was semi-quantified by adding a score for the proportion of cells staining (0: <1%; 1: 1 – 10%; 2: 10 – 50%; 3: >50%) to a score for the staining intensity (0 – absent; 1 – weak; 2 – moderate; 3 – strong). Slides of placental tissue were used as a positive control. Tumour slides processed with the primary antibody substituted with PBS were used as a negative control. Staining of normal tissue adjacent to the vascular tumour was used to assess endothelial specific staining.

The semi-quantitative analysis of all specimens is summarised in figure 3.65. The inflammatory vascular lesions formed a distinct block with high expression of all the angiogenic growth factors. The angiosarcoma and benign haemangiomas in contrast, showed a range of staining intensities. An inter-group comparison of the ranked immunohistochemistry scores showed angiosarcoma had a lower expression of angiogenic growth factors and their receptors than the benign haemangiomas or inflammatory vascular lesions (table 3.8), with the expression of VEGFR1, NRP1 and bFGF statistically significant (p=0.010, 0.001 and <0.001 respectively). The expression of FGFR1, Tie2 and Met were not statistically different. Analysis using the Mann-Whitney test to directly compare angiosarcomas with benign haemangiomas showed VEGF expression was significantly lower in angiosarcomas (p=0.028). VEGFR2 expression was not significantly different (p-0.08), and neither was Ang-2 (p=0.19). HGF expression was lower in benign haemangiomas than angiosarcomas but this was not statistically significant. Analysis using the Mann-Whitney test to compare angiosarcomas with the inflammatory vascular lesions showed VEGFR2, Ang-1, Ang-2 and HGF expression was significantly lower in angiosarcomas (p=0.006, 0.032, 0.010 and 0.029 respectively). VEGF expression was not significantly different (p=0.060).

The benign haemangiomas and inflammatory vascular lesions studied were selected from cases presenting in 2010. In contrast, the angiosarcoma tumour blocks were from cases presenting in 2000 – 2011. Angiosarcoma immunohistochemistry score significantly correlated with age of the tumour block (table 3.9). The strongest correlation with tumour block age was with the VEGFR1 score (correlation coefficient 0.810; p=<0.001). When angiosarcoma cases pre-2007 were excluded, VEGFR1 did not correlate significantly with tumour block age (correlation coefficient 0.546; p=0.205).

A repeat comparison of the ranked immunohistochemistry scores using the Kruskall-Wallis test, selecting out the angiosarcoma cases pre-2007 showed similar immunohistochemistry scores across the tumour groups (table 3.10). Only the expression of bFGF was significantly lower in angiosarcoma (p=0.014).

The expression of angiogenic growth factors and their receptors were compared between benign haemangiomas and the inflammatory vascular lesions (table 3.11). The inflammatory lesions had a higher expression of angiogenic factors with VEGFR2, Ang-2 and HGF statistically significant (p=0.039, 0.014 and 0.021 respectively).

The co-expression of angiogenic growth factors and their receptors were compared within tumour groups using Spearman's correlation coefficient. Analysis involved multiple testing of each angiogenic factor. To avoid over interpretation of the data, only results with a significance of <0.01 are presented. As angiogenic factor co-expression by the angiosarcoma tumours was biased by the age of the tumour block, this analysis was performed on cases from 2007 onwards. Only HGF and Met expression correlated (r=0.891; p=0.007). In the benign haemangioma group, VEGFR1 and Tie2 expression correlated (r=0.744; p=0.009). Angiogenic factor co-expression was not investigated in the inflammatory vascular lesions, as expression was high across all the factors.

VEGFR2, Ang-1, Ang-2 and Tie2 immunohistochemistry scoring was quantified separately by Dr Malee Fernando (collaborating histopathologist). There was good

inter-observer agreement between immunohistochemistry scores, which did not differ by more than one grade (r=0.846, 0.826, 0.681 and 0.705 for VEGFR2, Ang-1, Ang-2 and Tie2 respectively, calculated using Kendall's tau-b test). Representative images from the immunohistochemistry comparing angiosarcomas with benign haemangiomas and pyogenic granulomas are shown in figures 3.66 – 3.76.

3.5.3.3 Immunohistochemistry studies of tumour samples summary

The immunohistochemistry studies of human tumour samples demonstrated vascular tumours expressed a range of angiogenic growth factors and their receptors. Inflammatory vascular lesions were distinguished from benign haemangiomas by increased expression of VEGFR2, Ang-2 and HGF; however, the angiogenic growth factors studied did not distinguish between benign and malignant groups.

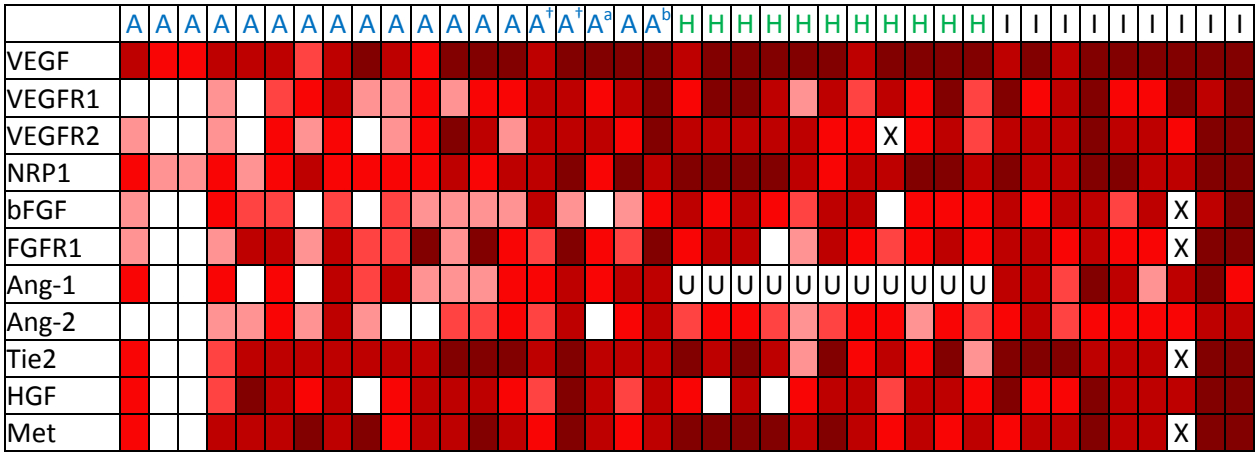

Key:

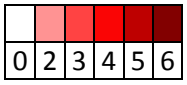

A - angiosarcoma
H - haemangioma
I - inflammatory vascular lesions
† - paired biopsy and excision specimens
a - STS2110
b - STS1011
X - tissue not available for analysis
U - unable to accurately score - difficult to distinguish angiopoieitin-1 staining of endothelial cells from surrounding collagen

Figure 3.65: Heat map summarising the semi-quantitative analysis from the immunohistochemistry studies. The angiosarcoma tumours are grouped together in chronological order (2000 to 2011), followed by the benign haemangiomas and then the inflammatory vascular lesions.

Mean Rank	N	VEGF	VEGFR1	VEGFR2	NRP1`	bFGF	FGFR1	Ang-1	Ang-2	Tie2	HGF	Met
Angiosarcoma	19	15.8	14.7	14.7	13.1	12.3	17.6	12.3	15.7	17.8	18.0	16.8
Haemangioma	11	24.3	22.9	21.0	26.1	24.3	18.3	-	20.0	18.5	16.9	22.4
Inflammatory	9	23.6	27.6	28.1	27.2	30.1	25.8	19.2	29.0	25.0	28.0	21.9
p value		**0.033**	**0.010**	**0.007**	**0.001**	**<0.001**	0.18	**0.032**	**0.013**	0.23	**0.043**	0.273

Table 3.8: Ranked immunohistochemistry scores, grouped by tumour type (angiosarcoma, benign haemangioma or inflammatory vascular lesion). Data shown represents the mean rank and *p* value, calculated using the Kruskall-Wallis test.

	N	VEGF	VEGFR1	VEGFR2	NRP1`	bFGF	FGFR1	Ang-1	Ang-2	Tie2	HGF	Met
Spearman Correlation Coefficient (r)	19	0.662	0.810	0.720	0.703	-	0.566	0.484	0.488	0.654	-	-
p value		**0.002**	**<0.001**	**0.001**	**0.001**	0.60	**0.012**	**0.036**	**0.034**	**0.002**	0.18	0.29

Table 3.9: Immunohistochemistry scores correlated with age of the angiosarcoma tumour blocks. Data shown represents the spearman correlation coefficient and *p* value.

Mean Rank	N	VEGF	VEGFR1	VEGFR2	NRP1`	bFGF	FGFR1	Ang-1	Ang-2	Tie2	HGF	Met
Angiosarcoma	7	14.6	13.2	12.9	10.4	7.4	14.4	7.3	14.0	14.7	13.2	11.7
Haemangioma	11	14.1	12.6	10.7	14.9	13.7	10.8	-	10.5	11.3	10.7	14.3
Inflammatory	9	13.5	16.4	17.1	15.7	18.5	16.4	9.4	18.3	15.5	18.7	13.9
p value		0.92	0.51	0.13	0.30	**0.014**	0.25	0.34	0.07	0.38	0.06	0.73

Table 3.10: Ranked immunohistochemistry scores, grouped by tumour type excluding angiosarcoma cases pre-2007. Data shown represents the mean rank and *p* value, calculated using the Kruskall-Wallis test.

Mean Rank	N	VEGF	VEGFR1	VEGFR2	NRP1`	bFGF	FGFR1	Ang-1	Ang-2	Tie2	HGF	Met
Haemangioma	11	10.7	9.3	7.8	10.3	8.4	8.2	-	7.8	8.7	7.9	10.1
Inflammatory	9	10.3	12.0	12.5	10.8	12.3	12.5	-	13.8	11.8	13.7	9.8
p value		0.83	0.29	**0.039**	0.83	0.11	0.08	-	**0.014**	0.22	**0.021**	0.89

Table 3.11: Ranked immunohistochemistry scores, grouped by tumour type (benign haemangioma versus inflammatory vascular lesion). Data shown represents the mean rank and *p* value, calculated using the Mann-Whitney test

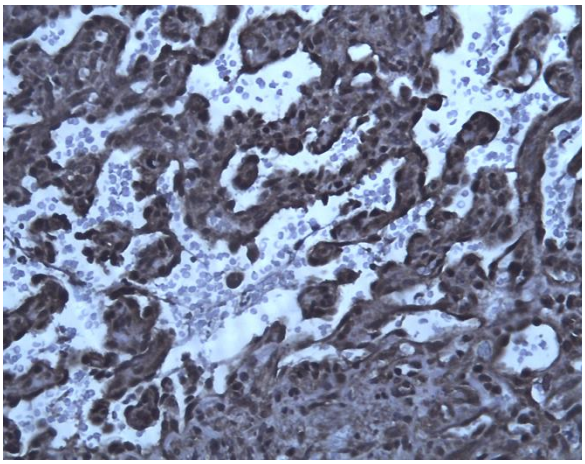

Angiosarcoma: Diffuse, strong VEGF expression

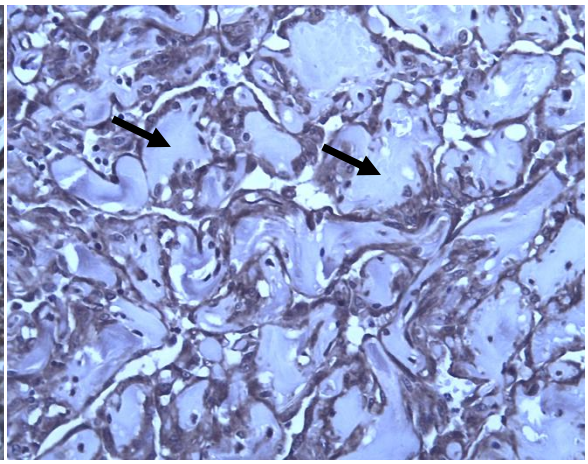

Angiosarcoma: Diffuse, moderately intense VEGF expression, with collagen fibres dissecting through the tumour (arrowed)

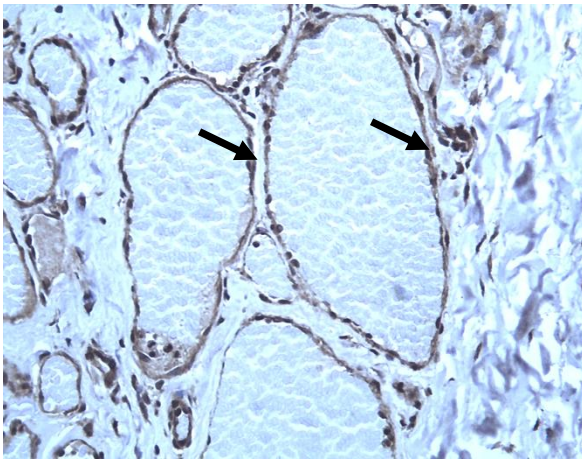

Benign haemangioma: Strong expression of VEGF seen in the thin endothelial cells (arrowed) that surround the large vascular spaces.

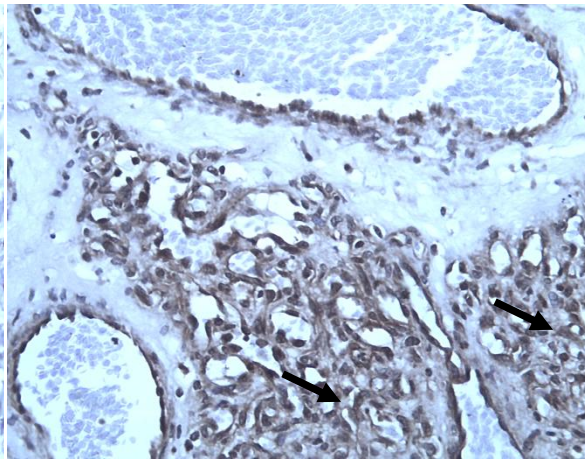

Pyogenic granuloma: Diffuse, strong expression of VEGF (arrowed)

Figure 3.66: Immunohistochemistry studies showing the diffuse expression of VEGF across all tumour groups (x20 magnification).

:

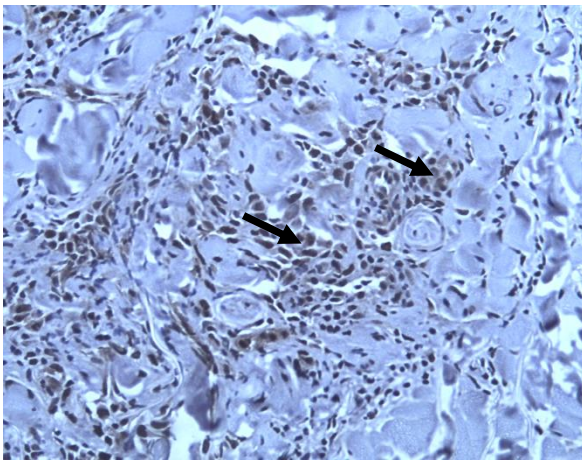

Angiosarcoma: Diffuse, moderately intense expression of VEGFR1 (arrowed)

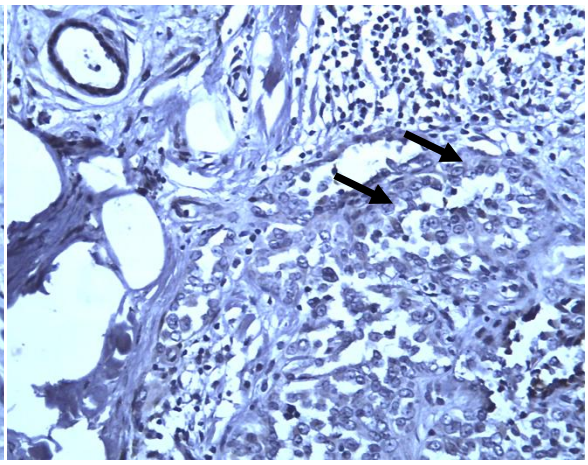

Angiosarcoma: Weak expression of VEGFR1 (arrowed)

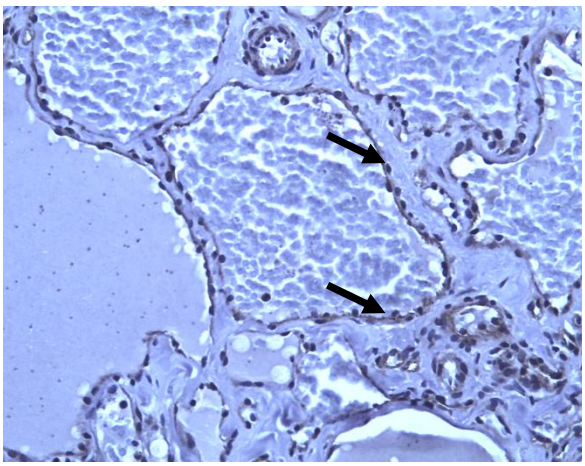

Benign haemangioma: Strong expression of VEGFR1 in the endothelial cells lining vascular spaces

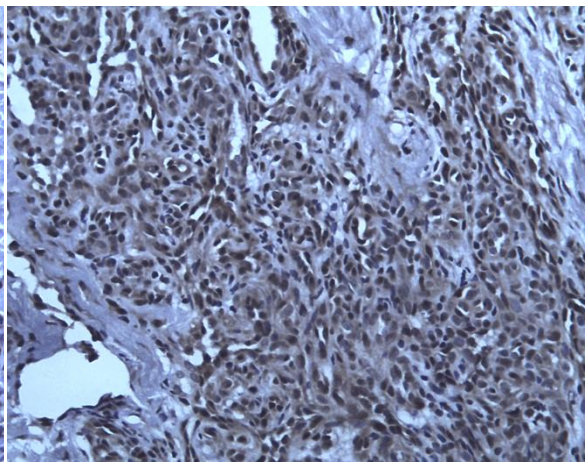

Pyogenic granuloma: Diffuse, strong VEGFR1 expression

Figure 3.67: Immunohistochemistry studies comparing the expression of VEGFR1 across all tumour groups (x20 magnification).

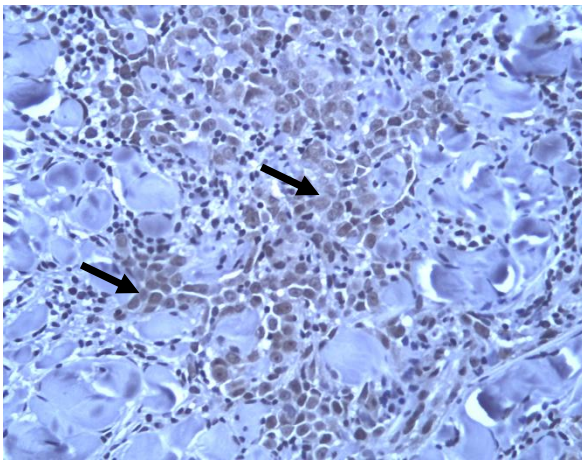

Angiosarcoma: Moderately intense nuclear and cytoplasmic VEGFR2 staining (arrowed)

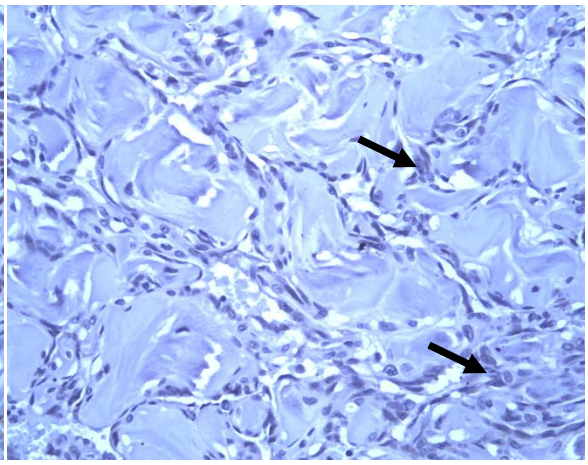

Angiosarcoma: Weak VEGFR2 staining (arrowed)

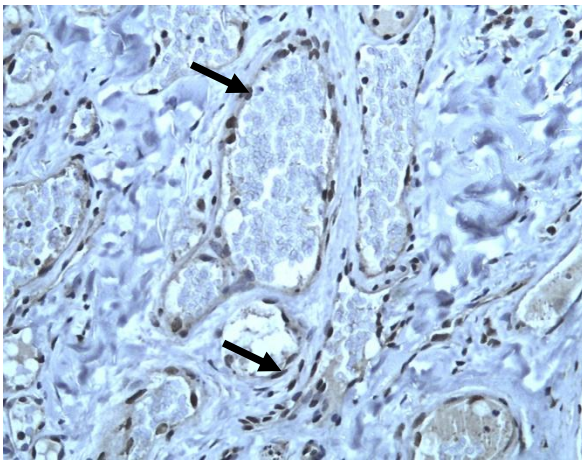

Benign haemangioma: Compact, nuclear staining (arrowed)

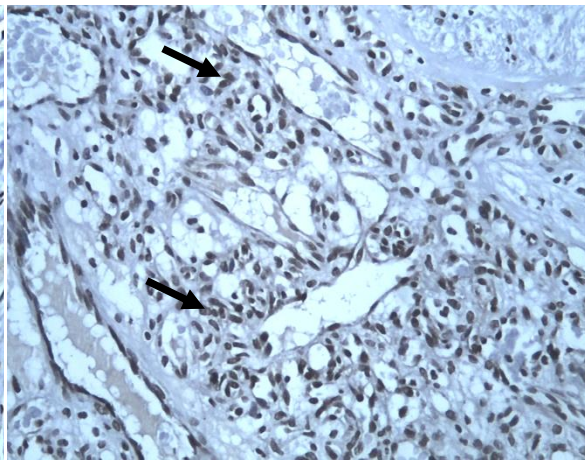

Pyogenic granuloma: Compact, strong nuclear VEGFR2 staining (arrowed)

Figure 3.68: Immunohistochemistry studies comparing the expression of VEGFR2 across all tumour groups (x20 magnification).

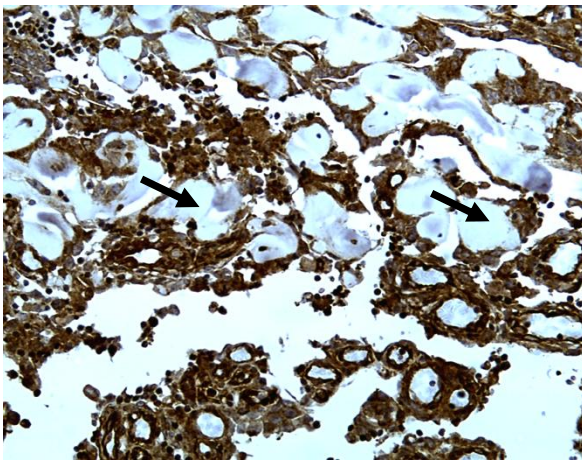

Angiosarcoma: Diffuse, strong NRP1 staining of tumour cells, dissected by collagen fibres (arrowed)

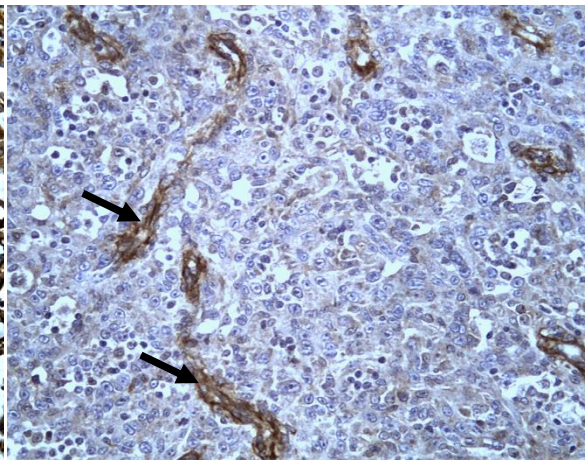

Angiosarcoma: Weak NRP1 staining of tumour cells, with intense staining focally around vascular channels (arrowed)

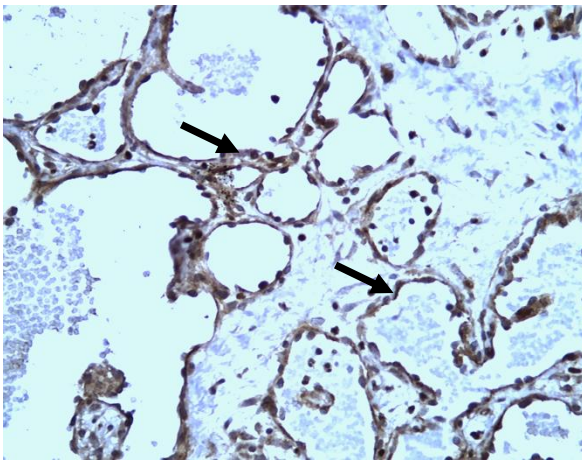

Benign haemangioma: Strong NRP1 staining of endothelial cells lining vascular spaces (arrowed)

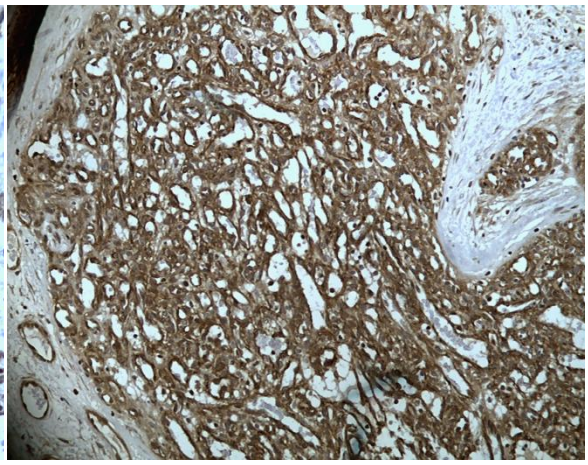

Pyogenic granuloma: Diffuse, strong NRP1 staining

Figure 3.69: Immunohistochemistry studies comparing the expression of NRP1 across all tumour groups (x20 magnification).

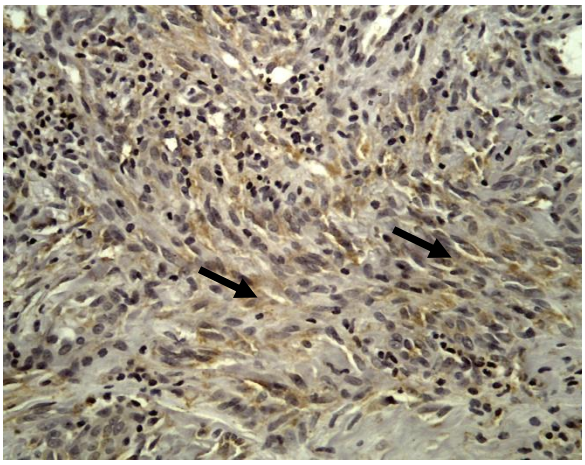

Angiosarcoma: Weak cytoplasmic bFGF staining in <50% of tumour cells (arrowed)

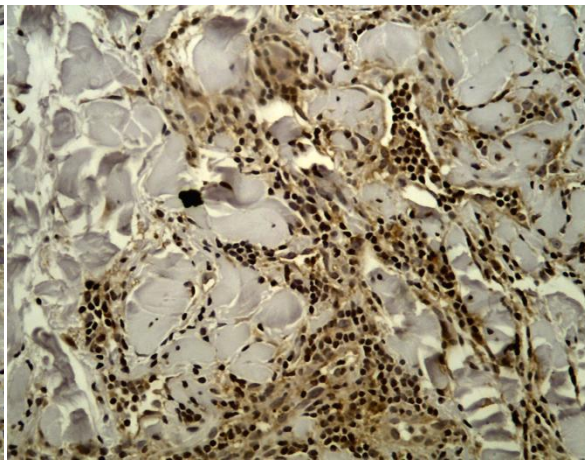

Angiosarcoma: Strong cytoplasmic bFGF staining in the majority of tumour cells

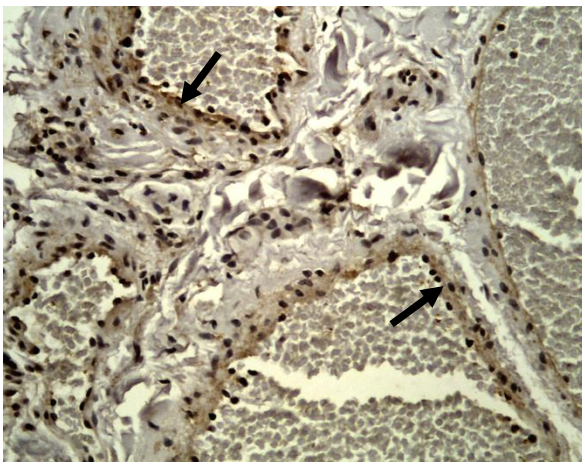

Benign haemangioma: Strong cytoplasmic bFGF staining in the endothelial cells lining the vascular spaces (arrowed)

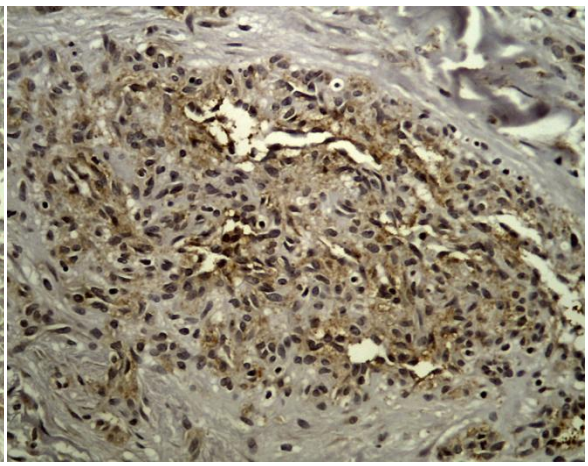

Pyogenic granuloma: Diffuse, strong cytoplasmic bFGF staining

Figure 3.70: Immunohistochemistry studies comparing the expression of bFGF across all tumour groups (x20 magnification).

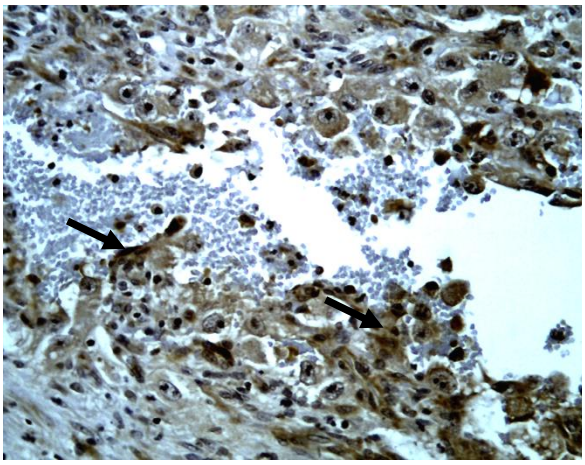

Angiosarcoma: Strong FGFR1 staining in epithelioid tumour cells (arrowed)

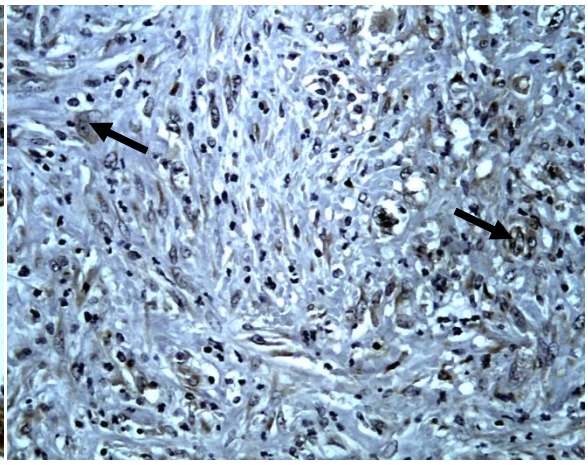

Angiosarcoma: Weak FGFR1 staining (arrowed) from the same tumour sample shown in the left hand panel

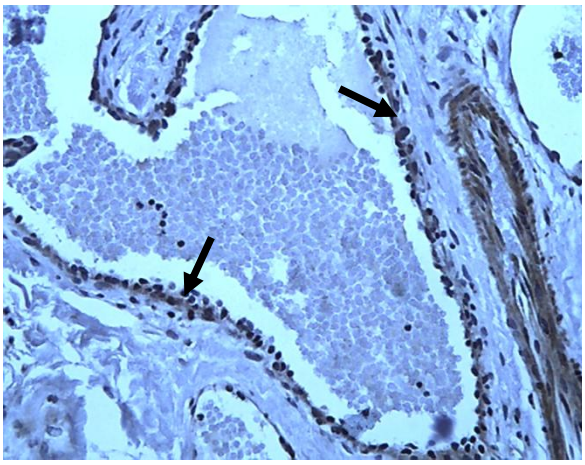

Benign haemangioma:FGFR1 staining of the endothelial cells lining the vascular spaces (arrowed) adjacent to a normal blood vessel

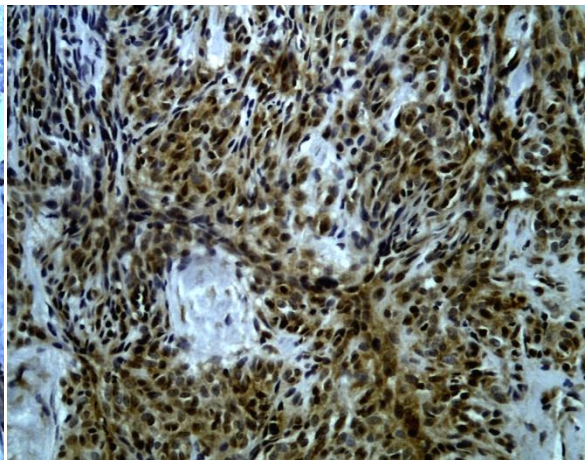

Pyogenic granuloma: Strong, diffuse FGFR1 staining

Figure 3.71: Immunohistochemistry studies comparing the expression of FGFR1 across all tumour groups (x20 magnification).

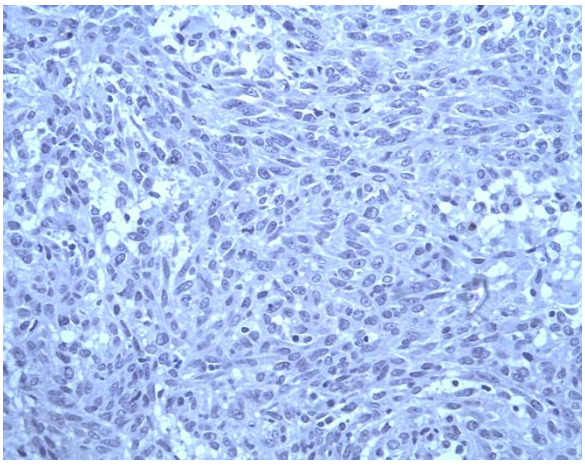

Angiosarcoma: Very weak, diffuse Ang-1 cytoplasmic staining of the tumour cells

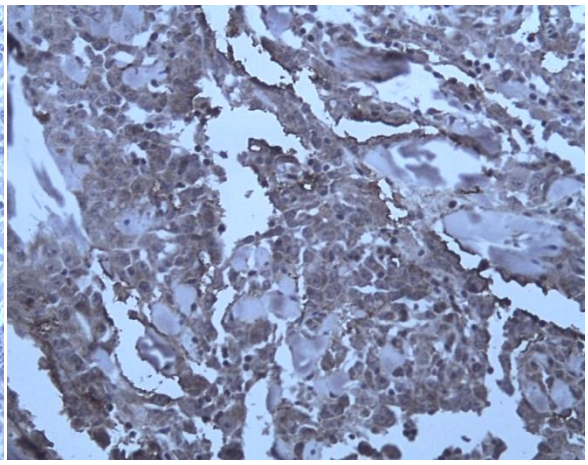

Angiosarcoma: Strong, diffuse Ang-1 staining

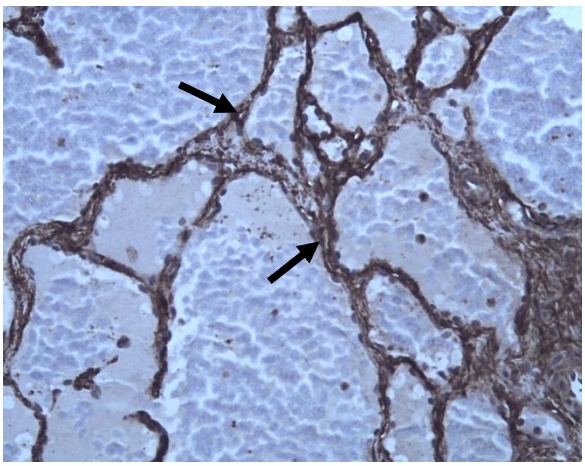

Benign haemangioma: Intense staining of the matrix surround the vascular spaces making accurate scoring of Ang-1 staining of the endothelial cells (arrowed) very difficult

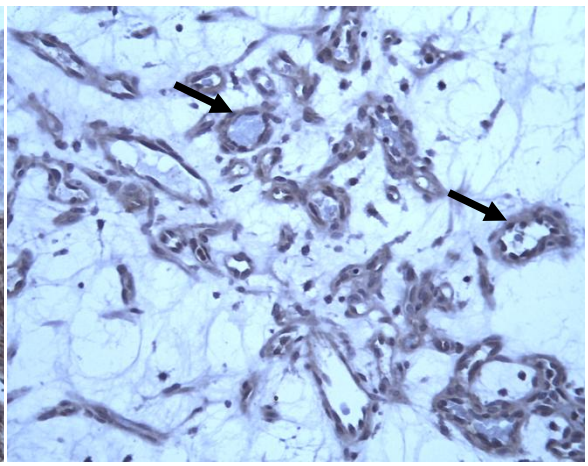

Pyogenic granuloma: Moderately intense Ang-1 staining (arrowed)

Figure 3.72: Immunohistochemistry studies comparing the expression of Ang-1 across all tumour groups (x20 magnification).

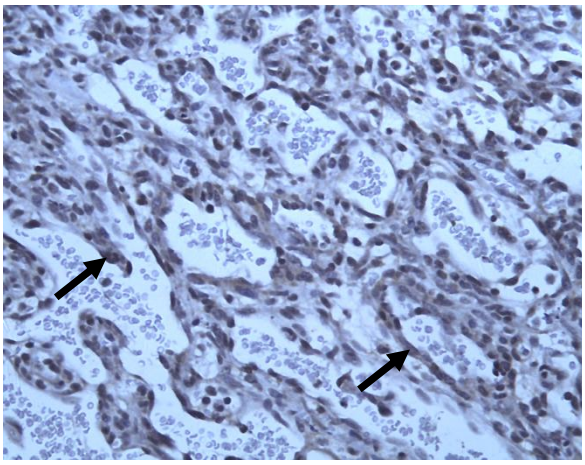

Angiosarcoma: Strong staining of Ang-2 around the vascular spaces (arrowed)

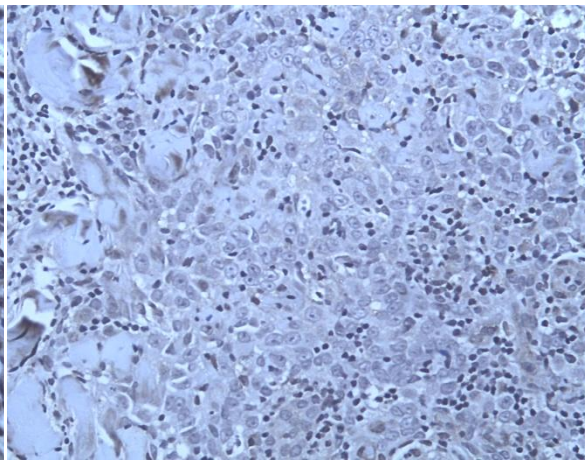

Angiosarcoma: Weak Ang-2 staining

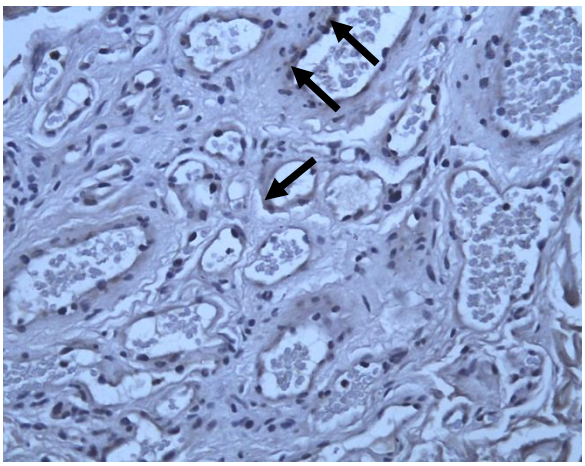

Benign haemangioma: Focal staining of endothelial cells lining the vascular spaces

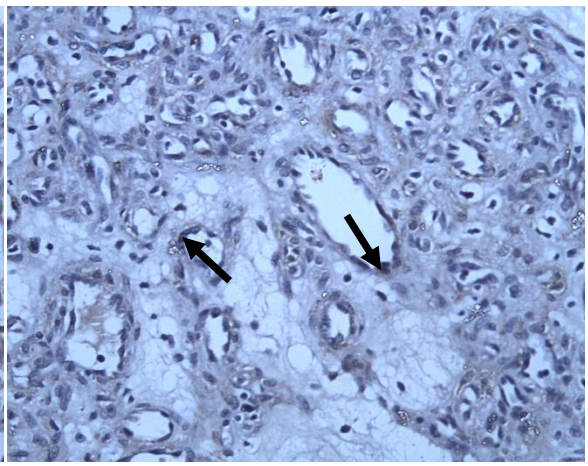

Pyogenic granuloma: Diffuse, moderately intense staining of Ang-2 (arrowed)

Figure 3.73: Immunohistochemistry studies comparing the expression of Ang-2 across all tumour groups (x20 magnification).

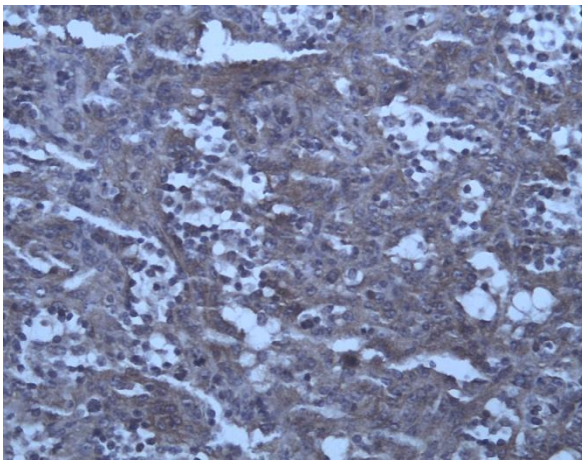

Angiosarcoma: Strong, diffuse Tie2 staining of epithelioid angiosarcoma cells

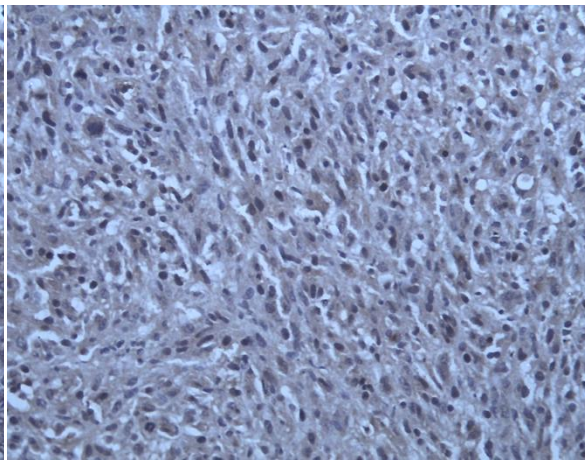

Angiosarcoma: Weaker Tie 2 staining in the same tumour, showing more spindle shaped tumour cells

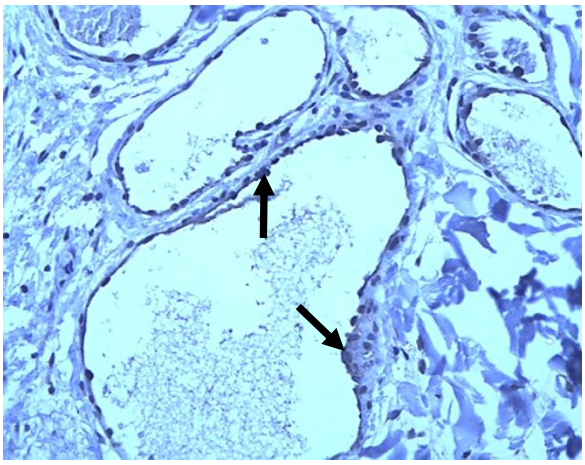

Benign haemangioma: Tie2 staining of endothelial cells lining the vascular spaces (arrowed)

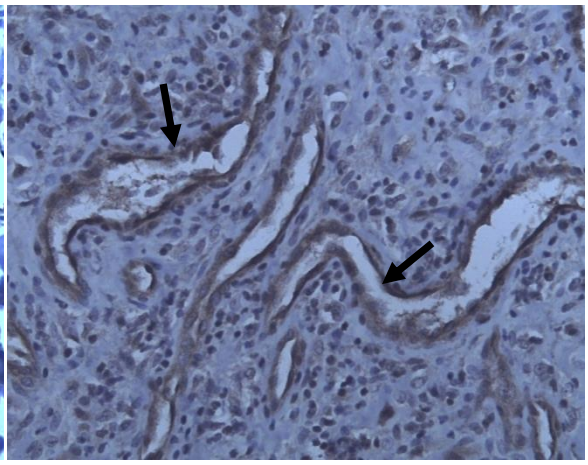

Pyogenic granuloma: Intense Tie2staining of endothelial cells lining vascular channels (arrowed)

Figure 3.74: Immunohistochemistry studies comparing the expression of Tie2 across all tumour groups (x20 magnification).

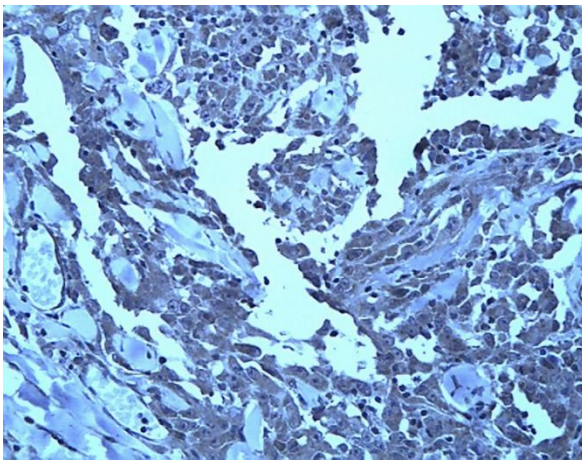

Angiosarcoma: Diffuse, strong HGF staining

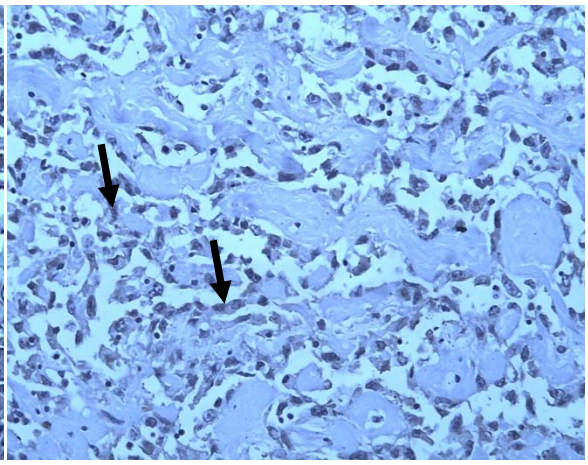

Angiosarcoma: Weak HGF staining (arrowed)

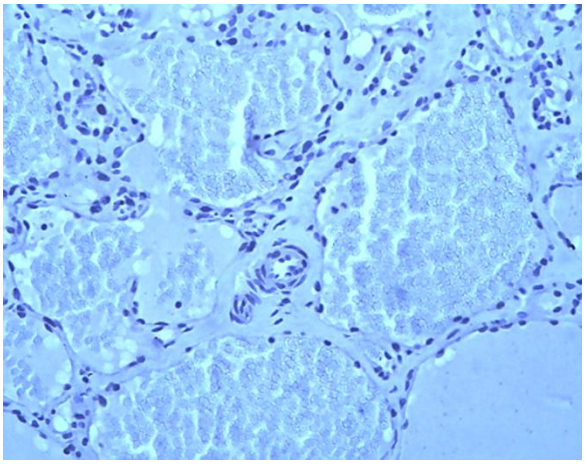

Benign haemangioma: Absent HGF staining

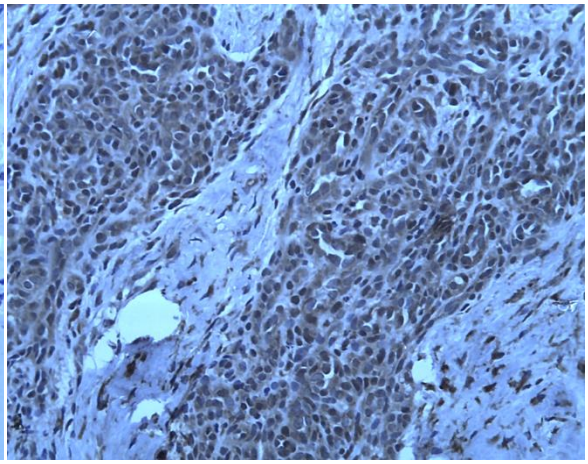

Pyogenic granuloma: Diffuse, strong HGF staining

Figure 3.75: Immunohistochemistry studies comparing the expression of HGF across all tumour groups (x20 magnification).

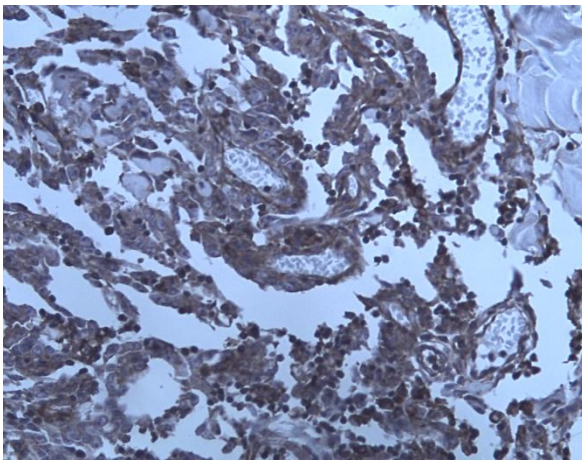

Angiosarcoma: Diffuse, strong expression of Met

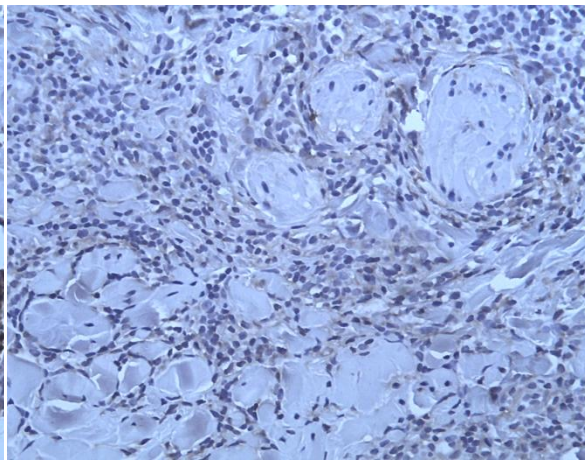

Angiosarcoma: Diffuse, weak expression of Met

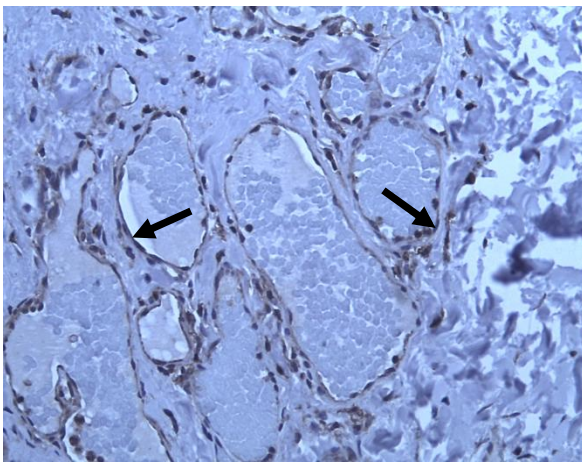

Benign haemangioma: Strong Met staining of endothelial cells lining the vascular spaces (arrowed)

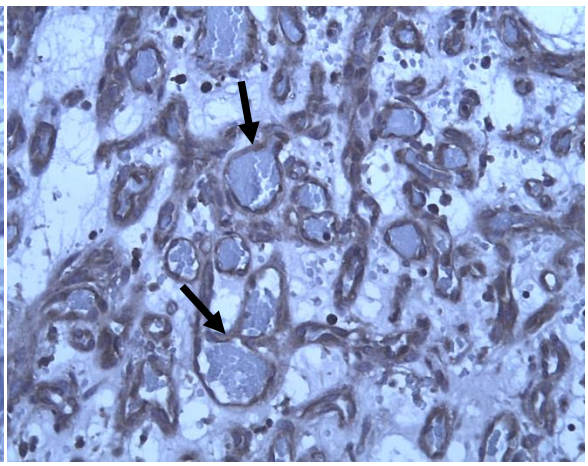

Pyogenic granuloma: Intense Met staining of vascular channels (arrowed)

Figure 3.76: Immunohistochemistry studies comparing the expression of Met across all tumour groups (x20 magnification).

3.5.4 Immunohistochemistry studies of canine vascular tumours

In contrast with humans, angiosarcomas are common in dogs. Through collaboration with the Animal Health Trust (Cambridge, UK), formalin fixed paraffin embedded tumour samples of canine angiosarcomas and benign haemangiomas were obtained for comparative immunohistochemistry studies to determine whether canine angiosarcoma could be used as a model for human angiosarcoma. Details of the tumour blocks studied are summarised in table 3.12.

	Histology	Tumour site	Date
Malignant vascular tumours	19 angiosarcomas	12 skin or subcutaneous 7 splenic	2004 - 2008
Benign vascular tumours	5 haemangiomas	Skin or subcutaneous	2004 - 2005

Table 3.12: Summary of the canine vascular tumours analysed

Canine angiosarcomas demonstrated similar morphological features to human angiosarcomas, including abnormal vascular channel formation by malignant endothelial cells, and dissecting bundles of collagen fibres (figure 3.77). Preliminary studies were performed to compare the pattern of VEGF and VEGFR2 expression in canine vascular tumours with human vascular tumours. Canine specific antibodies were not available commercially, and therefore the immunohistochemistry protocols used for the study of human tumours were utilised without modification (see section 2.6.4).

The canine angiosarcoma tumour cells showed a strong, diffuse staining pattern with antibody to VEGF, whilst the haemangiomas showed weak, compact staining (figure 3.78). Similarly, the canine angiosarcoma tumours showed moderately intense staining for antibody to VEGFR2, whilst the haemangiomas showed weak staining (figure 3.79). VEGFR2 staining of the canine tumour blocks was less intense than that seen with the human tumours. This difference in VEGFR2 staining compared to human samples may

reflect the age of the canine tumour blocks, or differences in antigen-antibody binding. Immunohistochemistry scores for canine haemangiomas and angiosarcomas were compared using the Mann-Whitney test. In contrast to the human samples, VEGF and VEGFR2 immunohistochemistry scores were significantly higher in the angiosarcomas than in the benign lesions (mean VEGF rank in haemangiomas 3.4 compared to 14.9 in angiosarcomas (p=0.001); mean VEGFR2 rank in haemangiomas 4.1, compared to 14.2 in angiosarcomas (p=0.002)).

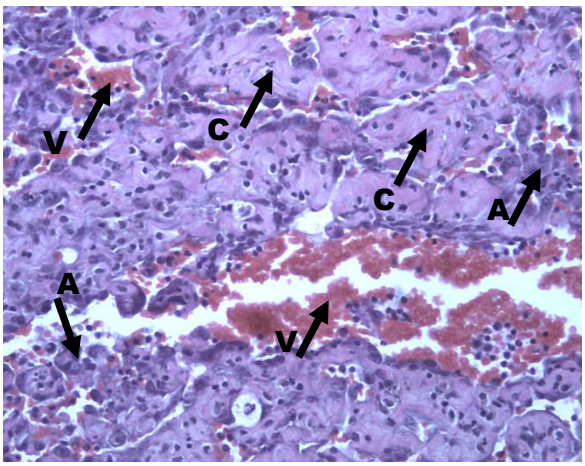

Canine angiosarcoma: Abnormal vascular channels (V), with malignant angiosarcoma tumour cells (A) and dissecting collagen fibres (C)

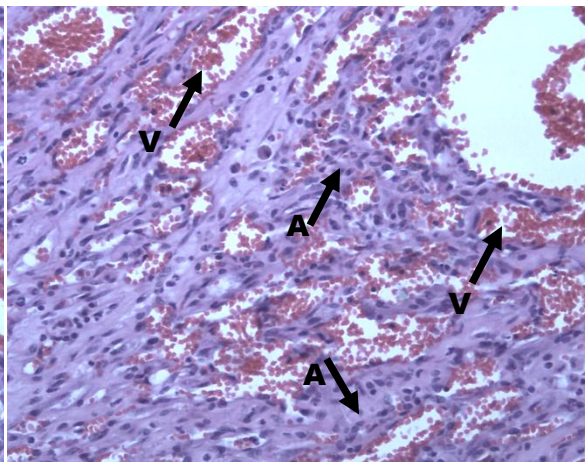

Canine angiosarcoma: Abnormal vascular channels (V) with malignant angiosarcoma tumour cells (A)

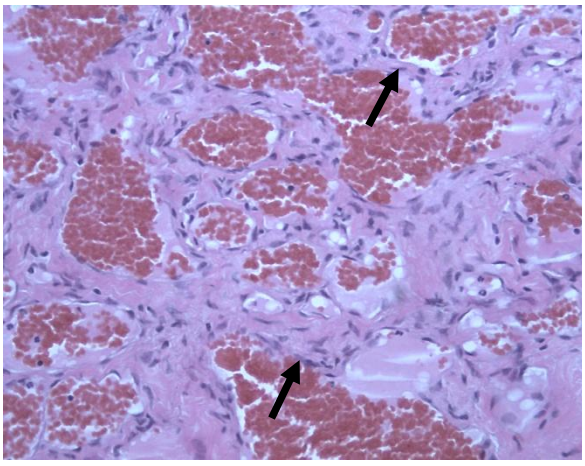

Canine haemangioma: Vascular spaces lined by benign endothelial cells (arrowed)

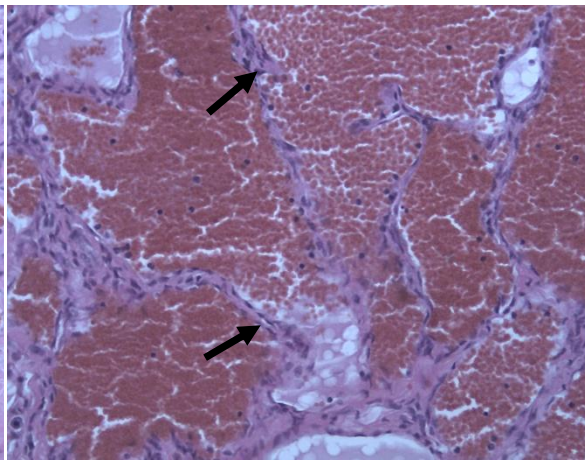

Canine haemangioma: Vascular spaces lined by benign endothelial cells (arrowed)

Figure 3.77: Haematoxylin & eosin stained canine vascular tumour (x20 magnification).

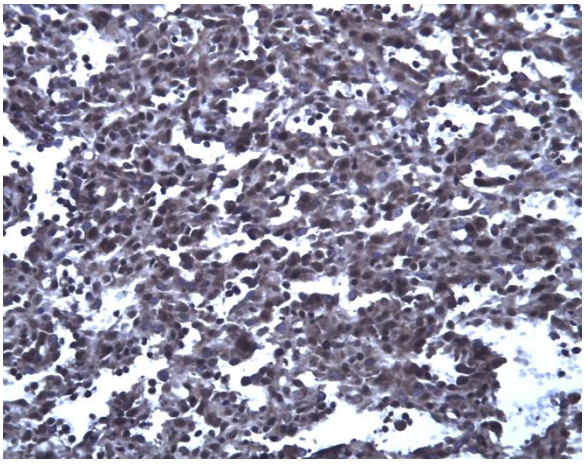

Canine angiosarcoma: Strong, diffuse VEGF staining of malignant endothelial cells

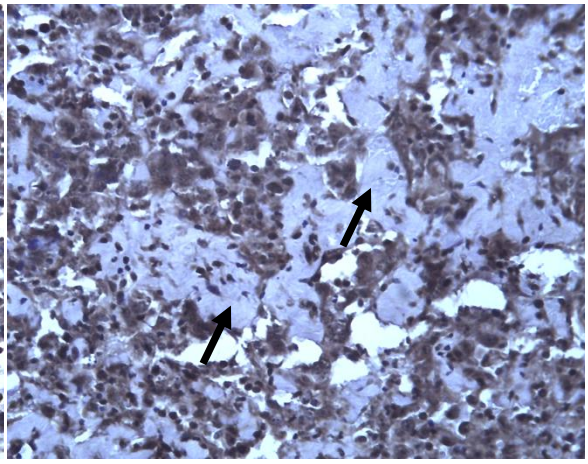

Canine angiosarcoma: Strong, diffuse VEGF staining of malignant endothelial cells, with dissecting collagen fibres (arrowed)

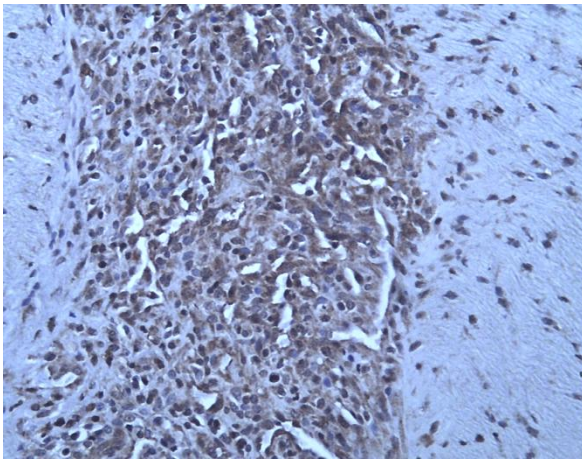

Canine angiosarcoma: Moderately intense VEGF staining of malignant endothelial cells

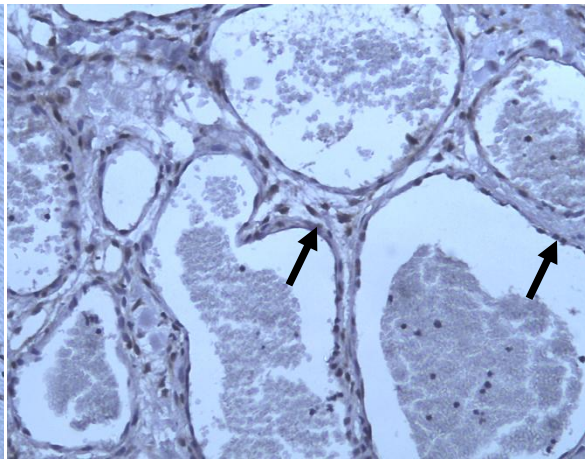

Canine haemangioma: Compact, nuclear VEGF staining of benign endothelial cells (arrowed)

Figure 3.78: Immunohistochemistry studies comparing the expression of VEGF in canine vascular tumours (x20 magnification).

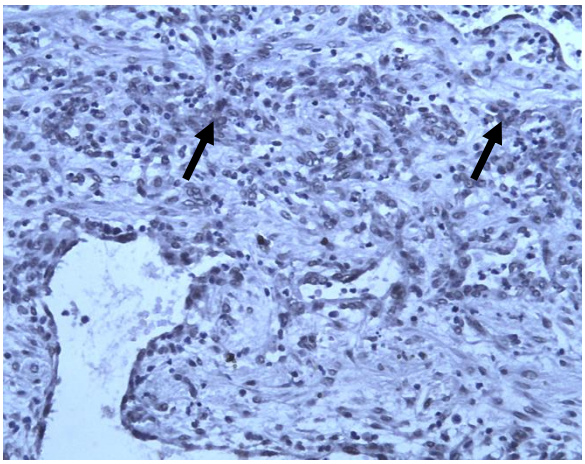

Canine angiosarcoma: Moderately intense VEGFR2 staining of malignant endothelial cells (arrowed)

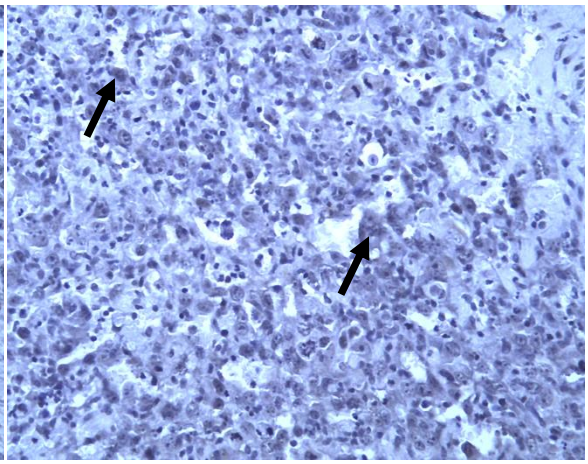

Canine angiosarcoma: Moderately intense VEGFR2 staining of malignant endothelial cells (arrowed)

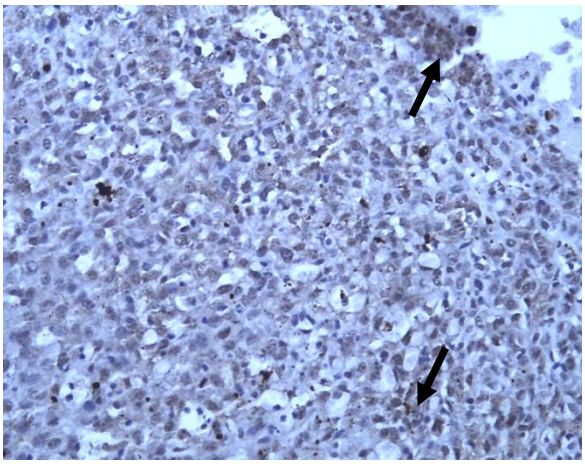

Canine angiosarcoma: Moderately intense VEGFR2 staining of malignant endothelial cells (arrowed)

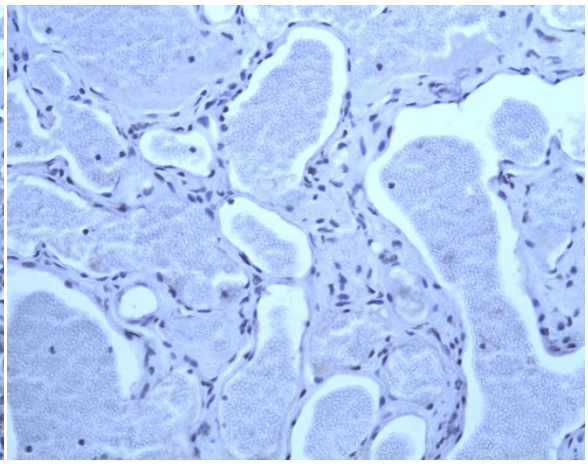

Canine haemangioma: No VEGFR2 staining of benign endothelial cells

Figure 3.79: Immunohistochemistry studies comparing the expression of VEGF2 in canine vascular tumours (x20 magnification).

4 Discussion

4.1 Characterisation Studies

ASM and ISO-HAS cell lines were separately developed from two patients with cutaneous angiosarcoma of the scalp. Similar to previously published reports[154, 158], ASM and ISO-HAS demonstrated Dil-Ac-LDL uptake and expressed CD31, vWF, VEGFR1 and VEGFR2, consistent with cells of endothelial origin. Cell morphology and immunocytochemistry studies suggested ASM and ISO-HAS consisted of a heterogeneous population of cells. However, flow cytometry studies showed that the cells were derived from a single population but expressed endothelial cell markers over a range of intensities.

In contrast to HuDMEC primary cell cultures, ASM and ISO-HAS showed accelerated growth kinetics and apparent limitless replicative potential *in vitro*. Functional assays also showed biological characteristics distinct from HuDMECs, with ASM and ISO-HAS demonstrating chaotic tubule formation on Matrigel, and significantly increased cell migration in Boyden chamber studies. Cytogenetic analysis had previously identified chromosomal abnormalities in ASM cells including the loss of whole chromosomes from homologues 4, 7, 8, 13, 15 and 16[154], and gene sequencing of ISO-HAS had shown the presence of a p53 mutation[156]. Neither ASM nor ISO-HAS cells formed tumours *in vivo* in CD1 nude mice. Krump-Konvalinkova *et al* were also unable to demonstrate ASM or ISO-HAS tumour formation in CD1 nude mice[154], though Masuzawa *et al* eported ISO-HAS tumourigenesis in profoundly immuno-compromised SCID mice pre-treated with anti-IL2 antibody[156].

Other angiosarcoma models considered included HAEND, EAhy926, SVR and ISOS-1 cells. HAEND cells were isolated from a human angiosarcoma of the liver[182]. It was not possible to source these cells, but it has previously been reported these cells were CD31, CD34 and vWF negative, and did not take up Dil-Ac-LDL, suggesting these cells were not of endothelial origin[158]. Both EAhy926 and SVR were synthetic cell lines.

EAhy926 was a hybrid cell line artificially formed by fusion of the lung cancer cell line A549 with an endothelial cell line (HuVECs)[157]. SVR was created by transfection of a primary murine endothelial cell line with retroviruses encoding for SV40 large T-antigen and activated H-ras[128], and *in vivo* form vascular tumours morphologically consistent with well differentiated angiosarcomas[128]. ISOS-1 cells were developed from the same cutaneous angiosarcoma as ISO-HAS, by subcutaneous transplantation of tumour fragments into SCID mice[155]. Cytogenetic analysis of ISOS-1 cells however demonstrated these cells had a murine rather than human phenotype[155].

ASM and ISO-HAS cells were derived from human cutaneous angiosarcomas, and the characterisation studies, together with the previously reported data, identified these cells as abnormal, potentially malignant, endothelial cells. ASM and ISO-HAS were therefore selected for further study as *in vitro* models most representative of human angiosarcoma.

4.2 Protein Expression

A targeted proteomic approach was used to compare ASM and ISO-HAS cell expression of angiogenic growth factors with that of HuDMECs and HDFs. The R&D Systems Proteome arrays enabled the simultaneous comparison of 55 angiogenesis related proteins. The levels of 42 phosphorylated receptor tyrosine kinases were also compared, including VEGFRs, Tie1 and 2, FGFRs and PDGFRs, and the levels of 46 phosphorylated protein kinases, including the signalling intermediaries promoting cellular response to VEGFR2 activation: cell proliferation (PLCy-1, MEK, ERK), cell growth (Akt, TOR, GSK-3, AMPK, p70 S6 kinase) cell migration (p38 MAPK, HSP27, Src, FAK, paxillin) and vascular permeability (eNOS) (figure 4.1)[38, 183].

These arrays were used as a tool to generate hypotheses for further study. Of note, the arrays did not measure absolute protein levels. Protein spot densities were dependent on antigen-antibody binding efficiency, which might not be equivalent across different proteins. The relative expression of individual proteins was therefore compared across

cell lines and culture conditions (e.g. to compare the expression of VEGF between ASM, ISO-HAS and HuDMECs, and between normoxia and hypoxia), but were not used to compare expression between different proteins within the same cell line (e.g. a direct comparison of Ang-1 with Ang-2 expression would in part be influenced by differences in antigen-antibody binding efficiencies). Comparisons of a large number of proteins across a small number of cell lines also increased the risk of declaring false positive associations. A two-fold difference in protein expression was initially used as a filter to identify proteins of interest. However, biological responses may not be linearly related to protein expression, and more subtle changes could also have profound biological effects. Patterns of expression across related proteins in cell signalling pathways were therefore also considered.

Other methods of comparing expression profiles between cell lines were considered. RNA studies are quantitative, but may not reflect actual protein expression levels, and an advantage of the R&D Systems Proteome arrays is that they enabled comparison of phosphorylated (active) protein kinases rather than total protein levels, which may be more biologically relevant. Unselected methods of measuring protein expression, such as iTRAQ, were also considered but differences between cell lines were likely to be lost within the general protein expression profiles.

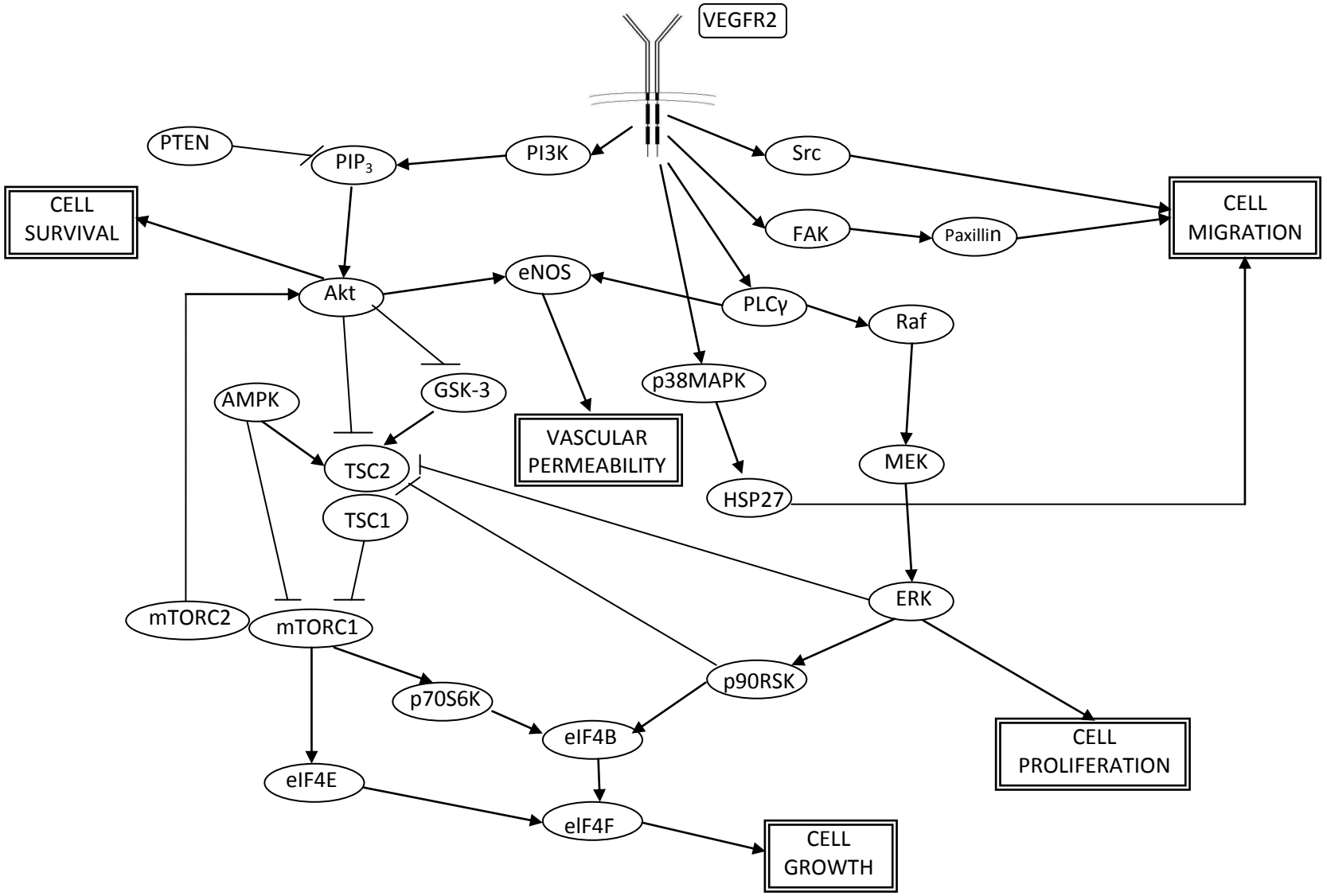

Figure 4.1: Signalling cascades recruited in response to VEGF activation of VEGFR2

Protein expression was principally studied in cell lysates. However, secreted angiogenesis related proteins in the cell supernatant may promote cell growth through autocrine or paracrine stimulation. Analysis of ASM and ISO-HAS cell supernatant was therefore also performed. This demonstrated quantitative differences with the proteins expressed in cell lysates. For example, bFGF was relatively high in ASM and ISO-HAS cell lysates, but the levels secreted into the cell supernatant were low. In contrast, levels of inflammatory cell chemoattractants including MCP-1 and GM-CSF were low in the cell lysates, but high in the cell supernatant. These studies highlighted the limitations of extrapolating from expression profiles based on cell lysate derived data only. If resources had permitted it would have been interesting to have studied the expression of angiogenesis related proteins in cell supernatant collected from HuDMEC cells, and to compare how levels in cell supernatant changed with incubation in hypoxic conditions.

Hypoxia is more representative of physiological conditions and therefore array studies were performed to assess the expression of angiogenesis related proteins in lysates of cells incubated in hypoxia. Compared to the studies in 21% O_2, greater differences were seen between the cell lines in expression of angiogenesis related proteins in 1% O_2, with increased expression of angiogenin, Ang-1, aFGF, HGF and VEGF by ASM and ISO-HAS cells compared to HuDMECs.

Despite studies demonstrating that ASM and ISO-HAS cells expressed a wide range of pro-angiogenic growth factors, phosphorylation of receptor tyrosine kinases in ASM and ISO-HAS cell lysates was restricted to a small number of receptors, suggesting limited autocrine or paracrine stimulation of ASM and ISO-HAS cells. The panel of phosphorylated receptor tyrosine kinases identified in studies of HuDMECs were predictable, including phosphorylation of VEGFR1, VEGFR2, VEGFR3 and Tie2, suggesting these array results were reliable. Under the same culture conditions, western blot studies suggested VEGFR2 was not phosphorylated at baseline in either ASM, ISO-HAS or HuDMEC cells, perhaps due to probing with a different primary

antibody from that used in the protein arrays. VEGFR2 phosphorylation was identified by western blot following stimulation of the cells with exogenous VEGF (50ng/ml), and following cell culture in hypoxic conditions (1% O_2). If further resources had permitted, it would have been interesting to explore whether the expression profiles of other phosphorylated kinases and receptor tyrosine kinases altered in hypoxic conditions.

Overall, few distinct differences emerged between the protein expression profiles of ASM, ISO-HAS and HuDMECs. This may reflect the use of semi-confluent, proliferating HuDMECs as a comparison group, rather than confluent, senescent cells, which more closely reflects endothelial cells of the normal vasculature, although re-creating these conditions *in vitro* would be difficult. Proteins of interest identified by the protein arrays for further study included VEGF/VEGFRs, mTOR/S6 kinase, MEK/ERK and ChkII.

4.2.1 VEGF

VEGF was significantly over expressed in ASM and ISO-HAS cell lysates compared to HuDMECs, and dramatically increased in hypoxic conditions. The increased VEGF expression was quantified and confirmed by ELISA. Western blot studies were performed to investigate the expression of VEGFA isoforms in ASM and ISO-HAS cell lysates and supernatants. Multiple protein bands were seen between 25 and 42 kDa which could reflect the concurrent expression of different VEGFA isofoms such as $VEGFA_{121}$, $VEGFA_{165}$ and $VEGFA_{189}$. The expression of PlGF, which is not bound by antibodies to VEGF including the anti-VEGFA antibody bevacizumab, was included in the angiogenesis related protein array. ASM and ISO-HAS expression of PlGF was not significantly different from HuDMECs. Expression of VEGFB and D were not investigated.

4.3 Drug Studies

Initial studies performed with doxorubicin and paclitaxel, current first and second line chemotherapy options for patients with advanced angiosarcoma, confirmed putative

ASM and ISO-HAS cell sensitivity to chemotherapy in cell viability assays. Angiosarcoma response to paclitaxel has not been directly compared with doxorubicin in clinical trials, but a retrospective analysis suggested similar overall response rates[104]. There has been particular interest in paclitaxel as a chemotherapy option for the treatment of angiosarcoma. Paclitaxel is classified alongside other anti-microtubule chemotherapy agents including vinca alkaloids[184]. However, in contrast to vinca alkaloids which inhibit microtubule formation, paclitaxel accelerates microtubule assembly and fixates mitotic spindle formation. Paclitaxel has anti-angiogenic properties, and inhibits endothelial cell differentiation and migration at sub-lethal doses[185].

4.3.1 VEGF targeted agents

Results from the angiogenesis related protein arrays and VEGF ELISA studies supported the study of VEGF targeted agents. Potential methods of targeting VEGF included:

- targeting the ligand, through antibodies against VEGF (e.g. bevacizumab)
- targeting the receptor, through tyrosine kinase inhibitors to inhibit VEGFR phosphorylation following ligand binding (e.g sunitinib or axitinib)
- inhibition of downstream signalling components including mTOR inhibitors (e.g. everolimus) or inhibitors of the MAPK pathway (e.g. the MEK inhibitor selumetinib)

Bevacizumab is a humanised monoclonal antibody to VEGF. *In vitro* studies with HUVECs have demonstrated bevacizumab binds to VEGF to inhibit receptor mediated functions including endothelial cell proliferation, survival and migration, without evidence of antibody-dependent cell-mediated cytotoxicity (ADCC)[186]. Clinical trials exploring the efficacy of bevacizumab have been summarised previously in table 1.1.

Tyrosine kinase inhibitors (TKIs) inhibit receptor and intracellular tyrosine kinases, and thus inhibit signal transduction pathways. There are numerous TKIs in clinical

development each with a different profile of kinase inhibition[39]. Sunitinib is a broad spectrum TKI[40]. A screening array of 242 kinases showed 0.3μmol/l sunitinib inhibited the activity of 49 kinases by more than 50% including VEGFR1-3, PDGFRs, KIT, FLT3, CSF-1R and RET[187]. Axitinib is more selective, principally inhibiting VEGFR1-3, PDGFR and KIT (table 4.1)[41]. At doses above 1μmol/l however axitinib also inhibits Abl, Aurora B, Arg, AMPK, Axl and MST2[41]. *In vitro*, axitinib reduced HUVEC survival and inhibited tubule formation by HuDMEC spheroids[41]. Axitinib is currently under study in a phase II clinical trial for advanced soft tissue sarcoma, including a cohort for angiosarcoma (ISRCTN:60791336). Clinical trials exploring the efficacy of bevacizumab have been summarised previously in table 1.2.

	Axitinib (nmol/l)	**Sunitinib (nmol/l)**
VEGFR1	0.1	NA
VEGFR2	0.2	5
VEGFR3	0.2	NA
KIT	1.7	0.3
PDGFRα	1.6	NA
PDGFRβ	5	2
FGFR1	215	180
Flt-3	>1000	1

Table 4.1: RTK inhibition profile of axitinib and sunitinib. Data shown represents the IC_{50} estimated from cellular inhibition studies[41, 187]. NA – not available

mTOR inhibitors inhibit formation of the mTOR1 complex, formed following activation of the PI3K/Akt signalling cascade. They thus inhibit phosphorylation of downstream S6 kinase and the release of eIF4E (eukaryotic translation initiation factor) following phosphorylation and inactivation of 4EBP1 (eIF4E binding protein) consequently modulating protein synthesis, cell proliferation and cell growth[188]. mTOR inhibitors have demonstrated clinical benefit in the treatment of advanced renal cell carcinoma[189], and in a recent phase III study of maintenance ridaforolimus after

chemotherapy for advanced soft tissue sarcoma, showed a small but statistically significant increase in progression free survival – angiosarcoma specific responses were unreported[190].

MEK is a central intermediary of the MAPK signalling cascade, and is phosphorylated in response to growth factor initiated activation of tyrosine kinase receptors, or through constitutive activation of upstream kinases including Ras or Raf. In contrast to other kinase inhibitors MEK inhibitors, including selumetinib, do not compete with ATP binding to inhibit MEK phosphorylation, but rather interfere with MEK binding and the subsequent activation of downstream ERK[191]. Evidence of clinical efficacy for selumetinib monotherapy has been demonstrated in studies of patients with advanced colorectal cancer[192] and melanoma[193].

4.3.2 VEGFR inhibition

Despite increased VEGF expression only minor responses to VEGFR inhibitors were observed in studies of ASM and ISO-HAS, with a modest response seen in assays with HuDMECs. ASM and ISO-HAS cell viability were significantly reduced using supra-pharmacological doses of TKI, possibly due to off target inhibitory effects involving other kinases such as Aurora B. Drug responses were not substantially enhanced by combining VEGF targeted agents with paclitaxel chemotherapy.

The functional assays may not have been sufficiently sensitive to detect biological responses to VEGFR inhibition. For example, the trypan blue dye exclusion assay to measure cell viability assessed response 120 hours after the addition of drug. This may not have been the optimum time point at which to measure response, however results from these assays were consistent with findings from the MTS assay which measured cell viability at 24 and 48 hours. Cell viability with the dye exclusion assay was measured at 120 hours to enable direct comparison with response to the other targeted agents.

Other studies measuring endothelial cell response to bevacizumab *in vitro* have often used large vessel endothelial cells (e.g. HuVECs) rather than microvascular endothelial cells (e.g. HuDMECs). However, different endothelial cell types are functionally and genetically distinct, and their response to vascular targeted agents may not be the same (Chi, 2003). As both ASM and ISO-HAS were derived from superficial cutanous angiosarcomas, comparison of drug response with dermal microvascular endothelial cells (HuDMECs) was considered most appropriate. Luthra *et al* showed bevacizumab (0.125mg/ml – 1.0mg/ml) had no significant effect on human microvascular endothelial cell viability[194], and a study by Deissler *et al* showed no effect of bevacizumab (0.25mg/ml) on retinal microvascular endothelial cell proliferation, although endothelial cell migration was inhibited[195]. Importantly, the study by Deissler *et al* also suggested bevacizumab stored at 4^0C for more than 2 weeks was significantly less potent than fresh aliquots of the drug. However repeated studies of ASM, ISO-HAS and HuDMEC using fresh aliquots of bevacizumab and axitinib produced similar results.

In other studies, tumour cell responses to bevacizumab have not been seen *in vitro*[33], but responses have been demonstrated *in vivo,* including reduction in tumour micro-vessel density in patients receiving neo-adjuvant bevacizumab for advanced colorectal cancer[196]. *In vivo* studies may therefore be required to determine angiosarcoma response to VEGFR inhibitors. Consistent with the *in vitro* data however, phase II clinical studies of single agent bevacizumab, sunitinib and sorafenib for the treatment of advanced angiosarcoma have proved disappointing with overall response rates less than 15% (see table 1.4). It has been proposed that angiosarcomas harbouring mutations of VEGFR2 may respond to VEGFR kinase inhibitors[72]. A previous molecular study of tumour samples from 22 angiosarcomas reported four cases with VEGFR2 mutations. *In vitro* these mutations induced VEGFR2 autophosphorylation sensitive to inhibition with sorafenib and sunitinib[72]. However, a recently published phase II study found no activating mutations of VEGFR2 in 41 patients with advanced angiosarcoma, and no evidence for efficacy of single agent

sorafenib in these patients, suggesting angiosarcomas harbouring VEGFR2 mutations are a rare sub-group[107].

Biological responses to stimulation with exogenous VEGF were not seen in functional assays with the malignant ASM and ISO-HAS cells, whilst increased tubule formation and cell migration were seen in response to stimulation with exogenous VEGF in studies with HuDMECs. The absence of ASM and ISO-HAS response to stimulation with exogenous VEGF could be ascribed to VEGFR saturation by excess endogenous VEGF, and this could partly explain their insensitivity to VEGF targeted therapy. However, the western blot studies of ASM, ISO-HAS and HuDMECs suggested VEGFR2 was not phosphorylated by the levels of endogenous VEGF expressed in normoxia. In contrast VEGFR2 was phosphorylated by the levels of endogenous VEGF expressed in hypoxia, and in response to exogenous VEGF (50ng/ml). Induced VEGFR2 phosphorylation was inhibited by VEGF targeted agents (bevacizumab and axitinib) but this did not translate into a response in functional assays.

Western blot studies may not have been sufficiently sensitive to detect all phosphorylated VEGFR2. VEGFR2 activates the MAPK signalling cascade through tyrosine1175[38], and therefore the principal antibody used in these studies probed for $pVEGFR2^{Y1175}$. VEGF binding to VEGFR2 also induces phosphorylation of other tyrosine residues including tyrosine951, which stimulates cell migration through activation of Src[38]. Western blot studies were not performed to confirm that axitinib and bevacizumab inhibited all the phosphorylation sites on VEGFR2, nor to assess phosphorylation status of other VEGFRs (1 and 3), nor to assess signalling mediated through VEGFR2 interaction with the non-tyrosine kinase co-receptors NRP1 and NRP2. Interestingly, recent data from studies using an *in vitro* model for infantile haemangioma suggested downstream ERK phosphorylation was initiated by VEGFA and VEGFB signalling through VEGFR1 rather than through VEGFR2[197], supporting further study of VEGFR1 activity in ASM and ISO-HAS.

Intrinsic activation of down-stream signalling cascades including the MAPK pathway may have muted ASM and ISO-HAS cell response to stimulation with exogenous VEGF. ERK, a central signalling intermediary of the MAPK pathway, may be phosphorylated as a consequence of mutated Ras or Raf upstream, or through autocrine or paracrine stimulation of the MAPK pathway by other secreted growth factors. Western blot studies of ASM and ISO-HAS cells showed basal activation of ERK. ERK phosphorylation increased in response to stimulation with exogenous VEGF, and decreased in the presence of VEGF targeted agents, conflicting with the lack of response seen in functional assays. Residual ERK phosphorylation following treatment with axitinib and bevacizumab however may have been sufficient to maintain biological response

The functional assays used to assess drug response were not specific to VEGF. The angiogenesis related protein array studies demonstrated ASM, ISO-HAS and HuDMECs expressed a broad panel of pro-angiogenic growth factors, which were not targets of VEGFR inhibitors. Whilst the protein expression studies suggested VEGF was a key growth factor, these other pro-angiogenic cytokines may have compensated for any attenuation in VEGF signalling. Consistent with this, resistance to VEGF targeted agents in the treatment of other malignancies, is mediated through other signalling pathways, including FGF, PDGF and Notch[198].

4.3.3 mTOR inhibition

The phosphorylated protein kinase array studies provided evidence to support investigating response to mTOR inhibitors, with increased levels of pAkt, pTOR, p70 S6 kinases, and decreased pAMPK in ASM and ISO-HAS cell lysates. Furthermore, an immunohistochemistry study reported high expression of pAkt and peIF4E in angiosarcomas[168], and another recent study by Italiano *et al* reported expression of pS6K and p4EBP1 in 17/40 (42%) angiosarcomas[119].

Compared to axitinib and bevacziumab, increased responses were seen to the mTOR inhibitor everolimus in cell viability assays with ASM and ISO-HAS. The biological effects of mTOR inhibitors include inhibition of angiogenesis, partly through decreased synthesis of VEGF by reduced expression of HIF-1α[173]. mTOR inhibitors have other effects, including reduced cell growth and cell proliferation. ASM and ISO-HAS response to everolimus cannot be solely attributed therefore to decreased VEGF synthesis. Furthermore, an immunohistochemistry study showed angiosarcoma expression of VEGF was not dependent on HIF-1α expression[199].

The contribution of endogenous VEGF to angiosarcoma biology remains unclear. This could be further explored *in vitro* using short interfering RNA (siRNA) to VEGF to decrease the synthesis of endogenous VEGF. However, an efficient methodology would be required to reduce the high VEGF expression levels in ASM and ISO-HAS to be comparable with those measured in HuDMECs.

4.3.4 MEK inhibition

The phosphorylated kinase array studies demonstrated intrinsic activation of the MAPK pathway, with elevated pMEK and pERK in ASM cells compared to HuDMECs, though these were not elevated in ISO-HAS cells. As previously discussed, the MAPK signalling cascade may be stimulated by endogenous growth factors, or through constitutive activation of MEK by mutated Ras or Raf.

A recent immunohistochemistry study identified expression of pERK in 12/39 (31%) angiosarcomas[119]. However another immunohistochemistry study of benign and malignant vascular tumours suggested pERK was significantly lower in malignant endothelial lesions[200]. There was also evidence to support the study of MEK inhibitors from pre-clinical studies of other malignant vascular tumours, specifically Kaposi's sarcoma. Kaposi's sarcoma lesions develop as a consequence of lymphatic endothelial cell infection with human herpes virus-8 (HHV-8). Viral interleukin-6 (vIL-6) and viral G protein coupled receptor (vGCPR) stimulate the MAPK signalling cascade,

and increase the secretion of pro-angiogenic growth factors, including Ang-2, reduced *in vitro* by MEK inhibition[201].

Consistent with the protein expression studies, the MEK inhibitor selumetinib inhibited both ASM cell viability and tubule formation. ISO-HAS response to selumetinib was seen in cell differentiation assays, but not in cell viability studies. The absence of an ISO-HAS response to MEK inhibition in the cell viability assays suggest the Raf/MEK/ERK pathway did not drive proliferation in these cells. Alternatively, as drug response was assessed at 6 hours in cell differentiation assays compared to 120 hours in cell viability assays, the difference in drug response could be due to adaptive changes in cell signalling pathways. A study of MEK inhibition in a panel of different cell lines, including non small cell lung cancer and melanoma cell lines, showed cell sensitivity to MEK inhibitiors required the presence of mutated Ras or Raf. In cell lines with wild type Ras or Raf, MEK inhibitors were associated with loss of pERK mediated feedback loops and consequently drug resistance[202]. A separate study of MEK inhibition showed drug efficacy was dependent upon the mutation status of the PI3K pathway[203], suggesting compensatory signalling through the PI3K/Akt/mTOR pathway may have limited the effects of MEK inhibition in ISO-HAS cells. Drug studies to assess ASM and ISO-HAS cell response to combination therapy with MEK inhibitor and Akt or mTOR inhibitor were not performed. No response was observed however to single agent MK2206, an Akt inhibitor, in ISO-HAS or ASM cell viability studies. If resources had permitted, studies to investigate changes in the phosphorylation status of key kinases in the PI3K/Akt/mTOR and Raf/MEK/ERK pathways in response to MEK inhibition would have been of interest.

4.3.5 Checkpoint II inhibition

Phosphorylated ChkII^{T68} and p53^{S15} were significantly elevated in ASM and ISO-HAS cells relative to HuDMECs. ChkII may be required to manage genomic instability, and both ChkII and p53 are activated by at these phosphorylation sites by ATM in response to DNA double strand breaks[204]. Phosphorylated ChkII induces cell cycle arrest,

promotes DNA repair and activates apoptosis[204]. The clinical utility of ChkII inhibitors is uncertain. It has been postulated that, in combination with anti-cancer therapies that induce double strand DNA breaks, including radiotherapy and chemotherapy agents such as topoisomerase inhibitors, ChkII inhibitors may be of benefit to patients with concurrent DNA repair pathway abnormalities[204]. However, the main effect of ChkII activation may be to induce apoptosis in response to DNA damage. Therefore, the clinical potential of ChkII inhibitors may reside in protecting normal tissue with functioning DNA repair pathways from undergoing apoptosis in response to exposure to radiotherapy.

ASM and ISO-HAS cell response to ChkII inhibition was investigated in monotherapy studies and in combination with the topoisomerase II inhibitor doxorubicin. C3742 (ChkII inhibitor II) was selected for study as it is specific for ChkII, whilst other ChkII inhibitors identified also inhibit ChkI, required for the repair of single strand DNA breaks. The results from the cell viability assays demonstrated no benefit of ChkII inhibition at the doses studied, and in ISO-HAS cells C3742 showed a protective effect, potentially through inhibition of pro-apoptotic signals.

4.3.6 DMXAA

DMXAA is a flavonic acid derivative vascular disrupting agent that reduces tumour blood flow and induces tumour necrosis. A recent phase III trial of DMXAA in combination with carboplatin-paclitaxel chemotherapy for advanced non small cell lung cancer showed no improvement in progression free survival compared to chemotherapy alone, although DMXAA was well tolerated[178].

DMXAA's anti-tumour properties are not fully understood. Within 30 minutes of administration *in vivo*, DMXAA induces apoptosis of tumour endothelial cells leading to reduction in tumour blood flow[205]. Endothelial cell death exposes the underlying basement membrane, inducing platelet activation, and leading to a localised increase in 5-HIAA (5-hydroxyindole-3-acetic acid), resulting in vascular constriction, and thus

tumour hypoxia and necrosis[206]. Within 4 hours of administration, through activation of nuclear factor kappa B (NF-κB), DMXAA induces tumour production of a number of cytokines including TNFα, interferon-γ (IFNγ) and IFNγ-inducible protein-10 (IP-10)[206]. Systemic administration of TNFα is highly toxic, but localised administration by isolated limb perfusion, in combination with melphalan chemotherapy, is used in the treatment of soft tissue sarcoma of the distal extremities[207]. TNFα appears important for mediating the response to DMXAA *in vivo*, with treatment less effective in TNF receptor-1 knockout mice[208]. In contrast to mouse tumour models, evidence from phase I clinical studies suggested minimal TNFα production in human tumours, potentially explaining the subsequent lack of efficacy seen in the phase III NSCLC trial[179]. However, the phase I clinical studies measured TNFα in plasma rather than assessment of intratumoural levels, and thus may have missed any focal TNFα expression. In any case, production of TNFα may not be necessary for tumour response. Thalidomide inhibits the synthesis of TNFα but, intriguingly, studies of DMXAA in combination with thalidomide showed an increased anti-tumour response, despite evidence of modulated TNFα expression[209].

At clinically relevant doses DMXAA profoundly inhibited ASM, ISO-HAS and HuDMEC cell viability and tubule formation. The mechanisms by which DMXAA exerted its effect were unclear. ELISA studies showed no significant increase in TNFα expression in ASM cells after 4 and 24 hours of exposure to DMXAA 100μg/ml. Assays to measure AnnexinV showed no increase in apoptotic ASM cells after exposure to 100μg/ml DMXAA for up to 24 hours. Previously reported *in vitro* studies with HUVECs showed a modest reduction in cell viability 24 hours after treatment with 100μg/ml DMXAA, with an estimated IC_{50} of 300μg/ml[210]. Compared to untreated HUVEC cells, apoptosis was not significantly increased at 100μg/ml DMXAA, but was increased at doses beyond 300μg/ml[210]. Other i*n vitro* studies with mouse endothelial cells (HECCP) showed apoptosis was induced after 3 hours of exposure to 400μg/ml DMXAA, and increased substantially after exposure for 24 hours[211]. No significant increase in

HECCP cell apoptosis was observed after 24 hours of exposure to 100µg/ml DMXAA, and a dose of 500µg/ml DMXAA was required to induce apoptosis in 50% of cells at 24 hours. These studies illustrate differences seen between the effects of DMXAA on endothelial cells *in vitro* with tumour response *in vivo.*

Overall, the results from studies with ASM cells suggested the method by which DMXAA exerted its effect did not involve TNFα expression or induction of apoptosis. Interestingly, a recent report proposed DMXAA as a multi-kinase inhibitor including, and most prominently, an inhibitor of VEGFR2[212]. VEGFR2 phosphorylation status was not studied in ASM, ISO-HAS or HuDMEC cells in response to treatment with DMXAA. The western blot studies previously described however demonstrated basal VEGFR2 phosphorylation levels in these cells were low or absent, suggesting VEGFR2 inhibition as an unlikely mechanism of response. Tubule formation was significantly inhibited in assays with ASM, ISO-HAS and HuDMEC cells, but these responses could have been mediated through a direct cytotoxic effect, rather than through a response involving the inhibition of VEGFRs. DMXAA inhibits a number of other kinases including the aurora kinases. As previously described, axitinib inhibits aurora B kinase at doses that reduced ASM and ISO-HAS cell viability in the extended dose studies, suggesting a common mechanism requiring further study.

In summary the *in vitro* drug studies show targeting ASM or ISO-HAS cells with inhibitors of a single pro-angiogenic growth factor such as VEGF was less efficacious than either targeting a common signalling intermediary such as MEK, or using less directed therapy such as the vascular disrupting agent DMXAA, or the chemotherapeutic agents doxorubicin or paclitaxel. Ideally, additional *in vitro* studies would investigate response to MEK inhibitiors or vascular disrupting agents in a wider panel of angiosarcoma samples, and subsequently investigate drug response within an *in vivo* system. However, angiosarcomas are rare, and suitable material for further study is limited. *In vivo* studies are needed to fully evaluate angiosarcoma response to

anti-angiogenic agents, as their target may be the tumour micro-environment rather than the tumour cells. ASM and ISO-HAS cells did not form tumours *in vivo,* and there are currently no animal models for angiosarcoma.

4.4 Human Angiosarcoma Tumour Samples

Fresh angiosarcoma tumour samples were collected intra-operatively following the patient's consent. After resection the tumour was transported on ice for immediate sampling by the collaborating histopathologist. Multiple biopsies were taken under macroscopic inspection of the tumour to identify suitable lesional tissue. The presence of viable, neoplastic cells within the study samples was inferred, and the precise architecture of the samples used in the protein array study and for tumour cell isolation was unknown. In addition to fresh angiosarcoma tumour samples, historical samples were retrieved from the pathology archives of Sheffield Teaching Hospitals NHS Trust for immunohistochemistry study.

4.4.1 Tumour cell isolates

Fresh angiosarcoma tumour samples were collected in order to isolate and study tumour cells *in vitro.* As angiosarcomas are rare the opportunity to collect samples occurred sporadically, which hampered any systematic study. Cell isolates were successfully established in two of four cases (STS0510 and STS1011), although immunocytochemistry study suggested these cell isolates were not of endothelial origin. Drug studies with VEGF targeted agents were performed using cell isolates from one case (STS1011). Results were consistent with the studies of ASM and ISO-HAS cells, demonstrating the feasibility of this approach. Paclitaxel profoundly reduced STS1011 cell viability. A modest response was observed to axitinib in cell viability and cell differentiation assays, but no response was seen to bevacizumab. The window for performing *in vitro* studies with the tumour isolates was short as the characteristics of the cell isolates evolved rapidly during culture. Few tubules were formed by passage 7 cells, in contrast to earlier passages, and passage 7 cells were also drug resistant.

4.4.2 Angiogenesis related protein array study of tumour samples

The expression profiles of angiogenesis related proteins derived from the human angiosarcoma tumour samples were broadly consistent with ASM and ISO-HAS expression profiles, supporting the study of these cell lines as an *in vitro* model of angiosarcoma. Differences, such as higher expression of matrix metalloproteinases (MMP-8 and MMP-9) by tumour tissue samples may reflect analysis of more complex samples. The immunohistochemistry studies of angiosarcoma tumour samples, and the protein expression studies of ASM and ISO-HAS, showed high expression of VEGF by malignant endothelial cells. The angiogenesis related protein array study of angiosarcoma tumour samples however showed low tumour expression of VEGF. An mRNA analysis of angiosarcoma samples also reported low tumour expression of VEGF[72]. The quantitative differences in expression likely reflect differences in methodology. Tumour architecture was not assessed by array studies, in contrast to immunohistochemistry, which quantifies both intensity and location of protein expression.

The expression profiles of the two de-differentiated liposarcomas were distinct from the angiosarcoma samples, with lower levels of expression of angiogenesis related proteins by the liposarcomas compared to the angiosarcomas. The expression of proteins such as angiogenin and TIMP-4 were similar across all samples. This finding may be genuine, but probably illustrates the semi-quantitative nature of these arrays and suggests the use of sensitive but not specific primary antibodies to detect these proteins. Macroscopically, in contrast to the angiosarcoma tumour samples, the lipoosarcoma specimens appeared gelatinous and were relatively avascular. The differences in protein expression may therefore reflect the proportion of endothelial cells in the samples. It would be of interest to compare angiogenesis related protein expression profiles of benign vascular tumours, including capillary haemangiomas and pyogenic granulomas, with angiosarcomas. The subsequent immunohistochemistry

studies of benign and malignant vascular tumours would predict however that any differences would be small.

4.4.3 Immunohistochemistry studies

Immunohistochemistry studies were performed to compare benign and malignant vascular tumour expression of angiogenic growth factors and their receptors. Two haemangioendotheliomas were included in the group of malignant vascular tumours. Haemangioendotheliomas are rare vascular tumours of intermediate malignant potential, with a low risk of metastasis compared to angiosarcomas[180]. Capillary and cavernous haemangiomas were included as examples of benign quiescent vascular tumours, and pyogenic granulomas and granulation tissue were included as examples of benign inflammatory lesions[181].

Results from the immunohistochemistry studies of angiosarcoma tumour samples were biased by a strong correlation between the immunohistochemistry score and the age of the tumour block, with staining intensity reduced or absent in older specimens. On average two or three patients with angiosarcoma presented annually to Sheffield Teaching Hospitals, and therefore to collect the cohort size used in these studies it was necessary to use tissue blocks from a ten year period. The age of the benign vascular tumour blocks was not matched with the age of the malignant vascular tumour blocks, but this should be considered for future studies.

4.4.3.1 VEGF and VEGFRs

The expression of VEGF and its receptors in angiosarcomas and haemangiomas has been reported previously in several immunohistochemistry studies. Tokuyama *et al* identified increased expression of VEGF and VEGFR2 in angiosarcomas compared to capillary and cavernous haemangiomas[213]. A comparison of VEGF expression by Dim *et al* also suggested VEGF expression was increased in angiosarcomas compared to haemangiomas[142]. However, cytoplasmic VEGF staining only was scored in this study. The tumour endothelial cells of benign vascular lesions have a compact nucleus

with a thin rim of cytoplasm, compared to the tumour endothelial cells of angiosarcoma which demonstrate prominent cytoplasm, and this difference may have biased their results. Zietz *et al* also demonstrated increased expression of VEGF in angiosarcomas compared to benign controls[144]. The controls used covered a range of conditions including normal skin, an angiofibroma, a lymphangioma and granulation tissue. Notably the two haemangioma cases included in this series scored moderate and strong expression of VEGF. In contrast, a small study by Brown *et al* found strong expression of VEGFR2 by angiosarcoma tumour cells, but weak expression of VEGFR1 and VEGF, whilst capillary haemangiomas showed strong expression of VEGFR2 and R1, and weak expression of VEGF[214]. Results from a large study by Itakura *et al* were comparable with the results presented here[145]. Staining intensity was not assessed by Itakura *et al*, but the proportion of cells staining positive was measured. In these studies VEGFA was expressed by the majority of tumour cells but VEGFR1 and VEGFR2 expression varied. In summary, whilst a variety of sources have demonstrated angiosarcomas express VEGF and their receptors, the quantity of the expression relative to benign vascular tumours is unproven.

4.4.3.2 Neuropilins

Neuropilins are transmembrane non-tyrosine kinase co-receptors first shown to bind class 3 semaphorins (Sema-3) to regulate neuronal development during embryogenesis[215]. Neuropilins are required for normal development of the vasculature, and are expressed by endothelial cells during physiological angiogenesis including wound healing. They are expressed by both endothelial cells of the tumour vasculature and by neoplastic cells, and increased expression is associated with tumour progression and a worse prognosis. As co-receptors they complex with VEGFR2 and facilitate signal transduction on binding with VEGF to promote angiogenesis. Neuropilins do not induce phosphorylation of ERK, but through activation of focal adhesion kinase (FAK) they stimulate endothelial cell migration[10]. Neuropilins have been identified as a mechanism of resistance to VEGF targeted therapy as the

neuropilin binding site on VEGF, encoded by exons 7 and 8, is distal to VEGFR and bevacizumab binding sites. Furthermore, neuropilins have been reported to bind a wide range of pro-angiogenic growth factors that includes FGF, PDGF, HGF and TGF-β[216]. Neuropilin expression in vascular tumours has not been previously studied. The immunohistochemistry studies reported here demonstrated expression of NRP1 in both benign and malignant vascular tumours. Pre-clinical studies have shown NRP1 blocking antibody enhanced the efficacy of VEGF targeted therapy[217], suggesting a potential drug combination to study for the treatment of angiosarcoma.

4.4.3.3 bFGF and FGFR1

Angiosarcoma expression of aFGF and bFGF were suggested by protein array studies of ASM, ISO-HAS and the five fresh angiosarcoma tumour samples. The immunohistochemistry studies however showed bFGF expression was significantly lower in angiosarcomas than in either benign tumour group, although the expression of its receptor FGFR1 was similar. Angiosarcoma expression of bFGF and FGFR was previously reported in an immunohistochemistry study of 7 cutaneous angiosarcomas, but this study did not include a comparison group[150]. aFGF and bFGF promote angiogenesis, and increase the expression of other pro-angiogenic growth factors including VEGF and Ang-2[24]. Furthermore, bFGF signalling can stimulate angiogenesis despite effective VEGFR inhibition[218], indicating a resistance mechanism to VEGF targeted therapy. Axitinib inhibits FGFR1 phosphorylation, with an IC_{50} of 215nmol/l (i.e. 83ng/ml)[41]. Minor responses were seen to axitinib at doses up to 250ng/ml in functional assays of ASM and ISO-HAS cells, suggesting co-inhibition of VEGF and FGF signalling was not beneficial. The efficacy of agents specifically targeting FGF however was not separately studied.

4.4.3.4 Angiopoietins

Endothelial cell response to angiopoietins is context dependent[14]. Through the Tie2 receptor, Ang-1 promotes endothelial cell survival and vessel integrity. Ang-2 is an Ang-1 antagonist that promotes vessel destabilisation. In the presence of VEGF, this

promotes endothelial cell proliferation, but in the absence of VEGF induces vessel regression. Antibodies specifically targeting Ang-2 have been shown to inhibit angiogenesis in pre-clinical models, and an antibody (AMG-386) was recently tested in a phase I trial[219]. Ang-2 expression is elevated relative to Ang-1 in the tumour vasculature of other malignancies[17]. Data on the expression of angiopoietins in angiosarcoma however is sparse. Given the functional response to Ang-2 in the presence of VEGF, Ang-2 expression was predicted to be high in angiosarcomas. Ang-2 expression was observed in both malignant and benign vascular tumours, with highest expression in inflammatory vascular lesions, and lowest expression in haemangiomas. The expression of Ang-1 was difficult to characterise as the extracellular matrix stained heavily with Ang-1 antibody. Tie2 staining in contrast was highly specific for endothelial cells. Ang-1 stained slides were therefore examined in parallel with Tie2 stained slides to assist the quantification of Ang-1 staining of endothelial cells. The endothelial cells lining the dilated vascular spaces of haemangiomas were flattened, with only a thin rim of cytoplasm visible. Therefore, in the majority of haemangioma samples it was not possible to reliably distinguish endothelial staining for Ang-1, from staining of neighbouring pericytes or the extracellular matrix. Ang-1 staining was therefore not scored in this tumour group. Angiosarcoma and inflammatory vascular tumour expression of Ang-1 were similar.

High Ang-2 serum levels have been reported in patients with metastatic angiosarcoma compared with localised disease[220]. In two cases of angiosarcoma Brown *et al* reported high expression of Tie2 and Ang-2, and low expression of Ang-1[221]. It was not possible to directly infer an Ang-2:Ang-1 expression ratio from the immunohistochemistry and protein array studies presented here. In hypoxia however, the Ang-2:Ang-1 expression ration increased in ASM and ISO-HAS cells compared to cells in normoxia. In both normoxic and hypoxic conditions Ang-2 expression was lower in ASM and ISO-HAS cells than in HuDMECs. Consistent with this, a previous

report identified higher Ang-2 expression in HuDMECs than ISO-HAS cells, with Ang-1 mRNA undetectable in either[220].

4.4.3.5 HGF and MET

Through the receptor tyrosine kinase MET, HGF promotes cell proliferation, migration and invasion, and protects cells from apoptosis[222]. Hypoxia increases MET transcription, and it has therefore been postulated that increased tumour hypoxia, as a consequence of anti-angiogenic therapy, promotes MET signalling and thus increases tumour invasion and metastasis[223]. HGF expression in angiosarcoma has not been previously studied. HGF expression was increased in ASM and ISO-HAS cells compared to HuDMECs, in both normoxia and hypoxia. HGF expression was significantly elevated in the inflammatory vascular lesions compared with the haemangioma group. However, whilst HGF expression correlated with MET expression, HGF expression was not significantly increased in angiosarcomas. MET inhibitors are in clinical development, including agents that inhibit binding of HGF to MET, and small molecule tyrosine kinase inhibitors[224] including crizotinib, a dual inhibitor of MET and ALK, which demonstrated response in non-small cell lung cancer patients harbouring the echinoderm microtubule associated protein-like 4 - anaplastic lymphoma kinase fusion oncogene (EML4-ALK)[225], and several compounds such as foretinib which inhibits both MET and VEGFRs[226].

In summary, and consistent with data obtained from the protein array studies, the immunohistochemistry analysis demonstrated angiosarcomas express a range of angiogenic growth factors and their receptors. This supports the conclusions drawn from the *in vitro* studies that targeting a single pro-angiogenic growth factor in the treatment of angiosarcoma would be less effective than targeting central signalling processes such as the MAPK pathway. This analysis identified other targets for future study to combine with inhibitors of VEGF, including NRP1 and HGF/MET.

4.5 Canine Angiosarcomas

As with their human counterpart, canine angiosarcomas are aggressive, locally invasive tumours of proliferating malignant endothelial cells. In contrast to human angiosarcomas however, canine angiosarcomas are common, accounting for 10% of all canine malignancies[167]. Angiosarcomas are more frequent in certain breeds (e.g. German Shepherds, Boxers and Golden Retrievers) indicating a genetic predisposition[227]. A viral aetiology has been postulated, though not been demonstrated[167]. Canine angiosarcomas frequently develop in the skin or soft tissue, though most commonly arise in the spleen. Response to anthracycline based chemotherapy has been reported but, as with human angiosarcomas, the overall prognosis is poor[228].

Similar to the immunohistochemistry results presented here, other studies have shown that canine angiosarcomas express increased VEGF and VEGFR2 compared to haemangiomas, and also express increased VEGFR1 and bFGF[229]. These findings contrast with those from the immunohistochemistry analysis of the human vascular tumours. Of note however, both the benign and malignant canine tumour blocks were collected over a similar period, with no relationship seen between the age of the tumour block and the staining intensity.

Canine sarcomas have been studied elsewhere as a model of human sarcomas, including a clinical study in dogs of mifamurtide for the treatment of osteosarcoma[230]. The clinical and pathological features of canine angiosarcoma suggest it represents a model with which to study the human disease.

4.6 Future Work

The role of Notch signalling in the pathogenesis of angiosarcoma was not studied. Studies have shown inhibition of Notch1 in mouse models leads to the formation of vascular tumours, including hepatic angiosarcomas[152, 153], and the importance of Notch in branching morphogenesis and in regulating endothelial cell expression of

receptors such as VEGFR2 and NRP1[30], identifies an area worth further study. The R&D Systems protein arrays did not assess the expression of Notch, or any of its signalling counterparts, and Notch was also not included in the immunohistochemistry studies. Future studies could assess the expression of DLL-4, Notch1, and the negative regulator Jag-1 in vascular tumours by immunohistochemistry, and the ASM and ISO-HAS cell lines used to investigate the effects of modulating the Notch pathway *in vitro*.

Through collaborations with the Animal Health Trust (Cambridge, UK) and the Van Andel Research Institute (VARI; Great Rapids, USA) canine angiosarcoma tumour samples have been obtained for future study. These samples include a large cohort of formalin fixed paraffin embedded tumour blocks of angiosarcoma and benign vascular lesions, and angiosarcoma tumour cell isolates for *in vitro* study. An mRNA study is proposed to compare canine angiosarcoma expression of angiogenic proteins and their receptors with benign canine vascular lesions. The canine angiosarcoma tumour cell isolates will be characterised *in vitro,* and their response to vascular targeted agents, including the MEK inhibitor selumetinib and the vascular disrupting agent DMXAA, will be assessed in cell viability and cell differentiation assays. The data obtained from these studies will be compared to the findings reported here from the study of human angiosarcoma samples. These studies will be supported by a grant from SarcomaUK.

It is expected that further *in vitro* studies will lead to the selection of a vascular targeted agent for a clinical trial in angiosarcoma. As angiosarcomas are rare in humans, a clinical trial would require national or international collaborations. The pre-clinical data presented here would suggest the study of a vascular disrupting agent such as DMXAA. Tumour response to DMXAA monotherapy could be assessed in a single arm phase II trial. The clinical development of DMXAA has halted however, as a consequence of the disappointing results observed in the phase III trials of DMXAA in combination with chemotherapy for advanced NSCLC. Other vascular disrupting agents in clinical development that could be trialled include combretastatin (CA-4-P).

The mechanism of action of CA-4-P is distinct from DMXAA. CA-4-P targets the cytoskeleton of tumour endothelial cells, causing collapse of the tumour vasculature and tumour necrosis[231]. Pre-clinical studies are necessary to indicate CA-4-P activity against the malignant endothelial cells of angiosarcoma. *In vitro* studies however may not inform tumour response, as CA-4-P does not directly induce endothelial cell death. The study of angiosarcoma response to CA-4-P may therefore require an *in vivo* model. Currently there are no established *in vivo* models for angiosarcoma. The canine angiosarcoma tumour cell isolates obtained from VARI form tumour xenografts with histological features consistent with angiosarcoma (unpublished data from VARI). These tumour cell isolates may therefore be used to study angiosarcoma response to vascular targeted agents *in vivo*.

A clinical trial of vascular targeted agents could also be considered in dogs presenting with angiosarcoma. This would provide a unique opportunity for the study of angiosarcoma tumour response to vascular targeted agents, and could inform the selection of an agent for clinical trial in humans.

5 References

1. Young RJ, Reed MW: Anti-angiogenic therapy: concept to clinic. *Microcirculation* 2012, 19(2):115-125.

2. Hanahan D, Weinberg RA: The hallmarks of cancer. *Cell* 2000, 100(1):57-70.

3. Menakuru SR, Brown NJ, Staton CA, Reed MW: Angiogenesis in pre-malignant conditions. *Br J Cancer* 2008, 99(12):1961-1966.

4. Hicklin DJ, Ellis LM: Role of the vascular endothelial growth factor pathway in tumor growth and angiogenesis. *J Clin Oncol* 2005, 23(5):1011-1027.

5. Shibuya M: Vascular endothelial growth factor-dependent and -independent regulation of angiogenesis. *BMB Rep* 2008, 41(4):278-286.

6. Ferrara N, Gerber HP, LeCouter J: The biology of VEGF and its receptors. *Nat Med* 2003, 9(6):669-676.

7. Harper SJ, Bates DO: VEGF-A splicing: the key to anti-angiogenic therapeutics? *Nat Rev Cancer* 2008, 8(11):880-887.

8. Shibuya M: Differential roles of vascular endothelial growth factor receptor-1 and receptor-2 in angiogenesis. *J Biochem Mol Biol* 2006, 39(5):469-478.

9. Hiratsuka S, Maru Y, Okada A, Seiki M, Noda T, Shibuya M: Involvement of Flt-1 tyrosine kinase (vascular endothelial growth factor receptor-1) in pathological angiogenesis. *Cancer Res* 2001, 61(3):1207-1213.

10. Zachary I, Gliki G: Signaling transduction mechanisms mediating biological actions of the vascular endothelial growth factor family. *Cardiovasc Res* 2001, 49(3):568-581.

11. Cébe-Suarez S, Zehnder-Fjällman A, Ballmer-Hofer K: The role of VEGF receptors in angiogenesis; complex partnerships. *Cell Mol Life Sci* 2006, 63(5):601-615.

12. Ewan LC, Jopling HM, Jia H, Mittar S, Bagherzadeh A, Howell GJ, Walker JH, Zachary IC, Ponnambalam S: Intrinsic tyrosine kinase activity is required for vascular endothelial growth factor receptor 2 ubiquitination, sorting and degradation in endothelial cells. *Traffic* 2006, 7(9):1270-1282.

13. Tammela T, Zarkada G, Wallgard E, Murtomäki A, Suchting S, Wirzenius M, Waltari M, Hellström M, Schomber T, Peltonen R *et al*: Blocking VEGFR-3 suppresses angiogenic sprouting and vascular network formation. *Nature* 2008, 454(7204):656-660.

14. Eklund L, Olsen BR: Tie receptors and their angiopoietin ligands are context-dependent regulators of vascular remodeling. *Exp Cell Res* 2006, 312(5):630-641.

15. Augustin HG, Koh GY, Thurston G, Alitalo K: Control of vascular morphogenesis and homeostasis through the angiopoietin-Tie system. *Nat Rev Mol Cell Biol* 2009, 10(3):165-177.

16. Shim WS, Ho IA, Wong PE: Angiopoietin: a TIE(d) balance in tumor angiogenesis. *Mol Cancer Res* 2007, 5(7):655-665.

17. Tait CR, Jones PF: Angiopoietins in tumours: the angiogenic switch. *J Pathol* 2004, 204(1):1-10.

18. Ostman A: PDGF receptors-mediators of autocrine tumor growth and regulators of tumor vasculature and stroma. *Cytokine Growth Factor Rev* 2004, 15(4):275-286.

19. Andrae J, Gallini R, Betsholtz C: Role of platelet-derived growth factors in physiology and medicine. *Genes Dev* 2008, 22(10):1276-1312.

20. Lu C, Shahzad MM, Moreno-Smith M, Lin YG, Jennings NB, Allen JK, Landen CN, Mangala LS, Armaiz-Pena GN, Schmandt R *et al*: Targeting pericytes with a PDGF-B aptamer in human ovarian carcinoma models. *Cancer Biol Ther* 2010, 9(3):176-182.

21. Simon MP, Navarro M, Roux D, Pouysségur J: Structural and functional analysis of a chimeric protein COL1A1-PDGFB generated by the translocation t(17;22)(q22;q13.1) in Dermatofibrosarcoma protuberans (DP). *Oncogene* 2001, 20(23):2965-2975.

22. Corless CL, Schroeder A, Griffith D, Town A, McGreevey L, Harrell P, Shiraga S, Bainbridge T, Morich J, Heinrich MC: PDGFRA mutations in gastrointestinal stromal tumors: frequency, spectrum and in vitro sensitivity to imatinib. *J Clin Oncol* 2005, 23(23):5357-5364.

23. Lieu C, Heymach J, Overman M, Tran H, Kopetz S: Beyond VEGF: inhibition of the fibroblast growth factor pathway and antiangiogenesis. *Clin Cancer Res* 2011, 17(19):6130-6139.

24. Presta M, Dell'Era P, Mitola S, Moroni E, Ronca R, Rusnati M: Fibroblast growth factor/fibroblast growth factor receptor system in angiogenesis. *Cytokine Growth Factor Rev* 2005, 16(2):159-178.

25. Wesche J, Haglund K, Haugsten EM: Fibroblast growth factors and their receptors in cancer. *Biochem J* 2011, 437(2):199-213.

26. Daniele G, Corral J, Molife LR, de Bono JS: FGF receptor inhibitors: role in cancer therapy. *Curr Oncol Rep* 2012, 14(2):111-119.

27. Gavine PR, Mooney L, Kilgour E, Thomas AP, Al-Kadhimi K, Beck S, Rooney C, Coleman T, Baker D, Mellor MJ *et al*: AZD4547: an orally bioavailable, potent, and selective inhibitor of the fibroblast growth factor receptor tyrosine kinase family. *Cancer Res* 2012, 72(8):2045-2056.

28. Horowitz A, Simons M: Branching morphogenesis. *Circ Res* 2009, 104(2):e21.

29. Siekmann AF, Covassin L, Lawson ND: Modulation of VEGF signalling output by the Notch pathway. *Bioessays* 2008, 30(4):303-313.

30. Phng LK, Gerhardt H: Angiogenesis: a team effort coordinated by notch. *Dev Cell* 2009, 16(2):196-208.

31. Roma J, Almazán-Moga A, Sánchez de Toledo J, Gallego S: Notch, wnt, and hedgehog pathways in rhabdomyosarcoma: from single pathways to an integrated network. *Sarcoma* 2012:DOI 10.1155/2012/695603.

32. Purow B: Notch inhibition as a promising new approach to cancer therapy. *Adv Exp Med Biol* 2012, 727:305-319.

33. Kim KJ, Li B, Winer J, Armanini M, Gillett N, Phillips HS, Ferrara N: Inhibition of vascular endothelial growth factor-induced angiogenesis suppresses tumour growth in vivo. *Nature* 1993, 362(6423):841-844.

34. Ellis LM, Hicklin DJ: VEGF-targeted therapy: mechanisms of anti-tumour activity. *Nat Rev Cancer* 2008, 8(8):579-591.

35. Jain RK: Normalizing tumor vasculature with anti-angiogenic therapy: a new paradigm for combination therapy. *Nat Med* 2001, 7(9):987-989.

36. O'Connor JP, Carano RA, Clamp AR, Ross J, Ho CC, Jackson A, Parker GJ, Rose CJ, Peale FV, Friesenhahn M *et al*: Quantifying antivascular effects of monoclonal antibodies to vascular endothelial growth factor: insights from imaging. *Clin Cancer Res* 2009, 15(21):6674-6682.

37. Gotink KJ, Verheul HM: Anti-angiogenic tyrosine kinase inhibitors: what is their mechanism of action? *Angiogenesis* 2010, 13(1):1-14.

38. Olsson AK, Dimberg A, Kreuger J, Claesson-Welsh L: VEGF receptor signalling - in control of vascular function. *Nat Rev Mol Cell Biol* 2006, 7(5):359-371.

39. Bergh J: Quo vadis with targeted drugs in the 21st century? *J Clin Oncol* 2009, 27(1):2-5.

40. Chow LQ, Eckhardt SG: Sunitinib: from rational design to clinical efficacy. *J Clin Oncol* 2007, 25(7):884-896.

41. Hu-Lowe DD, Zou HY, Grazzini ML, Hallin ME, Wickman GR, Amundson K, Chen JH, Rewolinski DA, Yamazaki S, Wu EY *et al*: Nonclinical antiangiogenesis and antitumor activities of axitinib (AG-013736), an oral, potent, and selective inhibitor of vascular endothelial growth factor receptor tyrosine kinases 1, 2, 3. *Clin Cancer Res* 2008, 14(22):7272-7283.

42. Kerbel R, Folkman J: Clinical translation of angiogenesis inhibitors. *Nat Rev Cancer* 2002, 2(10):727-739.

43. Hurwitz H, Fehrenbacher L, Novotny W, Cartwright T, Hainsworth J, Heim W, Berlin J, Baron A, Griffing S, Holmgren E *et al*: Bevacizumab plus irinotecan, fluorouracil, and leucovorin for metastatic colorectal cancer. *N Engl J Med* 2004, 350(23):2335-2342.

44. Saltz LB, Clarke S, Díaz-Rubio E, Scheithauer W, Figer A, Wong R, Koski S, Lichinitser M, Yang TS, Rivera F *et al*: Bevacizumab in combination with oxaliplatin-based chemotherapy as first-line therapy in metastatic colorectal cancer: a randomized phase III study. *J Clin Oncol* 2008, 26(12):2013-2019.

45. Sandler A, Gray R, Perry MC, Brahmer J, Schiller JH, Dowlati A, Lilenbaum R, Johnson DH: Paclitaxel-carboplatin alone or with bevacizumab for non-small-cell lung cancer. *N Engl J Med* 2006, 355(24):2542-2550.

46. Reck M, von Pawel J, Zatloukal P, Ramlau R, Gorbounova V, Hirsh V, Leighl N, Mezger J, Archer V, Moore N *et al*: Phase III trial of cisplatin plus gemcitabine with either placebo or bevacizumab as first-line therapy for nonsquamous non-small-cell lung cancer: AVAil. *J Clin Oncol* 2009, 27(8):1227-1234.

47. Reck M, von Pawel J, Zatloukal P, Ramlau R, Gorbounova V, Hirsh V, Leighl N, Mezger J, Archer V, Moore N *et al*: Overall survival with cisplatin-gemcitabine and bevacizumab or placebo as first-line therapy for nonsquamous non-small-cell lung cancer: results from a randomised phase III trial (AVAiL). *Ann Oncol* 2010, 21(9):1804-1809.

48. Perren TJ, Swart AM, Pfisterer J, Ledermann JA, Pujade-Lauraine E, Kristensen G, Carey MS, Beale P, Cervantes A, Kurzeder C *et al*: A phase 3 trial of bevacizumab in ovarian cancer. *N Engl J Med* 2011, 365(26):2484-2496.

49. Miller K, Wang M, Gralow J, Dickler M, Cobleigh M, Perez EA, Shenkier T, Cella D, Davidson NE: Paclitaxel plus bevacizumab versus paclitaxel alone for metastatic breast cancer. *N Engl J Med* 2007, 357(26):2666-2676.

50. Miles DW, Chan A, Dirix LY, Cortés J, Pivot X, Tomczak P, Delozier T, Sohn JH, Provencher L, Puglisi F *et al*: Phase III study of bevacizumab plus docetaxel compared with placebo plus docetaxel for the first-line treatment of human epidermal growth factor receptor 2-negative metastatic breast cancer. *J Clin Oncol* 2010, 28(20):3239-3247.

51. Robert NJ, Diéras V, Glaspy J, Brufsky AM, Bondarenko I, Lipatov ON, Perez EA, Yardley DA, Chan SY, Zhou X *et al*: RIBBON-1: randomized, double-blind, placebo-controlled, phase III trial of chemotherapy with or without bevacizumab for first-line treatment of human epidermal growth factor receptor 2-negative, locally recurrent or metastatic breast cancer. *J Clin Oncol* 2011, 29(10):1252-1260.

52. Rini BI, Halabi S, Rosenberg JE, Stadler WM, Vaena DA, Ou SS, Archer L, Atkins JN, Picus J, Czaykowski P *et al*: Bevacizumab plus interferon alfa compared with interferon alfa monotherapy in patients with metastatic renal cell carcinoma: CALGB 90206. *J Clin Oncol* 2008, 26(33):5422-5428.

53. Rini BI, Halabi S, Rosenberg JE, Stadler WM, Vaena DA, Archer L, Atkins JN, Picus J, Czaykowski P, Dutcher J *et al*: Phase III trial of bevacizumab plus interferon alfa versus interferon alfa monotherapy in patients with metastatic renal cell carcinoma: final results of CALGB 90206. *J Clin Oncol* 2010, 28(13):2137-2143.

54. Escudier B, Bellmunt J, Négrier S, Bajetta E, Melichar B, Bracarda S, Ravaud A, Golding S, Jethwa S, Sneller V: Phase III trial of bevacizumab plus interferon alfa-2a in patients with metastatic renal cell carcinoma (AVOREN): final analysis of overall survival. *J Clin Oncol* 2010, 28(13):2144-2150.

55. Friedman HS, Prados MD, Wen PY, Mikkelsen T, Schiff D, Abrey LE, Yung WK, Paleologos N, Nicholas MK, Jensen R *et al*: Bevacizumab alone and in combination with irinotecan in recurrent glioblastoma. *J Clin Oncol* 2009, 27(28):4733-4740.

56. Kindler HL, Niedzwiecki D, Hollis D, Sutherland S, Schrag D, Hurwitz H, Innocenti F, Mulcahy MF, O'Reilly E, Wozniak TF *et al*: Gemcitabine plus bevacizumab compared with gemcitabine plus placebo in patients with

advanced pancreatic cancer: phase III trial of the Cancer and Leukemia Group B (CALGB 80303). *J Clin Oncol* 2010, 28(22):3617-3622.

57. Motzer RJ, Hutson TE, Tomczak P, Michaelson MD, Bukowski RM, Rixe O, Oudard S, Negrier S, Szczylik C, Kim ST *et al*: Sunitinib versus interferon alfa in metastatic renal-cell carcinoma. *N Engl J Med* 2007, 356(2):115-124.

58. Motzer RJ, Hutson TE, Tomczak P, Michaelson MD, Bukowski RM, Oudard S, Negrier S, Szczylik C, Pili R, Bjarnason GA *et al*: Overall survival and updated results for sunitinib compared with interferon alfa in patients with metastatic renal cell carcinoma. *J Clin Oncol* 2009, 27(22):3584-3590.

59. Demetri GD, van Oosterom AT, Garrett CR, Blackstein ME, Shah MH, Verweij J, McArthur G, Judson IR, Heinrich MC, Morgan JA *et al*: Efficacy and safety of sunitinib in patients with advanced gastrointestinal stromal tumour after failure of imatinib: a randomised controlled trial. *Lancet* 2006, 368(9544):1329-1338.

60. Robert NJ, Saleh MN, Paul D, Generali D, Gressot L, Copur MS, Brufsky AM, Minton SE, Giguere JK, Smith JW *et al*: Sunitinib plus paclitaxel versus bevacizumab plus paclitaxel for first-line treatment of patients with advanced breast cancer: a phase III, randomized, open-label trial. *Clin Breast Cancer* 2011, 11(2):82-92.

61. Escudier B, Eisen T, Stadler WM, Szczylik C, Oudard S, Siebels M, Negrier S, Chevreau C, Solska E, Desai AA *et al*: Sorafenib in advanced clear-cell renal-cell carcinoma. *N Engl J Med* 2007, 356(2):125-134.

62. Llovet JM, Ricci S, Mazzaferro V, Hilgard P, Gane E, Blanc JF, de Oliveira AC, Santoro A, Raoul JL, Forner A *et al*: Sorafenib in advanced hepatocellular carcinoma. *N Engl J Med* 2008, 359(4):378-390.

63. Scagliotti G, Novello S, von Pawel J, Reck M, Pereira JR, Thomas M, Abrão Miziara JE, Balint B, De Marinis F, Keller A *et al*: Phase III study of carboplatin and paclitaxel alone or with sorafenib in advanced non-small-cell lung cancer. *J Clin Oncol* 2010, 28(11):1835-1842.

64. Kindler HL, Ioka T, Richel DJ, Bennouna J, Létourneau R, Okusaka T, Funakoshi A, Furuse J, Park YS, Ohkawa S *et al*: Axitinib plus gemcitabine versus placebo plus gemcitabine in patients with advanced pancreatic adenocarcinoma: a double-blind randomised phase 3 study. *Lancet Oncol* 2011, 12(3):256-262.

65. Sternberg CN, Davis ID, Mardiak J, Szczylik C, Lee E, Wagstaff J, Barrios CH, Salman P, Gladkov OA, Kavina A *et al*: Pazopanib in locally advanced or metastatic renal cell carcinoma: results of a randomized phase III trial. *J Clin Oncol* 2010, 28(6):1061-1068.

66. van der Graaf WT, Blay JY, Chawla SP, Kim DW, Bui-Nguyen B, Casali PG, Schöffski P, Aglietta M, Staddon AP, Beppu Y *et al*: Pazopanib for metastatic soft-tissue sarcoma (PALETTE): a randomised, double-blind, placebo-controlled phase 3 trial. *Lancet* 2012, 379(9829):1879-1886.

67. Herbst RS, Sun Y, Eberhardt WE, Germonpré P, Saijo N, Zhou C, Wang J, Li L, Kabbinavar F, Ichinose Y *et al*: Vandetanib plus docetaxel versus docetaxel as second-line treatment for patients with advanced non-small-cell lung cancer (ZODIAC): a double-blind, randomised, phase 3 trial. *Lancet Oncol* 2010, 11(7):619-626.

68. Young RJ, Brown NJ, Reed MW, Hughes D, Woll PJ: Angiosarcoma. *Lancet Oncol* 2010, 11(10):983-991.

69. Weiss S, Goldblum J: Malignant Vascular Tumours. In: *Enzinger & Weiss's Soft Tissue Tumours.* 4th edn. Edited by Weiss S, Goldblum J: Mosby; 2001: 917-937.

70. Coindre JM, Terrier P, Guillou L, Le Doussal V, Collin F, Ranchère D, Sastre X, Vilain MO, Bonichon F, N'Guyen Bui B: Predictive value of grade for metastasis development in the main histologic types of adult soft tissue sarcomas: a study of 1240 patients from the French Federation of Cancer Centers Sarcoma Group. *Cancer* 2001, 91(10):1914-1926.

71. Rouhani P, Fletcher CD, Devesa SS, Toro JR: Cutaneous soft tissue sarcoma incidence patterns in the U.S. : an analysis of 12,114 cases. *Cancer* 2008, 113(3):616-627.

72. Antonescu CR, Yoshida A, Guo T, Chang NE, Zhang L, Agaram NP, Qin LX, Brennan MF, Singer S, Maki RG: KDR activating mutations in human angiosarcomas are sensitive to specific kinase inhibitors. *Cancer Res* 2009, 69(18):7175-7179.

73. Fury MG, Antonescu CR, Van Zee KJ, Brennan MF, Maki RG: A 14-year retrospective review of angiosarcoma: clinical characteristics, prognostic factors, and treatment outcomes with surgery and chemotherapy. *Cancer J* 2005, 11(3):241-247.

74. Schlemmer M, Reichardt P, Verweij J, Hartmann JT, Judson I, Thyss A, Hogendoorn PC, Marreaud S, Van Glabbeke M, Blay JY: Paclitaxel in patients with advanced angiosarcomas of soft tissue: a retrospective study of the EORTC soft tissue and bone sarcoma group. *Eur J Cancer* 2008, 44(16):2433-2436.

75. Mark RJ, Poen JC, Tran LM, Fu YS, Juillard GF: Angiosarcoma. A report of 67 patients and a review of the literature. *Cancer* 1996, 77(11):2400-2406.

76. Abraham JA, Hornicek FJ, Kaufman AM, Harmon DC, Springfield DS, Raskin KA, Mankin HJ, Kirsch DG, Rosenberg AE, Nielsen GP *et al*: Treatment and outcome of 82 patients with angiosarcoma. *Ann Surg Oncol* 2007, 14(6):1953-1967.

77. Naka N, Ohsawa M, Tomita Y, Kanno H, Uchida A, Aozasa K: Angiosarcoma in Japan. A review of 99 cases. *Cancer* 1995, 75(4):989-996.

78. Fayette J, Martin E, Piperno-Neumann S, Le Cesne A, Robert C, Bonvalot S, Ranchère D, Pouillart P, Coindre JM, Blay JY: Angiosarcomas, a heterogeneous group of sarcomas with specific behavior depending on primary site: a retrospective study of 161 cases. *Ann Oncol* 2007, 18(12):2030-2036.

79. Rossi S, Fletcher CD: Angiosarcoma arising in hemangioma/vascular malformation: report of four cases and review of the literature. *Am J Surg Pathol* 2002, 26(10):1319-1329.

80. STEWART FW, TREVES N: Lymphangiosarcoma in postmastectomy lymphedema; a report of six cases in elephantiasis chirurgica. *Cancer* 1948, 1(1):64-81.

81. Huang J, Mackillop WJ: Increased risk of soft tissue sarcoma after radiotherapy in women with breast carcinoma. *Cancer* 2001, 92(1):172-180.

82. West JG, Weitzel JN, Tao ML, Carpenter M, West JE, Fanning C: BRCA mutations and the risk of angiosarcoma after breast cancer treatment. *Clin Breast Cancer* 2008, 8(6):533-537.

83. Bosetti C, La Vecchia C, Lipworth L, McLaughlin JK: Occupational exposure to vinyl chloride and cancer risk: a review of the epidemiologic literature. *Eur J Cancer Prev* 2003, 12(5):427-430.

84. Ron E: Cancer risks from medical radiation. *Health Phys* 2003, 85(1):47-59.

85. Locker GY, Doroshow JH, Zwelling LA, Chabner BA: The clinical features of hepatic angiosarcoma: a report of four cases and a review of the English literature. *Medicine (Baltimore)* 1979, 58(1):48-64.

86. Keymeulen K, Dillemans B: Epitheloid angiosarcoma of the splenic capsula as a result of foreign body tumorigenesis. A case report. *Acta Chir Belg* 2004, 104(2):217-220.

87. Ben-Izhak O, Kerner H, Brenner B, Lichtig C: Angiosarcoma of the colon developing in a capsule of a foreign body. Report of a case with associated hemorrhagic diathesis. *Am J Clin Pathol* 1992, 97(3):416-420.

88. Weiss WM, Riles TS, Gouge TH, Mizrachi HH: Angiosarcoma at the site of a Dacron vascular prosthesis: a case report and literature review. *J Vasc Surg* 1991, 14(1):87-91.

89. Okada M, Takeuchi E, Mori Y, Ichihara S, Usui A, Ueda Y: An autopsy case of angiosarcoma arising around a woven Dacron prosthesis after a Cabrol operation. *J Thorac Cardiovasc Surg* 2004, 127(6):1843-1845.

90. Ferrari D, Pignatti G, Bertoni F, Bacchini P, Giunti A: Angiosarcoma of bone following intramedullary nail fixation. *Orthopedics* 2001, 24(8):795-797.

91. McDonald DJ, Enneking WF, Sundaram M: Metal-associated angiosarcoma of bone: report of two cases and review of the literature. *Clin Orthop Relat Res* 2002(396):206-214.

92. Folpe AL, Johnston CA, Weiss SW: Cutaneous angiosarcoma arising in a gouty tophus: report of a unique case and a review of foreign material-associated angiosarcomas. *Am J Dermatopathol* 2000, 22(5):418-421.

93. Pawlik TM, Paulino AF, McGinn CJ, Baker LH, Cohen DS, Morris JS, Rees R, Sondak VK: Cutaneous angiosarcoma of the scalp: a multidisciplinary approach. *Cancer* 2003, 98(8):1716-1726.

94. Espat NJ, Lewis JJ, Woodruff JM, Antonescu C, Xia J, Leung D, Brennan MF: Confirmed angiosarcoma: prognostic factors and outcome in 50 prospectively followed patients. *Sarcoma* 2000, 4(4):173-177.

95. Holden CA, Spittle MF, Jones EW: Angiosarcoma of the face and scalp, prognosis and treatment. *Cancer* 1987, 59(5):1046-1057.

96. Meis-Kindblom JM, Kindblom LG: Angiosarcoma of soft tissue: a study of 80 cases. *Am J Surg Pathol* 1998, 22(6):683-697.

97. Weiss S, Lasota J, Miettinen M: Angiosarcoma of soft tissue. In: *WHO Classification Pathology and Genetics of Tumours of Soft Tissue and Bone.* 3rd edn. Edited by Fletcher C, Unni K, Mertens F: IARC Press; 2002: 175-177.

98. Calonje E, Fletcher C: Vascular Tumours. In: *Diagnostic Histopathology of Tumours. Volume 1*, 3rd edn. Edited by CDM F: Churchill Livingstone; 2007: 41-76.

99. Ohsawa M, Naka N, Tomita Y, Kawamori D, Kanno H, Aozasa K: Use of immunohistochemical procedures in diagnosing angiosarcoma. Evaluation of 98 cases. *Cancer* 1995, 75(12):2867-2874.

100. Casali PG, Jost L, Sleijfer S, Verweij J, Blay JY, Group EGW: Soft tissue sarcomas: ESMO clinical recommendations for diagnosis, treatment and follow-up. *Ann Oncol* 2008, 19 Suppl 2:ii89-93.

101. Demetri G, von Mehren M: Soft Tissue Sarcomas. NCCN Clinical Practise Guidelines in Oncology. In.: NCCN; 2009.

102. Eisenhauer EA, Therasse P, Bogaerts J, Schwartz LH, Sargent D, Ford R, Dancey J, Arbuck S, Gwyther S, Mooney M *et al*: New response evaluation criteria in solid tumours: revised RECIST guideline (version 1.1). *Eur J Cancer* 2009, 45(2):228-247.

103. Penel N, Bui BN, Bay JO, Cupissol D, Ray-Coquard I, Piperno-Neumann S, Kerbrat P, Fournier C, Taieb S, Jimenez M *et al*: Phase II trial of weekly paclitaxel for unresectable angiosarcoma: the ANGIOTAX Study. *J Clin Oncol* 2008, 26(32):5269-5274.

104. Italiano A, Cioffi A, Penel N, Levra MG, Delcambre C, Kalbacher E, Chevreau C, Bertucci F, Isambert N, Blay JY *et al*: Comparison of doxorubicin and weekly paclitaxel efficacy in metastatic angiosarcomas. *Cancer* 2012, 118(13):3330-3336.

105. Agulnik M, Okuno SH, Von Mehren M, Jovanovic B, Brockstein B, Benjamin RS, Evens AM: An open-label multicenter phase II study of bevacizumab for the treatment of angiosarcoma. *ASCO Meeting Abstracts* 2009, 27(15S):10522.

106. Maki RG, D'Adamo DR, Keohan ML, Saulle M, Schuetze SM, Undevia SD, Livingston MB, Cooney MM, Hensley ML, Mita MM *et al*: Phase II study of sorafenib in patients with metastatic or recurrent sarcomas. *J Clin Oncol* 2009, 27(19):3133-3140.

107. Ray-Coquard I, Italiano A, Bompas E, Le Cesne A, Robin YM, Chevreau C, Bay JO, Bousquet G, Piperno-Neumann S, Isambert N *et al*: Sorafenib for patients with advanced angiosarcoma: a phase II Trial from the French Sarcoma Group (GSF/GETO). *Oncologist* 2012, 17(2):260-266.

108. George S, Merriam P, Maki RG, Van den Abbeele AD, Yap JT, Akhurst T, Harmon DC, Bhuchar G, O'Mara MM, D'Adamo DR *et al*: Multicenter phase II trial of sunitinib in the treatment of nongastrointestinal stromal tumor sarcomas. *J Clin Oncol* 2009, 27(19):3154-3160.

109. Raina V, Sengar M, Shukla NK, Deo SS, Mohanty BK, Sharma D, Ray R, Das P, Rath GK: Complete response from thalidomide in angiosarcoma after treatment of breast cancer. *J Clin Oncol* 2007, 25(7):900-901.

110. Budd GT: Management of angiosarcoma. *Curr Oncol Rep* 2002, 4(6):515-519.

111. Fata F, O'Reilly E, Ilson D, Pfister D, Leffel D, Kelsen DP, Schwartz GK, Casper ES: Paclitaxel in the treatment of patients with angiosarcoma of the scalp or face. *Cancer* 1999, 86(10):2034-2037.

112. Nagano T, Yamada Y, Ikeda T, Kanki H, Kamo T, Nishigori C: Docetaxel: a therapeutic option in the treatment of cutaneous angiosarcoma: report of 9 patients. *Cancer* 2007, 110(3):648-651.

113. Ryan CW, von Mehren M, Rankin CJ, Goldblum JR, Demetri GD, Bramwell VH, Borden EC: Phase II intergroup study of sorafenib (S) in advanced soft tissue sarcomas (STS): SWOG 0505. *ASCO Meeting Abstracts* 2008, 26(15_suppl):10532.

114. Manner J, Radlwimmer B, Hohenberger P, Mössinger K, Küffer S, Sauer C, Belharazem D, Zettl A, Coindre JM, Hallermann C *et al*: MYC high level gene amplification is a distinctive feature of angiosarcomas after irradiation or chronic lymphedema. *Am J Pathol* 2010, 176(1):34-39.

115. DuBois S, Demetri G: Markers of angiogenesis and clinical features in patients with sarcoma. *Cancer* 2007, 109(5):813-819.

116. Wong KF, So CC, Wong N, Siu LL, Kwong YL, Chan JK: Sinonasal angiosarcoma with marrow involvement at presentation mimicking malignant lymphoma: cytogenetic analysis using multiple techniques. *Cancer Genet Cytogenet* 2001, 129(1):64-68.

117. Naka N, Tomita Y, Nakanishi H, Araki N, Hongyo T, Ochi T, Aozasa K: Mutations of p53 tumor-suppressor gene in angiosarcoma. *Int J Cancer* 1997, 71(6):952-955.

118. Zietz C, Rössle M, Haas C, Sendelhofert A, Hirschmann A, Stürzl M, Löhrs U: MDM-2 oncoprotein overexpression, p53 gene mutation, and VEGF up-regulation in angiosarcomas. *Am J Pathol* 1998, 153(5):1425-1433.

119. Italiano A, Chen CL, Thomas R, Breen M, Bonnet F, Sevenet N, Longy M, Maki RG, Coindre JM, Antonescu CR: Alterations of the p53 and PIK3CA/AKT/mTOR pathways in angiosarcomas: A pattern distinct from other sarcomas with complex genomics. *Cancer* 2012.

120. Domfeh AB, Fichera M, Hunt JL: Allelic loss of 3 different tumor suppressor gene loci in benign and malignant endothelial tumors of the head and neck. *Arch Pathol Lab Med* 2006, 130(8):1184-1187.

121. Guo T, Zhang L, Chang NE, Singer S, Maki RG, Antonescu CR: Consistent MYC and FLT4 gene amplification in radiation-induced angiosarcoma but not in other radiation-associated atypical vascular lesions. *Genes Chromosomes Cancer* 2011, 50(1):25-33.

122. Mentzel T, Schildhaus HU, Palmedo G, Büttner R, Kutzner H: Postradiation cutaneous angiosarcoma after treatment of breast carcinoma is characterized by MYC amplification in contrast to atypical vascular lesions after radiotherapy and control cases: clinicopathological, immunohistochemical and molecular analysis of 66 cases. *Mod Pathol* 2012, 25(1):75-85.

123. Fernandez AP, Sun Y, Tubbs RR, Goldblum JR, Billings SD: FISH for MYC amplification and anti-MYC immunohistochemistry: useful diagnostic tools in the assessment of secondary angiosarcoma and atypical vascular proliferations. *J Cutan Pathol* 2012, 39(2):234-242.

124. Przygodzki RM, Finkelstein SD, Keohavong P, Zhu D, Bakker A, Swalsky PA, Soini Y, Ishak KG, Bennett WP: Sporadic and Thorotrast-induced angiosarcomas of the liver manifest frequent and multiple point mutations in K-ras-2. *Lab Invest* 1997, 76(1):153-159.

125. Weihrauch M, Bader M, Lehnert G, Koch B, Wittekind C, Wrbitzky R, Tannapfel A: Mutation analysis of K-ras-2 in liver angiosarcoma and adjacent nonneoplastic liver tissue from patients occupationally exposed to vinyl chloride. *Environ Mol Mutagen* 2002, 40(1):36-40.

126. Garcia JM, Gonzalez R, Silva JM, Dominguez G, Vegazo IS, Gamallo C, Provencio M, España P, Bonilla F: Mutational status of K-ras and TP53 genes in primary sarcomas of the heart. *Br J Cancer* 2000, 82(6):1183-1185.

127. Bajaj A, Zheng Q, Adam A, Vincent P, Pumiglia K: Activation of endothelial ras signaling bypasses senescence and causes abnormal vascular morphogenesis. *Cancer Res* 2010, 70(9):3803-3812.

128. Arbiser JL, Moses MA, Fernandez CA, Ghiso N, Cao Y, Klauber N, Frank D, Brownlee M, Flynn E, Parangi S *et al*: Oncogenic H-ras stimulates tumor angiogenesis by two distinct pathways. *Proc Natl Acad Sci U S A* 1997, 94(3):861-866.

129. LaMontagne KR, Moses MA, Wiederschain D, Mahajan S, Holden J, Ghazizadeh H, Frank DA, Arbiser JL: Inhibition of MAP kinase kinase causes morphological reversion and dissociation between soft agar growth and in vivo tumorigenesis in angiosarcoma cells. *Am J Pathol* 2000, 157(6):1937-1945.

130. Perry B, Banyard J, McLaughlin ER, Watnick R, Sohn A, Brindley DN, Obata T, Cantley LC, Cohen C, Arbiser JL: AKT1 overexpression in endothelial cells leads to the development of cutaneous vascular malformations in vivo. *Arch Dermatol* 2007, 143(4):504-506.

131. Chang HW, Aoki M, Fruman D, Auger KR, Bellacosa A, Tsichlis PN, Cantley LC, Roberts TM, Vogt PK: Transformation of chicken cells by the gene encoding the catalytic subunit of PI 3-kinase. *Science* 1997, 276(5320):1848-1850.

132. Chen SY, Takeuchi S, Urabe K, Hayashida S, Kido M, Tomoeda H, Uchi H, Dainichi T, Takahara M, Shibata S *et al*: Overexpression of phosphorylated-ATF2 and STAT3 in cutaneous angiosarcoma and pyogenic granuloma. *J Cutan Pathol* 2008, 35(8):722-730.

133. Yamamoto T, Umeda T, Nishioka K: Immunohistological distribution of stem cell factor and kit receptor in angiosarcoma. *Acta Derm Venereol* 2000, 80(6):443-445.

134. Miettinen M, Sarlomo-Rikala M, Lasota J: KIT expression in angiosarcomas and fetal endothelial cells: lack of mutations of exon 11 and exon 17 of C-kit. *Mod Pathol* 2000, 13(5):536-541.

135. Hornick JL, Fletcher CD: Immunohistochemical staining for KIT (CD117) in soft tissue sarcomas is very limited in distribution. *Am J Clin Pathol* 2002, 117(2):188-193.

136. Komdeur R, Hoekstra HJ, Molenaar WM, Van Den Berg E, Zwart N, Pras E, Plaza-Menacho I, Hofstra RM, Van Der Graaf WT: Clinicopathologic assessment of postradiation sarcomas: KIT as a potential treatment target. *Clin Cancer Res* 2003, 9(8):2926-2932.

137. Yang JL, Hannan MT, Russell PJ, Crowe PJ: Expression of HER1/EGFR protein in human soft tissue sarcomas. *Eur J Surg Oncol* 2006, 32(4):466-468.

138. Thewes M, Elsner E, Wessner D, Engst R, Ring J: The urokinase plasminogen activator system in angiosarcoma, Kaposi's sarcoma, granuloma pyogenicum, and angioma: an immunohistochemical study. *Int J Dermatol* 2000, 39(3):188-191.

139. Sato Y: Role of ETS family transcription factors in vascular development and angiogenesis. *Cell Struct Funct* 2001, 26(1):19-24.

140. Naito S, Shimizu K, Nakashima M, Nakayama T, Ito T, Ito M, Yamashita S, Sekine I: Overexpression of Ets-1 transcription factor in angiosarcoma of the skin. *Pathol Res Pract* 2000, 196(2):103-109.

141. Dictor M, Bendsöe N, Runke S, Witte M: Major basement membrane components in Kaposi's sarcoma, angiosarcoma and benign vascular neogenesis. *J Cutan Pathol* 1995, 22(5):435-441.

142. Dim D, Ravi V, Tan J, Hicks D, Wong M: The actin-bundling motility protein fascin and vascular endothelial growth factor (VEGF) are universally over-expressed in human angiosarcoma. *ASCO Meeting Abstracts* 2007, 25(18_suppl):10068.

143. Tokuyama W, Mikami T, Masuzawa M, Okayasu I: Autocrine and paracrine roles of VEGF/VEGFR-2 and VEGF-C/VEGFR-3 signaling in angiosarcomas of the scalp and face. *Hum Pathol* 2010, 41(3):407-414.

144. Zietz C, Rössle M, Haas C, Sendelhofert A, Hirschmann A, Stürzl M, Löhrs U: MDM-2 oncoprotein overexpression, p53 gene mutation, and VEGF up-regulation in angiosarcomas. *Am J Pathol* 1998, 153(5):1425-1433.

145. Itakura E, Yamamoto H, Oda Y, Tsuneyoshi M: Detection and characterization of vascular endothelial growth factors and their receptors in a series of angiosarcomas. *J Surg Oncol* 2008, 97(1):74-81.

146. Yonemori K, Tsuta K, Ando M, Hirakawa A, Hatanaka Y, Matsuno Y, Chuman H, Yamazaki N, Fujiwara Y, Hasegawa T: Contrasting prognostic implications of platelet-derived growth factor receptor-β and vascular endothelial growth factor receptor-2 in patients with angiosarcoma. *Ann Surg Oncol* 2011, 18(10):2841-2850.

147. Arbiser JL, Larsson H, Claesson-Welsh L, Bai X, LaMontagne K, Weiss SW, Soker S, Flynn E, Brown LF: Overexpression of VEGF 121 in immortalized endothelial cells causes conversion to slowly growing angiosarcoma and high level expression of the VEGF receptors VEGFR-1 and VEGFR-2 in vivo. *Am J Pathol* 2000, 156(4):1469-1476.

148. Hasenstein JR, Kasmerchak K, Buehler D, Hafez GR, Cleary K, Moody JS, Kozak KR: Efficacy of Tie2 receptor antagonism in angiosarcoma. *Neoplasia* 2012, 14(2):131-140.

149. Wang H, Zhang Y, Toratani S, Okamoto T: Transformation of vascular endothelial cells by a point mutation in the Tie2 gene from human intramuscular haemangioma. *Oncogene* 2004, 23(53):8700-8704.

150. Yamamoto T, Umeda T, Yokozeki H, Nishioka K: Expression of basic fibroblast growth factor and its receptor in angiosarcoma. *J Am Acad Dermatol* 1999, 41(1):127-129.

151. Ravi V, Kim S, Dim D, Hicks D, Aggarwal C, Hostetter G, Cheney RT, Bittner M, Trump DL, Wong MK: Identification of therapeutic targets in angiosarcoma. *ASCO Meeting Abstracts* 2007, 25(18_suppl):10030.

152. Dill MT, Rothweiler S, Djonov V, Hlushchuk R, Tornillo L, Terracciano L, Meili-Butz S, Radtke F, Heim MH, Semela D: Disruption of Notch1 induces vascular remodeling, intussusceptive angiogenesis, and angiosarcomas in livers of mice. *Gastroenterology* 2012, 142(4):967-977.e962.

153. Liu Z, Turkoz A, Jackson EN, Corbo JC, Engelbach JA, Garbow JR, Piwnica-Worms DR, Kopan R: Notch1 loss of heterozygosity causes vascular tumors and lethal hemorrhage in mice. *J Clin Invest* 2011, 121(2):800-808.

154. Krump-Konvalinkova V, Bittinger F, Olert J, Bräuninger W, Brunner J, Kirkpatrick CJ: Establishment and characterization of an angiosarcoma-derived cell line, AS-M. *Endothelium* 2003, 10(6):319-328.

155. Masuzawa M, Fujimura T, Tsubokawa M, Nishiyama S, Katsuoka K, Terada E, Kunita S, Sakurai Y, Kato H: Establishment of a new murine-phenotypic angiosarcoma cell line (ISOS-1). *J Dermatol Sci* 1998, 16(2):91-98.

156. Masuzawa M, Fujimura T, Hamada Y, Fujita Y, Hara H, Nishiyama S, Katsuoka K, Tamauchi H, Sakurai Y: Establishment of a human hemangiosarcoma cell line (ISO-HAS). *Int J Cancer* 1999, 81(2):305-308.

157. Edgell CJ, McDonald CC, Graham JB: Permanent cell line expressing human factor VIII-related antigen established by hybridization. *Proc Natl Acad Sci U S A* 1983, 80(12):3734-3737.

158. Unger RE, Krump-Konvalinkova V, Peters K, Kirkpatrick CJ: In vitro expression of the endothelial phenotype: comparative study of primary isolated cells and cell lines, including the novel cell line HPMEC-ST1.6R. *Microvasc Res* 2002, 64(3):384-397.

159. Pusztaszeri MP, Seelentag W, Bosman FT: Immunohistochemical expression of endothelial markers CD31, CD34, von Willebrand factor, and Fli-1 in normal human tissues. *J Histochem Cytochem* 2006, 54(4):385-395.

160. Carter N, Ormerod M: Introduction to the principles of flow cytometry. In: *Flow Cytometry. Volume Oxford University Press*, 3rd edn. Edited by Ormerod M; 2000: 1-22.

161. Voyta JC, Via DP, Butterfield CE, Zetter BR: Identification and isolation of endothelial cells based on their increased uptake of acetylated-low density lipoprotein. *J Cell Biol* 1984, 99(6):2034-2040.

162. Arnaoutova I, George J, Kleinman HK, Benton G: The endothelial cell tube formation assay on basement membrane turns 20: state of the science and the art. *Angiogenesis* 2009, 12(3):267-274.

163. Staton CA, Reed MW, Brown NJ: A critical analysis of current in vitro and in vivo angiogenesis assays. *Int J Exp Pathol* 2009, 90(3):195-221.

164. EMEA: Avastin : EPAR - Scientific Discussion. In: *European Public Assessments Report.* Initial marketing - authorisation documents edn. http://www.ema.europa.eu/docs/en_GB/document_library/EPAR_-_Scientific_Discussion/human/000582/WC500029262.pdf; 2006.

165. Blumenthal RD, Goldenberg DM: Methods and goals for the use of in vitro and in vivo chemosensitivity testing. *Mol Biotechnol* 2007, 35(2):185-197.

166. Albelda SM, Muller WA, Buck CA, Newman PJ: Molecular and cellular properties of PECAM-1 (endoCAM/CD31): a novel vascular cell-cell adhesion molecule. *J Cell Biol* 1991, 114(5):1059-1068.

167. Tamburini BA, Phang TL, Fosmire SP, Scott MC, Trapp SC, Duckett MM, Robinson SR, Slansky JE, Sharkey LC, Cutter GR *et al*: Gene expression profiling identifies inflammation and angiogenesis as distinguishing features of canine hemangiosarcoma. *BMC Cancer* 2010, 10:619.

168. Lahat G, Dhuka AR, Hallevi H, Xiao L, Zou C, Smith KD, Phung TL, Pollock RE, Benjamin R, Hunt KK *et al*: Angiosarcoma: clinical and molecular insights. *Ann Surg* 2010, 251(6):1098-1106.

169. Faivre S, Delbaldo C, Vera K, Robert C, Lozahic S, Lassau N, Bello C, Deprimo S, Brega N, Massimini G *et al*: Safety, pharmacokinetic, and antitumor activity of SU11248, a novel oral multitarget tyrosine kinase inhibitor, in patients with cancer. *J Clin Oncol* 2006, 24(1):25-35.

170. Rugo HS, Herbst RS, Liu G, Park JW, Kies MS, Steinfeldt HM, Pithavala YK, Reich SD, Freddo JL, Wilding G: Phase I trial of the oral antiangiogenesis agent AG-013736 in patients with advanced solid tumors: pharmacokinetic and clinical results. *J Clin Oncol* 2005, 23(24):5474-5483.

171. Costa R, Carneiro A, Rocha A, Pirraco A, Falcão M, Vasques L, Soares R: Bevacizumab and ranibizumab on microvascular endothelial cells: A comparative study. *J Cell Biochem* 2009, 108(6):1410-1417.

172. Banerji U, Camidge DR, Verheul HM, Agarwal R, Sarker D, Kaye SB, Desar IM, Timmer-Bonte JN, Eckhardt SG, Lewis KD *et al*: The first-in-human study of the hydrogen sulfate (Hyd-sulfate) capsule of the MEK1/2 inhibitor AZD6244 (ARRY-142886): a phase I open-label multicenter trial in patients with advanced cancer. *Clin Cancer Res* 2010, 16(5):1613-1623.

173. Houghton PJ: Everolimus. *Clin Cancer Res* 2010, 16(5):1368-1372.

174. O'Donnell A, Faivre S, Burris HA, Rea D, Papadimitrakopoulou V, Shand N, Lane HA, Hazell K, Zoellner U, Kovarik JM *et al*: Phase I pharmacokinetic and pharmacodynamic study of the oral mammalian target of rapamycin inhibitor everolimus in patients with advanced solid tumors. *J Clin Oncol* 2008, 26(10):1588-1595.

175. Yap TA, Yan L, Patnaik A, Fearen I, Olmos D, Papadopoulos K, Baird RD, Delgado L, Taylor A, Lupinacci L *et al*: First-in-man clinical trial of the oral pan-AKT inhibitor MK-2206 in patients with advanced solid tumors. *J Clin Oncol* 2011, 29(35):4688-4695.

176. Garrett MD, Collins I: Anticancer therapy with checkpoint inhibitors: what, where and when? *Trends Pharmacol Sci* 2011, 32(5):308-316.

177. Baguley BC: Antivascular therapy of cancer: DMXAA. *Lancet Oncol* 2003, 4(3):141-148.

178. Lara PN, Douillard JY, Nakagawa K, von Pawel J, McKeage MJ, Albert I, Losonczy G, Reck M, Heo DS, Fan X *et al*: Randomized phase III placebo-controlled trial of carboplatin and paclitaxel with or without the vascular disrupting agent vadimezan (ASA404) in advanced non-small-cell lung cancer. *J Clin Oncol* 2011, 29(22):2965-2971.

179. Rustin GJ, Bradley C, Galbraith S, Stratford M, Loadman P, Waller S, Bellenger K, Gumbrell L, Folkes L, Halbert G *et al*: 5,6-dimethylxanthenone-4-acetic acid (DMXAA), a novel antivascular agent: phase I clinical and pharmacokinetic study. *Br J Cancer* 2003, 88(8):1160-1167.

180. Weiss S, Goldblum J: Haemangioendothelioma: Vascular Tumors of Intermediate Malignancy. In: *Enzinger & Weiss's Soft Tissue Sarcoma.* 4th edn. Edited by Weiss S, Goldblum J: Mosby; 2001: 891-915.

181. Weiss S, Goldblum J: Benign Tumors and Tumor-Like Lesions of Blood Vessels. In: *Enzinger & Weiss's Soft Tissue Sarcoma.* 4th edn. Edited by Weiss S, Goldblum J: Mosby; 2001: 837-890.

182. Hoover ML, Větvicka V, Hoffpauir JM, Tamburro CH: Human endothelial cell line from an angiosarcoma. *In Vitro Cell Dev Biol* 1993, 29A(3 Pt 1):199-202.

183. Karar J, Maity A: PI3K/AKT/mTOR Pathway in Angiogenesis. *Front Mol Neurosci* 2011, 4:51.

184. Rowinsky EK, Cazenave LA, Donehower RC: Taxol: a novel investigational antimicrotubule agent. *J Natl Cancer Inst* 1990, 82(15):1247-1259.

185. Belotti D, Vergani V, Drudis T, Borsotti P, Pitelli MR, Viale G, Giavazzi R, Taraboletti G: The microtubule-affecting drug paclitaxel has antiangiogenic activity. *Clin Cancer Res* 1996, 2(11):1843-1849.

186. Wang Y, Fei D, Vanderlaan M, Song A: Biological activity of bevacizumab, a humanized anti-VEGF antibody in vitro. *Angiogenesis* 2004, 7(4):335-345.

187. Kumar R, Crouthamel MC, Rominger DH, Gontarek RR, Tummino PJ, Levin RA, King AG: Myelosuppression and kinase selectivity of multikinase angiogenesis inhibitors. *Br J Cancer* 2009, 101(10):1717-1723.

188. Pópulo H, Lopes JM, Soares P: The mTOR Signalling Pathway in Human Cancer. *Int J Mol Sci* 2012, 13(2):1886-1918.

189. Motzer RJ, Escudier B, Oudard S, Hutson TE, Porta C, Bracarda S, Grünwald V, Thompson JA, Figlin RA, Hollaender N *et al*: Phase 3 trial of everolimus for metastatic renal cell carcinoma : final results and analysis of prognostic factors. *Cancer* 2010, 116(18):4256-4265.

190. Chawla SP, Blay J, Ray-Coquard IL, Le Cesne A, Staddon AP, Milhem MM, Penel N, Riedel RF, Bui Nguyen B, Cranmer LD *et al*: Results of the phase III, placebo-controlled trial (SUCCEED) evaluating the mTOR inhibitor ridaforolimus (R) as maintenance therapy in advanced sarcoma patients (pts) following clinical benefit from prior standard cytotoxic chemotherapy (CT). *ASCO Meeting Abstracts* 2011, 29(15_suppl):10005.

191. Chappell WH, Steelman LS, Long JM, Kempf RC, Abrams SL, Franklin RA, Bäsecke J, Stivala F, Donia M, Fagone P *et al*: Ras/Raf/MEK/ERK and PI3K/PTEN/Akt/mTOR inhibitors: rationale and importance to inhibiting these pathways in human health. *Oncotarget* 2011, 2(3):135-164.

192. Bennouna J, Lang I, Valladares-Ayerbes M, Boer K, Adenis A, Escudero P, Kim TY, Pover GM, Morris CD, Douillard JY: A Phase II, open-label, randomised study to assess the efficacy and safety of the MEK1/2 inhibitor AZD6244 (ARRY-142886) versus capecitabine monotherapy in patients with colorectal cancer who have failed one or two prior chemotherapeutic regimens. *Invest New Drugs* 2011, 29(5):1021-1028.

193. Kirkwood JM, Bastholt L, Robert C, Sosman J, Larkin J, Hersey P, Middleton M, Cantarini M, Zazulina V, Kemsley K *et al*: Phase II, open-label, randomized trial of the MEK1/2 inhibitor selumetinib as monotherapy versus temozolomide in patients with advanced melanoma. *Clin Cancer Res* 2012, 18(2):555-567.

194. Luthra S, Narayanan R, Marques LE, Chwa M, Kim DW, Dong J, Seigel GM, Neekhra A, Gramajo AL, Brown DJ *et al*: Evaluation of in vitro effects of bevacizumab (Avastin) on retinal pigment epithelial, neurosensory retinal, and microvascular endothelial cells. *Retina* 2006, 26(5):512-518.

195. Deissler HL, Deissler H, Lang GE: Actions of bevacizumab and ranibizumab on microvascular retinal endothelial cells: similarities and differences. *Br J Ophthalmol* 2012, 96(7):1023-1028.

196. Willett CG, Boucher Y, di Tomaso E, Duda DG, Munn LL, Tong RT, Chung DC, Sahani DV, Kalva SP, Kozin SV *et al*: Direct evidence that the VEGF-specific antibody bevacizumab has antivascular effects in human rectal cancer. *Nat Med* 2004, 10(2):145-147.

197. Boscolo E, Mulliken JB, Bischoff J: VEGFR-1 mediates endothelial differentiation and formation of blood vessels in a murine model of infantile hemangioma. *Am J Pathol* 2011, 179(5):2266-2277.

198. Ellis LM, Hicklin DJ: Pathways mediating resistance to vascular endothelial growth factor-targeted therapy. *Clin Cancer Res* 2008, 14(20):6371-6375.

199. Abedalthagafi M, Rushing EJ, Auerbach A, Desouki MM, Marwaha J, Wang Z, Fanburg-Smith JC: Sporadic cutaneous angiosarcomas generally lack hypoxia-inducible factor 1alpha: a histologic and immunohistochemical study of 45 cases. *Ann Diagn Pathol* 2010, 14(1):15-22.

200. Arbiser JL, Weiss SW, Arbiser ZK, Bravo F, Govindajaran B, Caceres-Rios H, Cotsonis G, Recavarren S, Swerlick RA, Cohen C: Differential expression of active mitogen-activated protein kinase in cutaneous endothelial neoplasms: implications for biologic behavior and response to therapy. *J Am Acad Dermatol* 2001, 44(2):193-197.

201. Vart RJ, Nikitenko LL, Lagos D, Trotter MW, Cannon M, Bourboulia D, Gratrix F, Takeuchi Y, Boshoff C: Kaposi's sarcoma-associated herpesvirus-encoded interleukin-6 and G-protein-coupled receptor regulate angiopoietin-2 expression in lymphatic endothelial cells. *Cancer Res* 2007, 67(9):4042-4051.

202. Friday BB, Yu C, Dy GK, Smith PD, Wang L, Thibodeau SN, Adjei AA: BRAF V600E disrupts AZD6244-induced abrogation of negative feedback pathways between extracellular signal-regulated kinase and Raf proteins. *Cancer Res* 2008, 68(15):6145-6153.

203. Wee S, Jagani Z, Xiang KX, Loo A, Dorsch M, Yao YM, Sellers WR, Lengauer C, Stegmeier F: PI3K pathway activation mediates resistance to MEK inhibitors in KRAS mutant cancers. *Cancer Res* 2009, 69(10):4286-4293.

204. Antoni L, Sodha N, Collins I, Garrett MD: CHK2 kinase: cancer susceptibility and cancer therapy - two sides of the same coin? *Nat Rev Cancer* 2007, 7(12):925-936.

205. Ching LM, Zwain S, Baguley BC: Relationship between tumour endothelial cell apoptosis and tumour blood flow shutdown following treatment with the antivascular agent DMXAA in mice. *Br J Cancer* 2004, 90(4):906-910.

206. Baguley BC, Ching LM: DMXAA: an antivascular agent with multiple host responses. *Int J Radiat Oncol Biol Phys* 2002, 54(5):1503-1511.

207. Deroose JP, van Geel AN, Burger JW, Eggermont AM, Verhoef C: Isolated limb perfusion with TNF-alpha and melphalan for distal parts of the limb in soft tissue sarcoma patients. *J Surg Oncol* 2012, 105(6):563-569.

208. Zhao L, Ching LM, Kestell P, Baguley BC: The antitumour activity of 5,6-dimethylxanthenone-4-acetic acid (DMXAA) in TNF receptor-1 knockout mice. *Br J Cancer* 2002, 87(4):465-470.

209. Cao Z, Joseph WR, Browne WL, Mountjoy KG, Palmer BD, Baguley BC, Ching LM: Thalidomide increases both intra-tumoural tumour necrosis factor-alpha production and anti-tumour activity in response to 5,6-dimethylxanthenone-4-acetic acid. *Br J Cancer* 1999, 80(5-6):716-723.

210. Woon ST, Hung SS, Wu DC, Schooltink MA, Sutherland R, Baguley BC, Chen Q, Chamley LW, Ching LM: NF-kappaB-independent induction of endothelial cell apoptosis by the vascular disrupting agent DMXAA. *Anticancer Res* 2007, 27(1A):327-334.

211. Ching LM, Cao Z, Kieda C, Zwain S, Jameson MB, Baguley BC: Induction of endothelial cell apoptosis by the antivascular agent 5,6-Dimethylxanthenone-4-acetic acid. *Br J Cancer* 2002, 86(12):1937-1942.

212. Buchanan CM, Shih JH, Astin JW, Rewcastle GW, Flanagan JU, Crosier PS, Shepherd PR: DMXAA (Vadimezan, ASA404) is a multi-kinase inhibitor targeting VEGFR2 in particular. *Clin Sci (Lond)* 2012, 122(10):449-457.

213. Tokuyama W, Mikami T, Masuzawa M, Okayasu I: Autocrine and paracrine roles of VEGF/VEGFR-2 and VEGF-C/VEGFR-3 signaling in angiosarcomas of the scalp and face. *Hum Pathol* 2010, 41(3):407-414.

214. Brown LF, Tognazzi K, Dvorak HF, Harrist TJ: Strong expression of kinase insert domain-containing receptor, a vascular permeability factor/vascular

endothelial growth factor receptor in AIDS-associated Kaposi's sarcoma and cutaneous angiosarcoma. *Am J Pathol* 1996, 148(4):1065-1074.

215. Staton CA, Kumar I, Reed MW, Brown NJ: Neuropilins in physiological and pathological angiogenesis. *J Pathol* 2007, 212(3):237-248.

216. Wild JR, Staton CA, Chapple K, Corfe BM: Neuropilins: expression and roles in the epithelium. *Int J Exp Pathol* 2012, 93(2):81-103.

217. Pan Q, Chanthery Y, Liang WC, Stawicki S, Mak J, Rathore N, Tong RK, Kowalski J, Yee SF, Pacheco G *et al*: Blocking neuropilin-1 function has an additive effect with anti-VEGF to inhibit tumor growth. *Cancer Cell* 2007, 11(1):53-67.

218. Welti JC, Gourlaouen M, Powles T, Kudahetti SC, Wilson P, Berney DM, Reynolds AR: Fibroblast growth factor 2 regulates endothelial cell sensitivity to sunitinib. *Oncogene* 2011, 30(10):1183-1193.

219. Herbst RS, Hong D, Chap L, Kurzrock R, Jackson E, Silverman JM, Rasmussen E, Sun YN, Zhong D, Hwang YC *et al*: Safety, pharmacokinetics, and antitumor activity of AMG 386, a selective angiopoietin inhibitor, in adult patients with advanced solid tumors. *J Clin Oncol* 2009, 27(21):3557-3565.

220. Amo Y, Masuzawa M, Hamada Y, Katsuoka K: Observations on angiopoietin 2 in patients with angiosarcoma. *Br J Dermatol* 2004, 150(5):1028-1029.

221. Brown LF, Dezube BJ, Tognazzi K, Dvorak HF, Yancopoulos GD: Expression of Tie1, Tie2, and angiopoietins 1, 2, and 4 in Kaposi's sarcoma and cutaneous angiosarcoma. *Am J Pathol* 2000, 156(6):2179-2183.

222. Trusolino L, Bertotti A, Comoglio PM: MET signalling: principles and functions in development, organ regeneration and cancer. *Nat Rev Mol Cell Biol* 2010, 11(12):834-848.

223. Gherardi E, Birchmeier W, Birchmeier C, Vande Woude G: Targeting MET in cancer: rationale and progress. *Nat Rev Cancer* 2012, 12(2):89-103.

224. Cecchi F, Rabe DC, Bottaro DP: Targeting the HGF/Met signalling pathway in cancer. *Eur J Cancer* 2010, 46(7):1260-1270.

225. Kwak EL, Bang YJ, Camidge DR, Shaw AT, Solomon B, Maki RG, Ou SH, Dezube BJ, Jänne PA, Costa DB *et al*: Anaplastic lymphoma kinase inhibition in non-small-cell lung cancer. *N Engl J Med* 2010, 363(18):1693-1703.

226. Eder JP, Shapiro GI, Appleman LJ, Zhu AX, Miles D, Keer H, Cancilla B, Chu F, Hitchcock-Bryan S, Sherman L *et al*: A phase I study of foretinib, a multi-targeted inhibitor of c-Met and vascular endothelial growth factor receptor 2. *Clin Cancer Res* 2010, 16(13):3507-3516.

227. Tamburini BA, Trapp S, Phang TL, Schappa JT, Hunter LE, Modiano JF: Gene expression profiles of sporadic canine hemangiosarcoma are uniquely associated with breed. *PLoS One* 2009, 4(5):e5549.

228. Wiley JL, Rook KA, Clifford CA, Gregor TP, Sorenmo KU: Efficacy of doxorubicin-based chemotherapy for non-resectable canine subcutaneous haemangiosarcoma. *Vet Comp Oncol* 2010, 8(3):221-233.

229. Yonemaru K, Sakai H, Murakami M, Yanai T, Masegi T: Expression of vascular endothelial growth factor, basic fibroblast growth factor, and their receptors (flt-1, flk-1, and flg-1) in canine vascular tumors. *Vet Pathol* 2006, 43(6):971-980.

230. MacEwen EG, Kurzman ID, Rosenthal RC, Smith BW, Manley PA, Roush JK, Howard PE: Therapy for osteosarcoma in dogs with intravenous injection of liposome-encapsulated muramyl tripeptide. *J Natl Cancer Inst* 1989, 81(12):935-938.

231. Kanthou C, Tozer GM: Microtubule depolymerizing vascular disrupting agents: novel therapeutic agents for oncology and other pathologies. *Int J Exp Pathol* 2009, 90(3):284-294.

Appendix - Contents